Quantification of Soil CO_2 Emissions under the Influence of Climate Change on the Qinghai-Tibet Plateau Based on Freely Accessible Data

Dissertation

der Mathematisch-Naturwissenschaftlichen Fakultät

der Eberhard Karls Universität Tübingen

zur Erlangung des Grades eines

Doktors der Naturwissenschaften

(Dr. rer. nat.)

vorgelegt von

Anna Bosch

aus Giengen an der Brenz

Tübingen

2016

Gedruckt mit Genehmigung der Mathematisch-Naturwissenschaftlichen Fakultät der Eberhard Karls Universität Tübingen.

Tag der mündlichen Qualifikation:	27.03.2017
Dekan:	Prof. Dr. Wolfgang Rosenstiel
1. Berichterstatter:	Prof. Dr. Thomas Scholten
2. Berichterstatter:	Prof. Dr. Volker Hochschild

Table of Contents

List of Figures

Figure 8: Spatial distribution of C stocks of the permafrost areas on the Qinghai-Tibet Plateau for 2015, 2050 and 2070. C stocks are in SI unit (kg m^{-2}). The spatial resolution of the grids is 1,000 m x 1,000 m.

Figure 9: Spatial distribution of absolute differences in C stocks of the permafrost areas on the Qinghai-Tibet Plateau between 2015 and 2050 and between 2015 and 2070. Absolute differences in C stocks are in SI unit (kg m^{-2}). The spatial resolution of the grids is 1,000 m x 1,000 m.

List of Tables

List of Abbreviations

BGB	Belowground Biomass
C	Carbon
CO_2	Carbon Dioxide
MAP	Mean Annual Precipitation
MAT	Mean Annual Temperature
PF	Permafrost
PFS	Permafrost Soils
Pg	Petagramm (1 Pg = 10^{15} g)
RCP	Representative Concentration Pathway
SR	Soil Respiration

1 Summary

Soil CO_2 emissions are of important significance for the global carbon cycle and, thus, for climate change. Soils function as main source of atmospheric CO_2 from terrestrial ecosystems. Even small changes in soil CO_2 emissions can accelerate global warming. Reciprocally, climate change influences soil CO_2 emissions. Against this background, it is highly essential to quantify potential soil CO_2 emissions in order to be able to project future developments of global warming.

In this context, the permafrost region of the Qinghai-Tibet Plateau is a key region for soil CO_2 emissions. Permafrost soils are considered as a CO_2 source with high potential. In consequence of thawing processes, large quantities of carbon stored in these soils become subject to microbial decomposition and are emitted as CO_2. Because of its large area (1.050×10^6 km^2) and high sensitivity to climate together with increasing permafrost degradation, the Qinghai-Tibet Plateau attains global significance.

The spatially and temporally extremely varying soil CO_2 emissions originating from different sources can be quantified by process-based models. These models generally incorporate various of the interacting, numerous controlling factors of soil CO_2 emissions. Limitations occur especially for large areas due to higher requirements with regard to input data and a general restricted knowledge of the key trigger mechanisms of soil CO_2 emissions. Therefore, empirical models still represent the commonly used type of model, being highly advantageous especially for large and remote areas with a high data scarcity as e.g. the Qinghai-Tibetan Plateau. Due to the large area difficult to access, field measurements are very costly and time consuming. Thus, they are strongly limited on the Qinghai-Tibetan Plateau. Consequently, area-explicit data sets mainly exhibit a low spatial resolution, are not comprehensive or freely accessible. However, freely available global datasets of a high resolution (~1 km) enable an application of empirical models to predict soil CO_2 emissions on the Qinghai-Tibet Plateau area-explicitly.

This thesis provides an approach to quantify CO_2 emissions from permafrost soils efficiently. Belowground biomass on the Qinghai-Tibet Plateau was calculated using empirical models since it represents a not yet area-explicitly quanitifed key input factor in empirical models for soil CO_2 emissions on the Qinghai-Tibet Plateau. Based on a

comparison of different regression models for quantifying current soil CO_2 emissions on the Qinghai-Tibet Plateau, the one closest representing field measurements throughout various vegetation zones was identified. Applying this model, which incorporates mean annual precipitation as input factor, future soil CO_2 emissions were predicted. Consequently, scenarios of climate change for mean annual precipitation underlie the predictions of potential soil CO_2 emissions for 2050 and 2070. To account for the high importance of permafrost in the study area, thawing-induced CO_2 emissions from those soils were calculated additionally using experimental data on carbon losses from permafrost soils that were taken from the literature. To quantify those CO_2 emissions, area-explicit carbon stocks were calculated for the Qinghai-Tibet Plateau.

This thesis highlights the quantitative dimension of CO_2 from permafrost soils on the Qinghai-Tibet Plateau for global warming, with 0.15 Pg C $year^{-1}$ fitting the order of magnitude of results of comparable studies. The thesis further demonstrates the impact of climate change especially on thawing-induced CO_2 emissions from permafrost soils. Their order of magnitude, approximately 4% of the annual average atmospheric increase of CO_2-C, justifies strategies for climate protection in particular.

By comparing the modeled results to data from field measurements, this thesis further indicates that empirical models represent suitable tools to adequately model and predict belowground biomass and soil CO_2 emissions. Using exclusively freely accessible data sets, this thesis further exemplifies a highly efficient quantification of complex phenomena on a regional scale at a high resolution. Data-scarce areas of global relevance potentially profit most.

2 Zusammenfassung

CO_2-Emissionen aus Böden stellen als wesentlicher Faktor im Kohlenstoffkreislauf eine besonders relevante Einflussgröße des Klimawandels dar. Böden bilden die Hauptquelle atmosphärischen CO_2s hinsichtlich terrestrischer Ökosysteme. Kleinste Veränderungen der Boden-CO_2-Emissionen können zu einer Verstärkung der globalen Erwärmung führen. Demgegenüber steht der Einfluss des Klimawandels auf den Ausstoß von CO_2 aus Böden. Vor dem Hintergrund dieser Wechselwirkung ist es von großer Bedeutung potentielle CO_2-Emissionen aus Böden zu quantifizieren, um zukünftige Entwicklungen abschätzen zu können.

Hierbei stellt das Permafrostareal des Qinghai-Tibet Plateaus eine bedeutende Untersuchungsregion dar. Im Zusammenhang mit der globalen Erwärmung gelten Permafrostböden als besonders große potentielle CO_2-Quelle. Der dort in außergewöhnlich hohen Mengen gespeicherte Kohlenstoff wird im Zuge von Auftauprozessen mikrobieller Zersetzung zugänglich und als CO_2 emittiert. Seine enorme Fläche (1.050×10^6 km^2) und ausgeprägte Klimasensibilität einhergehend mit zunehmender Permafrostdegradation verleihen dem Qinghai-Tibet Plateau globale Bedeutung.

Die außerordentlich stark räumlich und zeitlich variienden Boden-CO_2-Emissionen, die eine Vielzahl an wechselwirkenden Einflussfaktoren sowie unterschiedliche Quellen aufweisen, können durch prozessbasierte Modelle quantifiziert werden. Diese berücksichtigen grundsätzlich zahlreiche Einflussfaktoren. Ihre Anwendung ist vor allem für großflächige Gebiete eingeschränkt aufgrund von hierfür höheren Anforderungen an die Eingangsdaten. Empirische Modelle für Boden-CO_2-Emissionen, die sich auf wesentliche Einflussfaktoren konzentrieren, sind generell weit verbreitet und bieten insbesondere für ausgedehnte und entlegene Regionen, die wie z. B. das Qinghai-Tibet Plateau eine starke Datenknappheit aufweisen, große Vorteile. Aufgrund des schwer zugänglichen und ausgedehnten Gebietes sind Feldmessungen dort stark eingeschränkt. Infolgedessen ist die Erstellung von Datensätzen mit hohem Zeit- und Kostenaufwand verbunden. Des Weiteren sind diese meist räumlich schwach aufgelöst, räumlich unzusammenhängend oder nicht frei zugänglich. Diesen Datensätzen stehen frei zugängliche globale Datensätze mit hoher (~1 km) Auflösung gegenüber, die die Anwendung von empirischen Modellen zur Berechnung von flächendeckenden CO_2-Emissionen des Qinghai-Tibet Plateaus erlauben.

Diese Arbeit zeigt eine effiziente Quantifizierung von CO_2-Emissionen aus den Permafrostböden des Qinghai-Tibet Plateaus. Unter Anwendung von empirischen Modellen wurde die unterirdische Biomasse als ein bislang nicht flächendeckend quantifizierter wesentlicher Eingangsfaktor für empirische Modelle zu Boden-CO_2-Emissionen des Qinghai-Tibet Plateaus berechnet. Ein Modellvergleich zeigte, welches empirische Regressionsmodell am besten im Feld gemessene CO_2-Emissionen auf dem Qinghai-Tibet Plateau repräsentiert. Mit diesem Regressionsmodell, das auf dem mittleren Jahresniederschlag basiert, wurden aktuelle Boden-CO_2-Emissionen des Qinghai-Tibet Plateau berechnet. Darüber hinaus wurden basierend auf Klimawandelszenarien der mittleren Jahresniederschläge für 2050 und 2070 die potentiellen Boden-CO_2-Emissionen dieser Jahre quantifiziert. Aufgrund der besonderen Bedeutung des Permafrosts und seinem Auftauen im Untersuchungsgebiet, wurden die entsprechenden CO_2-Emissionen basierend auf experimentellen Daten zu Kohlenstoffverlusten aus Permafrostböden aus der Literatur zusätzlich ermittelt. Um diese durch das Auftauen des Permafrosts induzierten Boden-CO_2-Emissionen zu quantifizieren, wurden flächendeckend Kohlenstoffvorräte für das Qinghai-Tibet Plateau berechnet.

Die vorliegende Arbeit zeigt das quantitative Ausmaß von CO_2-Emissionen aus den Permafrostböden des Qinghai-Tibet Plateaus für die globale Erwärmung, das sich mit 0.15 Pg C $year^{-1}$ in der Größenordnung von Berechnungen vergleichbarer Studien bewegt. Die Arbeit weist darüber hinaus darauf hin, dass sich der Klimawandel insbesondere auf die CO_2-Emissionen quantitativ auswirkt, die durch das Auftauen des Permafrostes induziert werden. Hierbei wird mit annähernd 4% des mittleren, jährlichen atmosphärischen CO_2-C-Anstiegs eine Größenordnung erreicht, die Klimaschutzstrategien in besonderem Maße rechtfertigen.

Empirische Modelle zeigen sich im Hinblick auf die Berechnung sowohl der unterirdischen Biomasse als auch der Boden-CO_2-Emissionen als mit Feldmessungen vergleichbare, geeignete Methoden für flächendeckende Vorhersagen. Mit der Konzentration auf ausschließlich frei zugängliche Datensätze exemplifiziert die Arbeit eine hocheffiziente Quantifizierung komplexer Größen in feiner Auflösung auf der Regionalskala. Dies ist insbesondere für Gebiete mit grundsätzlich schwacher Datengrundlage und globaler Relevanz von großer Bedeutung

3 List of Publications in the Thesis

(1) A comparison of regression models to estimate belowground biomass on the Qinghai-Tibet Plateau. (ready for submission)

Manuscript 1, ready for submission as first author in Geoderma Regional 2017.
Coauthors: Corina Doerfer, Jin-Sheng He, Karsten Schmidt, Thomas Scholten.
The full publication can be found on page 82.

(2) Predicting soil respiration for the Qinghai-Tibet Plateau: An empirical comparison of regression models. (published)

Manuscript 2, published as first author in Pedobiologia 2016, Volume 59, Pages 41-49. DOI: http://dx.doi.org/10.1016/j.pedobi.2016.01.002.
Coauthors: Corina Doerfer, Jin-Sheng He, Karsten Schmidt, Thomas Scholten.
The full publication can be found on page 111.

(3) Potential CO_2 emissions from defrosting permafrost soils of the Qinghai-Tibet Plateau under different scenarios of climate change in 2050 and 2070. (published)

Manuscript 3, published as first author in Catena 2017, Volume 149, Pages 221-231. DOI: http://dx.doi.org/10.1016/j.catena.2016.08.035.
Coauthors: Corina Doerfer, Jin-Sheng He, Karsten Schmidt, Thomas Scholten.
The full publication can be found on page 138.

4 Introduction and State of the Art

4.1 Soil CO_2 Emissions as Integral to Global Carbon Cycling and Climate Change

Soil CO_2 emissions constitute a highly relevant component of climate change (Wang et al., 2008; Chen et al., 2010; Powlson et al., 2011; IPCC, 2013; Schuur et al., 2015). These greenhouse gas releases from soils account for approximately 25% of the carbon dioxide (CO_2) exchange globally (Cui, 2014), representing one of the largest carbon (C) flows within the global C cycle (Schlesinger and Andrews, 2000). Within terrestrial ecosystems, soils emit most CO_2, contributing approximately 98 ±12 Petagramm (Pg) C $year^{-1}$ to the global C budget (Schlesinger and Andrews, 2000; Valentini et al., 2000; Bond-Lamberty and Thomson, 2010a). Soils further contain the largest amount of C in terrestrial ecosystems with more than 3,150 Pg C (Sabine et al., 2003), which is more than four times the atmospheric CO_2-C pool (750 Pg C) (Jia et al., 2006). Of the atmospheric CO_2, ~10% passes through soil annually on a global scale (Bond-Lamberty and Thomson, 2010b). Therefore, a small increase in the amount of soil CO_2 efflux, especially across wide-spread areas such as the Qinghai-Tibet Plateau, can considerably influence atmospheric CO_2 concentrations, potentially exacerbating the greenhouse gas-driven climate change (Schlesinger and Andrews, 2000; Rodeghiero and Cescatti, 2005; Davidson and Janssens, 2006; Qiu, 2008; Rodeghiero et al., 2013; Ding et al., 2016). An increase of 1% of global soil CO_2 emissions (amounting to 67.7 Pg C $year^{-1}$) would be equivalent to annual CO_2 emissions from fossil fuels increasing by 14% (Schlesinger et al., 2000). This potential C-cycle feedbacks from soils to climate warming as global challenge of vital importance made this a focal research topic over the last two decades to be continued in future (Bahn et al., 2010; IPCC, 2013; Wu et al., 2014). The acceleration of global warming due to soil CO_2 emissions especially from permafrost soils (PFS) is regarded as highly relevant to future climate change (Melillo et al., 2002; Wang et al., 2008; Schuur et al., 2009). If it is to predict global warming successfully and in order to take adequate action, not only qualitative aspects are important to consider, a quantification of future soil CO_2 emissions becomes inevitable (Fang and Moncrieff, 2001).

4.2 Characterization of Soil CO_2 Emissions

4.2.1 Differentiation of Soil CO_2 Emissions by Sources

Generally, soil CO_2 emissions originate from two major sources: (i) soil respiration (SR) as biogenic source incorporating soil organic C and (ii) soil CO_2 production by carbonatic reactions of soil inorganic C (Ramnarine et al., 2012). SR is often subdivided into two components: autotrophic respiration consisting of root and root-associated (e.g., mycorrhizae) respiration, and heterotrophic respiration, constituted by microbial respiration in the course of soil organic matter decomposition (Joo et al., 2012). In contrast, Kuzyankov (2006) distinghuishes five components of SR. However, definitions and terms used vary in general especially with regard to the understanding of autotrophic respiration including or excluding root-associated respiration (Six et al., 2002; Kuzyankov, 2006). A significant difference between these components represent their turnover rates, ranging from a few minutes to thousands of years (Kuzyankov, 2006). The variation of these components with environmental changes such as e.g. climate change is not entirely congruent (Boone et al., 1998; Chen et al., 2010). To date, however, no fully convincing method to determine the corresponding indiviual contribution of the respective sources to total soil CO_2 emissions has been developed yet (Kuzyankov, 2006).

In general, both quantitatively and qualitatively, SR inheres distinctly higher significance for total soil CO_2 emissions than abiotic soil CO_2 emissions. The global pool of inorganic C comprises the minor part of the global C pool with only 700 to 900 Pg (Adams and Post, 1999). This as well as the higher biogenic production of soil CO_2 account for the fact that total soil CO_2 emissions mainly originate from SR (Raich and Schlesinger, 1992; Lou and Zhou, 2006). Further, SR is of greater importance than abiotic soil CO_2 emissions as SR is regarded as a main controlling factor for abiotic soil CO_2 emissions (Rovira and Vallejo 2008; Ramnarine et al., 2012). Limitations in measurement techniques lead to the fact that measured SR generally comprises total soil CO_2 emissions and the term ‘SR’ used in literature typically refers to total soil CO_2 emissions (Kuzyankov, 2006).

4.2.2 Controlling Factors of Soil CO_2 Emissions

In general, there is quite a number of biotic and abiotic factors controlling soil CO_2 emissions. Abiotic soil CO_2 emissions are mainly determined by SR, which is mostly regulated by soil temperature and soil water content (e.g. Raich and Tufekcioglu, 2000;

Singh and Gupta, 1977; Ramnarine et al., 2012). Water solubilizes organic matter, supports its availability, controls O_2 diffusion for the microbial activity and further directly influences physiological processes of soil biota (Harris, 1981; Linn and Doran 1984; Koizumi et al., 1999). In general, soil CO_2 emissions are lower at dry conditions (Liu et al., 2002). However, a soil water content usually above field capacity, results in anaerobic conditions reducing microbial activity and therefore soil CO_2 emissions. Near field capacity, soil CO_2 emissions are generally highest (Lou and Zhou, 2006). Temperature, in contrast, directly impacts metabolic activities (Koizumi et al., 1999). Soil CO_2 emissions generally increase with increasing temperature (Raich and Schlesinger 1992; Raich and Potter 1995; Kirschbaum 1995). They are highest at a temperature of 45 to 50 °C, however, their exact temperature sensitivity depend on their source (Atkin et al., 2000; Lou and Zhou, 2006). Soil moisture also influences the response of soil CO_2 emissions to temperature variation (Wisemann and Seiler, 2004). Other factors affecting soil CO_2 emissions include characteristics of vegetation (Raich and Tufekcioglu, 2000), especially ecosystem type (Saiz et al., 2006), net primary productivity (Raich and Potter, 1995), rates of plant photosynthesis (Högberg et al., 2001), litterfall supply (Davidson and Janssens, 2006), relative allocation of net primary production above- and belowground (Boone et al., 1998), root biomass and density (e.g., Ben-Asher et al., 1994; Geng et al. 2012), root nitrogen content (Ryan et al., 1996), population characteristics of the flora and fauna above- and belowground (Raich and Schlesinger 1992), microbial biomass (Ryan et al., 1996), grazing (Cao et al., 2004), and land-use regimes (Ewel et al., 1987). Soil characteristics, pronouncedly substrate quality (Raich and Schlesinger, 1992), soil organic matter quality and quantity (Taylor et al., 1989), soil physical and chemical features (e.g., Boudot et al., 1986) such as soil acidity (Raich and Schlesinger 1992), soil texture (Raich and Schlesinger 1992), decomposition dynamics (Jackson et al., 1998), quality and amount of organic C (Raich and Schlesinger, 1992), availability of soil nutrients (Raich and Tufekcioglu, 2000), and soil type (Koizumi et al., 1999) have further shown to exert influence on soil CO_2 emissions. Regarding soil types, sandy soil generally exhibits faster decompositon due to a higher pore space (Puttaso et al., 2011). In contrast, in clay and loam soils mineralization rates are retarded due to more frequent anaerobic conditions and both reposition and sequestration of soil organic matter in clay minerals and sesquioxides (Blume et al., 2010; Puttaso et al., 2011). Precipitation also controls soil CO_2 emissions (Rey et al., 2002) and is often considered being an important

predictor for soil CO_2 emissions on a regional scale (Lou and Zhou, 2006). Topographic characteristics (Fang et al., 1998) such as exposition (Kang et al., 2003) and the location on a slope (Hanson et al., 1993) regulate soil CO_2 emissions as well as altitude does (Nakane, 1975).

The dominance of an influencing factor differs among ecosystem types. For example, tundra is less influenced by its vegetation type than by climatic factors (Grogan and Chapin, 1999). Soil moisture is the prevalent influencing factor for deserts (Lou and Zhou, 2006). In general, warmer and more humid regions show higher rates of soil CO_2 emissions (Lou and Zhou, 2006).

4.2.3 Variability of Soil CO_2 Emissions

Variability of soil CO_2 emissions occurs in temporal and spatial dimensions (Davidson et al., 2006; Bond-Lamberty and Thomson, 2010b). For both dimensions, different scales evoke a dominance of different controlling factors (Lou and Zhou, 2006).

As to temporal scales, on a diurnal scale, soil temperature is prevalent except for forests due to their shading (Davidson et al., 2000) and arid soils with a higher relative humidity at night (Medina and Zelwer, 1972). Weekly variation of soil CO_2 emissions can be initiated by changing synoptic weather events (Subke et al., 2003). Seasonal patterns generally follow the respective limiting factor, which is temperature or moisture, depending on the climate and ecosystem type (Lou and Zhou, 2006). For example, in arid and semiarid regions, dynamics of soil moisture determine the amount of soil CO_2 emissions (Davidson et al., 2000). Interannual differences in soil CO_2 emissions are mainly related to climatic variables (Epron, 2004). Decadal and centennial variation is basically related to succesional sequences but may be overridden by general environmental changes (Luo and Zhou, 2006).

As to spatial scales, high variability characterizes soil CO_2 emissions as well (Bond-Lamberty and Thomson, 2010b). Even at the stand level with comparatively homogenous soils, studies have shown that soil CO_2 emssions rates from 150 samples within a plot size of 3.6 m^2 vary for about six times within two days (Griffin et al., 1996). Landscapes as spatially diverse areas in general, exibit a high, spatial variability of soil CO_2 emissions by nature, resulting from their heterogenity in climate, topography, soil, vegetation, landscape forms and anthropogenic disturbance (Lou and Zhou, 2006). High spatial variability is regarded inevitably inherent to soil CO_2 emissions on a regional scale depending on the ecosystem (Lou and Zhou, 2006). According to Raich

and Schlesinger´s global analysis (1992), average annual rates of soil CO_2 emissions are generally higher in forests than in grasslands. However, grasslands exhibit about 20% higher soil CO_2 emission rates than forests according to Raich and Tufekcioglu (2000). Tundra ecosystems release less soil CO_2 than grasslands and forests (Grogan and Chapin 1999). In deserts, plant production and consequently soil CO_2 emissions appear to be the lowest under the ecosystems, resulting from extreme environmental conditions (Raich and Schlesinger, 1992). Soil CO_2 emissions of wetlands vary strongly from lowest to highest rates under the ecosystem types (Melling et al., 2005).

4.3 Quantifying Soil CO_2 Emissions

As a multifactorial process with complex interactions and extreme variability across time and space (Section 4.2), soil CO_2 emissions have always been a challenge to measure and no procedure or model has been commonly accepted to quantify soil CO_2 emissions as a standard (Luo and Zhou, 2006).

Widely used methods for field measurements of soil CO_2 emissions are chamber systems and eddy-covariance systems (Morén and Lindroth, 2000). However, high efforts of time and costs required for classical soil data collection and mapping, especially for soil CO_2 emissions in large and remote areas such as the Qinghai-Tibet Plateau, necessitate cost-efficient methods (Scull et al., 2003; Behrens and Scholten, 2006; Behrens et al., 2010). With global change being one of the major challenges facing the world at present, quantifying soil CO_2 emissions is no longer a purely academic exercise, further highlighting this demand for efficient methods (Lou and Zhou, 2006). Models therefore largely contribute to capturing and predicting the amount of soil CO_2 emissions especially for large areas (Raich and Potter, 1995).

4.3.1 Models of Soil CO_2 Emissions

Basically, there are two types of models used to predict soil CO_2 emissions: (i) empirical models and (ii) process-based models.

Process-based models refer to the trigger mechanisms of soil CO_2 emissions (Luo and Zhou, 2006). They are capable of explaining spatial variation across regions and ecosystems (Lou and Zhou, 2006). Limitations occur according to the understanding of the basic mechanisms and especially for large areas due to higher requirements with regard to input data (Reichstein et al., 2003; Lou and Zhou, 2006).

An empirical model (e.g. by Raich and Schlesinger, 1992; Luo et al., 2005) usually focuses on a strongly reduced number of controlling factors of soil CO_2 emissions lowering the requirements for input data (Luo and Zhou, 2006).

4.3.2 Empirical Models

Various empirical regression models for soil CO_2 emissions have been developed based on field measured soil CO_2 emissions as a function of different biotic and abiotic variables (Table 1, Appendix). Biotic variables incorporated in empirical models are belowground biomass (BGB), vegetation (number of types, area), soil organic matter, leaf area index, litter, net primary production, organic layer thickness, gross primary production (annual), NDVI, and photosynthesis. Abiotic variables in empirical models include climatic varibles such as temperature [air temperature (annual, monthly, weekly, daily), ambient air temperature, soil temperature (matudinal, daily), litter temperature, moss temperature, chamber temperature], temperature sensitivity of soil CO_2 emission rate, maximum depth of respiration, precipitation (annual, monthly, daily, rainfall event), soil moisture, and depth of soil water table. Further abiotic variables used in empirical models are soil water matrix potential, coarse fraction in the soil, soil C (total, labile, refractory), pH value, soil CO_2 concentration, time, age, geographical position, nitrogen, ambient CO_2 concentration and thawed soil thickness. Because of their lower requirements concerning input data, they are highly advantageous for predictions in remote and large areas such as the Qinghai-Tibet Plateau. To date, the majority of studies on soil CO_2 emissions relies on empirical models (e.g. Subke et al., 2006).

4.4 Influence of Climate Change on Soil CO_2 Emissions

Climate change is presumed to be the main reason for the increasing global soil CO_2 emissions to the atmosphere (Jones et al., 2003). However, the climate sensitivity of soil CO_2 emissions is still a matter of debate (Wang et al., 2014a) and has been widely investigated in field studies and laboratory experiments and when modeling ecosystems (Davidson and Janssens, 2006; Tian et al., 2015).

4.4.1 Effect of Temperature Increase

Soil CO_2 emissions generally respond strongly to temperature with emission rates typically increasing with higher temperatures (Raich and Schlesinger 1992; Raich and Potter 1995; Kirschbaum 1995). Hence, in natural ecosystems subjected to experimental warming, soil CO_2 emissions rise in general (Rustad and Fernandez,

1998; Melillo et al., 2002). Given this sensitivity, most biogeochemical models such as the IMAGE model by Rotmans and den Elzen (1993), project a loss of soil C to the atmosphere as consequence of climate change (Schimel et al., 1994; McGuire et al., 1995; Cox et al., 2000). However, the sensitivity of soil CO_2 emissions to warming varies spatially (Luo and Zhou, 2006). Colder ecosystems are more responsive than warm regions (Kirschbaum, 1995). Especially in tundra and boreal ecosystems, soils have lost large amounts of C due to climate warming (Oechel et al., 1995; Goulden et al., 1998). Generally, the response to warming fades at higher temperatures (Luo and Zhou, 2006). The acclimatization, strongly controlled by clay and soil water content, is attributed to changes in the microbial community, alterations in enzymatic reactions (Luo et al., 2001), and faster decomposition that may result in a depleted labile pool of soil C (Kirschbaum, 2004).

4.4.1.1 Response of Heterotrophic Soil CO_2 Emissions

In response to global warming, heterotrophic respiration generally increases due to the stimulation of microbes that decompose exudates and the C-input of roots (Kirschbaum, 1995; Wang et al., 2014a). The increase results from higher biomass and stronger plant growth as consequence of climate warming (Kirschbaum, 1995; Wang et al., 2014a). Particularly in PFS, heterotrophic soil CO_2 emissions strongly increase due to global warming (Schuur et al., 2009). Permafrost (PF) is commonly defined as ground (soil or rock and included ice or organic material) at or below 0 °C for at least two consecutive years. As consequence of cold, water-logged soil conditions, organic matter tends to accumulate in PFS (Harden et al., 1992; Trumbore and Harden, 1997). Thus, warmer temperatures and thawing of PF with the associated lowering of the water table, expose large amounts of soil organic C to microbial breakdown that has been frozen before (Schuur et al., 2009). Although radiocarbon measurements indicate reduced turnover, almost the entire organic matter is part of the labile fractions that decompose fastest under global warming (Chapman and Thurlow, 1998; Lindroth et al., 1998). Consequently, large quantities of soil CO_2 emissions are released from these soils (Schuur et al., 2009). This is confirmed by the results of Oechel et al. (1995), indicating high amounts of soil organic matter lost in tundra soils in consequence of recent climate change in Alaska. Likewise, Goulden et al. (1998) revealed strong soil C losses in a boreal ecosystem in Manitoba (Canada) due to PF thawing in previous warmer years. As much as warming reduces soil moisture, however, microbial activity and thus heterotrophic soil CO_2 emissions

decrease, weakening the positive effect of higher temperatures on heterotrophic soil CO_2 emissions (Harte et al., 1995; Rustad and Fernandez, 1998).

4.4.1.2 Response of Autotrophic Soil CO_2 Emissions

In general, autotrophic soil respiration mostly increases through warming, likely caused by the alteration of various processes (Shaver et al., 2000). Climate warming potentially increases BGB, which in turn increases autotrophic respiration (Kirschbaum, 1995; Wang et al., 2014a). Longer growing seasons (Norby et al., 2003), changes in plant phenology (Dunne et al., 2003), higher plant growth (Wan et al., 2005), changes of species (Saleska et al., 2002), and raising mineralization rates and nitrogen availability in soils (Rustad et al., 2001; Mellilo et al., 2002) are further results of higher temperatures, resulting in higher soil CO_2 emissions. Through warming reduced soil moisture, however, decreases the activity of roots and thus autotrophic soil CO_2 emissions, counterbalancing the positive effect of higher temperatures on autotrophic soil CO_2 emissions (Harte et al., 1995; Rustad and Fernandez, 1998).

4.4.1.3 Feedback Effects of Climate Warming-Induced Soil CO_2 Emissions

Understanding the different responses of autotrophic and heterotrophic respiration to global warming in PFS is particularly important with regard to their potential impact on climate change (Hicks Pries et al., 2013). In general, with respect to the CO_2-induced global warming, only CO_2 derived from soil organic matter contributes to alterations of the CO_2 concentration in the atmosphere (Kuzyankov, 2006).

Autotrophic Respiration

Especially higher C loss through augmented autotrophic respiration is expected to be neutralized in terms of atmospheric CO_2 concentration through an elevated rate of photosynthesis (Schuur et al., 2015). This compensation mainly results from a higher plant uptake of C and its sequestration (Schuur et al., 2015). Higher temperatures, extended growing seasons and a higher concentration of atmospheric CO_2 potentially intensify plant growth (Shaver et al., 2000). Uptaken C can be sequestered in larger above- and belowground biomass (Sistla et al., 2013).

Heterotrophic Respiration

In contrast, higher soil CO_2 emissions resulting from thawing PF are, if at all, only partly offset by this negative feedback to global warming through enhanced soil CO_2 emissions (Schuur et al., 2015). As a result, high quantities of C may be released to the atmosphere (Dutta et al., 2006). Schlesinger and Andrews (2000) conclude that

under the influence of climatic change, soil C loss will be highest in boreal and tundra ecosystems, storing most labile organic matter and being exposed to the strongest predicted warming. Although the rate of CO_2 emissions is highly uncertain, for predictions of the magnitude and temporal occurrence of the effect, it is a crucial question (Schuur et al., 2009). Further, the rate of PFS CO_2 emissions is important for revealing its significance for climate change in the upcoming decades and beyond (Schuur et al., 2009). In fact, there is high confidence about PFS generating more CO_2 under warming (IPCC, 2013). Lately, PFS were estimated to contain more than 1,600 Pg C (Schuur et al., 2008), which is twice the atmospheric CO_2-C pool (Jia et al., 2006). Considering the remarkable C stock of PFS, their considerable climate change-induced degradation (Schaefer et al., 2011) and their original function as C sinks (Hicks Pries et al., 2012), the quantification of future CO_2 emissions from PFS gains high relevance for more comprehensive scenarios on the effect of climate change (Schuur et al., 2009). In fact, the thawing of PF with the decomposition of its C is regarded to bear the highest potential for a positive climate feedback under the influence of climate change from terrestrial ecosystems (Schuur et al., 2009).

4.4.2 Effect of Changes in Precipitation Patterns

Climate change does not only induce higher temperatures but also changes in precipitation patterns (IPCC, 2013). With precipitation as an important controlling factor, especially in xeric ecosystems (Lou and Zhou, 2006), soil CO_2 emissions are affected by global change also through alterations in the characteristics of precipitation (i.e., amount, temporal variability, spatial patterns) (Brevik, 2012). Generally, less precipitation decreases soil CO_2 emissions as reducing soil moisture resulting in lower microbial and root activity (e.g. Harper et al., 2005). Soil CO_2 emissions further react differently to temperature changes depending on precipitation, which is traced back to interactions between soil moisture and temperature (Lou and Zhou, 2006). Higher precipitation resulted in lower temperature sensitivity and vice versa as revealed in a study in Germany by Dörr and Münnich (1987). Through complex interactions, precipitation further influences several controlling factors of soil CO_2 emissions such as vegetation and grazing. As much as precipitation patterns change, also in combination to temperature, biomass productivity is affected (Fan et al., 2010). Consequently, as predicted, more frequent droughts reduce biomass productivity which increases grazing pressure and thus leads to altered soil CO_2 emissions (Cao et al., 2004; Fan et al., 2010). Grazing further influences PF thawing as decreasing

vegetation cover reduces the insulating effect of vegetation, resulting in quicker PF thaw on the Qinghai-Tibet Plateau (Hu et al., 2009) and consequently leading to higher CO_2 emissions induced by PF thaw.

4.4.3 Effect of Elevated CO_2 Concentrations

Soil CO_2 emissions generally increase with elevated atmospheric CO_2 concentrations due to a higher rate of photosynthesis and stimulated plant growth (King et al., 2004). The increased C supply belowground results in higher heterotrophic respiration as decomposition by microbial activity raises (Higgins et al., 2002). Further, as plant transpiration decreases with elevated CO_2, soil moisture increases, resulting in higher soil CO_2 emissions (Davidson et al., 1990).

4.5 Soil CO_2 Emissions on the Qinghai-Tibet Plateau

4.5.1 The Qinghai-Tibet Plateau as Key Region for Soil CO_2 Emissions

The Qinghai-Tibet Plateau is a key region for studies on soil CO_2 emissions under the influence of climate change (Geng et al., 2012). Due to its important role in the global C cycle generally, ecological sensitivity and large PF area (Cheng, 2005; Fan et al., 2010; Geng et al., 2012), it may release large quantities of soil CO_2 to the atmosphere under the influence of climate change, thus potentially amplifying global warming (Qiu, 2008; Ding et al., 2016).

4.5.1.1 Relevance to the Global Carbon Cycle

The Qinghai-Tibet Plateau influences the global C cycle as remarkably contributing to the global C budget (Geng et al., 2012). In its grasslands soils, 33.5 Pg organic C is stored, of which 37% (12.3 Pg C) is contained in the PFS (Luo et al., 2000; Genxu et al., 2002). The PF C pool thus accounts for nearly 1% of the global pool according to Ni (2002). With large amounts of soil CO_2 emissions released from these soils under climate change with no corresponding compensation regarding the atmospheric CO_2 concentration, the Qinghai-Tibet Plateau inheres the potential to accerlerate global warming (Qiu, 2008; Schuur et al., 2009; Ding et al., 2016).

4.5.1.2 Climate Sensitivity

The Qinghai-Tibet Plateau, where human impact is relatively low in general, appears to be highly ecologically sensitive to changes in its environments (Liu and Chen, 2000; Yang et al., 2009; Fan et al., 2010). Therefore, climate warming influences the Qinghai-Tibet Plateau in particular (Zhang et al., 2010). This is mainly due to its extreme elevation, qualifiying it to one of the regions most sensitive to global warming (Luo et

al., 2002; Zhong et al., 2010). In the future, the annual temperature of the plateau is expected to increase far above the global average with about 0.1 °C per decade as opposed to 0.3 °C per decade (Liu and Chen, 2000; Christensen et al., 2007; Qiu, 2008; Wang et al., 2008). The cryosphere, commonly considered the most sensitive indicator to climate change, undergoes rapid changes on the Qinghai-Tibet Plateau (Kang et al., 2010). Its PF increasingly degrades (Böhner and Lehmkuhl, 2005; Qiu, 2008; Baumann et al., 2009; IPCC, 2013). This process has been advancing even more than in other high-latitude, low-altitude PF regions over the last few decades (Yang et al., 2004), revealing the high climate sensitivity of the Qinghai-Tibet Plateau.

4.5.1.3 Prominence of Thawing Permafrost

The Qinghai-Tibet Plateau exhibits the largest high-altitude and low-latitude PF zone on earth with more than half of its total area influenced by PF (Cheng et al., 2005). Given the climate sensitivity of the plateau, the further strong degradation of Tibetan PF (Böhner and Lehmkuhl, 2005) will highly influence its soils mainly by changes in their temperature and moisture patterns (Zhang et al., 2003; Doerfer et al., 2013). Thus, global warming affects PF stability and distribution as well as vegetation and soil characteristics that intensively interact with soil CO_2 emissions through complex processes (Chapin et al., 2005). Large quantities of soil CO_2 emissions are expected to be released from thawed PF (Schuur et al., 2009; see Section 4.4.1.1). The degradation of PF on the Qinghai-Tibet Plateau on a large scale is generally expected to potentially exacerbate climate warming by its CO_2 emissions (Qiu, 2008; Ding et al., 2016).

4.5.2 Key Controlling Factors of Soil CO_2 Emissions

For the Qinghai-Tibet Plateau, almost two-thirds of which is covered by grassland (Wang et al., 2006; Yang et al., 2008), BGB has been shown to most strongly influence soil CO_2 emissions in grassland ecosystems at a regional scale due to the high root biomass density (Geng et al., 2012). In general, temperature and precipitation are widely considered as most effectively representing soil CO_2 emission variation in time and space (Bond-Lamberty and Thomson, 2010a; Hashimoto et al., 2015). For arid and semiarid areas that are characteristic for the PF-affected part of the plateau (Chapter 5), precipitation represents the most important predictor (Lou and Zhou, 2006). For regional scales, precipitation also serves as an important predictor (Lou and Zhou, 2006). BGB, the most important controlling factor for soil CO_2 emissions, is particularly related to elevation on the Qinghai-Tibet Plateau (Ohtsuka et al., 2008).

Precipitation and temperature are also assumed to predict the amount of root biomass for the Qinghai-Tibet Plateau well (Luo et al., 2005). Generally, however, little knowledge exists about biotic and abiotic factors that influence BGB (Vogt et al., 1996; Cairns et al., 1997), and there are no process-based models yet for its prediction. A very common approach to calculate BGB is using root:shoot ratios (e.g. Schroeder and Winjum, 1995, Eamus et al., 2002, Mokany et al., 2006). However, Cairns et al. (1997) concluded from their analysis of forests worldwide that the amount of root biomass is better estimated directly without the application of root:shoot ratios. Empirical models are, however, also based on aboveground biomass but further on diameter at breast height, inside and outside bark basal diameter, basal diameter in combination with the total height, aboveground biomass combined with the annual leaf growth rate, annual stem growth rate and annual root growth rate. Other regression models involve climatic variables as input parameter such as mean annual temperature (MAT), mean annual precipitation (MAP), January mean temperature and July mean temperature. Elevation as abiotic input factor is also used as base of a regression model (Table 2, Appendix).

4.5.3 Data Relevant to Quantifying Soil CO_2 Emissions

Data on soil CO_2 emissions collected in field measurements generally require high efforts of time and cost (Lou and Zhou, 2006). An area-explicit coverage of data sampling is unfeasible in view of the Qinghai-Tibet Plateau´s area (Sections 6.1.1 and 6.1.6). Even the identification and sampling of representative sites remain an expensive and tedious endeavor still tainted with concomitant uncertainties due to deficient regionalization and/or upscaling techniques. The input parameters of models require highly resoluted, area covering data sets, why an indirect quantification of soil CO_2 emissions can likewise result in high cost efforts. Generally, data for that region at a required spatial resolution are scarce due to the inaccessible and complex terrain (Liu and Chen, 2000; Wang et al., 2006). Various data sets lack of a fine (about 1 km^2) resolution that captures spatial environmental variability appropriately (e.g. ERA-Interim (Dee et al., 2014); APHRODITE (Yatagai et al., 2012)). Others are not spatially comprehensive, existent, available or highly cost-intensive (Sanchez et al., 2009; Hertel et al., 2010). On the other hand, several freely available global databases exist for selected environmental variables. They are often highly (about 1 km^2) resoluted and developed through the harmonization of different data sets with elaborated methods (e.g. WISE30sec data set (Batjes, 2015)). These data sets enable calculations on a regional scale as e.g. for the Qinghai-Tibet Plateau and allow for

reasonable interpretations of results from empirical models. Above all, as saving time and costs, they contribute to a high efficiency when answering research questions. This is particularly important if those research topics are connected to issues of worldwide, societal concern requiring action in a timely manner as e.g. climate change (IPCC, 2013). For area-explicit calculations on a regional scale as for the Qinghai-Tibet Plateau, they are, therefore, highly advantageous.

5 Objectives

This thesis aims at a quantification of soil CO_2 emissions under the influence of climate change on the Qinghai-Tibet Plateau.

Since quantifying soil CO_2 emissions, particularly on the Qinghai-Tibet Plateau, requires high efforts of time and costs as opposed to results needed in a timely manner (Section 4.5.3), this thesis further attempts to demonstrate an efficient approach to reasonably quantify soil CO_2 emissions on a regional scale. Hence, exclusively freely available data are used.

BGB represents a key influencing factor of soil CO_2 emissions on the Qinghai-Tibet Plateau (Section 4.5.2). To date however, no area-covering data set yet exists (Section 4.5.3). Therefore, in a first step, BGB is area-explicitly estimated by investigating the optimal empirical model for the quantification of this important C source *(Manuscript 1)*.

To apply the most adequate regression model when projecting future scenarios of general soil CO_2 emissions, this thesis further aims at the identification of the 'best-fit' model to quantify soil CO_2 emissions on the Qinghai-Tibet Plateau under current climatic conditions *(Manuscript 2)*.

The main objective is to assess potential soil CO_2 emissions from the Qinghai-Tibet Plateau. In order to consider the influence of future climate change, two scenarios of global warming are applied to project future soil CO_2 emissions. These scenarios are calculated for 2050 and 2070 as commonly used scenarios (e.g. in the IPCC, 2013) and for comparability to other studies that focus on the current century (Chapter 7). Moreover, soil CO_2 emissions potentially providing a positive climate feedback, are assumed to be felt over decades to centuries (Schuur et al., 2015). Since the large area of PFS inheres the highest potential for soil CO_2 emissions to increase atmospheric CO_2 concentrations without a corresponding compensation (Section 4.4.1.3), the study area comprises PF areas, focusing on continuous and extensive discontinuous PF as areas spatially dominated by PF.

The prominence of PF on the Qinghai-Tibet Plateau and its high importance for soil CO_2 emissions influenced by global warming (Sections 4.4.1.1 and 4.5.1.3), necessiate an additional calculation of soil CO_2 emissions induced by PF thaw owing to a lack of region-specific models. Hence, soil CO_2 emissions specifically induced by thawing PF and general soil CO_2 emissions are quantified separately *(Manuscript 3)*.

Prerequisite of a calculation of thawing-induced soil CO_2 emissions is the estimation of C stocks on the Qinghai-Tibet Plateau *(Manuscript 3)*.

In quantifying soil CO_2 emissions for the Qinghai-Tibet Plateau under the influence of climate change, this thesis addresses the following objectives:

(i) Identification of the most suitable, respectively, 'best-fit' regression model to quantify BGB as region-specific, important input factor to calculate soil CO_2 emissions *(Manuscript 1)*,

(ii) Identification of the most suitable, respectively, 'best-fit' regression model to quantify general soil CO_2 emissions *(Manuscript 2)*,

(iii) Estimation of soil organic C stocks to quantify thawing-induced soil CO_2 emissions *(Manuscript 3)*,

(iv) Quantification of potential soil CO_2 emissions induced by the thawing of PF due to global warming for 2050 and 2070 *(Manuscript 3)*, and

(v) Quantification of potential general and total soil CO_2 emissions under scenarios of climate change in 2050 and 2070 *(Manuscript 3)*.

(vi) Finally, the present thesis aims at providing information on an areawide future soil C loss under climate change scenarios. Moreover, the results are supposed to further support in identifying potential sources and sinks of C and in an enhanced understanding of the role of the PF C on the Qinghai-Tibet Plateau in the global C cycle in view of and under the influence of climate change.

6 Material and Methods

6.1 Study area

6.1.1 Geographical Position

The study area is on the Qinghai-Tibet Plateau, located in southwestern China. The plateau extends from 26°00′12" N to 39°46′50" N and from 73°18′52" E to 104°46′59" E with a maximum E-W distance of approximately 2,945 km and a maximum S-N distance of approximately 1,532 km. The altitude of the highest and youngest plateau worldwide amounts to 4,380 m on average. Its area extends to about 2.6 $\times 10^6$ km^2 (Zhang et al., 2002).

6.1.2 Geomorphology and its Effects on Climate

The Qinghai-Tibetan Plateau strongly influences the Asian Monsoon, representing an origin of a temperature anomaly for the mid-troposphere (Smith and Shi, 1995). Mountain ranges from east to west prevent moist air from the tropical Indian monsoonal system to reach the plateau (Domrös and Peng, 1988). In the north, the Kunlun Shan borders the plateau, continuing in the east as Bayan Har Shan from northwest to southeast (Hövermann and Lehmkuhl, 1994). The eastern part of the plateau is geomorphologically characterized by pronounced valleys of e.g. the Yangtze River (Weischet and Endlicher, 2000). Dividing the plateau in cold, arid northwestern highlands and a warm, moist southeast, the Transhimalaja is of climatic importance. Warm, moist airmasses from the subtropical East Asian monsoonal systems reach the plateau through the lowlands in the east (Weischet and Endlicher, 2000).

6.1.3 Climate

The unique geographical position of the Qinghai-Tibet Plateau prevails an azonal, plateau climate (Zhong et al., 2010; Zhuang et al., 2010) with strong solar radiation, low air temperature, large daily temperature variations and low differences between average annual temperatures (Zhong et al., 2010). Generally, a decrease both in temperature and in precipitation from the south-eastern to the north-western part of the plateau is apparent (Immerzeel et al., 2005), indicating the decreasing intensity of the East Asian monsoon (Harris, 2006). For the plateau, the average temperature of July, as warmest month, varies from 7 °C to 15 °C and from -1 °C to -7 °C in January, as coldest month. Average annual temperature is 1.6 °C (Yang et al., 2009). Precipitation amounts to about 413.6 mm a year (Yang et al., 2009), with more than 60 to 90% falling

in the wet and humid summer months (June to September) and 10% at maximum in the cool, arid winters (November to February) (Xu et al., 2008).

6.1.4 Vegetation

The topographic setting as well as atmospheric conditions determine the sequence of alpine meadows, steppes and deserts from southeast to northwest (Zheng, 1996; Pei et al., 2009). Alpine steppes and meadows dominate the undisturbed vegetation, with *Stipa species* respectively *Kobresia meadows* as major vegetation types. *Kobresia meadows* are the most wide-spread vegetation with mostly *Kobresia pygmea* and *K. tibetica* as perennial tussock grasses (Chang, 1981; Zhou et al., 2005). Most prevalent are *Stipa purpurea* and *Stipa subsessiliflora* as short and dense tussock grasses in the alpine steppe (Chang, 1981). Wetlands are dominated by *Kobresia littledalei*, *Carex lanceolata* and *Carex muliensis* (Chang, 1981). According to the long freezing periods, relatively short growing seasons characterize the plateau`s climate (Yu et al., 2010). Its vegetation is regarded as relatively natural (Schroeder and Winjum, 1995).

6.1.5 Soils

Complex pedogenetic processes on the Qinghai-Tibet Plateau, mainly solifluction, soil erosion and sedimentation of aeolian material, typically result in young and highly diverse soils with distinct degradation characteristics, exhibiting a strong influence by PF regimes (Baumann et al., 2014). Fluvial erosion and alluviums as degradation features particularly occur during the summer in the east due to high precipitation (Baumann et al., 2014). Soils affected by the dry winter monsoon with scarce vegetation are characterized by aeolian erosion and deposition (Xue et al., 2009; Dietze et al., 2012) and hence buried, relict, mainly humic horizons (Lehmkuhl, 1997). Leptosols, Leptic Cambisols, Haplic Regosols and Mollic Cryosols as poorly developed soils dominate steeply sloping areas. Gleysols and Gleyic Fluvisols mostly occur close to open waterbodies and in geomorphological depressions (Kaiser et al., 2007). In continuous PF, Gelic Gleysols, Gelic Cambisols, Cambic Cryosols and Permagelic/Gelic Histosols prevail. In discontinuous and sporadic PF areas, Cambisols are present (IUSS Working Group WRB, 2006). Felty topsoils typically dominate cold alpine meadows (Kaiser et al., 2008).

6.1.6 Permafrost

On this plateau, earth´s largest high-altitude and low-latitude PF zone is located (Cheng, 2005). Covering about 1.050 × 10^6 km^2, the PF zone is mainly part of the southwestern and central plateau (Figure 1).

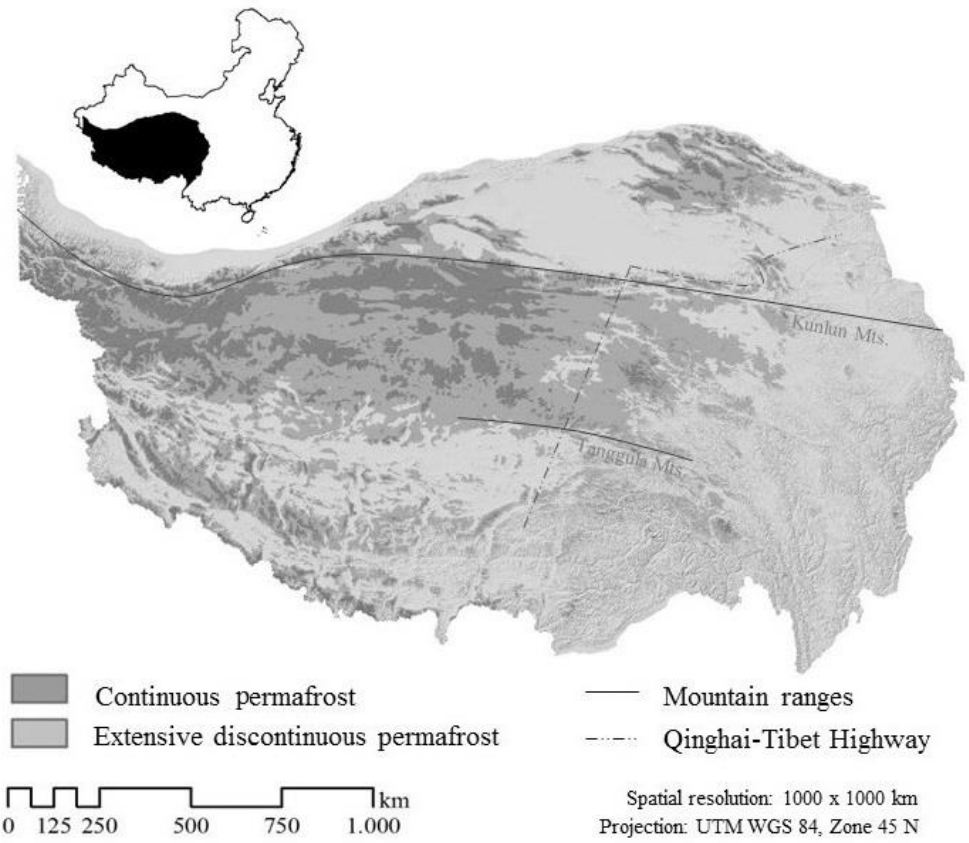

Fig. 1. Spatial extension of continuous and extensive discontinuous permafrost on the Qinghai-Tibet Plateau. The spatial resolution of the grids is 1,000 m x 1,000 m.

Overall, more than half of its area is influenced by PF (Cheng, 2005). Continuous PF mostly occurs in the interior and western Qinghai-Tibet Plateau, extending to the south of the Kunlun Mountains. Boundaries of the PF zone in the south are the Tanggula Mountains, merely dividing the plateau in half, and the 94 ° longitude in the east (Hövermann and Lehmkuhl, 1994; Cheng et al., 2013). In this central- western part, the PF is ice-poor (Jin et al., 2000), reflecting the fading impact of both monsoons. Continuous PF southernly occurs exclusively in mountainous regions higher than 4,600 – 4,700 m a.s.l. (Hövermann and Lehmkuhl, 1994). Thermokarst forming with water accumulation results from the degradation of PF (Niu et al., 2011). Discontinuous PF can be found in the northern, southern, and eastern regions on the Qinghai-Tibet

Plateau with more pronounced terrain. Here, the ground seasonally freezes and shows sporadic PF with taliks (Figure 2) (Jin et al., 2000; Cheng et al., 2013).

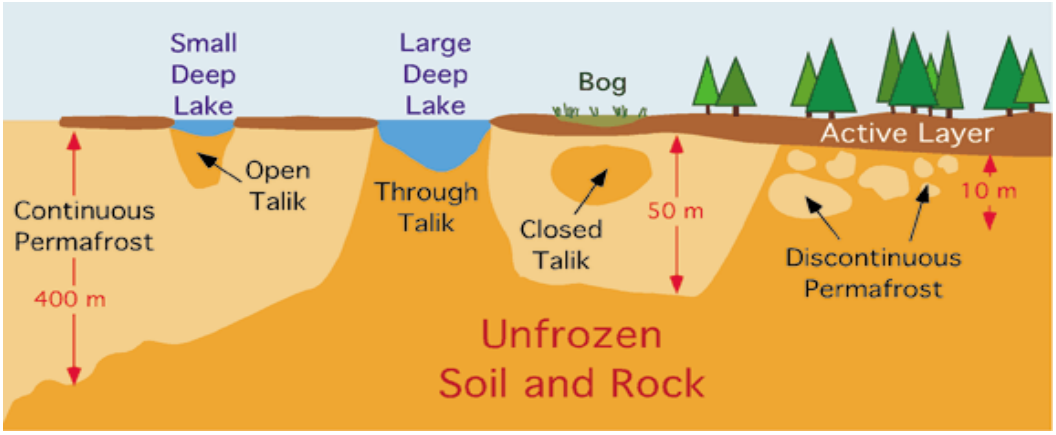

Fig. 2. Cross-sectional area of transition between continuous and discontinuous permafrost (Pidwirny, 2006).

Along the Qinghai-Tibet Highway, the PF zones stretches with a length of 550 km from north to south (Wang et al., 2006). On average, the active layer thickness amounts from 1 to 2 m in the zone of continuous PF, generally increasing along a north to south gradient and with elevation (Cheng and Wu, 2007). Daily freeze-thaw cycles frequently occur due to high temperature differences between days and nights from 25 to 40 °C (Ping et al., 2004).

6.2 Geodatabase and Processing

In this thesis, different freely available data sets were used, which were selected in terms of a fine spatial resolution (about 1,000 m x 1,000 m), area coverage, importance of the variable for the phenomenon to be modeled, and the existence of a corresponding model. All data sets were projected into the Universal Transverse Mercator coordinate system WGS 1984, Zone 45 N and exhibit a resolution of 1,000 m x 1,000 m.

Considering Manuscript 1 [objective (i)], the required data sets for recent MAP, MAT, July mean temperature, January mean temperature were obtained from the WorldClim data sets (Hijmans et al., 2005). They were compiled from a considerable number of various sources, such as the Global Historical Climate Network, World Meteorological Organization and the Food and Agricultural Organization, representing the current climate conditions from circa 1950 to 2000. Data from more than 71,000 climate stations worldwide recording for precipitation, and more than 45,000 climate stations

recording for temperature are integrated, with the Qinghai-Tibet Plateau as area with less densely distributed measurement points. Latitude, longitude and altitude served as independent variables (for more detailed information see Hijmans et al., 2005).

Elevation data were used from the Shuttle Radar Topography Mission, obtained from the WorldClim data sets (Hijmans et al., 2005).

To estimate recent soil CO_2 emissions [objective (ii)], the data sets for MAP and MAT from the WorldClim data sets were used. According to the results of Manuscript 1, the BGB data set based on MAT was used as input parameter.

To estimate organic C stocks [objective (iii)], the data sets for organic C content, gravel content and bulk density were obtained from the WISE30sec data set (Batjes, 2015) with a spatial resolution of 1,000 m x 1,000 m up to a soil depth of 2 m. This was compiled from different sources, such as the Harmonized World Soil Database, version 1.21 with marginal corrections, a climate zones map (Köppen-Geiger) used as co-variate and soil property estimations based on the ISRIC-WISE soil profile database. Soil properties were estimated based on statistical analyses of about 21,000 soil profiles. This was undertaken using an elaborate system of taxonomy-based transfer rules combined with expert-rules, which assess the consistency of the predictions within the pedons. WISE30sec is generally regarded as being appropriate for exploratory assessments at a resolution of 1,000 m x 1,000 m (for more detailed information see Batjes, 2015).

Considering objective (iv), the data sets for MAP in 2050 and 2070 under different scenarios of climate change originate from the WorldClim data sets as well. For 2050 and 2070, representing the average of modeled climate conditions from 2041 – 2060 and 2061 – 2080, respectively, there are four climate scenarios. The projections from ‘Community Climate System Model Version 4’ as one of the most common and current global climate models that is employed in the Fifth Assessment IPCC report as well, are used. The model, developed in international collaboration, is a coupled model combining four separate models that simulate the sea-ice, the atmosphere, oceans and land surface of the earth, and a fifth component that allows for an exchange of fluxes between these models. It is regarded to provide realistic simulations of the earth´s climate system at a resolution of 1,000 m x 1,000 m with reasonable fidelity (for more details see Gent et al., 2011). The four scenarios are projected by the global climate model for four different representative concentration pathways (RCPs) with a

spatial resolution of 1,000 m x 1,000 m (van Vuuren et al., 2011). The RCPs each describe different climate scenarios that are regarded being possible depending on future amounts of greenhouse gas emissions, land use change and air pollutants, covering a wide range of scenarios presented in the existing literature. They incorporate various different technological, political, social and economic futures influencing climate change. Each RCP has been developed under the usage of a different model. For RCP2.6, greenhouse gas emissions are assumed to be very low, for RCP4.5 medium-low, for RCP6.0 medium, and RCP8.5 is seen as high emission scenario. Air pollution is assumed to be medium-low for RCP2.6, medium for RCP4.5 and RCP6.0, and medium-high for RCP8.5. Data were harmonized, downscaled or converted using e. g. a carbon-cycle climate model or atmospheric chemistry model for emission data to be transformed into concentration data (for more details see van Vuuren et al., 2011 and for basic statistics on current MAP and MAP in 2050 and 2070 under the different scenarios see Table 3).

Table 3. Statistics on input data sets on MAP (mm) based on WorldClim data sets (Hijmans et al., 2005).

Year ***Scenario***	**2015**	**2050** ***RCP2.6***	**2050** ***RCP4.5***	**2050** ***RCP6.0***	**2050** ***RCP8.5***	**2070** ***RCP2.6***	**2070** ***RCP4.5***	**2070** ***RCP6.0***	**2070** ***RCP8.5***
					[mm]				
Mean	222.05	232.49	235.13	233.69	241.79	231.78	234.98	235.36	243.44
Min	32.36	35.36	34.58	35.08	35.44	34.40	33.36	35.40	36.40
Max	1237.18	1291.94	1287.11	1261.01	1243.34	1295.14	1338.14	1247.18	1303.71
Range	1204.82	1256.58	1252.53	1225.93	1207.9	1260.74	234.98	1211.78	1267.31
SD	137.67	143.70	145.73	144.207	148.66	143.81	147.32	145.33	151.12

Data for determining the extension of the PF zone of the Qinghai-Tibet Plateau were obtained from the Global PF Zonation Index Map (Gruber, 2012). The model underlying this map is based on established relationships between air temperature and occurring PF, which have been transformed into this model. Its parametrization has been undertaken based on published approximations. Air temperature and elevation represent the input parameters for the model. The input data to derive the modeled spatial PF extension are based on various climatic and physical-geographic data sets such as NCEP30 and SRTM30. PF extension classes used in the data are: continuous PF (90–100%), extensive discontinuous PF (50–90%), sporadic discontinuous PF (10–50%) and isolated patches (smaller than 10%) (for more details see Gruber, 2012).

6.3 Belowground Biomass Calculation and Model Evaluation

BGB was calculated using six empirical regression models developed by Luo et al. (2005) (Table 4). In the BGB samples, living and dead roots are included.

Table 4. Regression models to approximate belowground biomass by Luo et al. (2005) from Tibet.

Regression based on	Equation	Parameters
January mean temperature *x*	$y = 200/(1 + \exp(-0.1434x + 1.0789))$	*y* = root biomass density (Mg/ha), *x* = January mean temperature (°C)
July mean temperature *x*	$y = 200/(1 + \exp(-0.2245x + 4.6125))$	*y* = root biomass density (Mg/ha), *x* = July mean temperature (°C)
Annual mean temperature *x*	$y = 200/(1 + \exp(-0.1750x + 2.5543))$	*y* = root biomass density (Mg/ha), *x* = annual mean temperature (°C)
Annual precipitation *x*	$y = 200/(1 + \exp(-2.14E - 06x^2 - 0.00575x + 4.78))$	*y* = root biomass density (Mg/ha), *x* = annual precipitation (mm)
Annual mean temperature and annual precipitation *x*	$y = 200/(1 + \exp(-0.0001594x + 2.5869))$	*y* = root biomass density (Mg/ha), *x* = annual mean temperature x annual precipitation (°C x mm)
Altitude *x*	$y = -0.0209x + 104.89$	*y* = root biomass density (Mg/ha), *x* = altitude (m)

The ability of the models to predict BGB was investigated by a validation of the results with field measured results from other studies. The samples were taken by Luo et al. (2005), Yan et al. (2005), Wang et al. (2008), Yang et al. (2009), Li et al. (2011), Wu et al. (2011) and Geng et al. (2012) and are located in nine different vegetation types: Alpine steppe, alpine shrubs and meadows, desert grassland, dry valley forests, subtropical forests, alpine mixed forests, alpine spruce forests, timberline zone, and alpine desert covering altitudes from 1,900 m to 5,105 m a.s.l. (Figure 3). Not displayed in Figure 3 are the sites of Yan et al. (2005), who sampled in the central and northern central part, and Wu et al. (2011) (northeastern part).

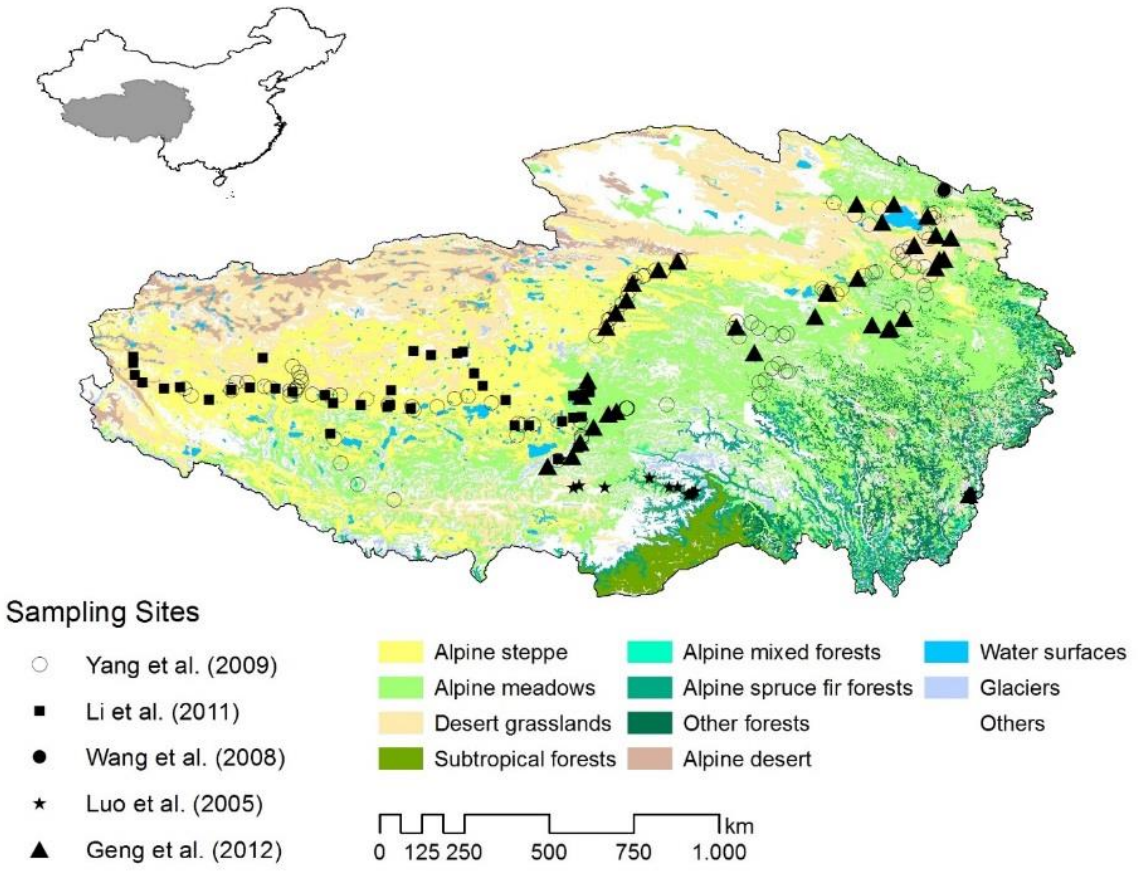

Fig. 3. Vegetation map of the Qinghai-Tibet Plateau based on data sets for Land Cover in Tibet with belowground biomass sampling localities of Luo et al. (2005), Wang et al. (2008), Yang et al. (2009), Li et al. (2011), and Geng et al. (2012) (Tibetan and Himalayan Library, 2002).

To account for the strong influence of vegetation type on BGB, ranges were compared for each vegetation zone. The ranges for the vegetation zones comprise those calculated grid pixel values that correspond to the precise geographical coordinates from the sampling sites of the literature data in the respective vegetation zone. Due to a lack of precise spatial information on the sites of Yan et al. (2005) and Wu et al. (2011), only the minima and maxima for the respective vegetation types could be considered. For the overall range of all field measured BGB values from all studies, all area-wide calculated BGB values for the whole plateau are compared to all field measured values, demonstrating variation. To allow for a direct point-to-point comparison, mean relative errors were calculated.

6.4 Calculation of Recent General Soil CO_2 Emissions and Model Evaluation

Soil CO_2 emissions were calculated using six different regression models (Table 5).

Table 5. Regression models based on MAT, MAP and BGB to approximate soil CO_2 emissions by Raich and Schlesinger (1992), Chimner (2004) and Behera et al. (1990).

Type of regression	Region, vegetation type	Equation	Parameters	Author(s)	r^2
Regression based on MAT *T*	Global	$SR = 25.6T + 300$	*SR* = annual SR rate (g C/m^2/yr), *T* = MAT (°C),	Raich and Schlesinger (1992) (MAT I)	0.42
	Micronesia and Hawaii, peatlands	$Y = 265.9 + (27.7 * MAT)$	*Y* = annual SR rate (g C m^{-2} yr^{-1}), *MAT* = MAT (°C)	Chimner (2004) (MAT II)	0.46
Regression based on MAP *P*	Global	$SR = 0.391P + 155$	*SR* = annual SR rate (gC/m^2/yr), *P* = MAP (mm)	Raich and Schlesinger (1992)	0.34
Regression based on MAT *T*, MAP *P*	Global	$SR = (9.26T) + (0.0127TP) + 289$	*SR* = annual SR rate (gC/m^2/yr), *T* = MAT (°C), *P* = MAP (mm)	Raich and Schlesinger (1992) (MATP I)	0.50
	Global	$SR = (9.88T) + (0.0344P) + (0.0112TP) + 268$	*SR* = annual SR rate (gC/m^2/yr), *T* = MAT (°C), *P* = MAP (mm)	Raich and Schlesinger (1992) (MATP II)	0.50
Regression based on root biomass	India, tropical forest soil	$y = 0.32x + 176.6$	*y* = SR (mg CO_2 m^{-2} h^{-1}), *x* = total root biomass (g m^{-2})	Behera et al. (1990)	0.89

To evaluate the power of the regression models applied in this study, the calculated values were compared to those reported by Cao et al. (2004), Zhang et al. (2005), Li et al. (2011), Zhang et al. (2009), Geng et al. (2012), Chen et al. (2014) and Wang et al. (2014b) (Tab. 2). The observation sites are located in three different vegetation types: alpine steppe, alpine meadows, and forest on altitudes from 3,000 m to 5,105 m a.s.l.. The sampling sites in the study from Chen et al. (2014), located in the eastern part of the plateau, are not displayed in Figure 4.

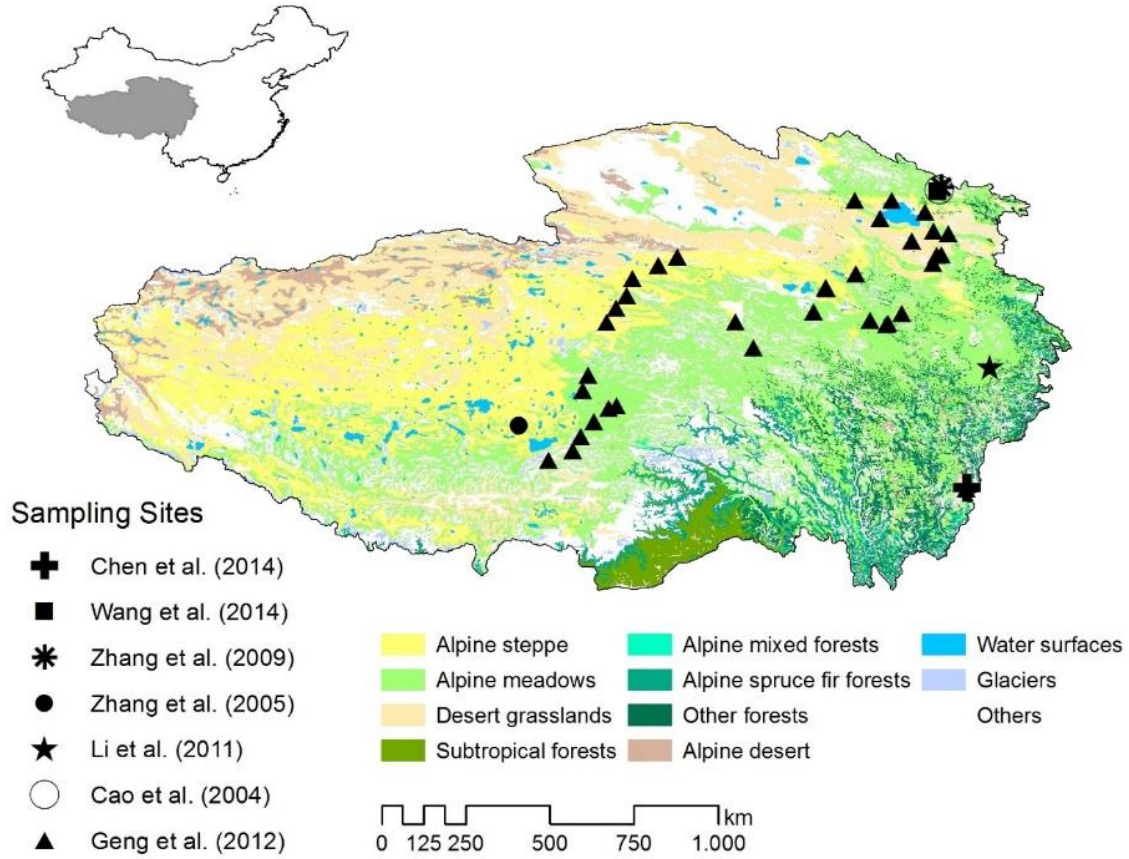

Fig. 4. Vegetation map of the Qinghai-Tibet Plateau based on data sets for land cover in Tibet with soil CO_2 emissions sampling localities of Cao et al. (2004), Zhang et al. (2005), Li et al. (2011), Zhang et al. (2009), Geng et al. (2012), and Wang et al. (2014b) (Tibetan and Himalayan Library, 2002).

All samples except the ones from the studies of Chen et al. (2014) and Wang et al. (2014b) were collected in the peak season of soil CO_2 emissions from June to August. Daily means were calculated based on several measurements per day in each study. To compare annual data calculated by the regression models, daily means were summed up to give annual soil CO_2 emissions values. However, this leads to a systematic overestimation of annual soil CO_2 emissions, because the daily means were estimated based on measurements during peak season months. A seasonality correction factor was therefore developed and implemented to account for this. This seasonality correction factor is based on calculations by Cao et al. (2004). The annual total sum of daily average soil CO_2 emission values is about 1.99 times higher than the estimation of annual soil CO_2 emission values where seasonal variation of soil CO_2 emissions is considered. Accordingly, all cumulative annual soil CO_2 emission values were corrected by a factor of 0.33 exept for the evaluation data from Chen et al. (2014) and Wang et al. (2014b) as provided as annual values a priori. The data of Chen et al. (2014) are based on measurements every ten days throughout an entire year after

having conducted extra measurements to find the optimal measurement time representing daily means. Wang et al. (2014b) summed daily means based on hourly measurements throughout four years to calculate annual estimates, which were averaged to one annual average value.

Ranges of the model-based soil CO_2 emission values of each vegetation zone are based on grid pixels according to the geographical coordinates from the field sampling sites of the literature data. Since information on precise georeferences was not given in Chen et al. (2014), personal communication with Ji Luo (2015) served as an additional source of information on the exact geographical position. The range of all field measurements throughout the different vegetation zones was compared to all calculated values of the whole plateau for each model. Moreover, the average of all field data to the average of all calculated soil CO_2 emission values for the whole plateau was compared for each model.

6.5 Calculation of Future Soil CO_2 Emissions

The calculation of future soil CO_2 emissions under the influence of climate change consists of two parts: (i) General soil CO_2 emission rates for the Qinghai-Tibet Plateau and (ii) specific soil CO_2 emission rates, that focus on the additional source of C made available by PF thaw on the Qinghai-Tibet Plateau in consequence of global warming. To obtain total future soil CO_2 emissions both parts were summed up.

General soil CO_2 emissions as one part were calculated using the regression model by Raich and Schlesinger (1992) based on MAP for each scenario in 2050 and 2070.

The second part of the total soil CO_2 emissions, the thawing-induced soil CO_2 emissions, are based on estimates from a synthesis of laboratory experiments. As there is no formulated regression model yet, results of incubation experiments with soil samples from the arctic region by Schaedel et al. (2014) were transferred to the study area in structural analogy to regression models. On average, 23.1% of the organic C can potentially be lost within 50 incubation years through PF thawing at a temperature of 5 °C, which corresponds to approximately 0.012‰ per day on average (Schaedel et al., 2014). As average from 1960 to 2000, 166 frost-free days per year occur on the Qinghai-Tibet Plateau and additional 3.1 days per further decade because of global warming (Zhang et al., 2014). Thus, the potential organic C loss from 2015 to 2050 amounts to 7.78% and to 12.45% until 2070 of the organic C stock in 2015. On average, the potential C loss from 2015 to 2050 is hence 0.222% per year and from

2015 to 2070 0.226% per year as result of thawing PF. The respecitve amounts of the CO_2 equivalents of the C loss were calculated based on the mass fraction of C present in CO_2.

C stocks for the estimation of thawing-induced soil CO_2 emissions for *k* layers were estimated as follows:

$$T_d = \sum_{i=1}^{k} \rho_i P_i D_i (1 - S_i), \quad (1)$$

where T_d is the total amount of organic C (Mg m^{-2}) over depth *d*, ρ_i is bulk density (Mg m^{-3}) of the layer *i*, P_i equals the proportion of organic C in layer *i* (g C g^{-1}), D_i is the thickness of this layer (m), and S_i is the volume of coarse fragments (> 2 mm) (Batjes, 1996). The proportion of thawing-induced CO_2 emissions to total CO_2 emissions was obtained as ratio for each year. To calculate this, means of total CO_2 emissions of all scenarios were averaged for each year.

7 Results

7.1 Total Soil CO_2 Emissions

7.1.1 Total Soil CO_2 Emissions in 2015 and 2050

Total soil CO_2 emissions from PFS of the Qinghai-Tibet Plateau generally increase by 2050 compared to 2015 (see Table 6 and Figure 6). Mean total CO_2 emissions in 2050 add up to 1,420.22 – 1,433.46 g CO_2 m^{-2} $year^{-1}$ (RCP2.6 and RCP8.5, respectively) as opposed to 1,415.59 g CO_2 m^{-2} in 2015. The difference between the lowest and highest mean CO_2 emission rates of the four scenarios is hence less than 1%. Differences in the minima and maxima of the different scenarios are likewise small as ranging from 737.90 g CO_2 m^{-2} $year^{-1}$ (RCP4.5) to 739.13 g CO_2 m^{-2} $year^{-1}$ (RCP8.5) (minima) and between 4,188.95 g CO_2 m^{-2} $year^{-1}$ (RCP2.6) and 4,224.77 g CO_2 m^{-2} $year^{-1}$ (RCP8.5) (maxima). In all scenarios, more values exceed the respective averages as reflected by the median values from 1,254.03 g CO_2 m^{-2} $year^{-1}$ (RCP6.0) to 1,267.53 g CO_2 m^{-2} $year^{-1}$ (RCP8.5). The mean of the thawing-induced CO_2 emissions adds up to 36.47% of the averaged means of the total CO_2 emissions.

Table 6: Statistics of total soil CO_2 emissions in 2015 and 2050 in g CO_2 m^{-2} $year^{-1}$.

Year (Scenario)	***2015 (Bosch et al. (2016))***	**2050 (RCP2.6)**	**2050 (RCP4.5)**	**2050 (RCP6.0)**	**2050 (RCP8.5)**
	g CO_2 m^{-2} $year^{-1}$				
Mean	*1,415.59*	1,420.22	1,423.87	1,421.76	1,433.46
Min	*737.08*	739.02	737.90	738.62	739.13
Max	*4,224.34*	4,188.95	4,190.54	4,195.69	4,244.77
Median	*1,246.86*	1,255.98	1,260.37	1,254.03	1,267.53

Highest decreases in total CO_2 emissions compared to the total CO_2 emissions in 2015 are located in the central part of the plateau (Figure 5).

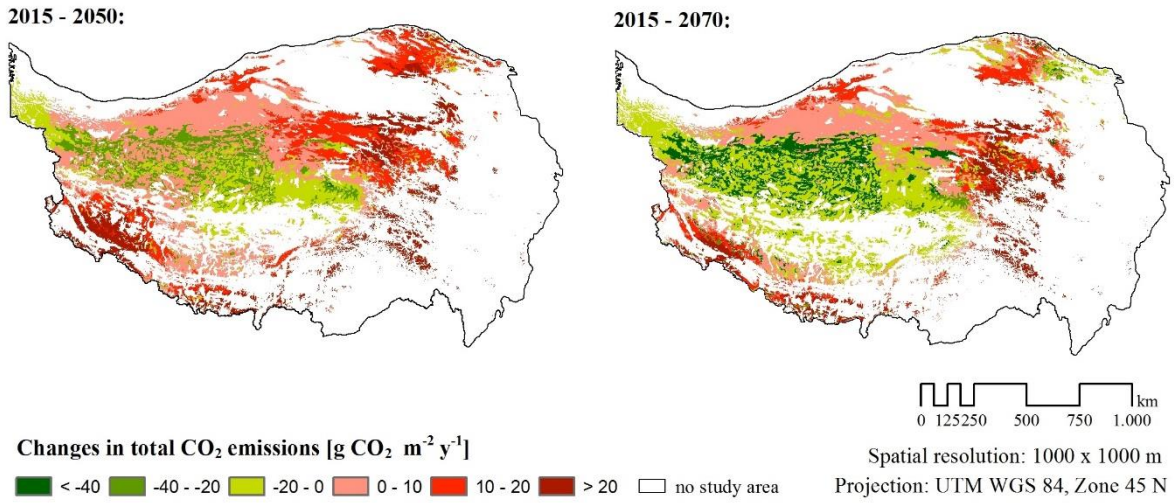

Fig. 5. Spatial distribution of absolute differences in total potential CO_2 emissions from permafrost areas on the Qinghai-Tibet Plateau between 2015 and 2050 and between 2015 and 2070 according to the RCP2.6 scenarios. Unit of changes in total CO_2 emissions is g CO_2 m^{-2} $year^{-1}$. The spatial resolution of the grids is 1000 m x 1000 m.

For all scenarios, about 70% of the CO_2 values amount to less than 1,000 g CO_2 m^{-2} (Table 7). In the highest class (>3664.21 g CO_2 m^{-2} y^{-1}), only 1 ‰ of the values appears, which corresponds to an area of 976–979 m^2. Differences between the scenarios with regard to the abundance of CO_2 values show to be less than 1% but can amount to an additional release of soil CO_2 of about 40,000,000 g CO_2 for an area of about 8,000 m^2.

Table 7: Abundance of CO_2 emission values per class of CO_2 emissions for the Qinghai-Tibet Plateau. CO_2 emission classes represent very low (>0 – 250 g C m^{-2} $year^{-1}$ / >0 – 916.05 g CO_2 m^{-2} $year^{-1}$), low (>250 – 500 g C m^{-2} $year^{-1}$ / >916.05 – 1832.10 g CO_2 m^{-2} $year^{-1}$), medium (>1832.10 g CO_2 m^{-2} $year^{-1}$ – 3664.21 g CO_2 m^{-2} $year^{-1}$ / >500 – 1000 g C m^{-2} $year^{-1}$), high (>3664.21 g CO_2 m^{-2} $year^{-1}$ / >1000 g C m^{-2} $year^{-1}$) and no (≤0 g CO_2 m^{-2} $year^{-1}$ / ≤0 g C m^{-2} $year^{-1}$) CO_2 emissions. Italicized values specify the area on the Qinghai-Tibet Plateau assigned to the respective CO_2 emission class.

Classes	**Scenario**	**RCP2.6**		**RCP4.5**		**RCP6.0**		**RCP8.5**	
	Year	**2050**	**2070**	**2050**	**2070**	**2050**	**2070**	**2050**	**2070**
		% *m^2*							
Very low		13.27 *135 902*	13.50 *138 276*	13.29 *136 118*	13.50 *138 286*	12.72 *130 224*	13.06 *133 737*	12.21 *125 037*	12.99 *132 997*
Low		69.25 *708 955*	69.18 *708 160*	69.13 *707 685*	69.00 *709 400*	69.74 *713 895*	69.57 *712 163*	69.90 *715 538*	69.33 *709 707*
Medium		17.36 *177 789*	17.24 *176 273*	17.49 *178 843*	17.11 *175 058*	17.44 *178 528*	17.27 *176 802*	17.78 *182 068*	17.83 *182 560*
High		0.09 *976*	0.08 *912*	0.09 *976*	0.08 *878*	0.09 *977*	0.08 *920*	0.09 *979*	0.09 *969*
No		0.00 *0*	0.00 *0*	0.00 *0*	0.00 *0*	0.00 *0*	0.00 *0*	0.00 *0*	0.00 *0*

7.1.2 Total Soil CO_2 Emissions in 2070

By 2070, mean CO_2 emissions of all scenarios for 2070 range from 1,409.73 g CO_2 m^{-2} $year^{-1}$ (RCP2.6) (Table 8) to 1,426.25 g CO_2 m^{-2} $year^{-1}$ (RCP8.5). The strongest difference between two scenarios therefore appears to be 1.15%. Like for the scenarios in 2050, minima (733.97 – 738.32 g CO_2 m^{-2} $year^{-1}$) and maxima (4,129.10 – 4,158.69 g CO_2 m^{-2} $year^{-1}$) are very close. Median values lie about 150 g CO_2 m^{-2} below averages (1,245.85 – 1,263.96 g CO_2 m^{-2} $year^{-1}$). For RCP2.6 (Figure 6) as well as for all scenarios, CO_2 emissions appear to be less than the CO_2 emissions of 2050. The mean of the thawing-induced CO_2 emissions adds up to 36.03% of the averaged means of the total CO_2 emissions. Like for 2050, the medians of the thawing-induced values amount to less than half of the mean and also like for 2050, strongest decreases in total CO_2 emissions compared to the total CO_2 emissions in 2015 are located in the central part of the plateau (Figure 5).

Table 8: Statistics of total soil CO_2 emissions in 2015 and 2070 in g CO_2 m^{-2} $year^{-1}$.

Year (Scenario)	***2015 (Bosch et al. (2016))***	**2070 (RCP2.6)**	**2070 (RCP4.5)**	**2070 (RCP6.0)**	**2070 (RCP8.5)**
			g CO_2 m^{-2} $year^{-1}$		
Mean	*1,415.59*	1,409.73	1,414.14	1,414.88	1,426.25
Min	*737.08*	735.46	733.97	736.89	738.32
Max	*4,224.34*	4,149.22	4,143.43	4,129.10	4,158.69
Median	*1,246.86*	1,245.85	1,249.51	1,251.36	1,263.96

Basic patterns of the abundance of total CO_2 emissions of 2050 and 2070 resemble each other strongly (Table 7). Again, the difference between the scenarios appears to be about 1%.

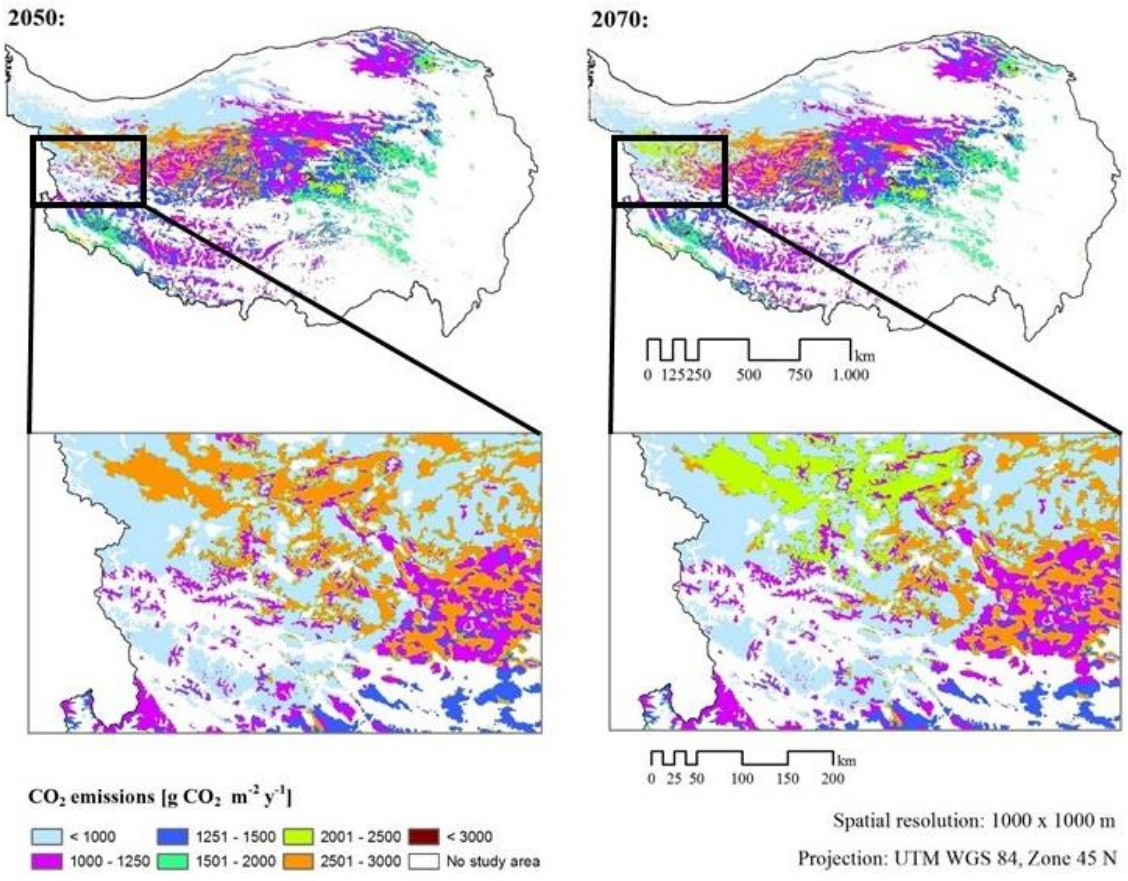

Fig. 6. Spatial distribution of total potential CO_2 emissions from permafrost areas on the Qinghai-Tibet Plateau in 2050 and 2070 according to the RCP2.6 scenarios. Unit of CO_2 emissions is g CO_2 m^{-2} $year^{-1}$. The spatial resolution of the grids is 1,000 m x 1,000 m.

7.2 General Soil CO_2 Emissions

7.2.1 Models for Belowground Biomass

To estimate BGB, the model with MAT exhibited closest agreements to the field measured data in general (Table 9). It overall performs best or second-best for most and largest vegetation zones. For the vegetation zones of alpine steppe, alpine mixed forests, and alpine spruce fir forests, the regression model based on MAP was distinctly preferable. When the model based on January mean temperature shows better results for a certain vegetation zone, the regression model based on MAT closes up very narrowly to it. Based on the comparison of ranges, minimum, maximum, and relative mean error for six models with regard to the samples of nine vegetation zones, the regression model based on MAT is the preferred model to calculate BGB on the Qinghai-Tibet Plateau.

Table 9: Range of belowground biomass for different vegetation types on the Qinghai-Tibet Plateau measured by Luo et al. (2005), Yan et al. (2005), Wang et al. (2008), Yang et al., (2009), Li et al. (2011), Wu et al. (2011), Geng et al. (2012) and calculated based on regression models.

Vegetation type		Luo et al. (2005) (n_{AS} =3; n_{AM} = 5; n_{DF} = 2; n_{SF} = 2; n_{AMF} = 3; n_{ASF} = 4; n_T = 3)	Yan et al. (2005) (n_{AS} =1; n_{AM} = 2)	Wang et al. (2008b) (n_{AM} = 12)	Yang et al. (2009) (n_{AS} = 73; n_{AM} = 35)	Li et al. (2011) (n_{AS} = 17; n_{AM} = 7; n_{DG} = 8; n_{AD} = 5)	Wu et al. (2011) (n_{AM} = 30)	Geng et al. (2012) (n_{AS} = 18; n_{AM} = 20)	All field samples	Regression model based on					
										January mean temperature	July mean temperature	MAT	MAP	MAT and MAP	Elevation
									[Mg ha^{-1}]						
Alpine steppe (AS)	Range	6-10	8.86	-	0.44-18.34	12.12-16.13	-	2.01-10.83	0.44-18.34	4.22-19.48	4.01-52.99	3.76-28.84	2.77-19.55	9.43-18.11	-14.15-50.86
	(Mean rel. error [%])									*(343.92)*	*(515.99)*	*(375.99)*	*(231.80)*	*(562.67)*	*(219.98)*
Alpine meadows (AM)	Range	9-32	24.90-100.48	17.97-145.67	0.82-27.84	26.67-49.30	13.40-24.74	5.43-93.93	0.82-145.67	4.36-28.81	4.12-47.34	3.76-31.90	4.54 - 49.39	9.96-20.48	-16.51-47.78
	(Mean rel. error [%])									*(91.71)*	*(111.75)*	*(97.46)*	*(110.08)*	*(124.87)*	*(142.51)*
Desert grasslands (DG)	Range	-	-	-	-	5.97-12.41	-	-	5.97-12.41	8.73-13.12 -	12.22-21.00 -	8.79-14.43 -	3.47-5.93 -	12.90-14.00 -	5.32-12.46 -
	(Mean rel. error [%])														
Dry Valley forests (DF)	Range	18-52	-	-	-	-	-	-	18-52	14.38-48.06	11.22-52.99	12.19-51.19	10.13-23.07	13.22-29.69	3.92-39.10
	(Mean rel. error [%])									*(14.16)*	*(25.34)*	*(17.13)*	*(49.65)*	*(34.85)*	*(51.68)*
Subtropical forests (SF)	Range	67-95	-	-	-	-	-	-	67-95	50.84-58.11	53.15-65.92	48.06-58.55	41.85-43.12	39.44-45.99	48.59-54.78
	(Mean rel. error [%])									*(30.18)*	*(23.19)*	*(31.32)*	*(46.30)*	*(45.17)*	*(33.84)*
Alpine mixed forests (AMF)	Range	23-36	-	-	-	-	-	-	23-36	45.82-50.74	45.21-52.51	44.02-53.86	24.31-44.09	29.26-37.05	38.64-45.21
	(Mean rel. error [%])									*(74.11)*	*(71.78)*	*(72.41)*	*(14.71)*	*(13.06)*	*(44.17)*

Alpine spruce fir forests (ASF)	Range *(Mean rel. error [%])*	21-49	-	-	-	-	-	-	21-49	34.22-38.86 *(44.61)*	28.58-34.78 *(32.08)*	31.09-39.35 *(42.81)*	19.14-45.41 *(47.27)*	20.98-34.19 *(26.63)*	26.14-40.77 *(39.66)*
Timberline (T)	Range *(Mean rel. error [%])*	7-27	-	-	-	-	-	-	7-27	21.69-25.21 *(85.93)*	15.49-18.97 *(56.63)*	18.85-21.53 *(80.60)*	15.39-49.39 *(224.25)*	15.78-20.48 *(84.22)*	13.57-25.19 *(110.00)*
Alpine desert (AD)	Range *(Mean rel. error [%])*	-	-	-	-	3.11-4.83	-	-	3.11-4.83	2.90-10.01 -	2.52-29.56 -	2.29-13.27 -	2.49-13.88 -	8.91-13.85 -	-23.35-36.87 -
All	Range *(Mean rel. error [%])*								0.44-145.67	0.53-159.11 -	0.13-173.93 -	0.43-167.66 -	0.00-57.09 -	2.04-199.99 -	-63.75-103.23 -

7.2.2 Models for General Soil CO_2 Emissions

The model based on MAP was the preferred model to calculate general soil CO_2 emissions for the study area as closest matching field measured data (Table 10). It typically best represents most and largest vegetation zones with regard to mean, relative error of the mean, minimum, maximum, and range of soil CO_2 emissions. Mean and mean relative error of alpine meadows and the vegetation types altogether constituted two exceptions with the BGB-based model providing more persuading results. However, the BGB-based model underperformed in general with an extremely high mean relative error. Even more disqualifying is the model´s particularly small range, covering less than 1% of the range of the field data throughout all vegetation zones. Additionally, for the alpine steppe vegetation zone, the MAT II-based model performed better than the MAP-based model. Nevertheless, the model with MAP as input parameter decidedly yielded most convincing results for alpine meadows, forests, and the range of the whole plateau. Thus, it is the preferred model to calculate general soil CO_2 emissions on the Qinghai-Tibet Plateau. Their spatial distribution is shown in Figure 7.

Table 10: Range of soil CO_2 emissions for different vegetation types on the Qinghai-Tibet Plateau measured by Cao et al. (2004), Zhang et al. (2005), Li et al. (2011), Zhang et al. (2009), Geng et al. (2012), Chen et al. (2014), Wang et al. (2014) and calculated based on regression models.

Vegetation type		Cao et al. (2004) (n = 1)	Zhang et al. (2005) (n = 1)	Li et al. (2011) (n = 1)	Zhang et al. (2009) (n = 60)	Geng et al. (2012) (n_{AS} = 18; n_{AM} = 20)	Chen et al. (2014) (n = 2)	Wang et al. (2014) (n = 1)	All field samples (n = 104)	Regression model based on					
										MAT I	MAT II	MAP	MAT and MAP I	MAT and MAP II	BGB
		[g C m^{-2} $year^{-1}$]													
Alpine steppe (AS)	Range	-	143.53	-	-	50.47-522.87	-	-	50.47-522.87	150.04-360.57	103.64-331.44	221.65-339.65	214.76-318.44	201.74-310.82	422.52-422.64
	Mean	-	-	-	-	-	-	-	254.6	262.86	225.71	283.17	270.64	260.60	422.57
	Median	-	-	-	-	-	-	-	245.9	274.39	238.19	279.87	274.54	263.33	422.57
	(Mean rel. error [%])	-	-	-	-	-	-	-	-	*(48.70)*	*(41.32)*	*(63.14)*	*(57.22)*	*(56.03)*	*(135.34)*
Alpine meadow (AM)	Range	555.37	-	714.17	326.15-1876.63	144.95-1666.97	-	696	144.95-1876.63	146.39-376.79	99.69-349.00	266.95-561.55	205.75-345.41	197.37-357.82	422.52-422.66
	Mean	-	-	-	-	-	-	-	828.77	293.36	258.87	333.22	285.82	280.66	422.59
	Median	-	-	-	-	-	-	-	795.95	311.39	278.23	333.48	295.7	290.37	422.6
	(Mean rel. error [%])	-	-	-	-	-	-	-	-	*(60.87)*	*(64.59)*	*(55.37)*	*(61.26)*	*(60.31)*	*(46.88)*
Forest (F)	Range	-	-	-	-	-	643.76-908.84	-	643.76-908.84	467.88-474.34	447.55-454.54	529.54-532.1	430.05-434.91	436.8-441.3	422.78-422.79
	Mean	-	-	-	-	-	-	-	776.3	471.11	451.04	530.82	432.48	439.05	422.78
	Median	-	-	-	-	-	-	-	-	-	-	-	-	-	-
	(Mean rel. error [%])	-	-	-	-	-	-	-	-	*(37.56)*	*(41.89)*	*(31.62)*	*(44.28)*	*(43.44)*	*(45.53)*
All	Range	-	-	-	-	-	-	-	50.47-1876.63	-223.07-914.4	-300.08-930.7	161.64-1762.17	15.83-1641.16	7.98-1639.56	422.48-423.76
	Mean	-	-	-	-	-	-	-	722.86	257.13	219.52	299.18	281.14	270.89	422.60
	Median	-	-	-	-	-	-	-	713.00	237.06	197.80	251.57	214.61	200.61	422.52
	(Mean rel. error [%])	-	-	-	-	-	-	-	-	*(64.42)*	*(69.63)*	*(58.61)*	*(61.10)*	*(62.52)*	*(41.53)*

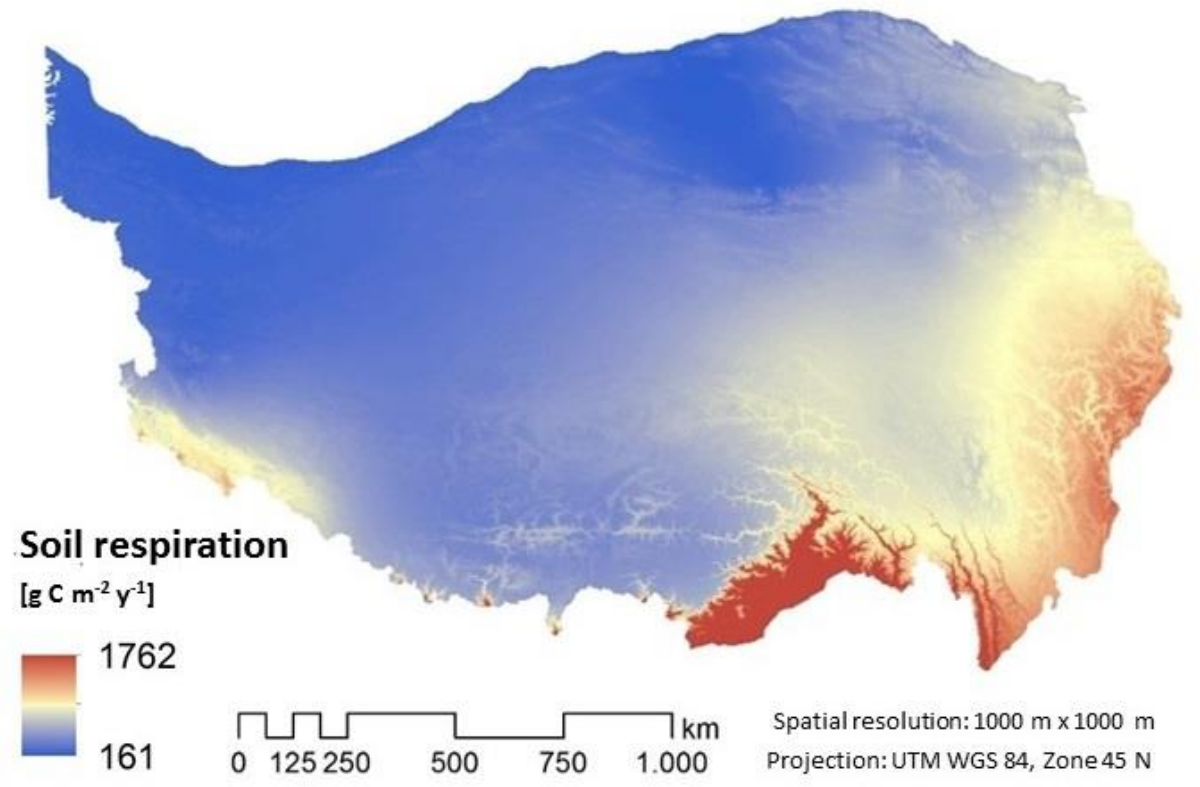

Fig. 7. Spatial distribution of general soil CO_2 emissions on the Qinghai-Tibet Plateau based on mean annual precipitation according to Raich and Schlesinger (1992). General soil CO_2 emissions, referred to as soil respiration, are in SI unit (g C m^{-2} $year^{-1}$). The spatial resolution of the grids is 1,000 m x 1,000 m.

7.2.3 General Soil CO_2 Emissions in 2015 and 2050

In 2050, general soil CO_2 emissions increase throughout all four climate change scenarios compared to general soil CO_2 emissions in 2015. The soil efflux raises by 18.80 g CO_2 m^{-2} $year^{-1}$ on average (2.11%). Variation in mean general soil CO_2 emissions between the four RCPs ranging from 901.02 to 914.34 g CO_2 m^{-2} $year^{-1}$ appears as 1.47% of their average (Table 11). Lowest general soil CO_2 emissions amount from 617.49 g CO_2 m^{-2} $year^{-1}$ (RCP4.5) to 622.36 g CO_2 m^{-2} $year^{-1}$ (RCP8.5). Maxima vary from 2,349.27 g CO_2 m^{-2} $year^{-1}$ (RCP8.5) to 2,418.95 g CO_2 m^{-2} $year^{-1}$ (RCP2.6). The statistical means of the general soil CO_2 emissions follow the same patterns as the ones of the total soil CO_2 emissions in 2050.

Table 11: Statistics of general soil CO_2 emissions in 2015 and 2050 in g CO_2 m^{-2} $year^{-1}$.

Year (Scenario)	*2015 (Bosch et al. (2016))*	2050 (RCP2.6)	2050 (RCP4.5)	2050 (RCP6.0)	2050 (RCP8.5)
		g CO_2 m^{-2} $year^{-1}$			
Mean	*886.92*	901.02	904.80	902.75	914.34
Min	*614.32*	618.59	617.49	618.18	622.36
Max	*2,340.46*	2,418.89	2,412.00	2,374.59	2,349.27
Median	*863.83*	855.15	860.21	855.26	859.62

7.2.4 General Soil CO_2 Emissions in 2070

Results show higher general soil CO_2 emissions for 2070 than for 2015, which applies to all RCPs. Mean annual soil CO_2 emissions range from 900.00 g CO_2 m^{-2} $year^{-1}$ (RCP2.6) to 916.78 g CO_2 m^{-2} $year^{-1}$ (RCP8.5) compared to 886.92 g CO_2 m^{-2} $year^{-1}$ in 2015 (Table 12). Compared to the general soil CO_2 emissions of 2050, differences between effluxes of a RCP in both years are very small with the biggest difference amounting to 2.44 g CO_2 m^{-2} $year^{-1}$ (RCP8.5). Minimum values vary between 615.73 g CO_2 m^{-2} $year^{-1}$ (RCP4.5) and 620.09 g CO_2 m^{-2} $year^{-1}$. Maximum general soil CO_2 emissions in 2070 differ more distinctly from those of 2050 (on average: 1.50%) compared to the differences between minima of 2050 and 2070 (on average: 0.19%). A greater difference between general soil CO_2 emissions of 2050 and 2070 occurs for median values ranging from 755.63 g CO_2 m^{-2} $year^{-1}$ (RCP2.6) to 765.63 g CO_2 m^{-2} $year^{-1}$ (RCP8.5) in 2070 (2050: 855.15 g CO_2 m^{-2} $year^{-1}$ – 860.21 g CO_2 m^{-2} $year^{-1}$). The statistical means of the general soil CO_2 emissions follow, again, the same patterns as the ones of the total soil CO_2 emissions in 2070.

Table 12: Statistics of general soil CO_2 emissions in 2015 and 2070 in g CO_2 m^{-2} $year^{-1}$.

Year (Scenario)	*2015 (Bosch et al. (2016))*	2070 (RCP2.6)	2070 (RCP4.5)	2070 (RCP6.0)	2070 (RCP8.5)
		g CO_2 m^{-2} $year^{-1}$			
Mean	*886.92*	900.00	904.62	905.13	916.78
Min	*614.32*	617.23	615.73	618.66	620.09
Max	*2,340.46*	2,423.50	2,485.10	2,354.76	2,435.97
Median	*863.83*	755.63	757.06	757.06	765.63

7.3 Heterotrophic Soil CO_2 Emissions Induced by Permafrost Thaw

7.3.1 Carbon Stocks

In total, 68.59 Pg C are stored in the PFS of the Qinghai-Tibet Plateau in 2015 according to our estimations based on the WISE30sec data sets. For 2050, C stocks sum up to 63.25 Pg C and to 60.05 Pg in 2070. On average, the PFS contains 67.00 kg C m^{-2} in 2015. Less C is stored in 2050 and 2070 with mean values of 61.79 kg C m^{-2} and 58.66 kg C m^{-2}, respectively. Figure 8 shows the spatial distribution of C stocks on the Qinghai-Tibet Plateau. The amount of C ranges from 6.72 to 387.13 kg m^{-2} in 2015, from 6.20 to 356.98 kg C m^{-2} in 2050 and from 5.88 to 338.92 kg C m^{-2} in 2070.

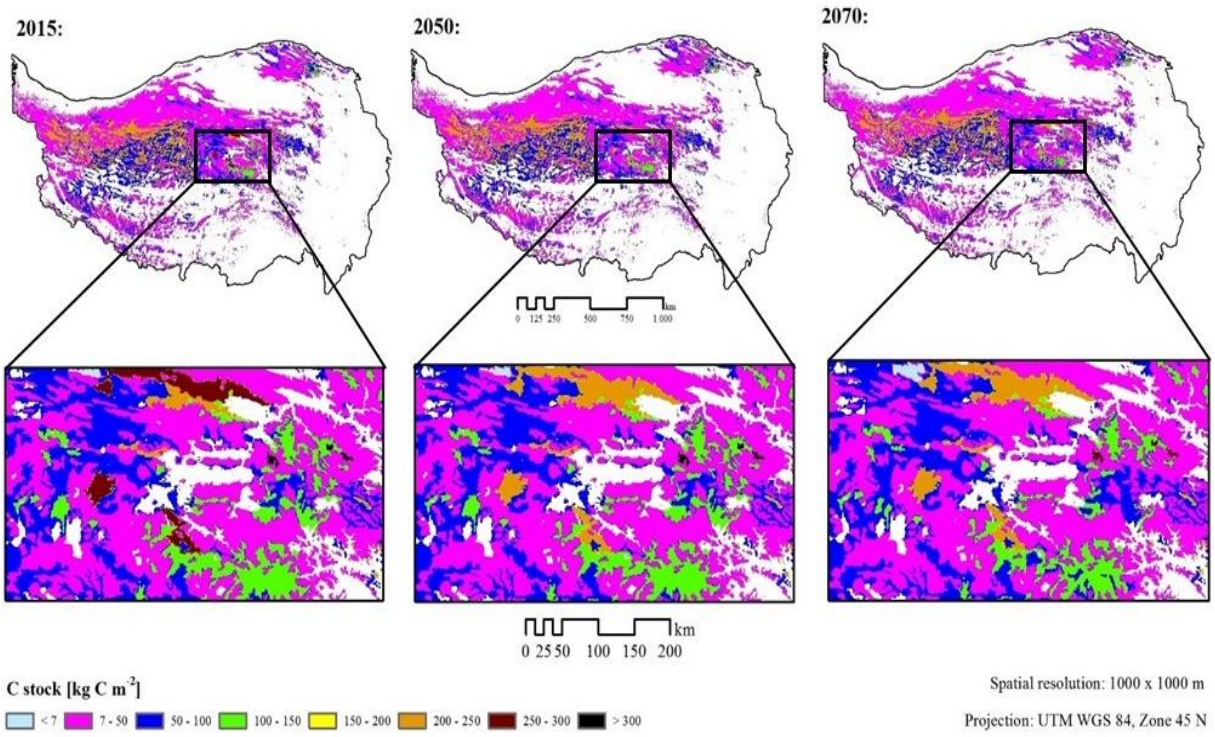

Fig. 8. Spatial distribution of C stocks of the permafrost areas on the Qinghai-Tibet Plateau for 2015, 2050 and 2070. C stocks are in SI unit (kg m^{-2}). The spatial resolution of the grids is 1,000 m x 1,000 m.

Strongest decreases of C stocks from 2015 to 2050 and from 2015 to 2070 are concentrated in the central part of the plateau for both periods (Figure 9).

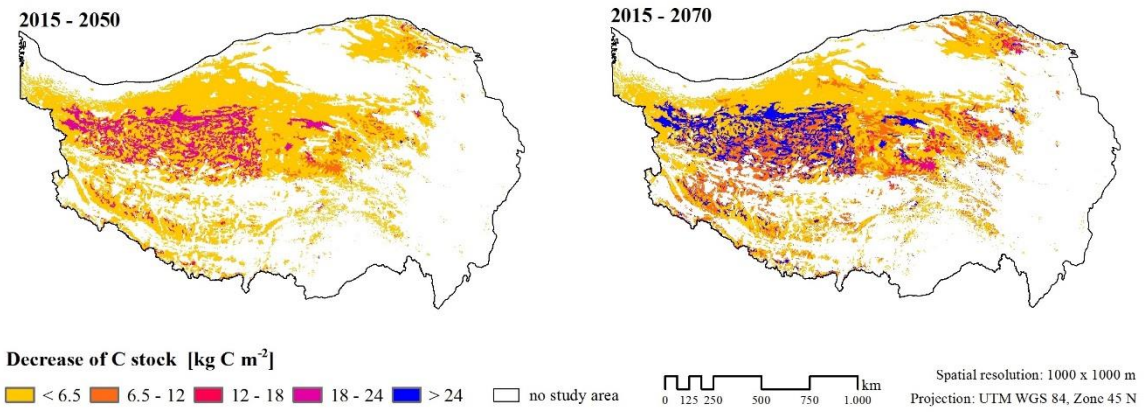

Fig. 9. Spatial distribution of absolute differences in C stocks of the permafrost areas on the Qinghai-Tibet Plateau between 2015 and 2050 and between 2015 and 2070. Absolute differences in C stocks are in SI unit (kg m^{-2}). The spatial resolution of the grids is 1,000 m x 1,000 m.

7.3.2 CO_2 Emissions

On the entire Qinghai-Tibet Plateau, every year 0.54 Pg CO_2 (0.15 Pg C) is released by the thaw of PF on average starting from 2015. From thawing PFS, annual soil CO_2 emissions decrease from mean 529.91 g CO_2 m^{-2} $year^{-1}$ in 2015 to 519.75 g CO_2 m^{-2} $year^{-1}$ and in 2050 to 510.13 g CO_2 m^{-2} $year^{-1}$ in 2070 (Table 13). Mean CO_2 emissions decrease by 3.7% on average between 2015 and 2070. For 2015, least CO_2 emissions originating from PFS C amount to 53.20 g CO_2 m^{-2} $year^{-1}$, for 2050 to 52.18 g CO_2 m^{-2} $year^{-1}$ and to 51.23 g CO_2 m^{-2} $year^{-1}$ for 2070. Maximum fluxes of soil CO_2 vary between 2,948.25 g CO_2 m^{-2} $year^{-1}$ (2070) and 3,134.91 g CO_2 m^{-2} $year^{-1}$ (2015). 50% of the values, however, remain below 236.19 g CO_2 m^{-2} $year^{-1}$ (2015). The results further show median values at 231.69 g CO_2 m^{-2} $year^{-1}$ for 2050 and 227.47 g CO_2 m^{-2} $year^{-1}$ for 2070, thereby amounting to less than half of the mean. For all scenarios and years, the range of the thawing-induced values of the entire Qinghai-Tibet Plateau appears to be broader than the range of the general soil CO_2 emissions.

Table 13: Statistics of PF soil CO_2 emissions in 2015, 2050 and 2070 in g CO_2 m^{-2} $year^{-1}$.

Year	2015	2050	2070
	g CO_2 m^{-2} $year^{-1}$		
Mean	529.91	519.75	510.30
Min	53.20	52.18	51.23
Max	3,134.91	3,002.82	2,948.25
Median	236.19	231.69	227.47

8 Discussion

8.1 Total Soil CO_2 Emissions

The calculation and analysis of total soil CO_2 emissions for 2015, 2050 and 2070 reveal that under all scenarios, the soil CO_2 emissions remain within the same order of magnitude (Tables 6 and 8). The average does not even alter more than 17.87 g CO_2 m^{-2} $year^{-1}$ (1.26% of mean total soil CO_2 emissions in 2015).

Thawing-induced soil CO_2 emissions in 2015, 2050 and 2070 account for 36.3% of total soil CO_2 emissions on average (Tables 6, 8 and 13). This closely lines up to the field measured results of Peng et al. (2015) with the amount of C additionally released due to warming and thawing PF reaching 18 to 29% in an alpine meadow on the plateau. In that study, there is no differentiation between altered soil CO_2 emissions induced by PF thaw and altered general soil CO_2 emissions due to a general higher plant and microbial metabolic activity as consequence of higher temperatures. However, it is to assume that most of the increase is related to the additional available PF C as Hicks Pries et al. (2013) obtained similar results when focusing on soil CO_2 emissions originating from PF C. In that study, old soil heterotrophic soil CO_2 emissions comprised up to approximately 18% of the remaining parts of soil CO_2 emissions under thawing PF.

Compared to direct CO_2 emission measurements on the Qinghai-Tibet Plateau, the range of total soil CO_2 emissions for all years and scenarios (733.97 – 4,224.77 g CO_2 m^{-2} $year^{-1}$) lies within the order of magnitude of field measurements (2,321.60 – 3,277.56 g CO_2 m^{-2} $year^{-1}$) as reported by Chen et al. (2014). Those field data have been measured in forests why representing higher sectors of this range of values. As not including PF-specific soil CO_2 emissions, the maximum value remains below the highest values with about 22.42%, roughly corresponding to the range of the ratio of PF-specific soil CO_2 emissions to total soil CO_2 emissions as reported by Peng et al. (2015) and discussed in this section. Wang et al. (2014b) measured a four-year average of 2,550.29 g CO_2 m^{-2} $year^{-1}$ in alpine meadows, which are characterized by a short growing season. Again, due to no PF at the measurement sites, these values would be higher under the influence of PF, then closely lining up to a typical soil CO_2 emission value for alpine meadows in a PF area. Less CO_2 emissions in 2070 mainly result from the decrease of thawing-induced soil CO_2 emissions over time, reflecting

the close relationship of soil CO_2 emissions to a decrease of C stocks in PF in the calculations.

The differences between the scenarios of total soil CO_2 emissions fully result from the differences between the general soil respiration rates for each scenario as the potential thawing-induced CO_2 emissions are represented by only one value per year due to the different calculation. Accordingly, values of mean, minimum, maximum and median share proportionally the same trends for total CO_2 emissions and general soil respiration. Differences between the scenarios of general soil CO_2 emissions appear to be about 1% what reflects the small differences between the scenarios of MAP as fully accounting for this. For all scenarios of 2070, CO_2 emissions appear to be less than the CO_2 emissions of 2050. This results mostly from the thawing-induced CO_2 loss, which is calculated as percentage of the respective C-stock, consequently decreasing with temporal progression.

Regarding the abundance of values in 2050, except for the entire lowest class and the medium class for the RCP8.5 scenario, more values of CO_2 emissions can generally be found in all scenarios of 2050. This corresponds to the result of general higher total CO_2 emissions in 2050, resulting from decreasing carbon stocks in the end.

As total soil CO_2 emissions have been obtained by adding up general soil CO_2 emissions and PF-specific CO_2 emissions, both, uncertainties and implications originate from their respective calculations as discussed below (Sections 8.2, 8.3). Further, the results of total soil CO_2 emissions are not fully accurate with exclusively adding up general and PF-specific CO_2 emissions, which, additionally, may partly overlap. These compartments do not include further region-specific phenomena (i.e., grazing) relevant to soil CO_2 emissions on the Qinghai-Tibet Plateau that can possibly change with global warming. Although the mechanisms of the relations have in general not been sufficiently clarified yet, changes in soil CO_2 emissions by grazing are relatively high with a decrease by about 50% when doubling grazing intensity on the Qinghai-Tibet Plateau (Cao et al., 2004). Moderate grazing reduces the C uptake in *Kobresia* turfs (Babel et al., 2014) indicating decreasing CO_2 emissions. Also, grazing influences PF thawing as decreasing vegetation cover reduces the insulating effect of vegetation, resulting in quicker PF thaw on the Qinghai-Tibet Plateau (Hu et al., 2009) and consequently leading to higher CO_2 emissions induced by PF thaw. Studies by Wen et al. (2013) and Cao et al. (2004) found vegetation degradation and grazing

effects comprising about 35% of the Qinghai-Tibet Plateau. Johnson and Matchett (2001) concluded that grazing resulted in a decrease of soil CO_2 emissions compared to an ungrazed tallgrass prairie, however, grazed prairie exhibited more soil CO_2 emissions than ungrazed prairie (Frank et al., 2002). Thus, although important, grazing effects do not exceed the order of magnitude of the remaining soil CO_2 emissions (Cao et al., 2004).

8.2 General Soil CO_2 Emissions

As projected by all four scenarios, the average increase of general soil CO_2 emissions from 2015 to 2050 with 2.1% lies in the order of magnitude of the results of the study of Melillo et al. (2002). They predict a long-term warming-induced C-loss in a PF-free area in the first six years amounting to averaged 28%, followed by 5% in the subsequent three years, and declining to no C-loss for the 10^{th} year. Acclimatization accounts for the weakening of general soil CO_2 emissions, which initially increased due to global warming (Luo et al., 2001). This decrease in temperature sensitivity can occur because of reduced root respiration and microbial activity as consequence of drier soils (Peterjohn et al., 1994), and limited substrate availability (Rustad and Fernandez, 1998). Although even decreasing, changes in general soil CO_2 emissions to 2070 likewise resemble this weak response of general soil CO_2 emissions to global warming.

The results further directly reflect the spatial and temporal variability of precipitation patterns as calculated by a linear regression model based on MAP, declining from northwest to southeast (Figure 7). Although with low mean relative error for two zones, BGB-based estimates of soil CO_2 emissions are most unrealistic with a range of only 1.28 g C m^{-2} $year^{-1}$. This narrow range results from the regression model used by Behera et al. (1990), since calculated BGB data based on MAT show reasonable results when compared to field measured data (Table 9). Indicated by its coefficient of determination ($r^2 = 0.66$), the model is a priori not capable to fully explain all variation. It is, moreover, developed for a very specific climate and vegetation zone (tropical forest soils in India), why the fully different climatic and environmental conditions lead to deviations due to limited transferablilty. Since the results of the BGB-based model still reflect basic patterns such as the main quantitative differences between the vegetation zones, the temporal resolution of the input data of the model development accounts for this. In this model, soil CO_2 emission rates are resoluted to hourly values, why upscaling to years is particularly sensitive to rounding errors and coefficients.

The fact that the best regression model for the calculation of soil CO_2 emissions incorporates MAP as key parameter reflects the particularly high sensitivity of the Qinghai-Tibet Plateau as arid and semiarid region to precipitation patterns (Rey et al., 2002). Generally, precipitation may override temperature as main controlling factor in such areas (Curiel Yuste et al., 2003). For the entire Qinghai-Tibet Plateau, precipitation is further regarded as the principle controlling factor for vegetation cover (Sun et al., 2013), indicating its importance for soil CO_2 emissions as a phenomenon that is generally closely connected to biomass (Section 4.2.2). Nevertheless, as much as precipitation does not occur linearly, as much does the influence of precipitation on soil CO_2 emissions proceed in a linear manner especially with regard to its regulation of soil moisture (Birch, 1958; Davidson et al., 2000; Lee et al., 2002; Liu et al., 2002; Lou and Zhou, 2006). Under low soil moisture conditions, soil CO_2 emissions are generally low, because bacteria act only on a basic metabolism and reduce their respiratory activity (Lou and Zhou, 2006). Medium soil moisture conditions lead to highest soil CO_2 emissions while high soil moisture has a reducing effect because anaerobic conditions shrink aerobic microbial activity (Lou and Zhou, 2006). The fact, that MAP does not naturally follow static patterns as depending on complex influencing factors is partly considered in the RCPs. The differences between the scenarios, amounting to about 1% reflect the small differences between the scenarios of MAP (Table 3) as fully accounting for this. With the mean CO_2 emission rate of RCP6.0 being lower than the one of the RCP4.5 in 2050, it is reflected that there is no linear correlation in general to radiative forcing values.

However, important uncertainties of the predicted values are generally associated with the regression model as not developed for this region and kind of application (Raich and Schlesinger, 1992). Since soil CO_2 emissions are the result of a number of complex processes altering over time and space with multiple influencing factors, the variability of soil CO_2 emissions may not be represented as accurate as e.g. by process-based models including more input variables (Reichstein and Beer, 2008). For instance, the influence of precipitation on soil CO_2 emissions depends on temperature (Schindlbacher et al., 2012). Nevertheless, the inclusion of more variables does not necessarily improve the accuracy of results in general as indicated by the lower performance of the regression models including MAP and MAT as input parameter (Table 10). However, it is to conclude that the results indicate highly complex

interactions between soil CO_2 emissions and various controlling factors besides MAP overall. Reflected by its coefficient of determination ($r^2 = 0.34$), the model, generally, is a priori not capable to fully explain the data variability. Moreover, the model does due to its formulated constant not realize values below 567.95 g CO_2 m^{-2} $year^{-1}$ that do exist on the Qinghai-Tibet Plateau (e.g. Geng et al., 2012). An upper limit of soil CO_2 emissions under high precipitation (Luo and Zhou, 2006) is not represented as well. Furthermore, the regression model is not developed for or with regard to future conditions where the sensitivity of soil CO_2 emissions to precipitation may differ. Additionally, inter-annual variability occurring due to hysteresis effects from droughts and impacts of rewetting (Birch, 1958; Davidson et al., 2000; Lee et al., 2002; Rey et al., 2002) can, by nature, not be represented by a linear regression model using MAP as only input factor.

Further uncertainties may arise from the difference between the spatial scales of the development and the application of the regression model. Raich and Schlesinger (1992) developed the regression model with regard to the global scale why region-specific characteristics may not be represented adequately. Even though the study area is a heterogeneous region also in terms of relevant influencing factors, the importance of influencing factors generally varies across spatial scales. This issue generally leads to the fact that results from different scales may even be contradictory (Reichstein and Beer, 2008). Therefore, in view of this multifactorial process and the input parameter, the regression model may not be as representative for the Qinghai-Tibet Plateau as for the globe (Section 4.2.3). For arid regions, only few measurements have been taken (Raich and Schlesinger, 1992), leading to a deficiency in applying the model for the study area. Nevertheless, in view of the high consistency of calculated values to field measurements (Table 10), this difference presumably does not lead to basic discrepancies. In general, incorporating other regression models for specific vegetation zones, however, might increase the accuracy of the calculation of the general soil CO_2 emissions.

Other important restrictions of the estimations result from limitations of the input data. For instance, the WorldClim data sets generally show lower precision for poorly sampled regions such as the Qinghai-Tibet Plateau and areas with complex topography (Hijmans et al., 2005; Böhner, 2006; Maussion et al., 2011). Further, the projections of the global climate model ‘Community Climate System Model, Version 4’ show uncertainties in predictions of precipitation on the Qinghai-Tibetan Plateau up to

10 mm per day when comparing to reference models (Gent et al., 2011), indicating the limitations of the model. The RCP projections generally inhere deficiencies resulting from the process of harmonizing different scenarios and models underlying the RCPs (Van Vuuren et al., 2011). As the years 2050 and 2070 represent an average from 2041 to 60 and from 2061 to 80 respectively, likely variation is not represented. Assumptions are too general or static such as a general stronger and stronger regulation of air pollution. They also may not only occur model-specifically but are important for other RCPs such as reforestation policies included in RCP4.5 but potentially also relevant to RCP2.6. Further uncertainties arise from the transfer of emissions to concentrations and radiative forcing. The RCPs do not represent those various possible translations. Moreover, the respective socio-economic scenario for each RCP is not representing the variety of possible developments (van Vuuren et al., 2011).

Furthermore, the high small-scale variability of soil CO_2 emissions especially in alpine meadows is generally not captured by the data resolution of 1,000 m x 1,000 m of all input data. The comparatively high values in alpine meadows, particularly of *Kobresia tibetica* plant communities, were not predicted by any regression model. This strong difference in soil CO_2 emission rates between these communities and other alpine meadow plant communities results in large differences of soil CO_2 emissions over short distances, which can only be represented with a higher spatial resolution.

The evaluation data (Table 10) used to decide on the best regression model to calculate general soil CO_2 emissions on the Qinghai-Tibet Plateau account for other restrictions. Firstly, they do not allow for deeper analysis as e.g. not covering all vegetation types. Moreover, although all studies use chamber-based methods for their measurements, there are differences between the various chamber methods that may cause further inaccuracies of the values. In addition, daily averages were calculated based on a different number and different times of measurements. For some of those studies, additional measurements were taken to determine the optimal number and time of measurements for the daily mean, however, discrepancies among the results remain. Also, the annual soil CO_2 emission values for forests have been estimated based on continuous measurements throughout one whole year in contrast to the values of all other studies where seasonality was not considered a major factor.

The estimation of annual values based on daily means of field measurements poses other constraints. The higher the temporal resolution of data, the higher the variability of the cumulative values. This tendency increases with larger differences in the target temporal resolution, which eventually ranges from seconds to a year. This may result in ranges of values that are too large. Further, the seasonality correction factor derived from the estimations by Cao et al. (2004) for alpine meadows might vary for other vegetation types such as forests with the cumulative soil CO_2 emissions in the peak month accounting for only about 20% of the total annual soil CO_2 emissions (Chen et al., 2014). The values provided by Cao et al. (2004) are estimations based on (i) data obtained from chamber method measurements, which have inherent limitations, and on (ii) equations based on soil temperature with an $r^2 = 0.82$.

It should be further noted that approximations for soil CO_2 emissions obtained from annual values in general are not as accurate as calculations from periodic or continuous data (Bahn et al., 2010).

Furthermore, the temperature change under global warming additionally alters soil CO_2 emissions compared to the results calculated based on the regression model with MAP as input parameter (Tables 6, 8, 11 and 12). This is due to the fact that the warming influences the impact of precipitation (Harte et al., 1995), which weakens the prediction capability of the model. Also, variation due to vegetation changes because of rapide desertification on the Qinghai-Tibet Plateau is not considered in this thesis (Xue et al., 2009). Until 2070, there is a predicted decrease in soil CO_2 emissions for the scenarios RCP2.6 and RCP4.5, while the emissions according to the RCP6.5 and RCP8.5 scenarios increase compared to 2050 (Tables 11, 12). Thereby it is revealed that precipitation patterns do not evolve linearly with further climate change (Table 3) but exhibit more complex patterns over time and space.

8.3 Heterotrophic Soil CO_2 Emissions Induced by Permafrost Thaw

The analysis of quantified soil CO_2 emissions from PF reflects distinctly higher pool sizes of C available to microbial decomposition due to the thaw of PF. Under the influence of climate warming, the PF C on the Qinghai-Tibet Plateau contributes 3.7% to the annual average atmospheric increase of CO_2-C (IPCC, 2013). This is 1.9% of the total global anthropogenic CO_2 emissions from fossil fuels (IPCC, 2013). With 0.15 Pg C $year^{-1}$, the thawing-induced CO_2 emissions from the Qinghai-Tibet Plateau

contribute approximately 0.2% to the annual global soil CO_2 emissions (91 Pg C) (Hashimoto et al., 2015).

With about 0.54 Pg CO_2 $year^{-1}$, the thawing-induced soil CO_2 emissions of the entire study area are, although in the same order of magnitude, about three times higher than what would be supposed based on the results of Schuur et al. (2009) and assuming an estimated area of global PF with about 22 * 10^6 km^2 according to Gruber (2012). Schuur et al. (2009) estimate 1 Pg C $year^{-1}$ (3.66 Pg CO_2 $year^{-1}$) as global C flux. Likewise, a model-based estimation, projecting emissions from PFS to a depth of 3 m to 7 - 17 Pg CO_2 until 2100 (Zhuang et al., 2006), is also lower than the results of this thesis (7.3.2). These and comparable estimates by Harden et al. (2012) are even considered being overestimated (Schädel et al., 2014). However, the results of Schuur et al. (2009) are highly uncertain since they are based on measurements on only one site. A recent, model-based study by Schuur et al. (2015) approximated 37 – 174 Pg C to lose from the global PF zone by 2100 under the RCP8.5 scenario. This corresponds to 0.09 Pg C $year^{-1}$ from the plateau on average, which is distinctly closer to an average of 0.15 Pg C $year^{-1}$ (Section 7.3.2). Generally, global annual soil CO_2 emissions are approximated to 63 – 120 Pg C (Raich and Schlesinger, 1992; Raich and Potter, 1995; Reichstein and Beer, 2008). This gives rise to the assumption that the calculated heterotrophic soil CO_2 emissions induced by PF thaw (Table 13) are as a whole to be revised upwards after further research.

Differences between the years 2050 and 2070 in thawing-induced CO_2 emissions reflect their linear calculation and decreasing C-stocks. As natural process, thawing of PF does, however, not progress strict linearily. Nevertheless, the relative high independence of temperature (Schädel et al., 2014) does not require further differentiations of different temperature scenarios.

The spatial distribution of CO_2 emissions with a concentration of high values in the central part of the plateau (Figure 6) resembles the spatial distribution of the C:N ratio in the study area. There, the C:N ratio ranges from 0 – 25 (Batjes, 2015). Highest C losses occur in this area (Figure 9), confirming the results of Schädel et al., (2014) that present the C:N ratio as most reliable predictor of C loss compared to either C or N concentration. The PF conditions, conserving fragmentary decomposed organic matter, may account for this positive relationship, which reflects the stabile presence of N in the system (Schädel et al., 2014).

The calculated C stocks (Figure 8), reflecting the decrease caused by the raised C decomposition as steadily declining from 2015 to 2070, appear to be reasonable in view of other studies on C stocks. They fit the order of magnitude of field measured data with about 10 kg C m^{-2} in PFS of alpine grasslands of the Qinghai-Tibet Plateau to a depth of less than 1 m (Wang et al., 2008; Doerfer et al., 2013) or 56.5 kg C m^{-2} in meadows (Mu et al., 2015) as examples. The global C stock estimates by Batjes (2015) clearly show the same patterns of the spatial distribution of C stocks on the Qinghai-Tibet Plateau overall with highest C stocks on the Qinghai-Tibet Plateau reaching global maxima. Carvalhais et al. (2014) approximates the global maximum for soil C stocks to 243 kg C m^{-2}, which is comparable to the maxima in this study. Compared to 450 Pg C (Zimov et al., 2006) in the Siberian loess PF (1 x 10^6 km^2), the C stock estimated in this study appears to be much lower, resulting from the fact that it covers only a depth to 2 m in contrast to 25 m as reported in Zimov et al. (2006). They also include roots and partly organic matter in their less spatially differentiated approximations as not considering coarse fragments in their calculations and using only one standard value for organic C content and bulk density which accounts for much higher values. Their uncertainty is further assessed as possibly deviating by several hundred Pg (McGuire et al., 2010). Moreover, an extreme spatial variability of soil organic C stocks on the Qinghai-Tibet Plateau has been reported (Mu et al., 2015), leading generally to a wide range in area-wide estimations. C stocks for the PF region on the Qinghai-Tibet Plateau were calculated with about 160 Pg C up to 25 m in a similar order of magnitude by Mu et al. (2015) compared to the estimates for the Siberian loess PF. However, the strong methodological differences to this study are to a large extent very similar next to a broader definition of the PF area. Genxu et al. (2002) estimate the C stock of the plateau´s grasslands to 33.5 Pg. However, they only consider the first 70 cm of the soil. The estimation of Mu et al. (2015) for the first two meters amount to about 27.9 Pg C for the PFS on the Qinghai-Tibet Plateau indicating that estimates in this study (Section 7.3.1) are reasonable. Since the calculations by Mu et al. (2015) are based on literature data from different studies, they expect deviations of several 10% regarding the C contents as base for their calculations due to different methodological approaches.

However, there are various sources of uncertainty relevant to the results of PF thaw-induced soil CO_2 emissions presented in this thesis. First of all, the amount of C stock

as basis for the estimation of PF-induced soil CO_2 emissions bears deficiencies arising from the input data.

The input data sets from the WISE30sec data inhere deficiencies that arise from processing simplifications resulting in prediction accuracies from 23 - 51% (point-based). Potential biases occur especially for soil characteristics “not observed” as the volumetric gravel content that was calculated using taxotransfer rules. The pragmatic combination of soil profile data from different sources led in the process of harmonizing and reclassification to generalizations (Batjes et al., 2015). With different soil analytical methods in nearly each country, even possibly varying between laboratories, comparability remains critical. To some extend these differences result from the fact that the analytical procedures depend on the soil type. However, no straightforward method of harmonization of the data exists (Batjes, 1999), why the synthesis of the data has proceeded pragmatically as in studies before at this scale (Batjes, 2002). Also, soil geographic as well as taxonomic gaps do exist. Generally, the soil profiles are spatially irregularly distributed. Further uncertainties originating from the spatial data and processes of aggregation, are not yet possible to be quantified at present. (Batjes et al., 2015). Moreover, the PF of the Qinghai-Tibet Plateau may reach a depth up to more than 130 m (Wang and French, 1995) and soil C stocks at least several 10 m (Mu et al., 2015). Consequently, the C stocks must be higher than the WISE30sec data set captures with a depth of 2 m. Thus, the thawing-induced CO_2 emissions in the field are higher, however, it is to assume that the PF thawing process does not reach this depth within the addressed years (Pang et al., 2012). Despite their limitations, however, the WISE30sec data sets provide the most recent, appropriate, area-explicit information on soil properties for the Qinghai-Tibet Plateau needed to calculate C stocks at a resolution of 1,000 m x 1,000 m to a depth of 2 m in order to assess potential soil CO_2 emissions on the Qinghai-Tibet Plateau.

In the Global PF Zonation Index Map, main uncertainties also occur for less studied areas such as the Qinghai-Tibet Plateau (Gruber, 2012), potentially affecting the extend of PF on the Qinghai-Tibet Plateau in this thesis. Generally, the high spatial variability of PF is not captured by the resolution at hand. The occurrence of permafrost is a result of the interaction of various influencing factors. The Global Permafrost Zonation Index Map, however, solely determines the existence of permafrost based on mean annual air temperature leading to deficiencies. Excluding topographic effects such as the exposition of hills to sun or temperature effects of snow warming the

underground are not represented. Likewise is deep permafrost not considered with its influence on near-surface conditions. The model on which the map is based on, further does not reproduce effects of valleys and depressions where inversions and the drainage of cold air often impact ground temperature. Vegetation effects and thermal characteristics of the ground are further not considered. Sub-grid variability may differ between grids which is also not reproduced by the map as well as transient effects (Gruber et al., 2012). Given the variety of definitions of PF, differences in the determination of the area covered by PF may occur (Gruber, 2012), resulting in deviations of the amount of calculated soil CO_2 emissions in this thesis. Further inaccuracies are assigned to limitations of the input data sets for the derivation of the spatial PF extension. Next to these uncertainties, areas with less than 50% coverage of PF were not included in this thesis, indicating that estimates for the PFS CO_2 emissions on the Qinghai-Tibet Plateau are possibly biased low. However, their inclusion would potentially have caused a stronger bias. Further uncertainties of the estimations of thawing-induced soil CO_2 emissions arise because the soils in the defined PF area are both horizontallly and vertically not continuously frozen. Hence, the amount of soil organic C made available for decomposition through thawing is less because an active layer exists and discontinuous PF areas are included.

The results of PF CO_2 emissions further do not represent the variation due to the non-linear character of the amount of frost-free days in a year. Indicated by the results by Zhang et al. (2014) using data from 73 meteorological stations on the plateau for the observation period from 1960 to 2010, the trend of the lengthening of the frost-free season does not follow linear patterns. They further report a dependence of the frost-free season lengthening on elevation since there are less additional frost-free days in areas higher than 3,000 m a.s.l. (3.1 days/decade) compared to areas below 3,000 m a.s.l. (4.7 days/decade) (Zhang et al., 2014), which leads to deviations in the presented results here.

Another limitation of the potential thawing-induced CO_2 emissions in the presented results (Section 7.3.2, Table 13) arise from the transfer of the incubation experiments as base for the calculations. The soil samples of the experiments originate from the northern circumpolar PF zone with different climatic and environmental conditions. As the soil samples, further, are taken from different studies, their sampling methods are not fully consistent inhering another potential source of uncertainty. Moreover, the

thawing experiments are executed under laboratory conditions that may deviate from the process in natural environments due to strong simplifications. Fresh litter additionally incorporated into the soil is not regarded as well as it is assumed that abiotic factors do not change in contrast to a natural environment (Schädel et al., 2014). Of special importance are drainage conditions altering thawing-induced C loss by 9 – 75% (Elberling et al., 2013) that the calculated results do not reproduce. The estimations of this study further do not consider the C quality. As parts of the C have undergone microbial decomposition before their inclusion in PF, C quality differs among pools (Schuur et al., 2008). The amount of C loss strongly depends on C quality as determining its turnover time (Shaver et al., 2000; Schädel et al., 2014), therefore leading to uncertainties in the calculated results. Uncertainty further arises from the extrapolation of the results up to 50 years, disregarding potential variation over time. It is further to expect that the linear developement of C loss over time assumed for the calculations presented here does not correspond to the natural course as climate change is characterized by a high complexity. Moreover, variation due to soil types is methodologically not considered in the calculation. According to Schädel et al. (2014), potential C loss is about four times higher in organic soils than in mineral soils. With organic soils hardly occuring in the study area (less than 0.1% on the entire Qinghai-Tibet Plateau) (FAO, 2012), soil CO_2 emissions are, however, accordingly only marginally lower than the results of this thesis suggest.

Overall, the quantification of soil CO_2 emissions on the Qinghai-Tibet Plateau under the influence of climate change is challenging, yet the results obtained based on freely accessible data appear to be reasonable when comparing to other studies. In general, using these freely accessible data inheres several limitations and uncertainties in general that have partly not even been quantified yet. Therefore, estimations based on them have to be used with caution in view of their deficiencies. In combining the different data sets with their respective limitations in data quality, the deficiencies become even more complex and less quantified. Also, the order of magnitude of potential deviations may change and results may not be as comparable e.g. absolute changes of general soil CO_2 emissions over time may range in a different order of magnitude than the changes over time of the thawing-induced soil CO_2 emissions in absolute numbers. In adding them up to total soil CO_2 emissions, this difference is less obvious and the results need to be interpreted carefully. However, on a regional scale as well as for exploratory investigations, the individual data sets are considered both

appropriate and advantageous as highly efficient suppliers of area-explicit data at a high resolution. As the combination of these freely accessible data sets even increases the inaccuracies of the results, they, as a matter of principle, cannot reach the precision of using a fully consistent data set. This approach obtains its appropriateness in view of the early stage of this research area together with its relevance to the vital problem of climate change necessitating results in a timely manner, and other approaches still being highly uncertain as well. Thereby, the high potential of freely accessible data to answer questions alike is strongly indicated. Although in terms of spatial resolution and standardization of methods they remain deficient, freely available data constitute a highly promising source especially for the addressing of problems needing a fast, facile, and low-cost estimate. Fields of research at an early stage, remote study areas with a high data scarcity or pilot schemes are naturally predestinated to operate with freely accessible databases.

However, the discussion shows that the results do not reflect the complexity of the phenomenon soil CO_2 emissions with high variability over space and time. It is further revealed that the results are, although reasonable, still highly uncertain.

The application of empirical regression models, has once more proven to be generally capable to deliver reasonable results, also for soil CO_2 emissions. Although soil CO_2 emission is a complex phenomenon, numerous studies, especially for large scales, have used very simple, many times solely climate-driven models to estimate soil CO_2 emissions (Raich and Schlesinger 1992; Raich et al., 2002). The simplification of this process inheres, however, a number of uncertainties, why these models have to be used with caution. Moreover, the transferability to other regions from the one the model has been developed for, inheres particular difficulties as climate and environment and the various factors involved typically differ. Nevertheless, with accepting a lower degree of precision, concentrating on the main patterns, empirical models still can be applied for other regions than the one it was developed for. Especially in combination of a data-scarce area where high precision is an unfeasible goal, empirical regression models are a method of choice. Also, for an efficient general or preliminary estimate, empirical models are in a diagnostic sense highly useful and the most suitable instruments at present as indicating basic patterns.

In general, the results show the high influence of climate change on soil CO_2 emissions. Especially for the PF areas, the amount of CO_2 being released to the

atmosphere reaches dimensions that clearly direct all efforts of mitigating climate change to strengthen. The amount of CO_2 releases from the PFS of the Qinghai-Tibet Plateau due to thawing is about 1.92% of the global anthropogenic emissions [7.8 Pg C $year^{-1}$ (IPCC, 2013)], pointing to the importance of PF areas on earth. Even though parts of the increased CO_2 emissions are supposed to be neutralized by a higher plant uptake, it is still important to consider that those soil CO_2 emissions are affected by climate change as well. This is important when measuring soil CO_2 emissions and interpreting the results as only parts of those emissions are being expected to be compensated inherent to the system and naturally within human timescales. Further, even if total soil CO_2 emissions do not alter strongly, depending on the share of its components, as e.g. PF thaw-induced CO_2 emissions, the impact on climate change might still be huge.

The Qinghai-Tibet Plateau is further well known as climate-sensitive region, which is confirmed by the results of this thesis. The thawing of PFS releases large quantities of CO_2 potentially accelerating climate change in turn. The large PF region on the Plateau together with its high sensitivity to global warming contribute to a remarkable extend to the atmospheric CO_2 budget.

To sum up, these potential soil CO_2 emissions from PFS on the Qinghai likely do not meet the degree of precision to be expected after further research and improved methodology. However, they indicate the large quantities of soil CO_2 emissions from the PF on the Qinghai-Tibet Plateau that could be transferred to the atmosphere and seriously impact global change.

9 Conclusions and Outlook

CO_2 emissions from soils on the Qinghai-Tibet Plateau potentially increase atmospheric CO_2 concentration, thus accelerating climate change. Although the estimates of this thesis are subject to several constraints, potential CO_2 emissions from those PFS range within an order of magnitude that appeals for strategies to reduce those CO_2 emissions. However, the main increase of soil CO_2 emissions on the Qinghai-Tibet Plateau results from global warming itself, indicating the importance of both national and international political solutions to manage anthropogenic CO_2 emissions in order to mitigate global warming. Regarding general CO_2 emissions from soils, altered land management practices support their reduction. Zero tillage, augmenting perennial grasses, preferring more manure from plant residues, crop rotations and especially changed grazing patterns (i.e., grazing in short rotation) decrease soil CO_2 emissions (Smith et al., 1997; Falloon et al., 2002; Mangalassery et al., 2014). In order to implement these strategies tightly focused, further research is needed to enhance the knowledge about the strength and time scales of those effects that are likely to vary spatially.

While this thesis confirms the meaning of the Qinghai-Tibetan Plateau for soil CO_2 emissions, there is still a lack of more precise knowledge about the amount of soil CO_2 emissions as least understood part in the global C cycle. Further research therefore should mainly target on improving models to reduce the limitations of estimates. Empirical models best are developed region-specific to address their particular characteristics as e.g. a prominence of PF. Further, models should be developed on different timescales to account for the variation of the controlling factors and their respective varying impact across scales of time. Differentiating between vegetation and ecosystem types would be of high importance for models especially when targeting the regional scale as naturally heterogenous area. With soil properties largely influencing soil CO_2 emissions, soil-specific models would increase the accuracy of approximations. According to the impact of topographic features, models could further increase their predictability if developed differentiated according to e.g. exposition.

This thesis confirms the influence of global warming on soil CO_2 emissions, however, this complex influence is not yet sufficiently understood. Contradicting results from different studies indicate the need to investigate the controlling factors of the sensitivity of general soil CO_2 emissions to climate change. With regard to the influence changing

over time, investigations should be carried out across different scales of time. Further, as the response to climate warming varies spatially, areas should be targeted specifically e.g. according to their degree of humidity and temperature.

Soil CO_2 emissions induced by the thaw of PF are quantitatively the most important part of soil CO_2 emissions relevant to climate change. Thus, the decomposition of PF C responding to future climate warming should be explicitly incorporated into current models predicting future global warming. Moreover, further research on this phenomenon is needed as, to date, only a small amount of data and experiments on the PF C release induced by warming exist. Modeling this process differentiated e.g. according to soil type respectively to the content of organic and mineral compartments could provide more accurate insights about the amount released.

Present freely accessible data are a useful, highly efficient resource in order to calculate a large-scale phenomenon with plausible results in a fine resolution. However, the databases still lack of a general higher spatial precision and a homogenous data basis. Especially poorly sampled regions require more data acquisition efforts to enhance the accuracy of the data sets and increase the spatial resolution. Objects of research that have not been well-investigated yet or still lack of the development of elaborated methods with high requirements for input data may benefit most from those data with regard to time and cost.

Empirical regression models provide a high potential to reasonably estimate complex processes even when applied not region-specific as this thesis indicates. Especially in view of the limitations of process-based models, empirical regression models are highly promising.

To sum up, as exemplified in this thesis, highly unknown, complex and under-investigated, yet highly relevant large-scale phenomena can be both efficiently and reasonably quantified by means of simple regression models and freely accessible data. Especially when targeting on preliminary results, this approach inheres strong advantages in terms of efficiency.

Finally, the results of this thesis provide information on an areawide future soil C loss under climate change scenarios on the Qinghai-Tibet Plateau. The results further support in identifying potential sources and sinks of C and in an enhanced

understanding of the role of the PF C on the Qinghai-Tibet Plateau in the global C cycle in view of and under the influence of climate change.

10 References

Adams, J. M. and Post, W. M., 1999. A preliminary estimate of changing calcrete carbon storage on land since the Last Glacial Maximum. Global Planetary Change 20, 243-256.

Atkin, O.K., Edwards, E.J., Loveys, B.R., 2000. Response of root respiration to changes in temperature and its relevance to global warming. New Phytologist 147, 141-154.

Babel, W., Biermann, T., Coners, H., Falge, E., Seeber, E., Ingrisch, J., Schleuß, P.-M., Gerken, T., Leonbacher, J., Leipold, Willinghöfer, S., Schützenmeister, K., Shibistova, O., Becker, L., Hafner, S., Spielvogel, S., Li, X., Xu, X., Sun, Y., Zhang, L., Yang, Y., Ma, Y., Wesche, K., Graf, H.-F., Leuschner, C., Guggenberger, G., Kuzyakov, Y., Miehe, G., Foken, 2014. Pasture degradation modifies the water and carbon cycles of the Tibetan highlands. Biogeosciences 11, 6633-6656.

Bahn, M., Reichstein, M., Davidson, E.A., Grünzweig, J., Jung, M., Carbone, M.S., Epron, D., Misson, L., Nouvellon, Y., Roupsard, Savage, K., Trumbore, S.E., Gimeno, C., Curiel Yuste, J., Tang, J., Vargas, R., Janssens, I.A., 2010. Soil respiration at meant annual temperature predicts annual total across vegetation types and biomes. Biogeosciences 7, 2147-2157.

Batjes, N.H., 2015. World soil propertiy estimates for broad-scale modelling (WISE30sec). Report 2015/01, ISRIC – World Soil Information, Wageningen.

Batjes, N.H., 2002. Soil parameter estimates for the soil types of the world for use in global and regional modelling (Version 2.1). ISRIC Report 2002/02c, International Food Policy Research Institute (IFPRI) and International Soil Reference and Information Centre (ISRIC), Wageningen. Available at:

http://www.isric.org/isric/webdocs/Docs/ISRIC_Report_2002_02c.pdf; accessed 12/2008., 58 p.

Batjes, N.H., 1999. Soil vulnerability mapping in Central and Eastern Europe: Issues of data acquisition, quality control and sharing. In: Naff, T. (Ed.), Data Sharing for International Water Resource Management: Eastern Europe, Russia and the

CIS. NATO Science Series 2: Environmental Security (Vol. 61). Kluwer Academic Publishers, Dordrecht, pp 187-206.

Batjes, N.H., 1996. Total carbon and nitrogen in the soils of the world. European Journal of Soil Science. 47, 151-163.

Baumann, F., Schmidt, K., Doerfer, C., He, J.-S., Scholten, T., Kühn, P., 2014. Pedogenesis, permafrost, substrate and topography: plot and landscape scale interrelations of weathering processes on the central-eastern Tibetan Plateau. Geoderma 226-227, 300-316.

Behera, N., Joshi, S.K., Pati, D.P., 1990. Root contribution to total soil metabolism in a tropical forest soil from Orissa, India. Forest Ecology and Management 36, 125-134.

Behrens T., Schmidt K., Zhu A.X., Scholten T., 2010. The ConMap approach for terrain-based digital soil mapping. European Journal of Soil Science 61, 133–143.

Behrens T., Scholten T., 2006. Digital soil mapping in Germany – a review. Journal of Plant Nutrition and Soil Science 169, 434–443.

Ben-Asher, J., Cardon, G.E., Peters, D., Rolston, D.E., Biggar, J.W., Phene, C.J., Ephrath, J.E., 1994. Determining root activity distribution by measuring surface carbon dioxide fluxes. Soil Science Society of America Journal 58, 926-930.

Birch, H.F., 1958. The effect of soil drying on humus decomposition and nitrogen availability. Plant and Soil 10, 9-31.

Blume, H.P., Brümmer, G.W., Horn, R., Kandeler, E., Kögel-Knabner, I., Kretzschmar, R., Stahr, K., Wilke, B.M., 2010. Scheffer/Schachtschabel: Lehrbuch der Bodenkunde. Spektrum Akademischer Verlag, Berlin.

Böhner, J., 2006. General climatic controls and topoclimatic variations in Central and High Asia. Boreas 35, 279-295.

Böhner, J., Lehmkuhl, F., 2005. Environmental change modelling for Central and High Asia: Pleistocene, present and future scenarios. Boreas 34, 220-231.

Bond-Lamberty, B., Thomson, A., 2010a. Temperature-associated increases in the global soil respiration record. Nature 464, 579-582.

Bond-Lamberty, B., Thomson, A., 2010b. A global database of soil respiration data. Biogeosciences 7, 1915-1926.

Boone, R.D., Nadelhoffer, K.J., Canary, J.D., Kaye, J.P., 1998. Roots exert a strong influence on the temperature sensitivity of soil respiration. Nature 396, 570-572.

Boudot, J.P. Bel Hadj, B.A., Chone, T., 1986. Carbon mineralization in andosols and aluminiumrich highland soils. Soil Biology and Biochemistry 18, 457-461.

Bouma, T.J., Nielsen, K.L., Eissenstata, D.M., Lynch, J.P., 1997. Estimating respiration of roots in soil, interactions with soil CO_2, soil temperature and soil water content. Plant and Soil 227, 215-221.

Bradford, M.A., Christian, A.D., Serita, D.F., Maddox,, T.R., Melillo, J.M., Mohan, J.E., Reynolds, J.F., Treseder, K.K., Wallenstein, M.D., 2008. Thermal adaption of soil microbial respiration to elevated temperature. Ecology Letters 11, 1316-1327.

Brevik, E.C., 2012. Soils and climate change: Gas fluxes and soil processes. Soil Horizons 53, 12-23.

Bunnell, F.L., Tait, D.E.N., Flanagan, P.W., van Cleve, K., 1977. Microbial respiration and substrate weight loss. I. A general model of the influences of abiotic variables. Soil Biology and Biochemistry 9, 33-40.

Buyanovsky, G.A., Wagner, G.H., Gantzer, C.J., 1986. Soil respiration in a winter wheat ecosystem. Soil Science Society of America Journal 50, 338-344.

Cairns, M.A., Brown, S., Helmer, E.H., Baumgardner, G.A., 1997. Root biomass allocation in the world´s upland forests. Oecologia 111, 1-11.

Cao, G., Tang, Y., Mo, W., Wang, Y., Li, Y., Zhao, x., 2004. Grazing intensity alters soil respiration in an alpine meadow on the Tibetan plateau. Soil Biology and Biochemistry 36, 237-243.

Carlyle, J.C., Than, U.B., 1988. Abiotic controls of soil respiration beneath an eighteen-year-old *Pinus radiate* stand in south-eastern Australia. Journal of Ecology 76, 654-62.

Carvalhais, N., Forkel, M., Khomik, M., Bellarby, J., Jung, M., Migliavacca, M., Mu, m:, Saatchi, S., Santoro, S., Santoro, M., Thurner, M., Weber, U., Ahrens, B., Beer, C., Cescatti, A., Randerson, J.T., Reichstein, M., 2014. Global covariation of carbon turnover times with climate in terrestrial ecosystems. Nature 514, 213-217.

Chang, D.H.S., 1981. The vegetation zonation of the Tibetan Plateau. Mountain Research and Development 1, 29–48.

Chapin III, F.S., Sturm, M., Serreze, M.C., McFadden, J.P., Key, J.R., Lloyd, A.H., McGuire, A.D., Rupp, T.S., Lynch, A. H., Schimel, J.P., Beringer, J., Chapman, W.L., Epstein, H.E., Euskirchen, E. S., Hinzman, L.D., Jia, G., Ping, C.-L., Tape, K.D., Thompson, C.D.C., Walker, D.A., Welker, J.M., 2005. Role of land-surface changes in Arctic summer warming. Science 310, 657–660.

Chapman, S.J., Thurlow, M., 1998. Peat respiration at low temperatures. Soil Biology and Biochemistry 30, 1013–1021.

Chen, H., Harmon, M.E., Griffiths, R.P., Hicks, W., 2000. Effects of temperature and moisture on carbon respiraed from decomposing woody roots. Forest Ecology and Management 138, 51-64.

Chen, X., Post, W., Norby, R., Classen, A., 2010. Modeling soil respiration and variations in source components using a multi-factor global climate change experiment. Climatic Change, 1-22.

Chen, Y., Luo, J., Li, W., Dong, Y., She, J., 2014. Comparison of soil respiration among three different subalpine ecosystems on eastern Tibetan Plateau, China. Soil Science and Plant Nutrition 60, 231-241.

Cheng, G., 2005. Permafrost studies in the Qinghai-Tibet Plateau for road construction. Journal of Cold Regions Engineering 19, 19-29.

Cheng, G., Wu, T., 2007. Responses of permafrost to climate change and their environmental significance, Qinghai-Tibet Plateau. Journal of Geophysical Research. 112 (F2).

Cheng, G., Jin, H., 2013. Permafrost and groundwater on the Qinghai-Tibet Plateau and in northeast China. Hydrogeology Journal 21, 5-23.

Chimner, R.A., 2004. Soil respiration rates of tropical peatlands in Micronesia and Hawaii. Wetlands 24, 51-56.

Christensen, J.H., Hewitson, B., Busuioc, A., Chen, A., Gao, X., Held, I., Jones, R., Kolli, R.K., Kwon, W.T., Laprise, R., Rueda, V. M., Mearns, L., Menéndez, Räisänen, J., Rinke, A., Sarr, A., Whetton, P., 2007. Regional Climate Projections. In: Solomon, S., Qin, D., Manning, M., Chen, Z., Marquis, M., Averyt, K.B., Tignor, M., Miller, H.L. (Eds.), Climate Change 2007: The Physical Science Basis. Contribution of Working Group I to the Fourth Assessment Report of the Intergovernmental Panel on Climate Change. Cambridge University Press, Cambridge, pp. 848-940.

Cook, F.J., Thomas, S.M., Kelliher, F.M., Whitehead, D., 1998. A model of one-dimensional steady-state carbon dioxide diffusion from soil. Ecological Modelling 109, 155-164.

Cox, P.M., Betts, R.A., Jones, C.D., Steven, A. S., Totterdell, J., 2000. Acceleration of global warming due to carbon-cycle feedbacks in a coupled climate model. Nature 408, 184-187.

Cui, S., Zhu, X., Wang, S., Zhang, Z., Xu, B., Luo, C., Zhao, L., Zhao, X., 2004. Effects of seasonal grazing on soil respiration in an alpine meadow on the Tibetan plateau. Soil Use and Management 30, 435-443.

Curiel Yuste, J., Janssens, I.A., Carrara, A., Meiresonne, L., Ceulemans, R., 2003. Interactive effects of temperature and precipitation on soil respiration in a temperate maritime pine forest. Tree Physiology 23, 1263-1270.

Curiel Yuste, J., Janssens, I.A., Ceulemans, R., 2005. Calibration and validation of an empirical approach to model soil CO_2 efflux in a deciduous forest. Biogeochemistry 73, 209-230.

Davidson, E.A., Belk, E., Boone, R.D., 1998. Soil water content and temperature as independent or confound factors controlling soil respiration in a temperature mixed hardwood forest. Global Change Biology 4, 217-227.

Davidson, E.A., Verchot, L.V., Cattanio, J.H., Ackermann, I.L., Carvalho, J.E.M., 2000. Effects of soil water content on soil respiration in forests and cattle pastures of eastern Amazonia. Biogeochemistry 48, 53-69.

Davidson, E.A., Janssens, I. A., 2006. Temperature sensitivity of soil carbon decomposition and feedbacks to climate change. Nature 440, 165-173.

Davidson, E.A., Janssens, I.A., Luo, Y., 2006. On the variability of respiration in terrestrial ecosystems: moving beyong Q_{10}. Global Change Biology 12, 154-164.

Davidson, E.A., Stark, J.M., Firestone, M.K., 1990. Microbial production and consumption of nitrate in an annual grassland. Ecology 71, 1968-1975.

Dee, D. P., Balmaseda, M., Balsamo, G., Engelen, R., Simmons, A. J., Thepaut, J.-N., 2014. Towards a consistent reanalysis of the climate system, Bulletin of the American Meteorological Society 95, 1235–1248.

del Grosso, S.J., Parton, W.J., Mosier, A.R., Holland, E.A., Pendall, E., Schimel, D.S., Ojima, D.S., 2005. Modeling soil CO_2 emissions from ecosystems. Biogeochemistry 73, 71-91.

Dietze, E., Hartmann, K., Diekmann, B., Ijmker, J., Lehmkuhl, F., Opitz, S., Stauch, G., Wunnemann, B., Borchers, A., 2012. An end-member algorithm for deciphering modern detrital processes from lake sediments of Lake Donggi Cona, NE Tibetan Plateau, China. Sedimentary Geology 243-244, 169–180.

Ding, J., Li, F., Yang, G., Chen, L., Zhang, B., Liu, L., Fang, K., Qin, S., Chen, Y., Peng, Y., Ji, C., He, H., Smith, P., Yang, Y., 2016. The permafrost carbon inventory on the Tibetan Plateau: a new evaluation using deep sediment cores. Global Change Biology 22, 2688-2701.

Domrös, M., Peng, G., 1988. The Climate of China. Springer-Verlag, Berlin.

Doerfer, C., Kuehn, P., Baumann, F., He, J.-S., Scholten, T., 2013. Soil organic carbon pools and stocks in permafrost-affected soils on the Tibetan Plateau. PLoS ONE 8(2): e57024.

Dörr, H., Münnich, K.O., 1987. Annual variation in soil respiration in selected areas of the temperate zone. Tellus 39B, 114-121.

Dunne, J., Harte, J., Taylor, K., 2003. Subalpine meadow flowering phenology responses to climate change: integrating experimental and gradient methods. Ecological Monograph 73, 69-86.

Dutta, K., Schurr, E.A.G., Neff, J.C., Zimov, S.A., 2006. Potential carbon release from permafrost soils of Northeastern Sibiria. Global Change Biology 12, 2336-2351.

Eamus, D., Chen, X., Kelley, E., Hutley, L.B., 2002. Root biomass and root fractional analyses of an open *Eucalyptus* forest in a savanna of north Australia. Australian Journal of Botany 50, 31-41.

Elberling, B., Michelsen, A., Schädel, C., Schuur, E.A.G., Christiansen, H.H., Berg, L., Tamstorf, M.P., Sigsgaard, C., 2013. Long-term CO_2 production following permafrost thaw. Nature Climate Change 3, 890-894.

Epron, D., Nouvellon, Y., Roupsard, O., Mouvondy, W., Mabiala, A., Saint-André, L., Joffre, R., Jourdan, C., Bonnefond, J.M., Berbigier, P., Hamel, O., 2004. Spatial and temporal variation of soil respiration in a *Eucalyptus* plantation in Congo. Forest Ecology and Management 202, 149-160.

Epron, D., Farque, D., Lucot, É., Badot, P.-M., 1999. Soil CO_2 efflux in a beech forest. Dependence on soil temperature and soil water content. Annals of Forest Science 56, 221-226.

Ewel, K.C., Cropper, W.P., Gholz, H.L.Jr, 1987. Soil CO_2 evolution in Florida slash pine plantation: I, Changes through time. Canadian Journal of Forest research 17, 330-333.

Falloon, P., Smith, P., Szabó, J., Pásztor, L., 2002. Comparison of approaches for estimating carbon sequestration at the regional scale. Soil Use and Management 18, 164-174.

Fan, J.-W., Shao, Q.-Q., Liu, J.-Y., Wang, J.-B., Harris, W., Chen, Z.-Q., Zhong, H.-P., Xu, X.-L., Liu, R.-G., 2010. Assessment of effects of climate change and grazing activity on grassland yield in the Three Rivers Headwaters Region of Qinghai-Tibet Plateau, China. Environmental Monitoring and Assessment 170, 571–584.

Fang, C., Moncrieff, J.B., 2001. The dependence of soil CO_2 efflux on temperature. Soil Biology and Biochemistry 33, 155-165.

Fang, C., Moncrieff, J.B., Gholz, H.L. Clark, K.L., 1998. Soil CO_2 efflux and its spatial variation in a Florida slash pine plantation. Plant and Soil 205, 135-146.

FAO/IIASA/ISRIC/ISSCAS/JRC, 2012. Harmonized World Soil Database (version 1.2). Luxemburg, Rome, Italy, IIASA, FAO.

Fernandez, D.P., Neff, J.C., Belnap, J., Reynolds, R.L., 2006. Soil respiration in the cold desert environment of the Colorado Plateau (USA): abiotic regulators and thresholds. Biogeochemistry 78, 247-265.

Frank, A.B., Liebig, M.A., Hanson, J.D., 2002. Soil carbon dioxide fluxes in northern semiarid grasslands. Soil Biology and Biochemistry 34, 1235-1241.

Fung, I.Y., Tucker, C. J., Prentice, K.C., 1987. Application of advanced very high resolution radiometer vegetation index to study atmosphere-biosphere exchange of CO_2. Journal of Geophysical Research 92, 2999-3015.

Geng, Y., Wang, Y., Yang, K., Wang, S., Zeng, H., Baumann, F., Kuehn, P., Scholten, T., He, J.-S., 2012. Soil Respiration in Tibetan alpine grasslands: belowground biomass and soil moisture, but not soil temperature, best explain the large-scale patterns. PLoS ONE 7, 1-12.

Gent, P. R., Danabasoglu, G., Donner, L.J., Holland, M.M., Hunke, E.C., Jayne, S.R., Lawrence, D.M., Neale, R.B., Rasch, P.J., Vertenstein, M., Worley, P.H., Yang, Z.-L., Zhang, M., 2011. The Community Climate System Model Version 4. Journal of Climatology 24, 4973-4991.

Genxu, W., Qian, J., Cheng, G., Lai, Y., 2002. Soil organic carbon pool of grassland soil son the Qinghai-Tibetan Plateau and its global implication. The Science of the Total Environment 291, 207-217.

Glinski, J., Stepniewski, W., 1985. Soil aeration and its role for plants. CRC Press, Boca Raton.

Goulden, M.L., Wofsy, S.C., Harden, J.W., Trumbore, S.E., Crill, P.M., Gower, S.T., Fires, T., Daube, B., Fan, S. M., Sutton, D.J., Bazzaz, A., Munger, J.W., 1998. Sensitivity of boreal forest carbon balance to soil thaw. Science 279, 214-217.

Griffin, K.L., Ross, P.D., Sims, D.A., Luo, V., Seemann, J.R., Fox, C. A., Ball, J.T., 1996. EcoCELLs, tools for mesocosm scale measurements of gas exchange. Plant, Cell and Environment 18, 1210-1221.

Grogan, P., Chapin, F.S., 1999. Arctic soil respiration: Effects of climate and vegetation depend on season. Ecosystems 5, 451-459.

Gruber, S., 2012. Derivation and analysis of a high-resolution estimate of global permafrost zonation. The Cryosphere 6, 221-233.

Gulledge, J., Schimel, J.P., 2000. Controls on soil carbon dioxide and methane fluxes in a variety of taiga forest stands in interior Alaska. Ecosystems 3, 269-282.

Gupta, S.R., Singh, J.S., 1981. Soil respiration in a tropical grassland. Soil Biology and Biochemistry 13, 261-268.

Han, G., Zhou, G., Xu, Z., Yang, Y., Liu, J., Shi, K., 2007. Biotic and abiotic factors controlling the spatial and temporal variation of soil respiration in an agricultural ecosystem. Soil Biology and Biochemistry 39, 418-425.

Hanson, P.J., Wullschleger, S.D., Bohlman, S.A., Todd, D.E, 1993. Seasonal and topographic patterns of forest floor CO_2 efflux from and upland oak forest. Tree Physiology 13, 1-15.

Hao, Q., Jiang, C., 2014. Contribution of root respiration to soil respiration in a rape (*Brassica campestris* L.) field in Southwest China. Plant Soil Environment 60, 8-14.

Harden, J.W., Sundquist, E.T., Stallard, R.F., Mark, R.K., 1992. Dynamics of soil carbon during deglaciation of the Laurentide Ice Sheet. Science 258, 1921-1924.

Harden, J.W., Koven, C.D., Ping, C.-L., Hugelius, G., McGuire, A.D., Camill, P., Jorgenson, T., Kuhry, P., Michaelson, G.J., O´Donnell, J.A., Schuur, E.A.G., Tarnocai, C., Johnsons, K., Grosse, G., 2012. Field information links permafrost carbon to physical vulnerabilities of thawing. Geophysical Research Letters 39, L15704.

Harper, C.W., Blair, J.M., Fay, P.A., Knap, A.K., Carlisle, J.D., 2005. Increased rainfall variability and reduced rainfall amount decreases soil CO_2 flux in a grassland ecosystem. Global Change Biology 11, 322-334.

Harris, N., 2006. The elevation history of the Tibetan Plateau and its implications for the Asian monsoon. Palaeogeography, Palaeoclimatology, Palaeoecology 241 (1), 4–15.

Harris, R.F., 1981. Effect of water potential on microbial growth and activity. In: Water potential relations in soil microbiology. J.F. Parr, W.R. Gardner, L.F. Elliott (Eds.). Soil Science Society of America, Madison, WI, USA, pp. 23-95.

Harte, J., Torn, M.S., Chang, F.R., Feifarek, B., Kinzig, A.P., Shaw, R., Shen, K., 1995. Global warming and soil microclimate: results from a meadow-warming experiment. Ecological Applications 5, 132-150.

Hashimoto, S., Carvalhais, N., Ito, A., Migliavacca, M., Nishina, K., Reichstein, M., 2015. Global spatiotemporal distribution of soil respiration modeled using a global databse. Biogeosciences 12, 4121-4132.

Hertel, T. W, Britz, W., Diffenbaugh, N.S., Ramankutty N., Villoria, N.B., 2010. A global, spatially explicit, open source data base for analysis of agriculture, forestry, and the environment: Proposal and institutional considerations. Department of Agricultural Economics, Purdue University. http://www.agecon.purdue.edu/foresight/proposal_spatial_database10-15-2010.pdf accessed 5/2016.

Hibbard, K.A., Law, B.E., Reichstein, M., Sulzman, J., 2005. An analysis of soil respiration across northern hemisphere temperate ecosystems. Biogeochemistry 73, 29-70.

Hicks Pries, C. E., Schuur, E.A.G., Crummer, K. G., 2012. Holocene Carbon stocks and carbon accumulation rates altered in soils undergoing permafrost thaw. Ecosystems 15, 162-173.

Hicks Pries, C., Schuur, E.A.G., Crummer, K.G., 2013. Thawing permafrost increases old soil and autotrophic respiration in tundra: partitioning ecosystem respiration using $\delta^{13}C$ and $\Delta^{14}C$. Global Change Biology 19, 649-661.

Higgins, P.A.T., Jackson, R.B., des Rosiers, J.M., Field, C.B., 2002. Root production and demography in a California annual grassland under elevated atmospheric carbon dioxide. Global Change Biology 8, 841-850.

Hijmans, R. J., Cameron, S.E., Parra, J.L., Jones, P.G., Jarvis, A., 2005. Very high resolution interpolated climate surfaces for global land areas. International Journal of Climatology 25, 1965-1978.

Högberg, P-. Nordgren, A., Buchmann, N., Taylor, A.F.S., Ekblad, A., Högberg, M.N., Nyberg, G., Ottosson-Löfvenius, M., Read, D.J., 2001. Large-scale forest girdling shows that current photosynthesis drives soil respiration. Nature 411, 789-792.

Holthausen, R.S., Caldwell, M.M., 1980. Seasonal dynamics of root system respiration in *Atriplex confertifolia*. Plant and Soil 55, 307-317.

Hövermann, J., Lehmkuhl, F., 1994. Vorzeitliche und rezente geomorphologische Hohenstufen in Ost- und Zentraltibet. Gottinger Geographische Abhandlungen 95, 15–69.

Hu, H., Wang, G., Liu, G., Li, T., Ren, D., Wang, Y., Cheng, H., Wang, J., 2009. Influences of alpine ecosystem degradation on soil temperature in the freezing-thawing process on Qinghai– Tibet Plateau. Environmental Geology 57, 1391–1397.

Huang, N., Zheng, N., 2013. Estimating soil respiration using spectral vegetation indices and abiotic factors in irrigated and rainfeld agroecosystems. Plant and Soil 367, 535-550.

Immerzeel, W., Quiroz, R., Jong, S., 2005. Understanding precipitation patterns and land use interaction in Tibet using harmonic analysis of SPOT VGT-S10 NDVI time series. International Journal of Remote Sensing 26, 2281–2296.

IPCC, 2013. Climate change 2013: The physical science basis. Contribution of working group I to the fifth assessment report of the Intergovernmental Panel on Climate Change (Stocker, T.F., D. Qin, G.-K. Plattner, M. Tignor, S.K. Allen, J. Boschung, A. Nauels, Y. Xia, V. Bex and P.M. Midgley (Eds.)). Cambridge University Press, Cambridge, United Kingdom and New York, NY, USA.

IUSS Working Group WRB, 2006. World reference base for soil resources. World Soil Resources Reports (103).

Jackson, R.B., Sala, O.E., Paruelo, J.M., Mooney, H.A., 1998. Ecosystem water fluxes for two grasslands in elevated CO_2: a modeling analysis. Oecologia 113, 537-546.

Janssens, I.A., Lankreijer, H., Matteucci, G., Kowalski, A.S., Buchmann, N., Epron, D., Pilegaard, K., Kutsch, W., Longdoz, B., Grünwald, T., Montagnani, l., Dore, S., Rebmann, C., Moors, E.J., Grelle, A., Rannik, Ü., Morgenstern, K., Oltchev, S., Clement, R., Guomundsson, J., Minerbi, S., Berbigier, P., Ibrom, A., Moncrieff, J., Aubinet, M., Bernhofer, C., Jensen, N.O., Vesala, T., Granier, A., Schulze, E.-D., Lindroth, A., Dolman, A.J., Jarvis, P.G., Ceulemans, R., Valentini, R., 2001. Productivity overshadows temperature in determining soil and ecosystem respiration across European forests. Global Change Biology 7, 269-278.

Jia, B., Zhou, G., Wang, Y., Wang, F., Wang, X., 2006. Effects of temperature and soil water-content on soil respiration of grazed and ungrazed Leymus chinensis steppes, Inner Mongolia. Journal of Arid Environments 67, 60-76.

Jin, H., Li, S., Cheng, G., Shaoling, W., Li, X., 2000. Permafrost and climatic change in China. Global and Planetary Change 26, 387–404.

Johnson, L.C., Matchett, J.R., 2001. Fire and grazing regulate belowground processes in a tallgrass prairie. Ecology 82, 3377-3389.

Jones, C.D., Cox, P.M., Essery, R.L.H., Roberts, *D.L.,* Woodage, M.J., 2003. Strong carbon cycle feedbacks in a climate model with interactive CO_2 and sulphate aerosols. Geophysical Research Letter 30.

Joo, S.J., Park, S.-U., Park, M.-S., Lee, C.S., 2012. Estimation of soil respiration using automatic chamber systems in an oak (*Quercus mongolica*) forest at the Nam-San site in Seoul, Korea.

Kaiser, K., Miehe, G., Barthelmes, A., Ehrmann, O., Scharf, A., Schult, M., Schlutz, F., Adamczyk, S., Frenzel, B., 2008. Turf-bearing topsoils on the central Tibetan Plateau, China: Pedology, botany, geochronology. Catena 73 (3), 300–311.

Kaiser, K., Schoch, W.H., Miehe, G., 2007. Holocene paleosols and colluvial sediments in Northeast Tibet (Qinghai Province, China): Properties, dating and paleoenvironmental implications. Catena 69 (2), 91–102.

Kang, S., Xu, Y., You, Q., Flügel, W.-A., Pepin, N., Yao, T., 2010. Review of climate and cryospheric change in the Tibetan Plateau. Environmental Research Letters 5, 1-8.

Kang, S., Doh, S., Lee, D.S. Lee, D. Jin, V.L., Kimball, J.S., 2003. Topographic and climatic controls on soil respiration in six temperate mixed-hardwood forest slopes, Korea. Global Change Biology 9, 1427-1437.

Kato, T., Hirota, M., Tang, Y., Cui, X., Li, Y., Zhao, X., Oikawa, T., 2005. Strong temperature dependence and no mos photosynthesis in winter CO_2 flux for a *Kobresia* meadow on the Qinghai-Tibetan plateau. Soil Biology and Biochemistry 37, 1966-1969.

Keith, H., Jacobsen, K.L., Raison, R.J., 1997. Effects of soil phosphorus availability, temperature and moisture on soil respiration in Eucalyptus pauciflora forest. Plant and Soil 190, 127-141.

King, J.S., Hanson, P.J., Bernhardt, E.Y., Deangelis, P., Norby, R.J., Pregitzer, K.S., 2004. A multiyear synthesis of soil respiration responses to elevated atmospheric CO_2 from four forest FACE experiments. Global Change Biology 10, 1027-1042.

Kirschbaum, M.U.F., 2004. Soil respiration under prolonged soil warming: Are rate reductions caused by acclimation or substrate loss? Global Change Biology 10, 1870-1877.

Kirschbaum M.U.F., 1995. The temperature dependence of soil organic matter decomposition, and the effect of global warming on soil organic storage. Soil Biology and Biochemistry 27, 753-760.

Koizumi, H., Konturi, M., Mariko, S., Nakadai, T., Bekku, Y., Mela, T., 1999. Soil respiration in three soil types in agricultural ecosystems in Finland. Acta Agriculturae Scandinavica, Section B, Plant and Soil 49, 65-74.

Kucera, C. L., Kirkham, D.R., 1971. Soil respiration studies in tallgrass prairie in Missouri. Ecology 52, 912-915.

Kuzyankov, Y., 2006. Sources of CO_2 efflux from soil and review of partitioning methods, Soil Biology and Biochemistry 38, 425-448.

Lavigne, M.B., Foster, R.J., Goodine, G., 2004. Seasonal and annual changes in soil respiration in relation to soil temperature, water potential and trenching. Tree Physiology 24, 415-424.

Lee, M.S., Nakane, K., Nakatsubo, T., Mo, W.H., Koizumi, 2002. Effect of rainfall events on soil CO_2 flux in a cool temperate deciduous broad-leaved forest. Ecological Research 17, 401-409.

Lehmkuhl, F., 1997. The spatial distribution of loess and loess-like sediments in the mountain areas of Central and High Asia. Zeitschrift für Geomorphologie 111, 97–116.

Li, G., Sun, S., 2011. Plant clipping may cause overestimation of soil respiration in a Tibetan alpine meadow, southwest China. Ecological Research 26, 497-504.

Li, X., Zhang, X., Wu, J., Shen, Z., Zhang, Y., Xu, X., Fan, Y., Zhao, Y., Yan, W., 2011. Root biomass distribution in alpine ecosystems of the northern Tibetan Plateau. Environmental Earth Sciences 64, 1911-1919.

Lindroth A, Grelle A., Moren A.S. 1998. Long-term measurements of boreal forest carbon balance reveal large temperature sensitivity. Global Change Biology 4, 443–450.

Linn, D.M., Doran, J.W., 1984. Effects of water-filled pore space on carbon dioxide and nitrous oxide production in tilled and nontilled soil. Soil Science Society of America Journal 48, 1267-1272.

Liu, X., Chen, B., 2000. Climatic warming in the Tibetan Plateau during recent decades. International Journal of Climatology 20, 1729-1742.

Liu, X., Wan, S., Su, B., Hui, D., Luo, Y., 2002. Response of soil CO_2 efflux to water manipulation in a tallgrass prairie ecosystem. Plant and Soil 240, 213-223.

Lloyd, C.R., 2001. The measurement and modelling of the carbon dioxide exchange at a high Arctic site in Svalbard. Global Change Biology 7, 405-426.

Lloyd, J., Taylor, J.A., 1994. On the temperature dependence of soil respiration. Functional Ecology 8, 315-323.

Lomander, A.K., Kätterer, T., Andrén, O., 1998. Modeling the effects of temperature and moisture on CO_2 evolution from top- and subsoil using a multi-compartment approach. Soil Biology and Biochemistry 30, 2023-2030.

Longdoz, B., Yernaux, M., Aubinet, M., 2000. Soil CO_2 efflux measurements in a mixed forest: impact of chamber disturbances, spatial variability and seasonal evolution. Global Change Biology 6, 907-917.

Luo, G.B., Zhang, G.L., Gong, Z.T., 2000. A real evaluation of organic carbon pools in cryic soils of China. In: Lal, R., Kimble, J.M., Stewart, B.A. (Eds.). Global Climate Change and Coil Regions Ecosystems. Advances in Soil Science. Lewis Publishers, Boca Raton, FL, pp. 211–222.

Luo, T., Brown, S., Pan, Y., Shi, P., Ouyang, H., Yu, Z., Zhu, H., 2005. Root biomass along subtropical to alpine gradients: global implication from Tibetan transect studies. Forest Ecology and Management 206. 349-363.

Luo, T., Li, W., Zhu, H., 2002. Estimated biomass and productivity of natural vegetation on the Tibetan Plateau. Ecological Applications 12, 980-997.

Luo, Y., Wan, S., Hui, D., Wallace, L., 2001. Acclimatization of soil respiration to warming in a tall grass prairie. Nature 413, 622-625.

Luo, Y., Zhou, X., 2006. Soil respiration and the environment. Elsevier, San Diego, USA.

Mangalassery, S., Sjögersten, S., Sparkes, D.L., Sturrock, C., Craigon, J., Mooney, S.J., 2014. To what extent can zero tillage lead to reduction in greenhouse gas emissions from temperate soils? Nature 4:4586, 1-8.

Martin, J.G., Bolstad, P.V., 2005. Annual soil respiration in broadleaf forests of northern Wisconsin: influence of moisture and site biological, chemical, and physical characteristics. Biogeochemistry 73, 149-182.

Maussion, F., Scherer, D., Finkelnburg, R., Richter, J., Yang, W., Yao, T., 2011. WRF simulation of a precipitation event over the Tibetan Plateau, China – an assessment using remote sensing and ground observations. Hydrology and Earth System Sciences 15, 1795-1817.

McGuire, A.D., Macdonals, R.W., Schuur, E.A.G., Harden, J., Kuhry, P., Hayes, D.J., Christensen, T.R., Heimann, M., 2010. The carbon budget of the northern cryosphere region. Current Opinion in Environmental Sustainability 2, 231-236.

McGuire, A.D., Melillo, J.M., Kicklighter, D.W., Joyce, L.A., 1995. Equilibrium responses of soil carbon to climate change: Empirical and process-based estimates. Journal of Biogeography 22, 785-796.

Medina, E., Zelwer, M., 1972. Soil respiration in tropical plant communities. In: Papers from a symposium on tropical ecology with an emphasis on organic productivity. Golley, P.M., Golley, F.B. (Eds.). University of Georgia, Athens, GA, pp. 245-269.

Melillo, J.M., Steudler, P.A., Aber, J.D., Newkirk, K., Lux, H., Bowles, F.P. Catricala, C., Magili, A., Ahrens, T., Morrisseau, S., 2002. Soil warming and carbon cycle feedback to the climate system. Science 298, 2173-2176.

Melling, L., Hatano, R., Goh, K.J., 2005. Soil CO_2 flux from three ecosystems in tropical peatland of Sarawak, Malaysia. Tellus 57B, 1-11.

Mielnick, P.C., Dugas, W.A., 2000. Soil CO_2 flux in a tallgrass prairie. Soil Biology and Biochemistry 32, 221-228.

Mokany, K., Raison, R.J., Prokushkin, A.S., 2006. Critical analysis of root:shoot ratios in terrestrial biomes. Global Change Biology 12, 84-96.

Morén, A.-S., Lindroth, A., 2000. CO_2 exchange at the floor of a boreal forest. Agricultural and Forest Meteorology 101, 1-14.

Mu, C., Zhang, T., Wu, Q., Peng, X., Cao, B., Zhang, X., Cao, B., Cheng, G., 2015. Editorial: Organic carbon pools in permafrost regions on the Qinghai-Xizang (Tibetan) Plateau. The Cryosphere 9, 479-486.

Nakadai, T., Yokozawa, M., Ikeda, H., Koizumi, H., 2002. Diurnal changes of carbon dioxide flux from bare soil in agricultural field in Japan. Applied Soil Ecology 19, 161-171.

Nakane, K., 1975. Dynamics of soil organic matter in different parts on a slope under evergreen oak forest. Japanese Journal of Ecology 25, 204-216.

Ni, J., 2002. Carbon storage in grasslands of China. Journal of Arid Environments 50, 205-218.

Niu, F., Lin, Z., Liu, H., Lu, J., 2011. Characteristics of thermokarst lakes and their influence on permafrost in Qinghai–Tibet Plateau. Geomorphology 132 (3-4), 222–233.

Norby, R.J., Hartz-Rubin, J.S., Verbrugge, M.J., 2003. Phenological responses in maple to experimental atmospheric warming and CO_2 enrichmeht. Global Change Biology 9, 1792-1801.

O'Connell, A.M., 1990. Microbial decomposition (respiration) of litter in eucalypt forests of south-western Australia: An empirical model based on laboratory incubations. Soil Biology and Biochemistry 22, 153-160.

Oberbauer, S.F., Gillespie, C.T., Cheng, W., Gebauer, R., Sala Serra, A., Tenhunen, J.D., 1992. Environmental effects of CO_2 efflux from riparian tundra in the northern foothills of the Brooks Range, Alaska. Oecologia 92, 569-577.

Oechel, W.C., Vourlitis, G.L., Hasting, S.J., Bochkarev, S.A., 1995. Change in Arctic CO_2 flux over two decades, Effects of climate change at Barrow, Alaska. Ecological Applications 5, 846-855.

Ohtsuka, T., Hirota, M., Zhang, X., Shimono, A., Senga, Y., Du, M., Yonemura, S., Kawashima, S., Tang, Y., 2008. Soil organic carbon pools in alpine to nival zones along an altitudinal gradient (4400-5300 m) on the Tibetan Plateau. Polar Science 2, 277-285.

Orchard, V. A., Cook, F., 1983. Relationship between soil respiration and soil moisture. Soil Biology and Biochemistry 15, 447-453.

Pang, Q., Zhao, L., Li, S., Ding, Y., 2012. Active layer thickness variations on the Qinghai-Tibet Plateau under the scenarios of climate change. Environmental Earth Sciences 66, 849-857.

Pei, Z.-Y., Ouyang, H., Zhou, C.-P., Xu, X.-L., 2009. Carbon Balance in an Alpine Steppe in the Qinghai-Tibet Plateau. Journal of Integrative Plant Biology 51, 521-526.

Peng, F., Xue, X., You, Q., Zhou, X., Wang, T., 2015. Warming effects on carbon release in a permafrost area of Qinghai-Tibet Plateau. Environmental Earth Sciences 73, 57-66.

Peterjohn, W.T., Melillo, J.M., Steudler, P.A., Newkirk, K.M., Bowles, F.P., Aber, J.D., 1994. Responses of trace gas fluxes and N availability to experimentally elevated soil temperatures. Ecological Applications 4, 617-625.

Peterson, K.M., Billings, W.D., 1975. Carbon dioxide flux from tundra soils and vegetation as related to temperature at Barrow, Alaska. American Midland Naturalist 94, 88-98.

Ping, C.-L., Qiu, G., Zhao, L., 2004. The periglacial environment of China, in: Kimble, J. (Ed.), Cryosols. Permafrost-Affected Soils. Springer, Berlin, pp. 275–291.

Powlson, D.S., Whitmore, A.P., Goulding, W.T., 2011. Soil carbon sequestration to mitigate climate change: a critical re-examination to identify the true and the false. European Journal of Soil Science 62, 42-55.

Puttaso, A., Vityakon, P., Saenjan, P., Treloges, V., Cadisch, G., 2011. Relationship between residue quality, decomposition patterns, and soil organic matter accumulation in a tropical sandy soil after 13 years. Nutrient Cycling in Agroecosystems 89, 159-174.

Qi, Y., Xu, M., Wu, J., 2002. Temperature sensitivity of soil respiration and its effects on ecosystem carbon budget: nonlinearity begets surprises. Ecological Modeling 153, 131-142.

Qiu, J., 2008. The third pole. Nature 454, 393-396.

Raich, J.W., Potter, C.S., 1995. Global patterns of carbon dioxide emissions from soils. Global Biogeochemical Cycles 9, 23-36.

Raich, J.W., Potter, C.S., Bhagawati, D., 2002. Interannual variability in global soil respiration, 1980-94. Global Change Biology 8, 800-812.

Raich, J.W., Schlesinger, W.H., 1992. The global carbon dioxide flux in soil respiration and its relationship to vegetation and climate. Tellus 44B, 81-99.

Raich, J.W., Tufekcioglu, A., 2000. Vegetation and soil respiration: Correlations and controls. Biogeochemistry 48, 71-90.

Ramnarine, R., Wagner-Riddle, C., Dunfield, K.E., Voroney, R.P., 2012. Contributions of carbonates to soil CO_2 emissions. Canadian Journal of Soil Science 92, 599-607.

Ratkowsky, D.A., Olley, J., McMeekin, T.A., Ball, A., 1982. Relationship between temperature and growth rate of bacterial cultures. Journal of Bacteriology 149, 1-5.

Reichstein, M., Beer, C., 2008. Soil respiration across scales: The importance of a model-data integration framework for data interpretation. Journal of Plant Nutrition and Soil Science 171, 344-354.

Reichstein, M., Rey, A., Freibauer, A., Tenhunen, J., Valentini, R., Banza, J., Casals, P., Cheng, Y., Grünzweig, J.M., Irvine, J., Joffre, R., Law, B.E., Loustau, D., Miglietta, F., Oechel, W., Ourcival, J.-M., Pereira, J.S., Peressotti, A., Ponti, F., Qi, Y., Rambal, S., Rayment, M., Romanya, J., Rossi, F., Tedeschi, V., Tirone, G., Xu, M., Yakirs, D., 2003. Modeling temporal and large-scale spatial variability of soil respiration from soil water availability, temperature and vegetation productivity indices. Global Biogeochemical Cycles 17, 1104.

Reiners, W.A., 1968. Carbon dioxide evolution from the floor of three Minnesota Forests. Ecology 49, 471-483.

Reth, S., Reichstein, M., Falge, E., 2005. The effect of soil water content, soil temperature, soil pH-value and the root mass on soil CO_2 efflux – a modified model. Plant and Soil 268, 21-33.

Rey, A., Pegoraro, E., Tedeschi, V., Parri, I.D., Jarvis, P.G., Valentini, R., 2002. Annual variation in soil respiration and its components in a coppice oak forest in central Italy. Global Change Biology 8, 851-866.

Richards, F.J., 1959. A flexible growth function for empirical use. Journal of Experimental Botany 10, 290-300.

Rochette, P., Desjardins, R.L., Pattey, E., 1991. Spatial and temporal variability of soil respiration in agricultural fields. Canadian Journal of Soil Science 71, 189-196.

Rodeghiero, M., Cescatti, A., 2005. Main determinants of forest soil respiration along an elevation/temperature gradient in the Italian Alps. Global Change Biology 11, 1024–1041.

Rodeghiero, M., Churkina, G. Martinez, C., Scholten, T. Gianelle, D., Cescatti. A., 2013. Components of forest soil CO_2 efflux estimated from $\Delta^{14}C$ values of soil organic matter. Plant Soil 364/1, 55-68.

Rotmans, J., den Elzen, M.G.J., 1993. Modelling feedback mechanisms in the carbon cycle: balancing the carbon budget. Tellus 45B, 301-320.

Rovira, P. and Vallejo, V. R., 2008. Changes in ^{13}C composition of soil carbonates driven by organic matter decomposition under Mediterranean climate: a field incubation experiment. Geoderma 144, 517-534.

Rustad, L.E., Campbell, J.L., Marion, G.M., Norby, R.J., Mitchell, M.J., Hartley, A.E., Gurevitch, J., 2001. A meta-analysis of the response of soil respiration, net nitrogen mineralization, and aboveground plant growth to experimental ecosystem warming. Oecologia 126, 543-562.

Rustad, L.E., Fernandez, I.J., 1998. Experimental soil warming effects on CO_2 and CH_4 flux from a low elevation spruce-fir forest soil in Maine, U.S.A. Global Change Biology 4, 597-605.

Ryan, M.G., Hubbard, R.M., Pongracic, S., Raison, R.J., McMurtie, R.E., 1996. Foliage fine-root, woody-tissue and stand respiration in Pinus radiate in relation to nitrogen status. Tree Physiology 16, 333-343.

Sabine, C.,S., Hemann, M., Artaxo, P., Bakker, D., Chen, C.T.A., Field, C.B., Gruber, N., Le Quere, C., Prinn, R.G., Richey, J.E., Romero-Lankao, P., Sathaye, J., Valentini, R., 2003. Current status and past trends of the carbon cycle. In: C.B. Field, M.R. Raupac (Eds.). Toward CO_2 stabilization: Issues, strategies, and consequences. Island Press, Washington, DC, USA.

Saiz, G. Green, C., Butterbach-Bahl, K., Kiese, R., Avitabile, V., Farrell, E. P., 2006. Seasonal and spatial variability of soil respiration in four Sitka spruce stands. Plant and Soil 287, 161-176.

Saleska, S.R., Shaw, M.R., Fischer, M.L., Dunne, J.A., Still, C.J., Holman, M.L., Harte, J., 2002. Plant community composition mediates both large transient decline and predicted long-term recovery of soil carbon under climate warming. Global Biogeochemical Cycles 16, 1055.

Sánchez, M.L., Ozores, M.I., Lo´ pez, M.J., Colle, R., De Torre, B., Garcı´a, M.A., Pe´rez, I., 2003. Soil CO2 fluxes beneath barley on the central Spanish plateau. Agricultural and Forest Meteorology 118, 85–95.

Sanchez, P. A., S. Ahamed, F. Carre, A. E. Hartemink, J. Hempel, J. Huising, P. Lagacherie, A. B. McBratney, N. J. McKenzie, M. d. L. Mendonca-Santos, B. Minasny, L. Montanarella, P. Okoth, C. A. Palm, J. D. Sachs, K. D. Shepherd, T.-G. Vagen, B. Vanlauwe, M. G. Walsh, L. A. Winowiecki, Zhang, G.-L. 2009. Digital Soil Map of the World. Science 325, 680-681.

Savage, K.E., Davidson, E.A., 2001. Interannual variation of soil respiration in two New England forests. Global Biogeochemical Cycles 15, 337-350.

Schaedel, C., Schuur, E.A.G., Bracho, R., Elberling, B., Knoblauch, C., Lee, H., Luo, Y., Shaver, G.R., Turetsky, M.R., 2014. Circumpolar assessment of permafrost C quality and its vulnerability over time using long-term incubation data. Global Change Biology 20, 641-652.

Schaefer, K., Zhang, T., Bruhwiler, L., Barrett, A.P., 2011. Amount and timing of permafrost carbon release in response to climate warming. Tellus 63B, 165-180.

Schimel, D.S., Braswell, B.H., Holland, A.B., McKeown, R., Ojima, D.S., Painter, T.H., Parton, W.J., Townsend, A.R., 1994. Climatic, edaphic, and biotic controls over the storage and turnover of carbon in soils. Global Biogeochemistry Cycles 8, 279-293.

Schindlbacher, A., Wunderlich, S., Borken, W., Kitzler, B., Zechmeister-Boltenstern, S., Jandl., R., 2012. Soil respiration under climate change: prolonged summer drought offsets soil warming effects. Global Change Biology 18, 2270-2279.

Schlentner, R.E., van Cleve, K., 1984. Relationships between CO_2 evolution from soil, substrate temperature, and substrate moisture in four mature forest types in interior Alaska. Canadian Journal of Forest Research 15, 97-106.

Schleser, G.H., 1982. The response of CO_2 evolution from soils to global temperature changes. Zeitschrift für Naturforschung 37a, 287-291.

Schlesinger, W.H., Andrews, J.A., 2000. Soil respiration and the global carbon cycle. Biogeochemistry 48, 7-20.

Schlesinger, W.H., Winkler, J.P., Megonigal, J.P., 2000. Soils and the global carbon cycle. In: The carbon cycle. Wigley, T.M.L., Schimel, D.S. (Eds.), Cambridge University Press, USA.

Schroeder, P.E., Winjum, J.K., 1995. Assessing Brazil's carbon budget I. Biotic carbon pools. Forest Ecology and Management 75, 77-86.

Schuur, E.A.G., McGuire, A.D., Schädel, C., Grosse, G., Harden, J.W., Hayes, D.J., Hugelius, G., Koven, C.D., Kuhry, P., Lawrence, D.M., Natalo, S.M., Olefeldt, D., Romanovsky, V.E., Schaefer, K., Turetsky, M.R., Treat, C.C., Vonk, J.E., 2015. Climate change and the permafrost carbon feedback. Nature 520, 171-179.

Schuur, E.A.G., Vogel, J.G., Crummer, K.G., Lee, H., Sickman, J.O., Osterkamp, T.E., 2009. The effect of permafrost thaw on old carbon release and net carbon exchange from tundra. Nature 459, 556-559.

Schuur, E.A.G., Bockheim, J., Canadell, J.G., Euskirchen, E., Field, C.B., Goryachkin, S.V., Hagemann, S., Kuhry, P., Lafleur, P.M., Lee, H., Mazhitova, G., Nelson, F.E., Rinke, A., Romanovsky, V.E., Shiklomanov, N., Tarnocai, C., Venensky, S., Vogel, J., Zimov, S.A., 2008. Vulnerability of permafrost carbon to climate change: Implications for the global carbon cycle. Bioscience 58, 710-714.

Scull P., Franklin J., Chadwick O.A., McArthur D., 2003. Predictive soil mapping: a review. Progress in Physical Geography 27, 171–197.

Shaver, G.R., Canadell, J., Chapin, F.S.III, Gurevitch, J., Harte, J., Henry, G., Ineson, P., Jonasson, S., Melillo, J., Pitelka, L., Rustad, L., 2000. Global warming and terrestrial ecosystems: A conceptual framework for analysis. Biosciences 50, 874-871.

Singh, J.S., Gupta, S.R., 1977. Plant decomposition and soil respiration in terrestrial ecosystems. Botanical Review 43, 449-528.

Sistla, S. A., Moore, J.C., Simpson, R.T., Gough, L., Shaver, G.R., Schimel, J.P., 2013. Long-term warming restructures Arctic tundra without changing net soil carbon storage. Nature 497, 615-618.

Six, J., Conant, R.T., Paul, E.A., Paustian, K., 2002. Stabilization mechanisms of soil organic matter: implications for C-saturation of soils. Plant and Soil 241, 155–176.

Skopp, J., Jawson, M.D., Doran, J.W., 1990. Steady-state aerobic microbial activity as a function of soil water content. Soil Science Society of America Journal 54, 1619-1625.

Smith, E., Shi, L., 1995. Reducing discrepancies in atmospheric heat budget of Tibetan Plateau by satellite-based estimates of radiative cooling and cloud-radiation feedback. Meteorology and Atmospheric Physics 56, 229–260.

Smith, P., Powlson, D.S., Glendining, M.J. Smith, J.U., 1997. Opportunities and Limitations for C sequestration in European Agricultural Soils through Changes in Management. In: Management of Carbon Sequestration in Soil. Advances in Soil Science. R. Lal, J.M. Kimble, R.F. Follett, B. A. Stewart (Eds.), CRC Press, Boca Raton, Florida, pp. 143-152.

Song, X., Yuan, H., Kimberley, M.O., Jiang, H., Zhou, G., Wang, H., 2013. Soil CO_2 flux dynamics in the two main plantation forest types in subtropical China. Science of the Total Environment 444, 363-368.

Sotta, E.D., Meir, P., Malhi, Y., Nobre, A.D., Hodnett, M., Grace, J., 2004. Soil CO_2 efflux in a tropical forest in the central Amazon. Global Change Biology 10, 601-607.

Subke, J.A., Inglima, I., Cotrufo, F.M., 2006. Trends and methodological impacts in soil CO_2 efflux partitioning: A metaanalytical review. Global Change Biology 12, 921-943.

Subke, J.A., Haln, V., Battipaglia, G., Linder, S., Buchmann, N., Cotrufo, M.F., 2003. Explaining temporal variation in soil CO_2 efflux in a mature spruce forest in southern Germany. Soil Biology and Biochemistry 34, 1467-1483.

Sun, J., Cheng, G., Fan, J., 2013. Soil respiration in response to short-term nitrogen addition in an alpine steppe in northern Tibet. Polish Journal of Ecology 61, 655-663.

Tang, J., Baldocchi, D.D., Xu, M., Misson, L., Goldstein, A.H., 2005. Tree photosynthesis modulates soil respiration on a diurnal time scale. Global Change Biology 11, 1298-1304.

Taylor, B.R., Parkinson, D., Parsons, WFJ., 1989. Nitrogen and lignin content as predictors of litter decay rates. A microcosm test. Ecology 70, 97–104.

Thierron, V., Lausdelout, H., 1996. Contribution of root respiration to total CO_2 efflux from the soil of a deciduous forest. Canadian Journal of Forest Research 26, 1142-1148.

Tian, H., Lu, C., Yang, J., Banger, K., Huntzinger, D.N., Schwalm, C.R., Michalak, A.M., Cook, R., Clais, P., Hayes, D., Huang, M., Ito, A., Jain, A.K., Lei, H., Mao, J., Pan, S., Post, W.M., Penh, S., Poulter, B., Ren, W., Ricciuto, D., Schaefer, K., Shi, X., Tao, B., Wang, W., Wei, Y., Yang, Q., Zhang, B., Zeng, N., 2015. Global patterns and controls of soil organic carbon dynamics as simulated by multiple terrestrial biosphere models: Current status and future directions. Global Biogeochemical Cycles 29, 775-792.

Tibetan and Himalayan Library, 2002. Land Cover (Tibet). http://www.thlib.org/places/maps/collections/show.php?id=387 (16.12.2014).

Trumbore, S.E., Harden, J.W., 1997. Accumulation and turnover of carbon in organic and mineral soils of the BOREAS northern study area. Journal of Geophysical. Research 102, 28817–28830.

Tufekcioglu, A., Raich, J.W., Isenhart, T.M., Schulz, R.C., 2001. Soil respiration within riparian buffers and adjacent crop fields. Plant and Soil 229, 117-124.

Valentini, R., Matteucci, G., Dolman, A.J., Schulze, E.-D., Rebmann, C., Moors, E., J., Granier, A., Gross, P., Jensen, N.O., Pilegaard, K., Lindroth, A., Grelle, A., Bernhofer, C., Grünwald, T., Aubinet, M., Ceulemans, R., Kowalski, A.S., Vesala, T., Rannik, Ü., Berbigier, P., Loustau, D., Guðmundsson, J., Thorgeirsson, H., Ibrom, A., Morgenstern., Clement, R., Moncrieff, J., Montagnani, L., Minerbi, S.,

Jarvis, P. G. 2000. Respiration as the main determinant of carbon balance in European forests. Nature 404, 861-865.

van Vuuren, D.P., Edmonds, J., Kainuma, M., Riahi, K., Thomson, A., Hibbard, K., Hurtt, G.C., Kram, T., Krey, V., Nakicenovic, N., Smith, S. J., Rose, S. K., 2011. The representative concentration pathways: an overview. Climatic Change 109, 5-31.

van`t Hoff, J.H., 1884. Études de dynamique chimique (Studies of chemical dynamics). Frederik Muller and Co., Amsterdam, the Netherlands.

Vogt, K.A., Vogt, D.J., Palmiotto, P.A., Boon, P., O´Hara, J., Asbjornsen, H., 1996. Review of root dynamics in forest ecosystems grouped by climate, climatic forest type and species. Plant Soil 187, 159-219.

Wan, S., Hui, D., Wallace, L.L., Luo, Y., 2005. Direct and indirect warming effects on ecosystem carbon processes in a tallgrass prairie. Global Biogeochemical Cycles 19, GB2014.

Wang, B., 2006. The Asian monsoon. Springer, New York, USA.

Wang, B., French, H., 1995. Permafrost on the Tibet Plateau, China. Quaternary Science Reviews 14, 225-274.

Wang, C.T., Long, R.J., Wang, Q.L., Jing, Z.C., Shi, J.J., 2009. Changes in plant diversity, biomass and soil C, in alpine meadows at different degradation stages in the headwater region of the three rivers, China, Land Degradation and Development 20, 187-198.

Wang, G., W., Li, Y., Wang, Y., Wu, Q., 2008. Effects of permafrost thawing on vegetation and soil carbon pool losses on the Qinghai-Tibet Plateau, China. Geoderma 143, 143-152.

Wang, J., Wu, Q., 2013. Annual soil CO_2 efflux in a wet meadow during active layer freeze-thaw changes on the Qinghai-Tibet Plateau. Environmental Earth Sciences 69, 855-862.

Wang, W., Guo, J., Oikawa, T., 2007. Contribution of root to soil respiration and carbon balance in disturbed and undisturbed grassland communities, northeast China. Journal of Biosciences 32, 375-384.

Wang, W., Ohse, K., Liu, J., Mo, W., Oikawa, T., 2005. Contribution of root respiration to soil respiration in C_3/C_4 mixed grassland. Journal of Biosciences 30, 507-514.

Wang, W.Y., Wang, Q.J., Li, S.X., Wang, G., 2006. Distribution and species diversity of plant communities along transect on the Northeastern Tibetan plateau. Biodiversity and Conservation 15, 1811–1828.

Wang, X., Liu, L., Piao, S., Janssens, I.A., Tang, J., Liu, W., Chi, Y., Wang, J., Xu, S., 2014a. Soil respiration under climate warming: differential response of heterotrophic and autotrophic respiration. Global Change Biology 20, 3229-3237.

Wang, Y., Liu, H., Chung, H., Yu, L., Mi, Z., Geng, Y., Jing, X., Wang, S., Zeng, H., Cao, G., Zhao, X., He, J.-S., 2014b. Non-growing-season soil respiration is controlled by freezing and thawing processes in the summer monsoon-dominated Tibetan alpine grassland. Global Biochemical Cycles 28, 1081-1095.

Weischet, W., Endlicher, W., 2000. Regionale Klimatologie Teil 2. Schweizerbart'sche Verlangsbuchhandlung, Stuttgart.

Wen, L., Dong, S., Li, Y., Wang, X., Li, X., Shi, J., Dong, Q., 2013. The impact of land degradation on the C pools in alpine grasslands of the Qinghai-Tibet Plateau. Plant and Soil 368, 329-340.

Wildung, R.E., Garland, T.R., Buschbom, R.L., 1975. The interdependent effects of soil temperature and water content on soil respiration rate and plant root decomposition in arid grassland soils. Soil Biology and Biochemistry 7, 373-378.

Wiseman, P.E., Seiler, J.R., 2004. Soil CO_2 efflux across four age classes of plantation loblolly pine (*Pinus taeda* L.) on the Virginia Piedmont. Forest Ecology and Management 192, 297-311.

Wu, J., Liu, Z., Huang, G., Chen, D., Shao, Y., Wan, S., Fu, S., 2014. Response of soil respiration and ecosystem carbon budget to vegetation removel in Eucalyptus plantations with contrasting areas. Scientific Reports 4, 6262.

Wu, Y., Wu, J., Deng, Y., Tan, H., Du, Y., Gu, S., Tang, Y., Cui, X., 2011. Comprehensive assessments of root biomass and production in a *Kobresia humilis* meadow on the Qinghai-Tibetan Plateau. Plant and Soil 338, 497-510.

Xu, M., Qi, Y., 2001. Soil surface CO_2 efflux and its spatial and temporal variations in a young ponderosa one plantation in northern California. Global Change Biology 7, 667-677.

Xu, Z. X., Gong, T., L., Li, J. Y., 2008. Decadal trend of climate in the Tibetan Plateau - regional temperature and precipitation. Hydrological Processes 22, 3056-65.

Xue, X., Guo, J., Han, B., Sun, Q., Liu, L., 2009. The effect of climate warming and permafrost thaw on desertification in the Qinghai–Tibetan Plateau. Geomorphology 108 (3-4), 182–190.

Yan, Y., Zhang, J.-G., Zhang, J.-H., Fan, J.-R., Li, H.-X., 2005. The belowground biomass in alpine grassland in Nakchu Prefecture of Tibet. Acta Ecologica Sinica 25, 2818-2823. (in Chinese)

Yang, M., Wang, S., Yao, T., Gou, X., Lu, A., Guo, X., 2004. Desertification and its relationship with permafrost degradation in Qinghai-Xizang (Tibet) plateau. Cold Regions Science and Technology 39, 47-53.

Yang, Y., Fang, J., Tang, Y., Ji, C., Zheng, C., He, J.-S., Zhu, B., 2008. Storage, patterns and controls of soil organic carbon in the Tibetan grasslands. Global Change Biology 14, 1592-1599.

Yang, Y., Fang J., Smith, P.,Tang, Y., Chen, A., Ji, C., Hu, H., Rao, S., Tan K.U.N., He, J.-S., 2009. Changes in topsoil carbon stock in the Tibetan grasslands between the 1980s and 2004. Global Change Biology 15, 2723-2729.

Yatagai, A., K. Kamiguchi, O. Arakawa, A. Hamada, N. Yasutomi, Kitoh, A., 2012. APHRODITE constructing a long-term daily gridded precipitation dataset for Asia based on a dense network of rain gauges. Bulletin of the American Meteorological Society 93, 1401–1415.

Yu, H.Y., Luedeling, E., Xu, J.C., 2010. Winter and spring warming result in delayed spring phenology on the Tibetan Plateau. Proceedings of the National Academy of Sciences of the United States of America 107, 22151–22156.

Yu, X., Zha, T., Pang, Z., Wang, X., Chen, G., Li, C., Cao, J., Jia, G., Li, X., Wu, H., 2011. Response of soil respiration to soil temperature and moisture in a 50-year-old oriental arborvitae plantation in China. pLoS ONE 6(12), e28397.

Zanchi, F.B., da Roncha, H.R., de Freitas, H. C., Kruijt, B., Waterloo, M.J., Manzi, A.O., 2009. Measurements of soil respiration and simple models dependent on moisture and temperature for an Amazonian southwest tropical forest. Biogeosciences Disscussions 6, 6147-6177.

Zhang Y., Li Bingyuan, Z., Du, 2002. The area and boundary of Qinghai-Tibet Plateau. Geographical Research, 21, 1–8. (in Chinese)

Zhang, D., Xu, W., Li, Jiayun, Cai, Z., An, D., 2014. Frost-free season lenghtening and ist potential cause in the Tibetan Plateau from 1960 to 2010. Theoretical and Applied Climatology 115, 441-450.

Zhang, L.H., Chen, Y.N., Zhao, R.F., Li, W.H., 2010. Significance of temperature and soil water content on soil respiration in three desert ecosystems in Northwest China. Journal of Arid Environments 74, 1200-1211.

Zhang, P., Tang, Y., Hirota, M., Yamamoto, A., Mariko, S., 2009. Use of a regression method to partition sources of ecosystem respiration in an alpine meadow. Soil Biology and Biochemistry 41, 663-670.

Zhang, X., Shi, P., Liu, Y., Ouyang, H., 2005. Experimental study on soil CO_2 emission in the alpine grassland ecosystem on Tibetan Plateau. Science in China Series D 48, 218-224.

Zhang, Y., Ohata, T., Kodata, T., 2003. Land-surface hydrological processes in the permafrost region of the eastern Tibetan Plateau. Journal of Hydrology 283, 41-56.

Zheng, D., 1996. The system of physico-geographical regions of the Qinghai-Xizang (Tibet) Plateau. Science in China, Series D 39, 410-417.

Zhong, L., Ma, Y., Salama M.S., Su, Z., 2010. Assessment of vegetation dynamics and their response to variations in precipitation and temperature in the Tibetan Plateau. Climatic Change 103, 519-535.

Zhou, H., Zhao, X., Tang, Y., Gu, S., Zhou, L., 2005. Alpine grassland degradation and its control in the source region of the Yangtze and Yellow Rivers, China. Grassland Science 51 (3), 191–203.

Zhou, T., Shi, P.J., Hui, D., Luo, Y., 2009. Spatial patterns in temperature sensitivity of soil respiration in China: Estimation with inverse modeling. Science in China Series C: Life Sciences 52, 982-989.

Zhuang, Q., He, J., Lu, Y., Ji, L., Xiao, J., Luo, T., 2010. Carbon dynamics of terrestrial ecosystems on the Tibetan Plateau during the 20th century: an analysis with a process-based biogeochemical model. Global Ecology and Biogeography 19, 649-662.

Zhuang, Q., Melillo, J.M., Sarofim, M.C., Kicklighter, D.W., McGuire, A.D., Felzer, B.S., Sokolov, A., Prinn, R.G., Steudler, P.A., Hu, S., 2006. CO_2 and CH_4 exchanges between land ecosystems and the atmosphere in northern high latitudes over the 21st century. Geophysical Research Letters 33, L17403.

Zimov, S.A., Davydov, S.P., Zimova, G.M., Davydova, A.I., Schuur, E.A.G., Dutta, K., Chapin III, F.S., 2006. Permafrost carbon: stock and decomposability of a globally significant carbon pool. Geophysical Research Letters 33, L20502.

Appendix

Manuscript 1

A Comparison of Regression Models to Estimate Belowground Biomass on the Qinghai-Tibet Plateau

Manuscript in preparation, targeted Geoderma Regional (2017)

Anna Bosch[a], Karsten Schmidt[a], Jin-Sheng He[b, c], Corina Doerfer[a], Thomas Scholten[a]

[a]University of Tuebingen, Department of Geosciences, Chair of Soil Science and Geomorphology, Tübingen, Germany

[b]Key Laboratory of Adaptation and Evolution of Plateau Biota, Northwest Institute of Plateau Biology, Chinese Academy of Sciences, Xining, 810008, China

[c]Department of Ecology, College of Urban and Environmental Sciences, and Key Laboratory for Earth Surface Processes of the Ministry of Education, Peking University, Beijing, 100871, China

Abstract

Ecosystems in alpine permafrost regions like the Qinghai-Tibet Plateau are highly sensitive to global warming. Climate change potentially triggers large carbon loss from this ecosystem and thus exerts a relevant positive feedback to the climate warming. However, quantifying soil carbon dynamics in these remote areas is a challenge, because data on belowground biomass (BGB) as important carbon supplier for soils are scarce. Our current study aims at the approximation of BGB for the Qinghai-Tibet Plateau. We compared six regression models based on January mean temperature, July mean temperature, mean annual temperature (MAT), mean annual precipitation (MAP) and elevation on their ability to predict BGB for the entire plateau. We used the

WorldClim and Shuttle Radar Topography Mission data sets to estimate BGB area-wide on a regional scale. Our predicted results (max. 199.99 Mg ha^{-1}) compared to directly measured BGB samples at field plots in different vegetation zones on the Qinghai-Tibet Plateau (max. 145.67 Mg ha^{-1}) appear to be reasonable. The basic difference in BGB between grasslands and forests is reflected by all regression models. The model based on MAT overall performs best for most and largest vegetation zones. Alpine steppe, alpine mixed forests and alpine spruce fir forests are distinctly better estimated by the MAP-based regression. For desert grasslands and the alpine desert, the MAT-based model is only negligibly outperformed by other models. With this quantification, a more accurate basis for the calculation of BGB at a large scale as input for an area-specific assessment of soil respiration is provided.

Keywords

Belowground biomass, regression model, Qinghai-Tibet Plateau

1 Introduction[1]

Soil respiration, as second largest flux of CO_2 to the atmosphere (Schlesinger and Andrews, 2000; Bond-Lamberty et al., 2010), crucially influences the global carbon cycle (Chen et al., 2010). With more than 1500 Pg C, soil contains most C in terrestrial ecosystems (Raich and Schlesinger, 1992; Amundson, 2001). Small raises in the amount of soil respiration can therefore impact atmospheric CO_2 concentrations, potentially increasing global warming (Rodeghiero and Cescatti, 2005; Davidson and Janssens, 2006; Rodeghiero et al., 2013; Wang et al., 2014).

Since more than two-thirds of terrestrial carbon is contained belowground (Klopatek, 2002) and thus, roots as well as microbes respire a considerable part of the CO_2 to the atmosphere that is assimilated in by plants, BGB is of key importance for soil respiration rates (Luo and Zhou, 2006; Moyano et al., 2009). Following Luo et al. (2005), in this study, BGB comprises in general the whole root biomass including living and dead roots. Living roots respire up to more than half of plant photosynthates a day

[1] Abbreviations: belowground biomass (BGB), carbon (C), carbon dioxide (CO_2), mean annual temperature (MAT), mean annual precipitation (MAP).

(Lambers et al., 1996). Autotrophic respiration may contribute 10 to more than 90% of total in situ soil respiration mainly influenced by vegetation type and season (Hanson et al., 2000). The decomposition of dead roots is also part of soil respiration as heterotrophic component with no reliable quantification yet (Kuzyakov, 2006). Roots contain a significant part of the total carbon of ecosystems (Kurz et al., 1996) and mostly contribute a large amount to the total biomass of the ecosystem (Cannell, 1982; Jackson et al., 1996). Potentially, in most ecosystems, soil organic C preponderantly originates from roots (Rasse et al., 2005). Rasse et al. (2005) further provide multitudinous evidence for root C being the dominant contributor to soil C and doing so all the more with increasing soil depth.

The ecologically fragile Qinghai-Tibet Plateau is a key region for examining ecosystem compartments due to its strong sensitivity and comparably low human impact (Liu and Chen, 2000; Yang et al., 2009; Fan et al., 2010). The highest and most spatially extensive plateau on earth is influenced by global warming (Zhang et al., 2010) and is highly susceptible, primarily due to its extreme elevation (Luo et al., 2002; Zhong et al., 2010). Its temperature is expected to increase far above average in the future (Liu and Chen, 2000; Christensen et al., 2007; Wang et al., 2008a). Climate change is even presumed to be the main reason for the increasing global loss of soil carbon to the atmosphere (Jones et al., 2003). BGB is the factor that spatial variation of soil respiration in grassland ecosystems on the Qinghai-Tibet Plateau mostly depends on at a regional scale due to a high root biomass density (Geng et al., 2012). Almost two thirds of the Qinghai-Tibet Plateau is covered by grassland (Wang et al., 2006; Yang et al., 2008). Therefore, an accurate basis for the area-specific quantification of BGB strongly supports the assessment and highly necessary understanding of soil respiration rates on the Qinghai-Tibet Plateau (Geng et al., 2012).

Quantifying root biomass by means of direct field measurements, commonly described as the most basic, direct and authentic method, is, however, strongly limited (Fang and Moncrieff, 2001) for cost and time reasons. Existing methodological difficulties further aggravate the quantification of BGB (Titlyanova et al., 1999). The various methods to sample roots have not been standardized yet, especially with respect to depth (Luo et al., 2005). Information about the definition of size classes, drying methods, as well as the inclusion of dead and live roots is likewise deficient (Cairns et al., 1997). For large areas, one possible solution is to apply predictive tools in order to quantify BGB.

However, little knowledge exists about biotic and abiotic factors that influence BGB (Vogt et al., 1996; Cairns et al., 1997) although some studies on grazing effects on BGB on the Qinghai-Tibetan Plateau have been conducted (Hafner et al., 2012; Unterregelsbacher et al., 2012; Shi et al., 2013; Babel et al., 2014). For example, only little knowledge exists about the stability of BGB, as it is for the aboveground biomass when short-term changes through human impact like grazing are primarily to be considered (Fan et al., 2010; Ingrisch et al., 2015). Additionally, phenological phenomena relevant to the amount of biomass like foliation, are issues of aboveground biomass (Fitter, 1996). Overgrazing has been shown to affect root biomass, even though much less than aboveground biomass (Unterregelsbacher et al., 2012). Further, while grazing exclusion can decrease of the total amount of BGB and stored C (Hafner et al., 2012; Shi et al., 2013), grazing-induced changes of vegetation can also decrease C storage in BGB (Babel et al., 2014). Nevertheless, as there is more directly measured and indirectly obtained data on aboveground biomass (Yang et al., 2009), a very common method to calculate BGB is using root:shoot ratios (e.g. Schroeder and Winjum, 1995; Eamus et al., 2002; Mokany et al., 2006). However, Cairns et al. (1997) conclude from their analysis from the world´s forests that the amount of root biomass is better estimated directly without the application of root:shoot ratios.

There are studies on quantified relationships between climate and BGB (Schulze et al., 1996). According to Gill et al. (2002) global literature synthesis, MAP and/or MAT can serve as main predictor for BGB in grasslands. Few transect studies show that BGB decreases with decreasing precipitation and likewise decreases with increasing altitude (Schulze et al., 1996). The most important limiting factors for the amount of root biomass of undisturbed vegetation comprise temperature and precipitation in general (Luo et al., 2005). Regression models of Luo et al. (2005) involve climatic variables as input parameter such as MAT, MAP, January mean temperature and July mean temperature and also elevation (Luo et al., 2005). However, high requirements for the input parameters of many more of such regression models are still opposed to a small number of sufficient data sets in case of the Qinghai-Tibet Plateau. Data for that region at a sufficient spatial resolution are scarce due to the inaccessible and complex terrain causing that lack of data. Various data sets lack of a fine (about 1 km^2) resolution that captures spatial environmental variability appropriately. Others are not spatially comprehensive, available or existent.

For the Qinghai-Tibet Plateau, Ohtsuka et al. (2008) showed BGB is closely related to elevation. Precipitation and temperature are also likely to well predict the amount of root biomass for the Qinghai-Tibet Plateau (Luo et al., 2005) as its vegetation is regarded as comparatively natural (Yang et al., 2009). However, parts in the humid southeast underlie human-induced changes where *Kobresia pygmaea* grows instead of forests and grasslands as presumed natural vegetation (Miehe et al., 2014).

Facing these issues, we aim at finding the most optimum available regression model for BGB on the Qinghai-Tibet Plateau in this study. The algorithm should allow to (1) calculate BGB on a large scale (2) reflect variation of BGB correspondingly to major vegetation types.

2 Material and Methods

2.1 Study area

Our study area, the Qinghai-Tibet Plateau, is located in southwestern China. With an area of about 2.6 $\times 10^6$ km^2, it fully covers Tibet and Qinghai provinces and partially Xinjiang, Gansu, Sichuan, and Yunnan provinces. As largest plateau on earth, the Qinghai-Tibet Plateau extends from 26°00′12" N to 39°46′50" N and from 73°18′52" E to 104°46′59" E with a maximum length of approximately 2 945 km from east to west and approximately 1 532 km from south to north. The altitude of the highest and youngest plateau amounts to 4 380 m on average (Zhang et al., 2002). Surface elevation sharply declines at the plateau´s border, particularly at the southern one. Overall, eastern and western regions highly differ with regard to geomorphology, vegetation and climatic characteristics (Smith and Shi, 1995). The unique geographical position of the Qinghai-Tibet Plateau prevails an azonal, plateau monsoon climate from subtropical parts to a temperate mountain climate (Zhuang et al., 2010; Zhong et al., 2010) with strong solar radiation, low air temperature, large daily temperature variations and limited differences between annual mean temperatures (Zhong et al., 2010). The mean temperature of July, the warmest month, varies from 7 °C to 15 °C and the coldest month, January, ranges from -1 °C to -7 °C, with the average annual temperature being 1.6 °C (Yang et al., 2009). Precipitation amounts to about 413.6 mm a year (Yang et al., 2009), with more than 60 - 90% falling in the wet and humid summers (June-September) and 10% at maximum in the cool, arid winters (November-February) (Xu et al., 2008). Generally, a decrease both in temperature and in precipitation from the south-eastern to the north-western part of the plateau is apparent

(Immerzeel et al., 2005). The topographic setting as well as atmospheric conditions determine the sequence of alpine forests, meadows, steppes and deserts from southeast to northwest (Fig. 1) following a climatic gradient from warm and humid to cold and arid according to the influence of the South Asian monsoon (Zheng, 1996; Pei et al., 2009).

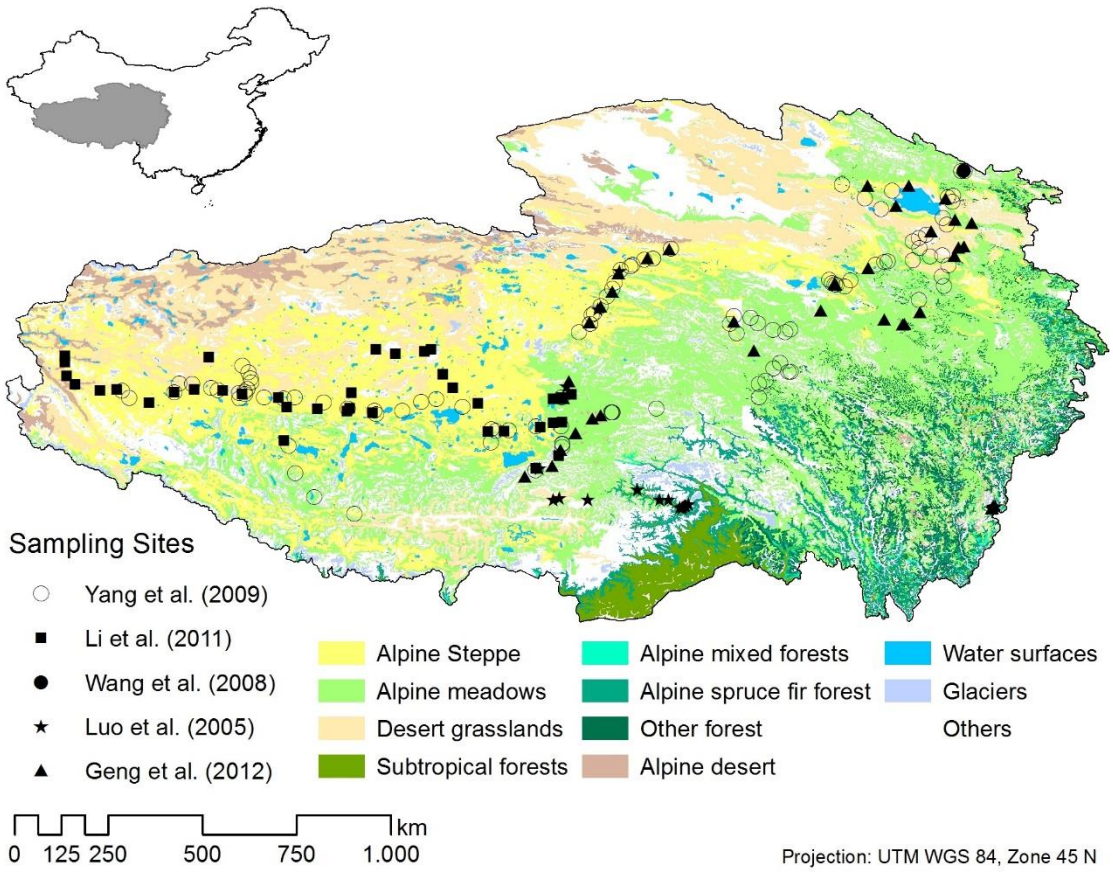

Fig. 1. Vegetation map of the Qinghai-Tibet Plateau based on data sets for Land Cover in Tibet with sampling localities of Luo et al. (2005), Wang et al. (2008b), Yang et al. (2009), Li et al. (2011), Geng et al. (2012) (Tibetan and Himalayan Library, 2002).

Alpine steppes and meadows dominate the vegetation, with *Kobresia* meadow as major vegetation type. Alpine grasslands bestride more than 60% of the study area (Wang et al., 2006). According to the long freezing periods, relatively short growing seasons characterize the plateau`s climate (Yu et al., 2010). Continuous, complex pedogenetic processes on the Qinghai-Tibet Plateau typically result in young and highly diverse soils with distinct degradation characteristics, exhibiting a strong influence by permafrost regimes (Baumann et al., 2014).

2.2 Geodatabase and processing

For the approximation of BGB from temperature, precipitation and elevation data, five data sets were used in this case study. All data sets were projected into the Universal Transverse Mercator coordinate system WGS 1984, Zone 45 N. The data were obtained from the WorldClim data set available at http://worldclim.com. This was compiled from a considerable number of various sources, such as the Global Historical Climate Network, World Meteorological Organization and the Food and Agricultural Organization, with a resolution of 1 x 1 km and representing the current climate conditions from ca. 1950 to 2000. Data from more than 71 000 climate stations worldwide (for precipitation), and more than 45 000 climate stations (for temperature) are integrated with the Qinghai-Tibet Plateau as area with less densely distributed measurement points. These were, however, interpolated using a thin-plate smoothing spline algorithm. Latitude, longitude and altitude served as independent variables. Elevation data were used from the Shuttle Radar Topography Mission with a spatial resolution of 1 x 1 km (for more detailed information see Hijmans et al., 2005). For our estimations, we used the following data sets: January mean temperature, July mean temperature, annual mean temperature, annual precipitation and altitude.

2.3 BGB calculation and evaluation

The data sets of WorldClim form the respective input parameters of the regression models, one combining MAT and MAP, for the calculations of BGB which were developed by Luo et al. (2005) (Table 1). In the BGB samples, living and dead roots are included.

Table 1. Regression models to approximate belowground biomass by Luo et al. (2005) from Tibet

Regression based on	Equation	Parameters
January mean temperature x	$y = 200/(1 + \exp(-0.1434x + 1.0789))$	y = root biomass density (Mg/ha), x = January mean temperature (°C)
July mean temperature x	$y = 200/(1 + \exp(-0.2245x + 4.6125))$	y = root biomass density (Mg/ha), x = July mean temperature (°C)
Annual mean temperature x	$y = 200/(1 + \exp(-0.1750x + 2.5543))$	y = root biomass density (Mg/ha), x = annual mean temperature (°C)
Annual precipitation x	$y = 200/(1 + \exp(-2.14E - 06x^2 - 0.00575x + 4.78))$	y = root biomass density (Mg/ha), x = annual precipitation (mm)

Annual mean temperature and annual precipitation x	$y = 200/(1 + \exp(-0.0001594x + 2.5869))$	y = root biomass density (Mg/ha), x = annual mean temperature x annual precipitation (°C x mm)
Altitude x	$y = -0.0209x + 104.89$	y = root biomass density (Mg/ha), x = altitude (m)

After the application of the regression models, we tested their ability to predict BGB by a validation of our results with field measured results of other studies (Table 2). The samples were taken by Luo et al. (2005), Yan et al. (2005), Wang et al. (2008b), Yang et al. (2009), Li et al. (2011), Wu et al. (2011) and Geng et al. (2012) located in nine different vegetation types: Alpine steppe, alpine shrubs and meadows, desert grassland, dry valley forests, subtropical forests, alpine mixed forests, alpine spruce forests, timberline zone and alpine desert. The respective vegetation type of the samples has been identified by each study. The validation sites altogether cover not only a broad range of the major vegetation types on the Qinghai-Tibet Plateau but also a variety of climatic conditions and altitudes (1900 m – 5105 m a.s.l.) spread out almost over the entire Qinghai-Tibet Plateau (Fig. 1). Not displayed in Fig. 1 are the sites of Yan et al. (2005), who sampled in the central and northern central part, and Wu et al. (2011) (northeastern part). Due to the rather unsystematic and scarce evaluation data set, we mainly compared ranges of the estimated BGB values. To account for the strong influence of vegetation type on BGB, this was performed for each vegetation zone. The ranges for the vegetation zones comprise those grid points´ values that correspond to the precise geographical coordinates from the sampling sites of the literature data in the respective vegetation zone. Due to a lack of precise spatial information on the sites of Yan et al. (2005) and Wu et al. (2011), only the minima and maxima for the respective vegetation types could be considered. For the overall range of all field measured values of all studies, all area-wide calculated values for the whole plateau are compared to all field measured values, demonstrating their variation. We further calculated the mean relative errors to allow for a direct point-to-point comparison.

3 Results

3.1 Variation of BGB with vegetation

The resulting BGB estimates of the tested regression models vary strongly with different vegetation types (Table 2, Fig. 2).

Table 2. Range of belowground biomass for different vegetation types on the Qinghai-Tibet Plateau measured by Luo et al. (2005), Yan et al. (2005), Wang et al. (2008b), Yang et al., (2009), Li et al. (2011), Wu et al. (2011), Geng et al. (2012) and calculated based on regression models.

Vegetation type		Luo et al. (2005) (n_{AS} =3; n_{AM} = 5; n_{DF} = 2; n_{SF} = 2; n_{AMF} = 3; n_{ASF} = 4; n_T = 3)	Yan et al. (2005) (n_{AS} =1; n_{AM} = 2)	Wang et al. (2008b) (n_{AM} = 12)	Yang et al. (2009) (n_{AS} = 73; n_{AM} = 35)	Li et al. (2011) (n_{AS} = 17; n_{AM} = 7; n_{DG} = 8; n_{AD} = 5)	Wu et al. (2011) (n_{AM} = 30)	Geng et al. (2012) (n_{AS} = 18; n_{AM} = 20)	All field samples	Regression model based on					
										January mean temperature	July mean temperature	MAT	MAP	MAT and MAP	Elevation
									[Mg ha^{-1}]						
Alpine steppe (AS)	Range	6-10	8.86	-	0.44-18.34	12.12-16.13	-	2.01-10.83	0.44-18.34	4.22-19.48	4.01-52.99	3.76-28.84	2.77-19.55	9.43-18.11	-14.15-50.86
	(Mean rel. error [%])									*(343.92)*	*(515.99)*	*(375.99)*	*(231.80)*	*(562.67)*	*(219.98)*
Alpine meadows (AM)	Range	9-32	24.90-100.48	17.97-145.67	0.82-27.84	26.67-49.30	13.40-24.74	5.43-93.93	0.82-145.67	4.36-28.81	4.12-47.34	3.76-31.90	4.54 - 49.39	9.96-20.48	-16.51-47.78
	(Mean rel. error [%])									*(91.71)*	*(111.75)*	*(97.46)*	*(110.08)*	*(124.87)*	*(142.51)*
Desert grasslands (DG)	Range	-	-	-	-	5.97-12.41	-	-	5.97-12.41	8.73-13.12 -	12.22-21.00 -	8.79-14.43 -	3.47-5.93 -	12.90-14.00 -	5.32-12.46 -
	(Mean rel. error [%])														
Dry Valley forests (DF)	Range	18-52	-	-	-	-	-	-	18-52	14.38-48.06	11.22-52.99	12.19-51.19	10.13-23.07	13.22-29.69	3.92-39.10
	(Mean rel. error [%])									*(14.16)*	*(25.34)*	*(17.13)*	*(49.65)*	*(34.85)*	*(51.68)*
Subtropical forests (SF)	Range	67-95	-	-	-	-	-	-	67-95	50.84-58.11	53.15-65.92	48.06-58.55	41.85-43.12	39.44-45.99	48.59-54.78
	(Mean rel. error [%])									*(30.18)*	*(23.19)*	*(31.32)*	*(46.30)*	*(45.17)*	*(33.84)*
Alpine mixed forests (AMF)	Range	23-36	-	-	-	-	-	-	23-36	45.82-50.74	45.21-52.51	44.02-53.86	24.31-44.09	29.26-37.05	38.64-45.21
	(Mean rel. error [%])									*(74.11)*	*(71.78)*	*(72.41)*	*(14.71)*	*(13.06)*	*(44.17)*

Alpine spruce fir forests (ASF)	Range *(Mean rel. error [%])*	21-49	-	-	-	-	-	-	21-49	34.22-38.86 *(44.61)*	28.58-34.78 *(32.08)*	31.09-39.35 *(42.81)*	19.14-45.41 *(47.27)*	20.98-34.19 *(26.63)*	26.14-40.77 *(39.66)*
Timberline (T)	Range *(Mean rel. error [%])*	7-27	-	-	-	-	-	-	7-27	21.69-25.21 *(85.93)*	15.49-18.97 *(56.63)*	18.85-21.53 *(80.60)*	15.39-49.39 *(224.25)*	15.78-20.48 *(84.22)*	13.57-25.19 *(110.00)*
Alpine desert (AD)	Range *(Mean rel. error [%])*	-	-	-	-	3.11-4.83	-	-	3.11-4.83	2.90-10.01 -	2.52-29.56 -	2.29-13.27 -	2.49-13.88 -	8.91-13.85 -	-23.35-36.87 -
All	Range *(Mean rel. error [%])*								0.44-145.67	0.53-159.11 -	0.13-173.93 -	0.43-167.66 -	0.00-57.09 -	2.04-199.99 -	-63.75-103.23 -

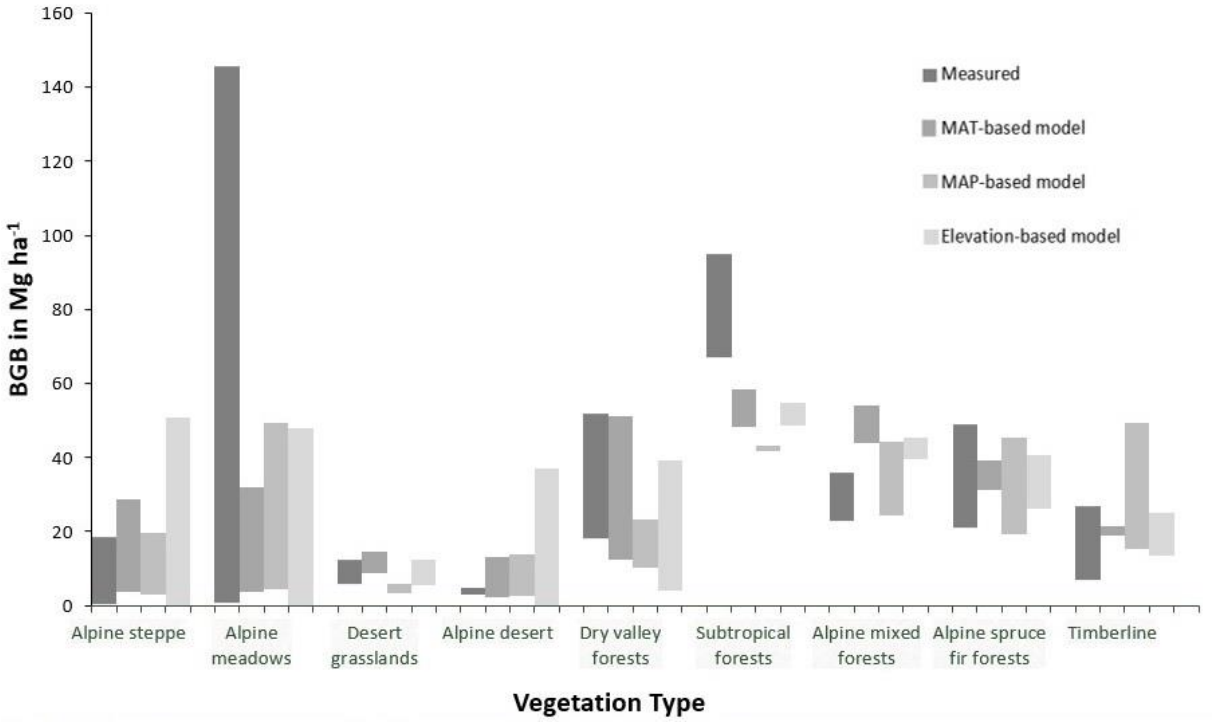

Fig. 2. Range of belowground biomass for different vegetation types on the Qinghai-Tibet Plateau measured by Luo et al. (2005), Yan et al. (2005), Wang et al. (2008b), Yang et al., (2009), Li et al. (2011), Wu et al. (2011), Geng et al. (2012) and modeled using MAT, MAP and elevation as input for regression models.

They amount up to 199.99 Mg ha^{-1}. The field measured values overall vary between 0.44 and 145.67 Mg ha^{-1}. Pixel values below zero Mg ha^{-1} arise from the regression model based on elevation, representing areas higher than 5015 m. Due to the linearity of the elevation-based regression model, this can be regarded as a predicted limit of vegetation wherefrom BGB is zero. Ohtsuka et al. (2008) found no vegetation cover on the Qinghai-Tibet Plateau for as high as 5300 m and above. Ohtsuka et al. (2008) observed a peak of BGB at 4800 - 4950 m at an altitudinal gradient from 4400 – 5300 m. It is, however, not manifested in the calculations of the regression model based on elevation due to its linear character. This likewise holds true for some variety in the altitude of the limit of vegetation. For example, BGB was at 29.90 Mg ha^{-1} at an altitude of 5105 m at some sampling site of Geng et al. (2012), which is to regard as an exception compared to other values at high altitudes. But again, the regression model based on elevation does not represent such variety. However, with providing no positive values for the amount of BGB at an elevation higher than 5015 m under the assumption this stands for BGB being zero, this regression model still reflects an approximated limit of vegetation and amount of BGB related to increasing elevation.

3.2 BGB of grasslands

For the vegetation zone of alpine steppe, the range of BGB values calculated based on MAP (2.77 – 19.55 Mg ha^{-1}) best represents the range of all directly measured BGB samples (0.44 – 18.34 Mg ha^{-1}). With > 50% of the samples amounting to less than 4 Mg ha^{-1}, the MAT-based model then most closely lines up to the range of the field measurements. The regression with elevation as input parameter tends to overestimate BGB a number of times and so does the regression model based on July mean temperature, however, not as much as the elevation-based model. The mean relative error is lowest for the elevation-based model (219.98%), followed by the model based on MAP. The regression model that combines MAT and MAP as input parameter shows the lowest range (9.34 – 18.11 Mg ha^{-1}) and smooths spatial variation, but lies within the range of directly measured BGB samples.

In alpine meadows, the directly measured values of all evaluation studies, regardless of the respective samplings´ geographic location, number and spatial extension, clearly exhibit highest ranges (up to 127.7 Mg ha^{-1}) of the amount of root biomass compared to all other vegetation types. This is due to the very high differences in BGB even between various meadow plant communities and causes strong small-scale variability [*Wang et al.,* 2008b]. All regression models do not predict these high values for special plant communities. Further, the high spatial variabilty within the small distances between single plant communities differing highly in their BGB cannot be represented in a 1 x 1 km resolution. Comparing the ranges of the calculated values, the regression based on elevation is closest to what can be assumed as most realistic range of BGB values on the Qinghai-Tibet Plateau for alpine meadows. Although the minimum value of that regression (-16.51 Mg ha^{-1}), indicating no BGB, does not fit to the respective value of comparison (29.90 Mg ha^{-1}), it is still most consistent to the given range of root biomass values with 2.73 Mg ha^{-1} as next lowest, positive value. It does not reflect some peak at 4800 - 4950 m, compared to the observations for 4400 - 5300 m by Ohtsuka et al. (2008), but the evaluation data sets as well as the other regression models likewise do not show some peak values. The models including MAP respectively the July mean temperature almost reflect the height of the range of the direct measurements as much as the elevation-based regression, with the slightly higher minimum values (4.54 Mg ha^{-1} and 4.12 Mg ha^{-1} compared to 2.73 Mg ha^{-1} and one further, more appropriate prediction of the MAT-based model with 3.76 Mg ha^{-1})

as main difference. Mean relative errors are lowest for the model based on January mean temperature, narrowly followed by the model based on MAT.

Desert grasslands´ BGB is best calculated using the regression model based on elevation with values between 5.32 Mg ha^{-1} and 12.46 Mg ha^{-1}. These are with regard to minimum, maximum and width of range almost equal to Li et al. (2011) field values (5.97 - 12.41 Mg ha^{-1}). Almost as accurate are the results of the estimations with the models based on January mean temperature and MAT (8.73 - 13.12 Mg ha^{-1} and 8.79 - 14.43 Mg ha^{-1}). With a minimum value (12.22 Mg ha^{-1}) almost above the maximum of Li et al. (2011) measurements, the regression including July mean temperature clearly overestimates BGB, whereas the MAP-based model distinctly underestimates root biomass (3.47 – 5.93 Mg ha^{-1}). The regression model based on MAP and MAT likewise does not appear suitable for the approximation of BGB due to its typical small range (12.90 – 14.00 Mg ha^{-1}).

3.3 BGB of forests

In contrast to the alpine grasslands, all forest vegetation types show relatively higher amounts of BGB in direct measurements. This holds true for the calculations of all regression models.

For dry valley forests, the minima of all regression models (3.92 – 14.38 Mg ha^{-1}) clearly underestimate the minimum of the field BGB (18 Mg ha^{-1}). In contrast, the maxima of all temperature-based regressions (48.06 – 52.99 Mg ha^{-1}) arise well in accordance to Luo et al.`s (2005) directly measured root biomass (52 Mg ha^{-1}). Considering the sampling method of Luo et al. (2005) with a maximum digging depth at 1.5 m, it is to assume that the field measurements did not capture all roots. *Quercus* can reach a rooting depth up to more than 10 m under extreme, especially dry, conditions (Stone and Kalisz, 1991). As the samples of Luo et al. (2005) were taken in a dry river valley, the rooting zone presumeably reaches more depth than 1.5 m. Therefore, although underestimating the minimum slightly stronger than the regression model based on monthly mean temperatures of January and a higher mean relative error, the regression model based on MAT shows best performance for dry valley forests with a more accurate maximum value.

Root biomass in subtropical forests is underestimated by all regression models. Not even the range of their maximum values (43.12 – 65.92 Mg ha^{-1}) catches up with the minimum of Luo et al.`s (2005) field measurements (67 Mg ha^{-1}). No regression model

reflects the range of the direct measurements (28 Mg ha^{-1}). The widest range amounts to 12.77 Mg ha^{-1} (regression based on July mean temperature) and the lowest to 1.27 Mg ha^{-1} (MAP-based regression). Here, the complexity of control factors on the occurence of strongly differing vegetation types is demonstrated, reflected by the uncertainty of all regression models when calculating BGB for the vegetation type of subtropical forests. This results partially from the fact that they deterministically give expression to only one or two influencing factors on BGB. Mean relative errors are close for all regression models (23.19 – 46.30%).

BGB in alpine mixed forests calculated by regression models is best represented by those including MAP as their input parameter. All regressions based only on temperature data or elevation data with minimum values ranging from 38.64 – 45.82 Mg ha^{-1} overestimate the amount of root biomass compared to field measured data (23 – 36 Mg ha^{-1}). The regression model using MAT (44.02 – 53.86 Mg ha^{-1}) as input factor does so mostly. The minimum value (38.64 Mg ha^{-1}) of those regression models is lower than the maximum value (36 Mg ha^{-1}) of the field measurements. The minimum value of the regression model solely based on MAP (29.26 Mg ha^{-1}) accurately meets up with the minimum value of the directly measured data (23 Mg ha^{-1}) whereas the minimum value of the regression with MAP and MAT as input parameters is higher (28.86 Mg ha^{-1}). In contrast, the maximum value of the latter one (37.05 Mg ha^{-1}) closely lines up with the maximum of the field data (36 Mg ha^{-1}) whereas values of the MAP-based regression are highest at 44.09 Mg ha^{-1}. Even though the MAP-based regression model´s deviation of its extreme values in relation to the field data´s extreme values is higher (9.39 Mg ha^{-1}) than the one of the regression based on MAP and MAT (4.31 Mg ha^{-1}) and the mean relative error is higher (14.71% versus 13.06%, respectively), it is regarded to best calculate the amount of root biomass in alpine mixed forests. A better performance is concluded with regard to the possible rooting depth compared to the digging depth of the field measured BGB together with the assumption that even the directly measured field data thus understimate actual BGB.

As to the alpine spruce fir forests, all regression models based on temperature input variables underestimate the maximum of the direct measurements (49 Mg ha^{-1}) with highest values ranging from 34.19 to 45.41 Mg ha^{-1}. Except for the models including MAP, all regression models also overestimate the minimum of the field data

(21 Mg ha^{-1}) with lowest values from 26.14 Mg ha^{-1} to 34.22 Mg ha^{-1}. Both minimum and maximum values of directly measured data are best approximated by the regression based on MAP (19.14 – 45.41 Mg ha^{-1}). Mean relative errors range from 26.63 – 47.27% with the MAP and MAT-based model accounting for the lowest. Although better than the solely temperature-based regressions, the regression model including only MAP as input factor still performs better in terms of the range of BGB amounts in alpine spruce fir forests.

The timberlines BGB data of Luo et al. (2005) are characterized by relatively wide ranging values (7 – 27 Mg ha^{-1}). Only the regression model based on MAP also reflects that broad range (15.39 – 49.39 Mg ha^{-1}) but generally overestimates root biomass values strongly and has the highest mean relative error. Also the fact that that regression model calculated the maximum value of all timberline sampling sites for just the sampling site with the minimal field measured value, disqualifies it as most optimum way to derive estimates of BGB in timberline zones. All other regression models lie with their approximations within the range of the field data, but none of them reflects the high variation in the amount of BGB. They rather exhibit particularly small ranges. Generally wider ranges would, however, be more appropriate for a zone of especially high variation in vegetation cover. This is due to the high small-scale variability as typical feature of vegetation in a timberline zone, respectively BGB. That character can easlily be identified via direct single spot measurements but not by means of pixel-based calculations with a resolution of 1 x 1 km. The vegetation zone is best represented by the calculations of the elevation-based model. However, given all these issues, the timberline zone cannot be crucial when deciding which regression-based estimate represents most realistic BGB values for the Qinghai-Tibet Plateau.

3.4 BGB of alpine desert

For alpine deserts, the regression model based on mean temperatures of January with values between 2.90 Mg ha^{-1} and 10.01 Mg ha^{-1} most accurately lines up with the direct measurements (3.11 – 4.83 Mg ha^{-1}). The regression models based on MAT and MAP show similar estimations (2.29 Mg ha^{-1} – 13.27 Mg ha^{-1} and 2.49 Mg ha^{-1} – 13.88 Mg ha^{-1}, respectively). All other regression models overestimate the field samplings even stronger and, moreover, exhibit far wider ranges exept for the regression based on both MAP and MAT.

Overall, basic patterns such as the difference in the amount of BGB between grasslands and forests are clearly reflected by all regression models. Also, subtropical forests are next to the timberline zone the vegetation type that shows most uncertainties when attempting to accurately calculate BGB based on regression models. Generally, for forest vegetation, except the subtropical one and the timberline, the MAP-based regression is given preference as the one to approximate closest estimates to what has been measured directly in the field. This is true for forest vegetation with high amounts of precipitation. It also reflects the high influence of precipitation on forest vegetation on the Qinghai-Tibet Plateau, although precipitation is not the defining influencing feature in contrast to the alpine desert. A further exception among forest vegetation types are dry valley forests. Their BGB is better estimated by the MAT-based regression, indicating the importance of the actual amount of precipitation next to a general influence of precipitation and vegetation type. Nevertheless, the influence of precipitation respectively moisture on ecosystem properties is generally complex depending on scales (Baumann et al., 2009) and permafrost types (Doerfer et al., 2013) among other factors (Gill et al., 2002). For all grassland types, however, it are the regression models based on MAT and mean temperatures of January as well as the elevation-based regression that perform clearly best in the alpine steppe, alpine meadows, desert grassland and further in the alpine desert. As exeption, the alpine steppe, is, second to the elevation-based model, more accurately estimated by the MAP-based model with the lowest mean relative error.

4 Discussion

With the MAT-based regression as most appropriate model to calculate BGB for the entire plateau, temperature as main controlling factor of BGB is reflected. Generally, BGB increases with higher temperatures (Faget et al., 2013). However, as the temperature increases beyond the species-dependent optimum temperature for maximum root growth, the development of roots decreases (Faget et al., 2013). Nevertheless, responses of BGB to temperature increases in view of climate change remain still unclear and appear to be complex. This is not only due to the fact that the temperature change is unlikely to be steady and monotonic but also because the few existing studies on that matter e.g. in grasslands highly differ in their results from higher, lower to unchanged root biomass (Bai et al., 2010; De Boeck et al., 2008; Fitter et al., 1999). The importance of the MAP-model for forests stresses the influence of

precipitation on BGB. Altered precipitation patterns due to climate change, however, strongly resemble the complexity of temperature changes that are concomitant to climate warming. Generally, increased precipitation leads to more BGB (Li et al., 2014), however, the increase in biomass will be greater for the aboveground biomass than for BGB (Xu and Zhou, 2005). Lower precipitation or droughts do, however, also result in an increase of BGB as an adaption to water stress (Li et al., 2014). Nevertheless, further influencing factors such as vegetation-specific characteristics or the influence of elevated CO_2-levels in the atmosphere always have to be taken into account additionally for any predictions in general (Li et al., 2014). Increased BGB potentially leads to higher soil respiration as root respiration and also the heterotrophic respiration increases (Schuur et al., 2015). With regard to its atmospheric C-input, however, this is presumably outbalanced by the higher C uptake of increased plant photosynthesis and its sequestration (Schuur et al., 2015).

Calculating BGB by the application of a regression model with an input data set resoluted to 1 x 1 km, however, inheres various sources of uncertainties. Main uncertainties of the predicted values arise from the background of the regression models by Luo et al. (2005). Indicated by their coefficient of determination (r^2 = 0.59 - 0.65), they are not capable to fully explain the data variability reflecting highly complex interdependencies between BGB and all its controlling factors. Incorporating data from the authors with BGB data mentioned in this study into model development would presumably strengthen their explanatory power as e.g. including more vegetation zones. Facing the potential degree of precision of this study´s aim, methodological differences concerning the sampling would be negligible.

Further deficiencies in the calculations of all regression models may rise from the developement of the WorldClim data sets that show lower precision for poorly sampled regions like the Qinghai-Tibet Plateau and montainous areas (Böhner, 2006; Maussion et al., 2011; Hijmans et al., 2005). The same holds true for areas on the plateau with a complex topography where a 1 x 1 km resolution does not capture all potential variation (Hijmans et al., 2005).

Next to this, high small-scale variability of BGB especially in alpine meadows and the timberline zone is not captured by a data resolution of 1 x 1 km. The comparatively very high values in alpine meadows of two specific plant communities are not predicted by any regression model. Excluding the samples that purely consist of the communities

Kobresia tibetica and *Kobresia littledalei* (7 out of all 115 samples of the alpine meadows) with a BGB between 49.55 – 145.67 Mg ha^{-1}, decreases the range of the field measured values to about one third (with a maximum of 53.91 Mg ha^{-1}) of the range of all samples of the alpine meadows. Predominantly occuring at wet sites, their plant physiological characteristics enable them to develop an extensive root system in this environment resulting in a distinctly higher BGB (Wang et al., 2006). This contrast in BGB between these communities and all other alpine meadow plant communities results in wide differences of the BGB within short distances which can only be represented by a higher spatial resolution.

The evalutation data used in this study account for another weakness. All studies delivering those evalutation data lack information concerning the inclusion of dead roots in their sampling that may alter the amount of the respective BGB. Also, actual BGB may be higher as digging depths generally may not fully cover the actual rooting depth.

Moreover, the degradation of vegetation comprising about 35% of the Qinghai-Tibet Plateau that has decreasing effects on the BGB (Wang et al., 2009; Wen et al., 2013) is not integrated in our estimations and limits these predictions of BGB.

To sum up, according to the analysis of the results against the background of the dependence of BGB on vegetation, it is the MAT-based regression model that is generally recommended for area-wide, pixel-based calculations of root biomass on the Qinghai-Tibet Plateau (Fig. 3).

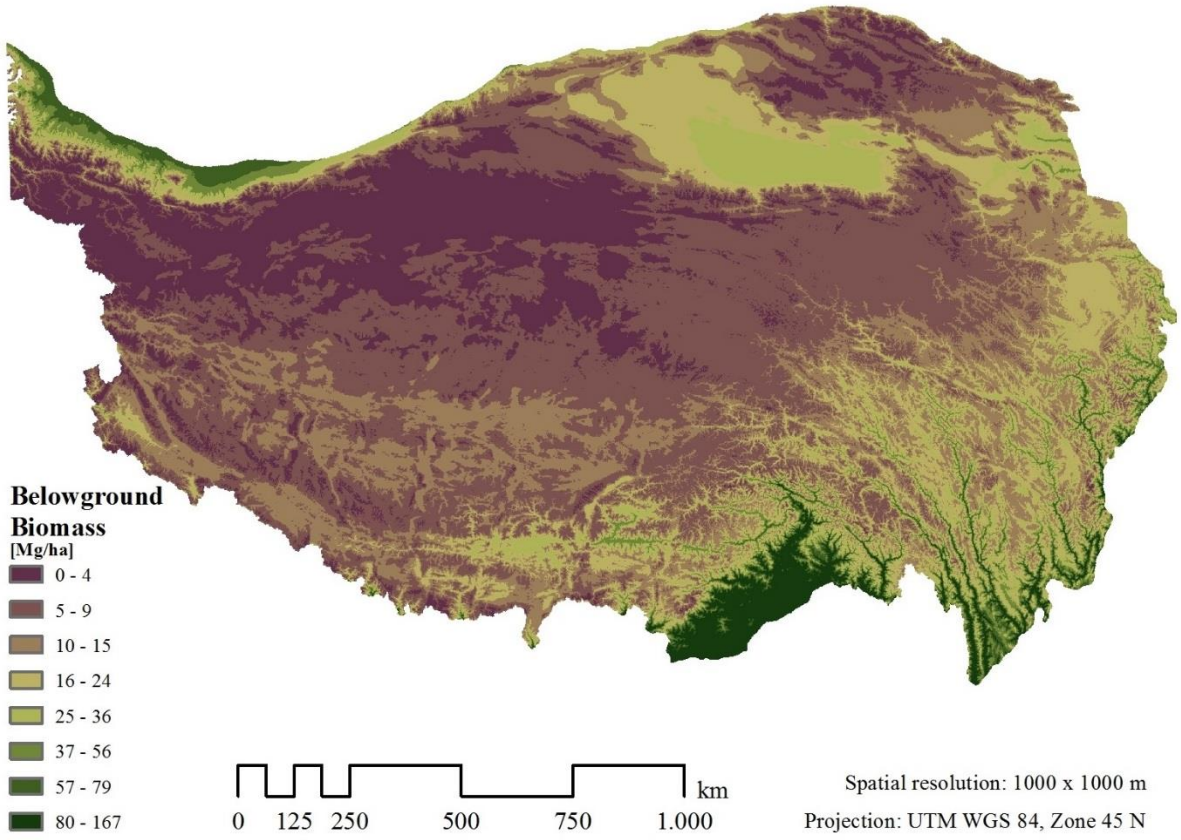

Fig. 3. Spatial distribution (grid 1 x 1 km) of belowground biomass on the Qinghai-Tibet Plateau based on MAT according to a regression model of Luo et al. (2005). Belowground biomass is in SI unit (Mg ha^{-1}).

Considering the fact that this regression is most powerful for the alpine meadows overall, clearly better performs for dry valley forests than the MAP-based model and is close to the best models in the alpine steppe, it is to be given preference over all other regression models. Although the regression model based on MAP performs better in the alpine steppe, alpine mixed forests and in alpine spruce fir forests, with regard to the relatively large area of the Qinghai-Tibet Plateau covered by alpine grasslands in contrast to the much smaller areas with forests or no vegetation, the regression model based on MAT is regarded being most optimum for an area-wide, pixel-based calculation of BGB on the Qinghai-Tibet Plateau. Especially because the MAP-based regression model does not reflect the ranges of field measured data in all vegetation zones as much as the MAT-based regression model does. In general, estimations executed with this methodology, may for many cases primarily deliver an approximate magnitude and reveal spatial distribution.

4 Conclusions

Estimates of BGB are fundamental to understanding carbon dynamics and soil respiration of terrestrial ecosystems. As data collection on root biomass requires extremely high time and cost efforts, data at a sufficient spatial resolution for large areas, especially for the Qinghai-Tibet Plateau, are generally scarce.

To overcome this restriction of limited data, we tested regression models which can be run with climate and elevation data and thus being advantageous for an area-wide calculation of scenarios.

Results of various studies indicate the important role of temperature, precipitation and elevation with regard to the amount of BGB. We conclude that the regression model based on MAT achieves best performance to calculate BGB according to our evalutation data sets. It can be run with limited data and accounts for the most important and spread-out vegetation zones on the Qinghai-Tibet Plateau, considering that for special vegetation types an incorporation of other regressions would enhance the accuracy of the approximation. Our approach of estimating BGB with scarce data is well within the same range of directly measured field data from other studies on the Qinghai-Tibet Plateau used for evaluation. It further fulfills our requirement to overcome the necessity of aboveground biomass data. The spatially distinct BGB calculation allows for assessing an area-specific soil respiration potential on the Qinghai-Tibet Plateau.

5 Acknowledgements

We thank the Ev. Studienwerk Villigst e. V. that funded this study conducted within the framework of the research project PERMATRANS. The support by the German Federal Ministry for Education and Research (BMBF, grant No. 03G0810A) is highly acknowledged. The data used are listed in the references and tables, and can be obtained at URL: http://worldclim.com (last access 11.05.2017). We further thank Katie Tay and Timo Giesmann for proof reading the article.

6 References

Amundson, R., 2001. The carbon budget in soils. Annu. Rev. Earth Planet. Sci. 29, 535-562.

Babel, W., Biermann, T., Coners, H., Falge, E., Seeber, E., Ingrisch, J., Schleuß, P.-M., Gerken, T., Leonbacher, J., Leipold, T., Wilinghöfer, S., Schützenmeister, K., Shibistova, O., Becker, L., Hafner, S., Spielvogel, S., Li, X., Xu, X., Sun, Y., Zhang, L., Yang, Y., Ma, Y., Wesche, K., Graf, H.-F., Leuschner, C., Guggenberger, G., Kuzyakov, Y., Miehe, G., Foken, T., 2014. Pasture degradation modifies the water and carbon cycles of the Tibetan highlands, Biogeosciences 11, 6633-6656.

Bai, W.M., Wan, S.Q., Niu, S.L., Liu, W.X., Quansheng, C., Wang, Q.B., 2010. Increased temperature and precipitation interact to affect root production, mortality, and turnover in a temperate steppe: implications for ecosystem C cycling. Glob. Change Biol. 16, 1306–1316.

Baumann, F., He, J.-S., Schmidt, K., Kühn, P., Scholten, T., 2009. Pedogenesis, permafrost, and soil moisture as controlling factors for soil nitrogen and carbon contents across the Tibetan Plateau. Glob. Change Biol. 15, 3001-3017.

Baumann, F., Schmidt, K., Doerfer, C., He, J.-S., Scholten, T., Kühn, P., 2014. Pedogenesis, permafrost, substrate and topography: plot and landscape scale interrelations of weathering processes on the central-eastern Tibetan Plateau. Geoderma 226-227, 300-316.

Böhner, J., 2006. General climatic controls and topoclimatic variations in Central and High Asia. Boreas 35, 279-295.

Bond-Lamberty, B., Thomson, A., 2010. A global database of soil respiration data. Biogeosciences 7, 1915-1926.

Cairns, M.A., Brown, S., Helmer, E.H., Baumgardner, G.A., 1997. Root biomass allocation in the world´s upland forests. Oecologia 111, 1-11.

Cannell, M.G.R., 1982. World forest biomass and primary production data. Academic Press, London, New York.

Chen, X., Post, W., Norby, R., Classen, A., 2010. Modeling soil respiration and variations in source components using a multi-factor global climate change experiment. Climatic Change, 1-22.

Christensen, J.H., Hewitson, B., Busuioc, A., Chen, A., Gao, X., Held, I., Jones, R., Kolli, R.K., Kwon, W.T., Laprise, R., Rueda, V. M., Mearns, L., Menéndez, Räisänen, J., Rinke, A., Sarr, A., Whetton, P., 2007. Regional Climate Projections. In: Solomon, S., Qin, D., Manning, M., Chen, Z., Marquis, M., Averyt, K.B., Tignor, M., Miller, H.L. (Eds.), Climate Change 2007: The Physical Science Basis. Contribution of Working Group I to the Fourth Assessment Report of the Intergovernmental Panel on Climate Change. Cambridge University Press, Cambridge, pp. 848-940.

Davidson, E.A., Janssens, I. A., 2006. Temperature sensitivity of soil carbon decomposition and feedbacks to climate change. Nature 440, 165-173.

De Boeck HJ, Lemmens C, Zavalloni C., Gielen, B., Malchair, S., Carnol, M., Merckx, R., Van den Berge, J., Ceulemans, R., Nijs, I., 2008. Biomass production in experimental grasslands of different species richness during three years of climate warming. Biogeosciences 5, 585–594.

Doerfer, C., Kuehn, P., Baumann, F., He, J.-S., Scholten, T., 2013. Soil organic carbon pools and stocks in permafrost-affected soils on the Tibetan Plateau. PLoS ONE 8(2): e57024.

Duan, A.M., Wu, G.X., 2005. Role of the Tibetan Plateau thermal forcing in the summer climate patterns over subtropical Asia. Clim. Dyn. 24, 793-807.

Eamus, D., Chen, X., Kelley, E., Hutley, L.B., 2002. Root biomass and root fractional analyses of an open *Eucalyptus* forest in a savanna of north Australia. Aust. J. Bot. 50, 31-41.

Faget, M., Blossfeld, S., Jahnke, S., Huber, G., Schurr, U., Nagel, K.A., 2013. Temperature effects on root growth. In: Eshel, A., Beeckham, T. (Eds.), Plant roots, the hidden half. CRC Press, New York, pp. 31-1 – 31-11.

Fan, J.-W., Shao, Q.-Q., Liu, J.-Y., Wang, J.-B., Harris, W., Chen, Z.-Q., Zhong, H.-P., Xu, X.-L., Liu, R.-G., 2010. Assessment of effects of climate change and grazing activity on grassland yield in the Three Rivers Headwaters Region of Qinghai-Tibet Plateau, China. Environ. Monit. Assess. 170, 571–584.

Fang, C., Moncrieff, J.B., 2001. The dependence of soil CO_2 efflux on temperature. Soil Biol. Biochem. 33, 155-165.

Fitter, A., 1996. Characteristics and functions of root systems. Respiratory patterns in roots in relation to their functioning. In: Waisel, Y., Eshel, A., Kafkaki, K., Dekker, M. (Eds.), Plant roots, the hidden half. Inc., New York, pp. 1-20.

Fitter, A.H., Self, G.K., Brown, T.K., Bogie, D.S., Graves, J.D., Benham, D., Ineson, P., 1999. Root production and turnover in an upland grassland subjected to artificial soil warming respond to radiation flux and nutrients, not temperature. Oecologia 120, 575–581.

Geng, Y., Wang, Y., Yang, K., Wang, S., Zeng, H., Baumann, F., Kuehn, P., Scholten, T., He, J.-S., 2012. Soil Respiration in Tibetan alpine grasslands: belowground biomass and soil moisture, but not soil temperature, best explain the large-scale patterns. PLoS ONE 7, 1-12.

Gill, R.A., Kelly, R.H., Parton, W.J., Day, K.A., Jackson, R.B., Morgan, J.A., Scurlock, J.M.O., Tieszen, L.L., Castle, J.V., Ojima, D.S., Zhang, X.S., 2002. Using simple environmental variables to estimate belowground productivity in grasslands. Global Ecol. Biogeogr. 11, 79-86.

Hafner, S., Unterregelsbacher, S., Seeber, E., Becker, L., Xu, X., Li, X., Guggenberger, G., Miehe, G., Kuzyakov, Y., 2012. Effect of grazing on carbon stocks and assimilate partitioning in a Tibetan montane pasture revealed by $^{13}CO_2$ pulse labeling, Glob. Change Biol. 18, 528-538.

Hanson, P.J., Edwards, N.T., Garten, C.T., Andrews, J.A., 2000. Separating roots and soil microbial contributions to soil respiration: a review of methods and observations. Biogeochemistry 48, 115-146.

Hijmans, R. J., Cameron, S.E., Parra, J.L., Jones, P.G., Jarvis, A., 2005. Very high resolution interpolated climate surfaces for global land areas. Int. J. Climat. 25, 1965-1978.

Immerzeel, W., Quiroz, R., Jong, S., 2005. Understanding precipitation patterns and land use interaction in Tibet using harmonic analysis of SPOT VGT-S10 NDVI time series. Int. J. Remote Sens. 26, 2281–2296.

Ingrisch, J., Biermann, T., Seeber, E., Leipold, T., Li, M., Ma, Y., Xu, X., Miehe, G., Guggenberger, G., Foken, T., Kuzyakov, Y., 2015. Carbon pools and fluxes in an Tibetan alpine *Kobresia pygmaea* pasture partitioned by coupled eddy-covariance measurements and $^{13}CO_2$ pulse labeling, Sci. Total Environ. 505, 1213-1224.

Jackson, R.B., Canadell, J., Ehleringer, J.L., Mooney, H.A., Sala, O.E., Schulze, E.D., 1996. A global analysis of root distributions for terrestrial biomes. Oecologia 108, 389-411.

Jia, B., Zhou, G., Wang, Y., Wang, F., Wang, X., 2006. Effects of temperature and soil water-content on soil respiration of grazed and ungrazed *Leymus chinensis* steppes, Inner Mongolia. J. Arid Environ. 67, 60-76.

Jones, C.D., Cox, *P.M.,* Essery, R.L.H., Roberts, *D.L.,* Woodage, M.J., 2003. Strong carbon cycle feedbacks in a climate model with interactive CO_2 and sulphate aerosols. Geophys. Res. Lett. 30.

Klopatek, J.M., 2002. Belowground carbon pools and processes in different age stands of Douglas-fir. Tree Physiol. 22, 197-204.

Kurz, W.A., Beukema, S.J., Apps, M.J., 1996. Estimation of root biomass and dynamics for the carbon budget model of the Canadian forest sector. Can. J. For. Res. 26, 1973-1979.

Kutzbach, J. E., Liu, X., Liu, Z., Chen, G., 2008. Simulation of the evolutionary response of global summer monsoons to orbital forcing over the past 280,000 years. Climate Dynamics 30, 567-579.

Kuzyakov, Y., 2006. Sources of CO_2 efflux from soil and review of partitioning methods, Soil Biol. Biochem. 38, 425-448.

Lambers, H., Scheurwater, I., Atkin, O. K., 1996. Respiratory patterns in roots in relation to their functioning. In: Waisel, Y., Eshel, A., Kafkaki, K., Dekker, M. (Eds.), Plant Roots, the Hidden Half. Inc., New York, 323-362.

Li, X., Zhang, X., Wu, J., Shen, Z., Zhang, Y., Xu, X., Fan, Y., Zhao, Y., Yan, W., 2011. Root biomass distribution in alpine ecosystems of the northern Tibetan Plateau. Environ. Earth Sci. 64, 1911-1919.

Li, Z., Zhang, Y., Yu, D., Zhang, N., Lin, J., Zhang, J., Tang, J., Wang, J., Mu, C., 2014. The influence of precipitation regimes and elevated CO_2 on photosynthesis and biomass accumulation and partitioning in seedlings of the rhizomatous perennial grass *Leymus chinensis*. PLoS ONE 9(8): e103633.

Liu, X., Chen, B., 2000. Climatic warming in the Tibetan Plateau during recent decades. Int. J. Climat. 20, 1729-1742.

Luo, Y., Zhou, X., 2006. Soil respiration and the environment. Elsevier, San Diego.

Luo, T., Brown, S., Pan, Y., Shi, P., Ouyang, H., Yu, Z., Zhu, H., 2005. Root biomass along subtropical to alpine gradients: global implication from Tibetan transect studies. Forest Ecology and Management 206. 349-363.

Luo, T., Li, W., Zhu, H., 2002. Estimated biomass and productivity of natural vegetation on the Tibetan Plateau. Ecol. Appl. 12, 980-997.

Maussion, F., Scherer, D., Finkelnburg, R., Richter, J., Yang, W., Yao, T., 2011. WRF simulation of a precipitation event over the Tibetan Plateau, China – an assessment using remote sensing and ground observations. Hydrol. Earth Syst. Sci. 15, 1795-1817.

Miehe, G., Miehe, S., Böhner, J., Kaiser, K., Hensen, I., Madsen, D., Liu, J., Opgenoorth, L., 2014. How old is the human footprint in the world´s largest alpine ecosystem? A review of multiproxy records from the Tibetan Plateau from the ecologists' viewpoint. Quat. Sci. Rev. 86, 190-209.

Mokany, K., Raison, R.J., Prokushkin, A.S., 2006. Critical analysis of root:shoot ratios in terrestrial biomes. Glob. Change Biol. 12, 84-96.

Moyano, F.E., Owen, A., Bahn, M., Bruhn, D., Burton, A.J., Heinemeyer, A., Kutsch, W.L., Wieser, G., 2009. Respiration from roots and the mycorrhizosphere. In: Kutsch, W.L., Bahn, M., Heinemeyer, A. (Eds.), Soil carbon dynamics. An integrated methodology. Cambridge University Press, New York, 127-156.

Ohtsuka, T., Hirota, M., Zhang, X., Shimono, A., Senga, Y., Du, M., Yonemura, S., Kawashima, S., Tang, Y., 2008. Soil organic carbon pools in alpine to nival zones along an altitudinal gradient (4400-5300 m) on the Tibetan Plateau. Polar Science 2, 277-285.

Pei, Z.-Y., Ouyang, H., Zhou, C.-P., Xu, X.-L., 2009. Carbon Balance in an Alpine Steppe in the Qinghai-Tibet Plateau. J. Integr. Plant Biol. 51, 521-526.

Raich, J.W., Schlesinger, W.H., 1992. The global carbon dioxide flux in soil respiration and its relationship to vegetation and climate. Tellus 44B, 81-99.

Rasse, D.P., Rumpel, C., and M.-F. Dignac, 2005. Is soil carbon mostly root carbon? Mechanisms for a specific stabilization, Plant Soil 269, 341-356.

Rodeghiero, M., Cescatti, A., 2005. Main determinants of forest soil respiration along an elevation/temperature gradient in the Italian Alps. Glob. Change Biol. 11, 1024–1041.

Rodeghiero, M., Churkina, G. Martinez, C., Scholten, T. Gianelle, D., Cescatti. A., 2013. Components of forest soil CO_2 efflux estimated from $\Delta^{14}C$ values of soil organic matter. Plant Soil 364/1, 55-68.

Schlesinger, W.H., Andrews, J.A., 2000. Soil respiration and the global carbon cycle. Biogeochemistry 48, 7-20.

Schroeder, P.E., Winjum, J.K., 1995. Assessing Brazil's carbon budget I. Biotic carbon pools. For. Ecol. Manage. 75, 77-86.

Schulze, E.-D., Mooney, H.A., Sala, O.E., Jobbagy, E., Buchmann, N., Bauer, G., Canadell, J., Jackson, R.B., Loreti, J., Oesterheld, M., Ehleringer, J.R., 1996. Rooting depth, water availability, and vegetation cover along an aridity gradient in Patagonia. Oecologia 108, 530-511.

Schuur, E.A.G., McGuire, A.D., Schädel, C., Grosse, G., Harden, J.W., Hayes, D.J., Hugelius, G., Koven, C.D., Kuhry, P., Lawrence, D.M., Natalo, S.M., Olefeldt, D., Romanovsky, V.E., Schaefer, K., Turetsky, M.R., Treat, C.C., Vonk, J.E., 2015. Climate change and the permafrost carbon feedback. Nature 520, 171-179.

Shi, X.-M., Li, X.G., Li, C.T., Zhao, Y., Shang, Z.H., Ma, Q., 2013. Grazing exclusion decreases soil organic C storage at an alpine grassland of the Qinghai-Tibetan Plateau, Ecol. Eng. 57, 183-187.

Smith, E., Shi, L., 1995. Reducing discrepancies in atmospheric heat budget of Tibetan Plateau by satellite-based estimates of radiative cooling and cloud-radiation feedback. Meteorol. Atmos. Phys. 56, 229–260.

Stone, E.L., Kalisz, P.J., 1991. On the maximum extent of tree roots. For. Ecol. Manage. 46, 59-102.

Tibetan and Himalayan Library, 2002. Land Cover (Tibet). http://www.thlib.org/places/maps/collections/show.php?id=387 (16.12.2014).

Titlyanova, A.A., Romanova, I.P., Kosykh, N.P., Mironycheva-Tokareva, N.P., 1999. Pattern and process in above-ground and below-ground components of grassland ecosystems. J. Veg. Sci. 10, 307-320.

Unterregelsbacher, S., Hafner, S., Guggenberger, G., Miehe, G., Xu, X., Liu, J., Kuzyakov, Y., 2012. Response of long-, medium- and short-term processes of the carbon budget to overgrazing-induced crusts in the Tibetan Plateau, Biogeochemistry 111, 187-201.

Vogt, K.A., Vogt, D.J., Palmiotto, P.A., Boon, P., O´Hara, J., Asbjornsen, H., 1996. Review of root dynamics in forest ecosystems grouped by climate, climatic forest type and species. Plant Soil 187, 159-219.

Wang, B., Bao, Q., Hoskins, B., Wu, G., Liu, Y., 2008a. Tibetan Plateau warming and precipitation change in East Asia. Geophys. Res. Lett. 35.

Wang, C., Cao, G., Wang, Q., Jing, Z., Ding, L., Long, R., 2008b. Changes in plant biomass and species composition of alpine *Kobresia* meadows along altitudinal gradient on the Qinghai-Tibetan Plateau. Sci. China Ser. C: Life Sciences 51, 86-94.

Wang, C.T., Long, R.J., Wang, Q.L., Jing, Z.C., Shi, J.J., 2009. Changes in plant diversity, biomass and soil C, in alpine meadows at different degradation stages in the headwater region of the three rivers, China, Land Degrad. Develop. 20, 187-198.

Wang, S., Jin, H., Li, S., Zhao, L., 2000. Permafrost degradation on the Qinghai-Tibet Plateau and its environmental impacts. Permafrost Periglacial Process. 11, 43-53.

Wang, W.Y., Wang, Q.J., Li, S.X., Wang, G., 2006. Distribution and species diversity of plant communities along transect on the Northeastern Tibetan plateau. Biodivers. Conserv. 15, 1811–1828.

Wang, X., Liu, L., Piao, S., Janssens, I.A., Tang, J., Liu, W., Chi, Y., Wang, J., Xu, S., 2014. Soil respiration under climate warming: differential response of heterotrophic and autotrophic respiration, Glob. Change Biol. 20, 3229-3237.

Wen, L., Dong, S., Li, Y., Wang, X., Li, X., Shi, J., Dong, Q., 2013. The impact of land degradation on the C pools in alpine grasslands of the Qinghai- Tibet Plateau, Plant Soil 368, 329-340.

WorldClim – Global Climate Data. http://www.worldclim.com (16.12.2014).

Wu, Y., Wu, J., Deng, Y., Tan, H., Du, Y., Gu, S., Tang, Y., Cui, X., 2011. Comprehensive assessments of root biomass and production in a *Kobresia humilis* meadow on the Qinghai-Tibetan Plateau. Plant Soil 338, 497-510.

Xu, Z.X., Gong, T., L., Li, J. Y., 2008. Decadal trend of climate in the Tibetan Plateau - regional temperature and precipitation. Hydrol. Process. 22, 3056-65.

Xu, Z.Z., Zhou, G.S., 2005. Effects of water stress and high nocturnal temperature on photosynthesis and nitrogen level of a perennial grass Leymus chinensis. Plant Soil 269, 131–139.

Yan, Y., Zhang, J.-G., Zhang, J.-H., Fan, J.-R., Li, H.-X., 2005. The belowground biomass in alpine grassland in Nakchu Prefecture of Tibet. Acta Ecol. Sin. 25, 2818-2823. (in Chinese)

Yang, Y., Fang J., Smith, P.,Tang, Y., Chen, A., Ji, C., Hu, H., Rao, S., Tan K.U.N., He, J.-S., 2009. Changes in topsoil carbon stock in the Tibetan grasslands between the 1980s and 2004. Glob. Change Biol. 15, 2723-2729.

Yang, Y., Fang, J., Tang, Y., Ji, C., Zheng, C., He, J.-S., Zhu, B., 2008. Storage, patterns and controls of soil organic carbon in the Tibetan grasslands. Glob. Change Biol. 14, 1592-1599.

Yu, H.Y., Luedeling, E., Xu, J.C., 2010. Winter and spring warming result in delayed spring phenology on the Tibetan Plateau. Proc. Natl. Acad. Sci. U. S. A. 107, 22151–22156.

Zhang, Y., Li Bingyuan, Z., Du, 2002. The area and boundary of Qinghai-Tibet Plateau. Geographical Research, 21, 1–8. (in Chinese)

Zhang, Y., Wang, G., Wang, Y., 2010. Response of biomass spatial pattern of alpine vegetation to climate change in permafrost region of the Qinghai-Tibet Plateau, China. J. Mt. Sci. 7, 301-314.

Zheng, D., 1996. The system of physico-geographical regions of the Qinghai-Xizang (Tibet) Plateau. Sci. China Ser. D 39, 410-417.

Zhong, L., Ma, Y., Salama M.S., Su, Z., 2010. Assessment of vegetation dynamics and their response to variations in precipitation and temperature in the Tibetan Plateau. Clim. Chang. 103, 519-535.

Zhuang, Q., He, J., Lu, Y., Ji, L., Xiao, J., Luo, T., 2010. Carbon dynamics of terrestrial ecosystems on the Tibetan Plateau during the 20th century: an analysis with a process-based biogeochemical model. Glob. Ecol. Biogeogr. 19, 649-662.

Manuscript 2

Predicting Soil Respiration for the Qinghai-Tibet Plateau: An Empirical Comparison of Regression Models

Pedobiologia 59 (2016) 41-49

Anna Bosch[a], Corina Doerfer[a], Jin-Sheng He[b, c], Karsten Schmidt[a], Thomas Scholten[a]

[a]University of Tuebingen, Department of Geosciences, Chair of Soil Science and Geomorphology, Tübingen, Germany

[b]Key Laboratory of Adaptation and Evolution of Plateau Biota, Northwest Institute of Plateau Biology, Chinese Academy of Sciences, Xining, 810008, China

[c]Department of Ecology, College of Urban and Environmental Sciences, and Key Laboratory for Earth Surface Processes of the Ministry of Education, Peking University, Beijing, 100871, China

Abstract

Alpine ecosystems like the Qinghai-Tibet Plateau strongly respond to global warming. Their soils, containing large carbon stocks, release more carbon dioxide as a possible consequence. Reciprocally, this may intensify climate warming. The Qinghai-Tibet plateau´s large and almost inaccessible terrain results in a general data scarcity for this area making the quantification of soil carbon dynamics challenging. The current study provides an area-wide estimation of soil respiration for the Qinghai-Tibet Plateau, which is a key region for climate change studies due to its size and sensitivity. We compared the ability of six regression models to predict soil respiration that were developed within different studies and are based on mean annual air temperature, mean annual precipitation and belowground biomass. We used the WorldClim data sets to approximate annual soil respiration on a regional scale. Compared to field measurements of soil respiration at single spots in different vegetation zones on the

Qinghai-Tibet Plateau (max. 1876.63 g C m^{-2} y^{-1}), our predicted results (max. 1765.13 g C m^{-2} y^{-1}) appear to be consistent. The basic difference between grasslands and forests in soil respiration is indicated by all regression models, however, a more precise differentiation between vegetation types is only exhibited by the regression model based on mean annual precipitation. Overall, this model performs best for most and the largest vegetation zones. Nevertheless, the approximations of the model based on mean annual temperature by Raich and Schlesinger (1992) with a lower constant better represent the vegetation zone of the alpine steppe. With this spatial estimation of soil respiration at a regional scale, a basis for assessing an area-specific potential of greenhouse gas emissions on the Qinghai-Tibet Plateau is provided. Moreover, we quantify a complex soil ecological process for this data-scarce area.

1 Introduction[2]

Soil respiration (SR), defined as the carbon dioxide (CO_2) efflux to the atmosphere, fundamentally impacts the global carbon cycle (Chen et al., 2010). Apart from oceans, soil emits the most carbon dioxide contributing approximately 98 ±12 Pg C $year^{-1}$ to the global carbon budget (Bond-Lamberty and Thomson, 2010a; Schlesinger and Andrews, 2000; Valentini et al., 2000). With more than 1500 Pg C, soils hold the largest amount of carbon in terrestrial ecosystems (Amundson, 2001; Raich and Schlesinger, 1992) roughly double that of the atmospheric CO_2-C pool (Jia et al., 2006). On a global scale, ~ 10% of the atmospheric CO_2 passes through soil annually (Bond-Lamberty and Thomson, 2010b). Therefore, a small increase in the amount of soil CO_2 efflux, especially across wide-spread areas, can considerably influence atmospheric CO_2 concentrations, potentially increasing global warming (Rodeghiero and Cescatti, 2005, 2013; Davidson and Janssens, 2006; Schlesinger and Andrews, 2000).

The ecologically fragile Qinghai-Tibet Plateau is a key region for examining ecosystem processes due to its sensitivity and comparatively low human impact (Fan et al., 2010; Yang et al., 2009; Liu and Chen, 2000). Moreover, the plateau is of high significance for studies on soil respiration (SR) (Geng et al., 2012) because of its important role in the global carbon cycle and remarkable contribution to the global carbon budget. As

[2] Abbreviations: soil respiration (SR), carbon (C), carbon dioxide (CO_2), mean annual temperature (MAT), mean annual precipitation (MAP), belowground biomass (BGB)

the highest and spatially most extended plateau on earth, the Qinghai-Tibet Plateau influences both regional and global climates significantly (Zhong et al., 2010; Wang et al., 2006). It has also been called the ‘driving force’ or ‘amplifier’ of global warming (Kang et al., 2010) due to its large size and high altitude but also because of its effects by means of thermal and mechanical forces (Kutzbach et al., 2008; Duan and Wu, 2005; Manabe and Terpstra, 1974). However, climate change likewise influences the Qinghai-Tibet Plateau (Zhang et al., 2010). It is one of the regions of highest sensitivity to global warming mainly due to its extreme elevation (Zhong et al., 2010; Zhang et al., 2007; Luo et al., 2002). The plateau´s temperature is expected to increase far above average in the future (Wang et al., 2008; Christensen et al., 2007; Liu and Chen, 2000). The cryosphere, commonly considered as the most sensitive indicator to climate change, undergoes rapid changes on the Qinghai-Tibet Plateau (Kang et al., 2010). There, earth´s largest high-altitude and low-latitude permafrost zone, with more than half of its total area influenced by permafrost (Cheng, 2005), shows increasing permafrost degradation (Böhner and Lehmkuhl, 2005; Baumann et al., 2009). This process has been advancing even more than in other high-latitude, low-altitude permafrost regions over the last few decades (Yang et al., 2004). As expected, the further degradation of Tibetan permafrost (Böhner and Lehmkuhl, 2005; Wang et al., 2000) will highly influence its soils mainly by changes in their temperature and moisture patterns (Doerfer et al., 2013; Zhang et al., 2003). Thus, global warming impacts permafrost stability and distribution as well as vegetation and soil characteristics that intensively interact with SR through complex processes (Chapin et al., 2005). Climate warming is even presumed to be the main reason for the increasing global loss of soil carbon to the atmosphere (Jones et al., 2003). This calls attention to the need of a deep understanding of the quantity of SR on the Qinghai-Tibet Plateau (Geng et al., 2012).

Various complex processes characterize SR, representing the activity of soil biota (Reth et al., 2005). Basically, SR is diveded into two components: autotrophic respiration, consisting of root and root-associated (e.g., mycorrhizae) respiration, and heterotrophic respiration, constituted by microbial respiration in the course of soil organic matter decomposition (Joo et al., 2012). Although not entirely congruent (Boone et al., 1998), both of these parts of SR vary with environmental changes (Chen et al., 2010). The variability of SR occurs in temporal and spatial dimensions, both vertically and horizontally (Davidson and Trumbore, 1995). Generally, there is quite a

number of biotic and abiotic factors influencing soil CO_2 efflux. Soil respiration is mostly regulated by soil temperature and soil water content (e.g. Raich and Tufekcioglu, 2000; Singh and Gupta, 1977). Water solubilizes organic matter and supports its availability, whereas temperature directly impacts metabolic activities (Koizumi et al., 1999). Soil moisture also controls the response of SR to temperature variation (Wisemann et al., 2004). Other factors affecting soil CO_2 emissions include vegetation (Raich and Tufekcioglu, 2000), soil characteristics, precipitation (Rey et al., 2002), topography (Fang et al., 1998), and land-use regimes (Ewel et al., 1987).

As a multifactorial process with complex interactions and high variability across time and space, SR has always been a challenge to measure and no procedure or model has been commonly accepted as a standard yet (Luo et al., 2006). Widely used methods for field measurements, however, are chamber systems and eddy-covariance systems (Morén and Lindroth, 2000) although they are, in general, highly time and cost intensive (Luo et al., 2006). One possible solution for SR measurement is to apply predictive tools especially for large areas. Due to a lack of data and knowledge of fundamental process components, mechanistic or process-based modelling remains likewise challenging and is still unable to represent SR fully reliable (Luo et al., 2006).

Empirical models have been widely applied for the estimation of likewise complex processes such as soil erosion, which is estimated most commonly with the Universal Soil Loss Equation (Da Silva, 2004). Various regression models for SR have been developed based on field measured SR as a function of different biotic and abiotic variables. These models usually focus on a strongly reduced number of controlling factors of SR (Luo et al., 2006) and thus, potentially overcome the restrictions of limited data, which is especially relevant to large-scale predictions in remote areas. Those empirical models include such climatic variables as mean annual temperature (MAT) and mean annual precipitation (MAP) as input parameters as well as biotic variables such as belowground biomass (BGB). These climatic and biotic variables will be compared in this study.

For the Qinghai-Tibet Plateau, almost two-thirds of which is covered by grassland (Yang et al., 2008; Wang et al., 2006), BGB has been shown to most strongly influence grassland ecosystem SR at a regional scale due to high root biomass density (Geng et al., 2012). In general, temperature and precipitation are widely considered as most effectively representing SR variation in time and space (Bond-Lamberty and Thomson,

2010a; Hashimoto et al., 2015) while MAT and MAP are important candidates as predictors for annual SR. We assume the Qinghai-Tibetan Plateau to represent a global-scale ecosystem given it has both highly heterogenic climate and vegetation. Nevertheless, data for the Qinghai-Tibet Plateau at a sufficient spatial and temporal resolution are generally scarce. Even though the Plateau's unique role in climate change studies due to its ecological sensibility, the inaccessible and complex terrain complicates research activities resulting in this lack of data. Despite their limitations, empirical models are therefore highly advantageous for predicting SR of the Qinghai-Tibetan Plateau due to its size and specific data acquisition requirements. The need for quantifying highly complex soil ecological processes more accurately for sparsely sampled areas, especially in light of climate change, is captured by such an approach and exemplarily executed for the Qinghai-Tibet Plateau.

Mindful of these challenges, we aim at determining the best regression model for estimating SR on the Qinghai-Tibet Plateau in this study. The ideal algorithm should allow for (1) the calculation of SR on a large scale and (2) for variation with major vegetation types.

2 Material and Methods

2.1 Study area

Our study area, the Qinghai-Tibet Plateau, is located in southwestern China. With an area of about 2.6 $\times 10^6$ km^2, it fully covers Tibet and Qinghai provinces, and partially Xinjiang, Gansu, Sichuan, and Yunnan provinces. As the largest plateau on earth, the Qinghai-Tibet Plateau extends from 26°00′12" N to 39°46′50" N and from 73°18′52" E to 104°46′59" E with a maximum length of approx. 2 945 km from east to west and approx. 1 532 km from south to north. The average altitude of the plateau is 4380 m (Zhang et al., 2002). Surface elevation sharply declines at its border, particularly at the southern end. Overall, eastern and western regions differ markedly with regard to geomorphology, vegetation and climatic characteristics (Smith and Shi, 1995). The unique geographical position of the Qinghai-Tibet Plateau results in an azonal, plateau monsoon climate from a subtropical to a temperate mountain climate (Zhuang et al., 2010; Zhong et al., 2010) with strong solar radiation, low air temperature, large daily temperature variations yet low differences between annual mean temperatures (Zhong et al., 2010). The mean temperature in July, the warmest month, varies from 7 °C to 15 °C and from -1 °C to -7 °C in January, the coldest month. Average annual

temperature is 1.6 °C (Yang et al., 2009). Precipitation amounts to about 413.6 mm per year (Yang et al., 2009), with more than 60-90% falling in the wet and humid summers (June-September) and 10% at maximum in the cool, arid winters (November-February) (Xu et al., 2008). Summer precipitation can be less than 50 mm in the northwest (Xu et al., 2008). Generally, a decrease both in temperature and in precipitation from the south-eastern to the north-western part of the plateau is apparent (Immerzeel et al., 2005). The topographic setting as well as atmospheric conditions determine the sequence of alpine forests, meadows, steppes and deserts from southeast to northwest (Fig. 1), which follows a climatic gradient from warm and humid to cold and arid according to the influence of the South Asian monsoon (Pei et al., 2009; Zheng, D., 1996).

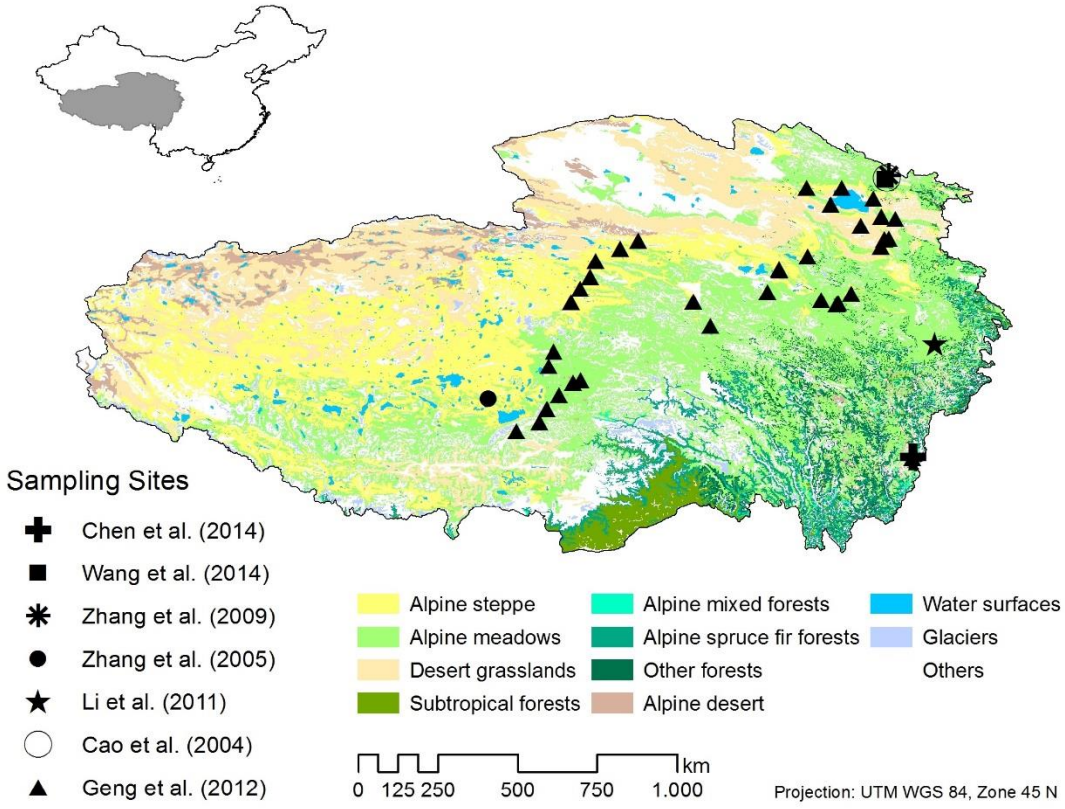

Fig. 1. Vegetation map of the Qinghai-Tibet Plateau based on data sets for land cover in Tibet with sampling localities of Cao et al. (2004), Zhang et al. (2005), Li et al. (2011), Zhang et al. (2009), Geng et al. (2012), Wang et al. (2014) (Tibetan and Himalayan Library, 2002).

Alpine steppes and meadows dominate the undisturbed vegetation with *Stipa* species and *Kobresia* meadows as major vegetation types. Alpine grasslands cover more than 60% of the study area (Yang et al., 2008; Wang et al., 2006). Long freezing periods

and thus, relatively short growing seasons characterize the plateau`s climate (Yu et al., 2010). Its vegetation is regarded as comparatively natural (Schroeder et al. 1995), although parts of the plateau in the humid Southeast have undergone human-induced changes with *Kobresia pygmaea* growing instead of forests and grasslands (Miehe et al., 2014). Continuous, complex pedogenetic processes on the Qinghai-Tibet Plateau typically result in young and highly diverse soils with distinct degradation characteristics, exhibiting a strong influence by permafrost regimes (Baumann et al., 2014).

2.2 Geodatabase and processing

In this case study, three data sets were used to estimate SR from temperature, precipitation and belowground biomass data. All data sets were projected into the Universal Transverse Mercator coordinate system WGS 1984, Zone 45 N. The data sets for MAT and MAP were obtained from the WorldClim data set available at http://worldclim.com. This latter database was compiled from a considerable number of various sources, such as the Global Historical Climate Network, World Meteorological Organization and the Food and Agricultural Organization, with a resolution of 1 x 1 km and representing the current climate conditions from ca. 1950 to 2000. Data from climate stations were interpolated with latitude, longitude and altitude as independent variables (for more detailed information see Hijmans et al., 2005). BGB data with a spatial resolution of 1 x 1 km have been generated by the application of an exponential regression model developed by Luo et al. (2005). When modeling, they incorporated various climate and vegetation data of the Qinghai-Tibet Plateau and presented the different resulting models based on various input parameters. When these models were compared, the model with MAT as an input parameter excels when applied to the Qinghai-Tibet Plateau (Bosch et al., unpublished results). We therefore use the data set generated with this MAT-dependent model in the present study. The input MAT data set of this calculated BGB data set also originate from WorldClim data (Bosch et al., unpublished results).

2.3 Soil Respiration Calculation and Evaluation

SR was calculated based on MAT, MAP and BGB using six different regression models (Tab. 1).

Table 1. Regression models to approximate soil respiration.

Type of regression	Region, Vegetation Type	Equation	Parameters	Author(s)	r^2
Regression based on mean annual temperature T	Global	$SR = 25.6T + 300$	SR = annual soil respiration rate (g C/m^2/yr), T = mean annual temperature (°C),	Raich and Schlesinger (1992) (MAT I)	0.42
	Micronesia and Hawaii, peatlands	$Y = 265.9 + (27.7 * MAT)$	Y = annual soil respiration rate (g C m^{-2} yr^{-1}), MAT = mean annual temperature (°C)	Chimner (2004) (MAT II)	0.46
Regression based on mean annual precipitation P	Global	$SR = 0.391P + 155$	SR = annual soil respiration rate (gC/m^2/yr), P = mean annual precipitation (mm)	Raich and Schlesinger (1992)	0.34
Regression based on mean annual temperature T, mean annual precipitation P	Global	$SR = (9.26T) + (0.0127TP) + 289$	SR = annual soil respiration rate (gC/m^2/yr), T = mean annual temperature (°C), P = mean annual precipitation (mm)	Raich and Schlesinger (1992) (MATP I)	0.50
	Global	$SR = (9.88T) + (0.0344P) + (0.0112TP) + 268$	SR = annual soil respiration rate (gC/m^2/yr), T = mean annual temperature (°C), P = mean annual precipitation (mm)	Raich and Schlesinger (1992) (MATP II)	0.50
Regression based on root biomass	India, tropical forest soil	$y = 0.32x + 176.6$	y = soil respiration (mg CO_2 m^{-2} h^{-1}), x = total root biomass (g m^{-2})	Behera et al. (1990)	0.89

Due to a scarce spatial data resolution for deriving the amount of SR on the Qinghai-Tibet Plateau, we made use of field observations of SR from other studies (Tab. 2). To evaluate the power of the regression models applied in this study, we compared our results with those reported by Cao et al. (2004), Zhang et al. (2005), Li et al. (2011), Zhang et al. (2009), Geng et al. (2012), Chen et al. (2014) and Wang et al. (2014). The observation sites are located in three different vegetation types: alpine steppe, alpine meadows and forest. These vegetation types were identified in each of the studies we used for comparison. Thus, the evaluation sites comprise the widest-spread vegetation types and the majority of vegetation cover on the plateau (Fig. 1). The sites also cover various climatic conditions and altitudes (3000 m – 5105 m a.s.l.). The sampling sites of Chen et al. (2004) located in the eastern part of the plateau are not displayed in Figure 1.

All samples except the ones from the studies of Chen et al. (2004) and Wang et al. (2014) were collected in the peak season of soil respiration from June to August. Daily means were calculated based on several measurements per day in each study. To compare annual data calculated by the regression models, we summed up daily means to give annual SR values. However, this leads to a systematic overestimation of annual SR, because the daily means were estimated based on measurements during peak season months. We therefore developed and implemented a seasonality correction factor to account for this. This seasonality correction factor is based on calculations by Cao et al. (2004). The annual total sum of daily average SR values is about 1.99 times higher than the estimation of annual SR values where seasonal variation of SR is considered. We accordingly corrected all cumulative SR annual values by a factor of 0.33 exept for the evaluation data from Chen et al. (2004) and Wang et al. (2014). The data of Chen et al. (2004) are based on measurements every 10 days throughout an entire year after having conducted extra measurements to find the optimal measurement time representing daily means. Wang et al. (2014) summed daily means based on hourly measurements throughout four years to calculate annual estimates, which we averaged to one mean annual value.

Ranges of the model-based SR values of each vegetation zone are based on grid points according to the geographical coordinates from the field sampling sites of the literature data. Since information on precise georeferences was not given in Chen et al. (2014), personal communication with Ji Luo (2015) served as an additional source of information. The range of all field measurements throughout the different vegetation zones is compared to all calculated values of the whole plateau for each model. Moreover, we compared the mean of all field data to the mean of all calculated SR values for the whole plateau for each model.

3 Results and Discussion

The resulting SR estimates of the applied regression models ranged from a low of -300.08 to a maximum of 1762.17 g C m^{-2} y^{-1}. All estimates generally fit the order of magnitude of the data measured in the field (Tab. 2).

Table 2. Range of soil respiration for different vegetation types on the Qinghai-Tibet Plateau measured by Cao et al. (2004), Zhang et al. (2005), Li et al. (2011), Zhang et al. (2009), Geng et al. (2012), Chen et al. (2014), Wang et al. (2014) and calculated based on regression models.

Vegetation type		Cao et al. (2004) (n = 1)	Zhang et al. (2005) (n = 1)	Li et al. (2011) (n = 1)	Zhang et al. (2009) (n = 60)	Geng et al. (2012) (n_{AS} = 18; n_{AM} = 20)	Chen et al. (2014) (n = 2)	Wang et al. (2014) (n = 1)	All field samples (n = 104)	Regression model based on					
										MAT I	MAT II	MAP	MAT and MAP I	MAT and MAP II	BGB
		[g C m^{-2} y^{-1}]													
Alpine steppe (AS)	Range	-	143.53	-	-	50.47-522.87	-	-	50.47-522.87	150.04-360.57	103.64-331.44	221.65-339.65	214.76-318.44	201.74-310.82	422.52-422.64
	Mean	-	-	-	-	-	-	-	254.6	262.86	225.71	283.17	270.64	260.60	422.57
	Median	-	-	-	-	-	-	-	245.9	274.39	238.19	279.87	274.54	263.33	422.57
	(Mean rel. error [%])	-	-	-	-	-	-	-	-	*(48.70)*	*(41.32)*	*(63.14)*	*(57.22)*	*(56.03)*	*(135.34)*
Alpine meadow (AM)	Range	555.37	-	714.17	326.15-1876.63	144.95-1666.97	-	696	144.95-1876.63	146.39-376.79	99.69-349.00	266.95-561.55	205.75-345.41	197.37-357.82	422.52-422.66
	Mean	-	-	-	-	-	-	-	828.77	293.36	258.87	333.22	285.82	280.66	422.59
	Median	-	-	-	-	-	-	-	795.95	311.39	278.23	333.48	295.7	290.37	422.6
	(Mean rel. error [%])	-	-	-	-	-	-	-	-	*(60.87)*	*(64.59)*	*(55.37)*	*(61.26)*	*(60.31)*	*(46.88)*
Forest (F)	Range	-	-	-	-	-	643.76-908.84	-	643.76-908.84	467.88-474.34	447.55-454.54	529.54-532.1	430.05-434.91	436.8-441.3	422.78-422.79
	Mean	-	-	-	-	-	-	-	776.3	471.11	451.04	530.82	432.48	439.05	422.78
	Median	-	-	-	-	-	-	-	-	-	-	-	-	-	-
	(Mean rel. error [%])	-	-	-	-	-	-	-	-	*(37.56)*	*(41.89)*	*(31.62)*	*(44.28)*	*(43.44)*	*(45.53)*
All	Range	-	-	-	-	-	-	-	50.47-1876.63	-223.07-914.4	-300.08-930.7	161.64-1762.17	15.83-1641.16	7.98-1639.56	422.48-423.76
	Mean	-	-	-	-	-	-	-	722.86	257.13	219.52	299.18	281.14	270.89	422.60
	Median	-	-	-	-	-	-	-	713.00	237.06	197.80	251.57	214.61	200.61	422.52
	(Mean rel. error [%])	-	-	-	-	-	-	-	-	*(64.42)*	*(69.63)*	*(58.61)*	*(61.10)*	*(62.52)*	*(41.53)*

Negative pixel values arose from the regression models involving MAT as input parameter, representing areas where the model MAT is -9.59 °C and below as for the case of Chimner (2004). The linear regression models did not adequately describe the shape of the true temperature-SR relation for very low temperatures. We, therefore, showed negative results as zero by assuming that negligible metabolic activity occurs below a certain threshold. In Chimner´s (2004) model this threshold was -9.59 °C. An approximate limit of respiratory processes related to a minimum temperature was thereby reflected. The variation of SR with vegetation types was resembled by all regression models, however, to a different extent (Tab. 2, Fig. 2).

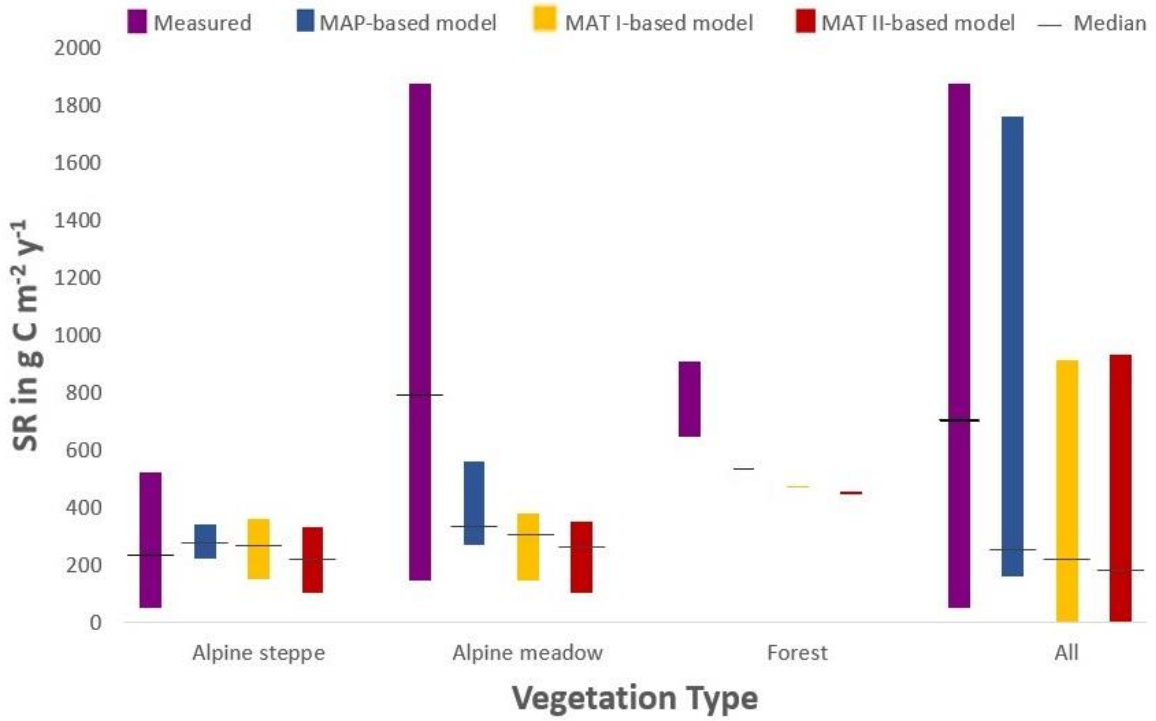

Fig. 2. Range of soil respiration for different vegetation types on the Qinghai-Tibet Plateau measured by Cao et al. (2004), Zhang et al. (2005), Li et al. (2011), Zhang et al. (2009), Geng et al. (2012), Chen et al. (2014) and calculated based on the mean annual precipitation-based, mean annual temperature I-based and mean annual temperature II-based regression models.

3.1 SR of grasslands

The ranges of all regression models were within the range of the directly measured SR samples (50.47 - 522.87 g C m^{-2} y^{-1}) for the vegetation zone of alpine steppe. The range of the calculations of the model based on MAT by Raich and Schlesinger (1992) (MAT II) (103.64 – 331.44 g C m^{-2} y^{-1}) most closely matched the range of the field measured samples followed by the MAT I-based model and MAP-based model (150.04

- 360.57 g C m^{-2} y^{-1} and 221.65 - 339.65 g C m^{-2} y^{-1}, respectively). Also, the relative error was lowest for the MAT II-based model (Tab. 2, Fig. 3).

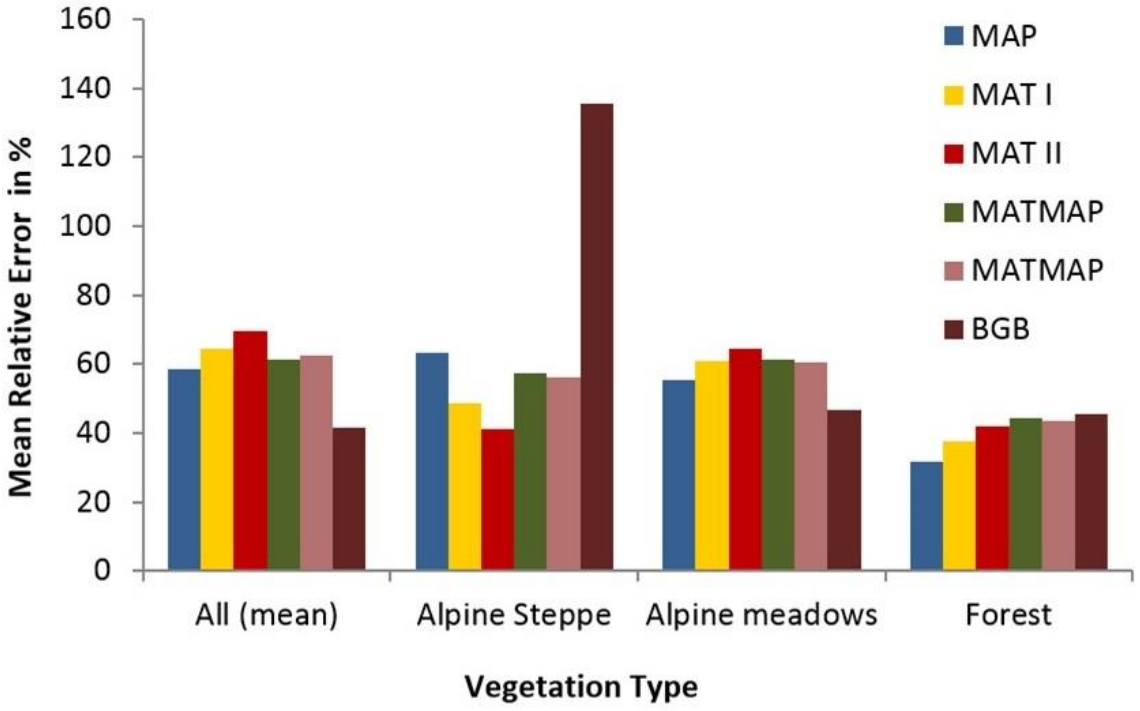

Fig. 3. Mean relative error of regression model estimates for the sampling sites of the respecitve vegetation zones.

Ranges, absolute minimum and maximum SRs estimated by the regression models that combine MAT and MAP as input parameters (with the higher constant: MATP I; with the lower constant: MATP II) were very similar (MATP I: 214.76-318.44 g C m^{-2} y^{-1}; MATP II: 201.74 – 310.82 g C m^{-2} y^{-1}) but were less congruent with the directly measured values than particularly the MAT-based regression models. The result of the MAT II-based model with regard to its absolute minimum value estimation was closest to the field measured data, although it was the maximum SR of the BGB-based model (422.64 g C m^{-2} y^{-1}) that corresponded best to the absolute maximum of the field data. However, the range of SR values predicted by the BGB-based model was a large number of times smaller than the range of the directly measured values. Moreover, the relative error of BGB-based model SR estimates was the highest. Thus, the MAT II-based regression model most closely represented the field measurements for the vegetation of alpine steppe.

The alpine meadows field values generally exhibited a wider range and higher minimum and maximum values (144.95 - 1876.63 g C m^{-2} y^{-1}) than the field data for

the alpine steppe. Generally, this comparatively wide range resulted from large differences in SR even between plant communities causing extremely high small-scale variability (Zhang et al., 2009) that cannot be reflected in the 1 x 1 km resolution at hand. Excluding samples that purely consisted of *Kobresia tibetica* with SR values of 565.58 to 1876.63 g C m^{-2} y^{-1} (Zhang et al., 2009; n = 20) and from 594.05 to 1666.97 g C m^{-2} y^{-1} for the three samples of Geng et al. (2012), the maximum value would have been distinctly lower (1410.71 g C m^{-2} y^{-1}). With 7 exceptions out of a total of 76 samples, all SR samples would be below 1000 g C m^{-2} y^{-1}, which clearly shows that the range of the vast majority was lower and about one third to one half smaller (144.95 to below 1000 g C m^{-2} y^{-1}). Predominantly occuring at wet sites, the plant physiological characteristics of *Kobresia tibetica* communities enable them to develop an extensive root system in this environment resulting in a much higher BGB (Wang et al., 2008) and consequently in strongly increased SR (Geng et al., 2012; Zhang et al., 2009). None of the regression models predicted such extraordinarily high values for these special plant communities. The spatial variability within the small distances between single plant communities that differed highly in their SR cannot be represented by a 1 x 1 km resolution as well. Of all regression models, however, the MAP-based one best concurred with the direct measurements except for the minimum. The minimum values of the models including MAT as the input parameter align more closely with smaller relative errors of only up to 0.01% in the minima for the MAT I-based model. It was nevertheless the MAP-based regression model which prooved to be the most appropriate for the alpine meadows as its mean relative error was lowest (55.37%) except from the model based on BGB (46.88%). The latter, however, is not adequate due its extremly small range (422.52 – 422.66 g C m^{-2} y^{-1}). The recognition that the MAP-based model as most appropriate one was further confirmed by the fact that this model was the only one to clearly distinguish between alpine steppe and alpine meadows.

3.2 SR of forests

Compared to the average field measurement value of grasslands excluding *Kobresia tibetica* samples (622.05 g C m^{-2} y^{-1}) and compared to the model-based values for grasslands, higher SR values generally occurred in forests which was also reflected by the calculations of all models. The models that included MAT as an input parameter performed very similarly; however, their estimates (430.05 - 474.34 g C m^{-2} y^{-1}) are not as close to the field measured values (643.76 - 908.84 g C m^{-2} y^{-1}) as the

approximations calculated by the MAP-based regression model (529.54 - 532.1 g C m^{-2} y^{-1}). Throughout all vegetation zones, the BGB-based results exhibited a small range within the range of MAT-based estimates. The MAP-based model had one of the lowest one (31.62%) relative mean errors compared to all other models (37.56 – 45.53%). The regression model based on MAP showed the closest approximations to field measurements and thus, performed best for the forest vegetation zone.

For the Qinghai-Tibetan Plateau as a whole, the regression models involving MAP as the input parameter were closest to all field measurement data of grassland types and forests with respect to the mean SR, the relative error of the mean, the minimum, the maximum and range. However, two exceptions were noted for the BGB-based model. These were the mean and the mean relative error for all data that arose from the comparatively static character of the values from the BGB-based model throughout the vegetation zones. This model was generally most inadequate with the highest mean relative error. It also underperformed with a particularly small range representing less than 1% of the field data range which appeared to be characteristic for this model throughout all vegetation zones. The model solely based on MAP, was the best model also in comparison to the regression models that included MAP as an input parameter. This was true especially for the mean value and its relative error (299.18 g C m^{-2} y^{-1}; 58.61%), indicating the peculiar importance of precipitation for SR in rather arid regions (Curiel Yuste et al., 2003).

Overall, the estimates of all regression models were within the order of magnitude of the values based on field measurements. All model-based estimates indicated the basic difference in SR between grasslands and forests. For the alpine steppe vegetation zone, the MAT II-based regression model was preferable as it most closely approximated direct field measurements. On the other hand, the regression model with MAP as an input parameter decidedly performed best for alpine meadows, forests and the range of the whole plateau. Generally, although developed for very different regions, both MAT-based models behave similarly across all vegetation types.

However, important uncertainties of the predicted values are associated with the regression models. Indicated by their coefficient of determination (r^2 = 0.34 – 0.88), the models cannot fully explain the data variability. This reflects highly complex interdependencies between SR and all its controlling factors. Moreover, discrepancies

would be expected since none of the regression models have been developed for the Qinghai-Tibet Plateau or for this certain kind of application.

Further deficiencies in the calculations of all regression models may arise from the development of the WorldClim data sets that show lower precision for poorly sampled regions like the Qinghai-Tibet Plateau (Maussion et al., 2011; Böhner, 2006; Hijmans et al., 2005). The same holds true for areas on the plateau with complex topography where a 1 x 1 km resolution does not capture all potential variation (Hijmans et al., 2005). Additionally, the input data set with BGB data exhibits limitations especially for forests and extraordinary high values (Bosch et al., unpublished results).

Furthermore, high small-scale variability of SR especially in alpine meadows is not captured by a data resolution of 1 x 1 km. The comparatively high values in alpine meadows, particularly of *Kobresia tibetica* plant communities, were not predicted by any regression model. This strong difference in SR rates between these communities and other alpine meadow plant communities results in large differences of SR over short distances, which can only be represented with higher spatial resolution. Moreover, vegetation degradation and grazing effects comprising about 35% of the Qinghai-Tibet Plateau and their decreasing influence on SR (Wen et al., 2013; Cao et al., 2004) were not integrated in our estimations and constraints these predictions of SR.

The evaluation data used in this study account for another weakness. Although all studies use chamber-based methods for their measurements, there are differences between the various chamber methods that may cause further inaccuracies of the values. In addition, daily means were calculated based on a different number of daily measurements and measurement times. Although for some of the studies, extra measurements were taken to determine the optimal number and time of measurement for the daily mean, discrepancies among the results remain. Also, the annual SR values for forests have been estimated based on continuous measurements throughout one whole year in contrast to the values of all other studies where seasonality was not considered a major factor.

The estimation of annual values based on daily means of field measurements poses other constraints. The higher the temporal resolution of data, the higher the variability of the cumulative values. This tendency increases with larger differences in the target temporal resolution, which eventually ranges from seconds to a year. This may result

in ranges of values that are too large. The seasonality correction factor derived from the estimations by Cao et al. (2004) for alpine meadows might vary for other vegetation types such as forests as the cumulative SR in the peak month accounts for only about 20% of the total annual SR (Chen et al., 2014). The larger difference in SR between forests and grasslands compared to the difference between alpine steppes and alpine meadows can be explained as forests can often adjust better to environmental (e.g. temperature) variation. Furthermore, the values provided by Cao et al. (2004) are themselves estimations based on (1) data obtained from chamber method measurements, which have inherent limitations, and on (2) equations based on soil temperature with an $r^2 = 0.82$. It should be noted that approximations for SR obtained from annual values in general are inevitably not as accurate as calculations from periodic or continuous data. However, a recent study (Wang et al., 2014b) provides hourly data throughout four years. We developed a seasonality correction factor of *0.55 based on their results, which corresponded to the one we used based on Cao et al.´s (2004) results. The relative error of the annual total of SR based on cumulative daily means is hence lower than for Cao et al.´s (2004). In Wang et al.´s (2014) study, however, the daily mean refers to the whole growing season in contrast to the daily means of all other evaluation data studies including Cao et al. (2004), which refer to the peak months in the growing season. Therefore, the seasonality correction factor based on the results of Cao et al. (2004) still achieved more accurate results.

In conclusion, we recommend the MAP-based regression model for area-wide, pixel-based calculations of SR on the Qinghai-Tibet Plateau (Fig. 4) given our analysis of the results in view of the dependence of SR on vegetation.

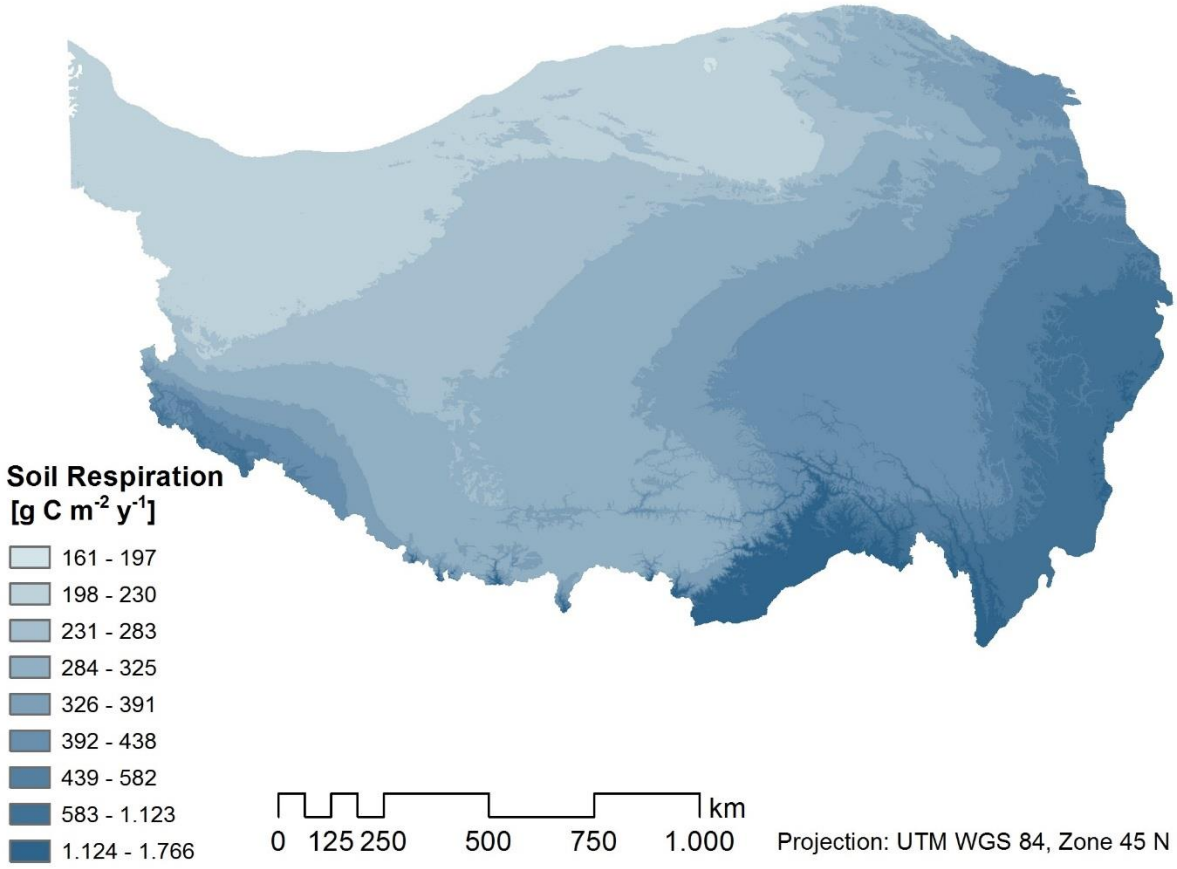

Fig. 4. Spatial distribution of soil respiration on the Qinghai-Tibet Plateau based on mean annual precipitation according to Raich and Schlesinger (1992). Soil respiration is in SI unit (Mg ha^{-1}). The spatial resolution of the grids is 1 x 1 km.

Considering the fact that this regression model only performs worse than the models including MAT as an input parameter for the minimum value in the alpine steppe and, first and foremost, clearly excels for alpine meadows and forests, it is to be given preference over all regression models. More importantly, the MAP-based regression model is the only one that shows a clear difference between the vegetation types alpine steppe and alpine meadows. We, therefore, consider it as the superior model for a pixel-based calculation of SR on the Qinghai-Tibet Plateau. Our study provides an area-wide quantification of a multifactorial soil ecological process assessed by a comparison of different regression models against the background of strong data limitations.

4 Conclusion

Estimates of SR are crucial in understanding soil carbon dynamics of terrestrial ecosystems. Since SR data collection requires significant time and cost, data at a sufficient spatial resolution for large areas, especially for the Qinghai-Tibet Plateau, are generally scarce.

To overcome this restriction of limited data, we tested regression models which can be run with climate and BGB data, which is advantageous for an area-wide calculation of scenarios.

Results of various studies indicate the important role of temperature, precipitation and BGB with regard to SR. We conclude from our study that the regression model based on MAP performs best in calculating SR for the Qinghai-Tibet Plateau according to the comparision with our evaluation data sets and other regression models. The MAP-based model can be run with limited data and best represents the most important and spread-out vegetation zones on the Qinghai-Tibet Plateau. The incorporation of other regression models would, however, improve the accuracy of SR approximations for special vegetation types. Our approach of estimating SR with scarce data is well within the same range of directly measured field data from other studies on the Qinghai-Tibet Plateau. The spatially distinct SR calculation at a comparatively high spatial resolution allows for assessing potential area-specific greenhouse gas emission on the Qinghai-Tibet Plateau.

5 Acknowledgements

We thank the Ev. Studienwerk Villigst e. V. that funded this study conducted within the framework of the research project PERMATRANS. The support by the German Federal Ministry for Education and Research (BMBF, grant No. 03G0810A) is also acknowledged. We also thank Ji Luo (Institute of Mountain Hazards and Environment, Chinese Academy of Sciences and Ministry of Water Conservancy, Chengdu, China) for his support via messaging.

6 References

Amundson, R., 2001. The carbon budget in soils. Annu. Rev. Earth Planet. Sci. 29, 535-562.

Baumann, F., He, J.-S., Schmidt, K., Kühn, P., Scholten, T., 2009. Pedogenesis, permafrost, and soil moisture as controlling factors for soil nitrogen and carbon contents across the Tibetan Plateau. Glob. Change Biol. 15, 3001-3017.

Baumann, F., Schmidt, K., Doerfer, C., He, J.-S., Scholten, T., Kühn, P., 2014. Pedogenesis, permafrost, substrate and topography: plot and landscape scale interrelations of weathering processes on the central-eastern Tibetan Plateau. Geoderma 226-227, 300-316.

Behera, N., Joshi, S.K., Pati, D.P., 1990. Root contribution to total soil metabolism in a tropical forest soil from Orissa, India. For. Ecol. Manage. 36, 125-134.

Böhner, J., Lehmkuhl, F., 2005. Environmental change modelling for Central and High Asia: Pleistocene, present and future scenarios. Boreas 34, 220-231.

Böhner, J., 2006. General climatic controls and topoclimatic variations in Central and High Asia, Boreas 35, 279-295.

Bond-Lamberty, B., Thomson, A., 2010a. Temperature-associated increases in the global soil respiration record. Nature 464, 579-582.

Bond-Lamberty, B., Thomson, A., 2010b. A global database of soil respiration data. Biogeosciences 7, 1915-1926.

Boone, R.D., Nadelhoffer, K.J., Canary, J.D., Kaye, J.P., 1998. Roots exert a strong influence on the temperature sensitivity of soil respiration. Nature 396, 570-572.

Bosch, A., Doerfer, C., He, J.-S., Schmidt, K., Scholten, T., 2015. A Comparison of Regression Models to estimate Belowground Biomass on the Qinghai-Tibet Plateau. Catena (submitted 12.09.2015, CATENA4511) (under review).

Cao, G., Tang, Y., Mo, W., Wang, Y., Li, Y., Zhao, X., 2004. Grazing intensity alters soil respiration in an alpine meadow on the Tibetan plateau. Soil Biol. Biochem. 36, 237-243.

Chapin III, F.S., Sturm, M., Serreze, M.C., McFadden, J.P., Key, J.R., Lloyd, A.H., McGuire, A.D., Rupp, T.S., Lynch, A. H., Schimel, J.P., Beringer, J., Chapman,

W.L., Epstein, H.E., Euskirchen, E. S., Hinzman, L.D., Jia, G., Ping, C.-L., Tape, K.D., Thompson, C.D.C., Walker, D.A., Welker, J.M., 2005. Role of land-surface changes in Arctic summer warming. Science 310, 657–660.

Chen, X., Post, W., Norby, R., Classen, A., 2010. Modeling soil respiration and variations in source components using a multi-factor global climate change experiment. Climatic Change, 1-22.

Chen, Y., Luo, J., Li, W., Dong, Y., She, J., 2014. Comparison of soil respiration among three different subalpine ecosystems on eastern Tibetan Plateau, China. Soil Sci. Plant Nutr. 60, 231-241.

Cheng, G., 2005. Permafrost studies in the Qinghai-Tibet Plateau for road construction. Journal of Cold Regions Engineering 19, 19-29.

Chimner, R.A., 2004. Soil respiration rates of tropical peatlands in Micronesia and Hawaii. Wetlands 24, 51-56.

Christensen, J.H., Hewitson, B., Busuioc, A., Chen, A., Gao, X., Held, I., Jones, R., Kolli, R.K., Kwon, W.T., Laprise, R., Rueda, V. M., Mearns, L., Menéndez, Räisänen, J., Rinke, A., Sarr, A., Whetton, P., 2007. Regional Climate Projections. In: Solomon, S., Qin, D., Manning, M., Chen, Z., Marquis, M., Averyt, K.B., Tignor, M., Miller, H.L. (Eds.), Climate Change 2007: The Physical Science Basis. Contribution of Working Group I to the Fourth Assessment Report of the Intergovernmental Panel on Climate Change. Cambridge University Press, Cambridge, pp. 848-940.

Curiel Yuste, J., Janssens, I.A., Carrara, A., Meiresonne, L., Ceulemans, R., 2003. Interactive effects of temperature and precipitation on soil respiration in a temperate maritime pine forest. Tree Physiol., 23, 1263-1270.

Da Silva, A.M., 2004. Rainfall erosivity map for Brazil. Catena 57, 251-259.

Davidson, E.A., Janssens, I.A., 2006. Temperature sensitivity of soil carbon decomposition and feedbacks to climate change. Nature 440, 165-173.

Davidson, E.A., Janssens, I.J., Luo, Y., 2006. On the variability of respiration in terrestrial ecosystems: moving beyond Q10. Glob. Change Biol. 12, 154-164.

Doerfer, C., Kuehn, P., Baumann, F., He, J.-S., Scholten, T., 2013. Soil organic carbon pools and stocks in permafrost-affected soils on the Tibetan Plateau. PLoS ONE 8(2): e57024.

Duan, A.M., Wu, G.X., 2005. Role of the Tibetan Plateau thermal forcing in the summer climate patterns over subtropical Asia. Clim. Dyn. 24, 793-807.

Ewel, K.C., Cropper, W.P., Gholz, H.L., 1987. Soil CO_2 evolution in Florida slash pine plantations: II. Importance of root respiration. Can. J. For. Res. 17, 330-333.

Fan, J.-W., Shao, Q.-Q., Liu, J.-Y., Wang, J.-B., Harris, W., Chen, Z.-Q., Zhong, H.-P., Xu, X.-L., Liu, R.-G., 2010. Assessment of effects of climate change and grazing activity on grassland yield in the Three Rivers Headwaters Region of Qinghai-Tibet Plateau, China. Environ. Monit. Assess. 170, 571–584.

Fang, C., Moncrieff, J.B., Gholz, H.L. Clark, K.L., 1998. Soil CO_2 efflux and its spatial variation in a Florida slash pine plantation. Plant Soil 205, 135-146.

Geng, Y., Wang, Y., Yang, K., Wang, S., Zeng, H., Baumann, F., Kuehn, P., Scholten, T., He, J.-S., 2012. Soil Respiration in Tibetan alpine grasslands: belowground biomass and soil moisture, but not soil temperature, best explain the large-scale patterns. PLoS ONE 7, 1-12.

Hashimoto, S., Carvalhais, N., Ito, A., Migliavacca, M., Nishina, K., Reichstein, M., 2015. Global spatiotemporal distribution of soil respiration modeled using a global databse. Biogeosciences 12, 4121-4132.

Hijmans, R. J., Cameron, S.E., Parra, J.L., Jones, P.G., Jarvis, A., 2005. Very high resolution interpolated climate surfaces for global land areas. Int. J. Climat. 25, 1965-1978.

Immerzeel, W., Quiroz, R., Jong, S., 2005. Understanding precipitation patterns and land use interaction in Tibet using harmonic analysis of SPOT VGT-S10 NDVI time series. Int. J. Remote Sens. 26, 2281–2296.

Jia, B., Zhou, G., Wang, Y., Wang, F., Wang, X., 2006. Effects of temperature and soil water-content on soil respiration of grazed and ungrazed *Leymus chinensis* steppes, Inner Mongolia. J. Arid Environ. 67, 60-76.

Jones, C.D., Cox, *P.M.,* Essery, R.L.H., Roberts, *D.L.,* Woodage, M.J., 2003. Strong carbon cycle feedbacks in a climate model with interactive CO_2 and sulphate aerosols. Geophys. Res. Lett. 30.

Joo, S.J., Park, S.-U., Park, M.-S., Lee, C.S., 2012. Estimation of SR using automatic chamber systems in an oak (*Quercus mongolica*) forest at the Nam-San site in Seoul, Korea.

Kang, S., Xu, Y., You, Q., Flügel, W.-A., Pepin, N., Yao, T., 2010. Review of climate and cryospheric change in the Tibetan Plateau. Environ. Res. Lett. 5, 1-8.

Kirschbaum M.U.F., 1995. The temperature dependence of soil organic matter decomposition, and the effect of global warming on soil organic storage. Soil Biol. Biochem. 27, 753-760.

Koizumi, H., Konturi, M., Mariko, S., Nakadai, T., Bekku, Y., Mela, T., 1999. SR in thress soil types in agricultural ecosystems in Finland. Acta Agriculturae Scandinavica, Section B, Plant Soil 49, 65-74.

Kutzbach, J. E., Liu, X., Liu, Z., Chen, G., 2008. Simulation of the evolutionary response of global summer monsoons to orbital forcing over the past 280,000 years. Clim. Dyn. 30, 567-579.

Li, G., Sun, S., 2011. Plant clipping may cause overestimation of soil respiration in a Tibetan alpine meadow, southwest China. Ecol. Res. 26, 497-504.

Liu, X., Chen, B., 2000. Climatic warming in the Tibetan Plateau during recent decades. Int. J. Climat. 20, 1729-1742.

Luo, T., Li, W., Zhu, H., 2002. Estimated biomass and productivity of natural vegetation on the Tibetan Plateau. Ecol. Appl. 12, 980-997.

Luo, T., Brown, S., Pan, Y., Shi, P., Ouyang, H., Yu, Z., Zhu, H., 2005. Root biomass along subtropical to alpine gradients: global implication from Tibetan transect studies. For. Ecol. Manage. 206. 349-363.

Luo, Y., Zhou, X., 2006. Soil respiration and the environment. Elsevier, San Diego.

Manabe, S., Terpstra, T., 1974. The effects of mountains on the general circulation of the atmosphere as identified by numerical experiments. J. Atmos. Sci. 31, 3-42.

Maussion, F., Scherer, D., Finkelnburg, R., Richter, J., Yang, W., Yao, T., 2011. WRF simulation of a precipitation event over the Tibetan Plateau, China – an assessment using remote sensing and ground observations, Hydrol. Earth Syst. Sci. 15, 1795-1817.

Miehe, G., Bach, K., Miehe, S., Kluge, J., Yang, Y., La, D., Sonam, C., Wesche, K., 2011. Alpine steppe plant communities of the Tibetan highlands. Appl. Veg. Sci. 14, 547-560.

Miehe, G., Miehe, S., Böhner, J., Kaiser, K., Hensen, I., Madsen, D., Liu, J., Opgenoorth, L., 2014. How old is the human footprint in the world´s largest alpine ecosystem? A review of multiproxy records from the Tibetan Plateau from the ecologists' viewpoint. Quat. Sci. Rev. 86, 190-209.

Morén, A.-S., Lindroth, A., 2000. CO_2 exchange at the floor of a boreal forest. Agric. For. Meteorol. 101, 1-14.

Pei, Z.-Y., Ouyang, H., Zhou, C.-P., Xu, X.-L., 2009. Carbon Balance in an Alpine Steppe in the Qinghai-Tibet Plateau. J. Integr. Plant Biol. 51, 521-526.

Raich, J.W., Schlesinger, W.H., 1992. The global carbon dioxide flux in soil respiration and its relationship to vegetation and climate. Tellus 44B, 81-99.

Raich, J.W., Tufekcioglu, A., 2000. Vegetation and soil respiration: Correlations and controls. Biogeochemistry 48, 71-90.

Reth, S., Reichstein, M., Falge, E., 2005. The effect of soil water content, soil temperature, soil pH-value and the root mass on soil CO_2 efflux – a modified model. Plant Soil 268, 21-33.

Rey, A., Pegoraro, E., Tedeschi, V., Parri, I.D., Jarvis, P.G., Valentini, R., 2002. Annual variation in SR and its components in a coppice oak forest in central Italy. Glob. Change Biol. 8, 851-866.

Rodeghiero, M., Cescatti, A., 2005. Main determinants of forest soil respiration along an elevation/temperature gradient in the Italian Alps. Glob. Change Biol. 11, 1024–1041.

Rodeghiero, M., Churkina, G. Martinez, C., Scholten, T. Gianelle, D., Cescatti. A., 2013. Components of forest soil CO_2 efflux estimated from $\Delta^{14}C$ values of soil organic matter. Plant Soil 364/1, 55-68.

Schlesinger, W.H., Andrews, J.A., 2000. Soil respiration and the global carbon cycle. Biogeochemistry 48, 7-20.

Schroeder, P.E., Winjum, J.K., 1995. Assessing Brazil's carbon budget I. Biotic carbon pools. For. Ecol. Manage. 75, 77-86.

Singh, J.S., Gupta, S.R., 1977. Plant decomposition and soil respiration in terrestrial ecosystems. Bot. Rev. 43, 449-528.

Smith, E., Shi, L., 1995. Reducing discrepancies in atmospheric heat budget of Tibetan Plateau by satellite-based estimates of radiative cooling and cloud-radiation feedback. Meteorol. Atmos. Phys. 56, 229–260.

Valentini, R., Matteucci, G., Dolman, A.J., Schulze, E.-D., Rebmann, C., Moors, E., J., Granier, A., Gross, P., Jensen, N.O., Pilegaard, K., Lindroth, A., Grelle, A., Bernhofer, C., Grünwald, T., Aubinet, M., Ceulemans, R., Kowalski, A.S., Vesala, T., Rannik, Ü., Berbigier, P., Loustau, D., Guðmundsson, J., Thorgeirsson, H., Ibrom, A., Morgenstern., Clement, R., Moncrieff, J., Montagnani, L., Minerbi, S., Jarvis, P. G. 2000. Respiration as the main determinant of carbon balance in European forests. Nature 404, 861-865.

Wang, B., Bao, Q., Hoskins, B., Wu, G., Liu, Y., 2008. Tibetan Plateau warming and precipitation change in East Asia. Geophys. Res. Lett. 35.

Wang, S., Jin, H., Li, S., Zhao, L., 2000. Permafrost degradation on the Qinghai-Tibet Plateau and its environmental impacts. Permafrost Periglacial Process. 11, 43-53.

Wang, W.Y., Wang, Q.J., Li, S.X., Wang, G., 2006. Distribution and species diversity of plant communities along transect on the Northeastern Tibetan plateau. Biodivers. Conserv. 15, 1811–1828.

Wang, C., Cao, G., Wang, Q., Jing, Z., Ding, L., Long, R., 2008. Changes in plant biomass and species composition of alpine *Kobresia* meadows along altitudinal gradient on the Qinghai-Tibetan Plateau, Sci. China Ser. C 51, 86-94.

Wang, X., Liu, L., Piao, S., Janssens, I.A., Tang, J., Liu, W., Chi, Y., Wang, J., Xu, S., 2014. Soil respiration under climate warming: differential response of heterotrophic and autotrophic respiration, Glob. Change Biol. 20, 3229-3237.

Wang, Y., Liu, H., Chung, H., Yu, L., Mi, Z., Geng, Y., Jing, X., Wang, S., Zeng, H., Cao, G., Zhao, X., He, J.-S., 2014. Non-growing-season soil respiration is controlled by freezing and thawing processes in the summer monsoon-dominated Tibetan alpine grassland. Global Biochem. Cy. 28, 1081-1095.

Wen, L., Dong, S., Li, Y., Wang, X., Li, X., Shi, J., Dong, Q., 2013. The impact of land degradation on the C pools in alpine grasslands of the Qinghai- Tibet Plateau, Plant Soil 368, 329-340.

Wiseman, P.E., Seiler, J.R., 2004. Soil CO_2 efflux across four age classes of plantation loblolly pine (*Pinus taeda* L.) on the Virginia Piedmont. Forest Ecology and Management 192, 297-311.

Xu, Z. X., Gong, T., L., Li, J. Y., 2008. Decadal trend of climate in the Tibetan Plateau - regional temperature and precipitation. Hydrol. Process. 22, 3056-65.

Yang, M., Wang, S., Yao, T., Gou, X., Lu, A., Guo, X., 2004. Desertification and its relationship with permafrost degradation in Qinghai-Xizang (Tibet) plateau. Cold Reg. Sci. Technol. 39, 47-53.

Yang, Y., Fang J., Smith, P.,Tang, Y., Chen, A., Ji, C., Hu, H., Rao, S., Tan K.U.N., He, J.-S., 2009. Changes in topsoil carbon stock in the Tibetan grasslands between the 1980s and 2004. Glob. Change Biol. 15, 2723-2729.

Yang, Y., Fang, J., Tang, Y., Ji, C., Zheng, C., He, J.-S., Zhu, B., 2008. Storage, patterns and controls of soil organic carbon in the Tibetan grasslands. Glob. Change Biol. 14, 1592-1599.

Yu, H.Y., Luedeling, E., Xu, J.C., 2010. Winter and spring warming result in delayed spring phenology on the Tibetan Plateau. Proc. Natl. Acad. Sci. U. S. A. 107, 22151–22156.

Zhang Y., Li Bingyuan, Z., Du, 2002. The area and boundary of Qinghai-Tibet Plateau. Geographical Research, 21, 1–8. (in Chinese)

Zhang, Y., Ohata, T., Kodata, T., 2003. Land-surface hydrological processes in the permafrost region of the eastern Tibetan Plateau. J. Hydrol. 283, 41-56.

Zhang, X., Shi, P., Liu, Y., Ouyang, H., 2005. Experimental study on soil CO_2 emission in the alpine grassland ecosystem on Tibetan Plateau. Sci. China Ser. D 48, 218-224.

Zhang, Y., Tang, Y., Jiang, J., Yang, Y., 2007. Characterizing the dynamics of soil organic carbon in grasslands on the Qinghai-Tibetan Plateau. Sci. China Ser. D 50, 113-120.

Zhang, P., Tang, Y., Hirota, M., Yamamoto, A., Mariko, S., 2009. Use of a regression method to partition sources of ecosystem respiration in an alpine meadow. Soil Biol. Biochem. 41, 663-670.

Zhang, Y., Wang, G., Wang, Y., 2010. Response of biomass spatial pattern of alpine vegetation to climate change in permafrost region of the Qinghai-Tibet Plateau, China. J. Mt. Sci. 7, 301-314.

Zheng, D., 1996. The system of physico-geographical regions of the Qinghai-Xizang (Tibet) Plateau. Sci. China Ser. D 39, 410-417.

Zhong, L., Ma, Y., Salama M.S., Su, Z., 2010. Assessment of vegetation dynamics and their response to variations in precipitation and temperature in the Tibetan Plateau. Clim. Chang. 103, 519-535.

Zhuang, Q., He, J., Lu, Y., Ji, L., Xiao, J., Luo, T., 2010. Carbon dynamics of terrestrial ecosystems on the Tibetan Plateau during the 20th century: an analysis with a process-based biogeochemical model. Glob. Ecol. Biogeogr. 19, 649-662.

Supplementary material

Appendix I. Abundance of soil respiration values of the regression models per class of soil respiration flux for the Qinghai-Tibet Plateau. Soil respiration flux classes represent low (>0 – 625 g C m^{-2} y^{-1}), medium (>625 – 1250 g C m^{-2} y^{-1}), high (> 1250 g C m^{-2} y^{-1}) and no (≤0 g C m^{-2} y^{-1}) soil respiration.

Soil respiration flux class	Regression model based on					
	MAT I	MAT II	MAP	MAT and MAP I	MAT and MAP II	BGB
			[%]			
low	97.95	96.5	97.85	98.12	98.09	100
medium	1.69	1.95	1.79	1.59	1.62	0
high	0	0	0.34	0.27	0.27	0
no	0.34	1.53	0	0	0	0

Appendix II. Area on the Qinghai-Tibet Plateau assigned to a soil respiration flux class. Soil respiration flux classes represent low (>0 – 625 g C m^{-2} y^{-1}), medium (>625 – 1250 g C m^{-2} y^{-1}), high (> 1250 g C m^{-2} y^{-1}) and no (≤0 g C m^{-2} y^{-1}) soil respiration.

Soil respiration flux class	Regression model based on					
	MAT I	MAT II	MAP	MAT and MAP I	MAT and MAP II	BGB
			[km^2]			
low	2,605,965	2,567,346	2,603,333	2,610,528	2,609,621	2,660,303
medium	45,063	52,064	47,662	42,404	43,264	0
high	0	0	9,308	7,371	7,418	0
no	9,275	40,893	0	0	0	0

Manuscript 3

Potential CO_2 emissions from defrosting permafrost soils of the Qinghai-Tibet Plateau under different scenarios of climate change in 2050 and 2070

Catena 149 (2017) 221-231

Anna Bosch[a], Karsten Schmidt[a], Jin-Sheng He[b, c], Corina Doerfer[a], Thomas Scholten[a]

[a]University of Tuebingen, Department of Geosciences, Chair of Soil Science and Geomorphology, Tübingen, Germany

[b]Key Laboratory of Adaptation and Evolution of Plateau Biota, Northwest Institute of Plateau Biology, Chinese Academy of Sciences, Xining, 810008, China

[c]Department of Ecology, College of Urban and Environmental Sciences, and Key Laboratory for Earth Surface Processes of the Ministry of Education, Peking University, Beijing, 100871, China

Abstract

Permafrost soils store enormous quantities of organic carbon. Especially on the alpine Qinghai-Tibet Plateau, global warming induces strong permafrost thawing, which strengthens the microbial decomposition of organic carbon and the emission of the greenhouse gas carbon dioxide (CO_2). Enhanced respiration rates may intensify climate warming in turn, but the magnitude of future CO_2 emissions from this data-scarce region in a changing climate remains highly uncertain. Here, we aim at an area-wide estimation of future potential CO_2 emissions for the permafrost region on the Qinghai-Tibet Plateau as key region for climate change studies due to its size and sensitiveness. We calculated four potential soil respiration scenarios for 2050 and 2070 each. Using a regression model, results from laboratory experiments and C stock estimations from other studies, we provide an approximation of total potential soil CO_2

emissions on a regional scale ranging from 737.90 g CO_2 m^{-2} y^{-1} - 4224.77 g CO_2 m^{-2} y^{-1}. Our calculations as first estimate of thawing-induced CO_2 emissions (51.23 g CO_2 m^{-2} y^{-1} – 3002.82 g CO_2 m^{-2} y^{-1}) from permafrost soils of the Qinghai-Tibet Plateau under global warming appear to be consistent to measurements of C loss from thawing permafrost soils measured within other studies. Thawing-induced soil CO_2 emissions from permafrost soils with a organic C content ranging from 2.42 g C kg^{-1} to 425.23 g C kg^{-1} increase general soil respiration by at least about one third on average at a temperature of 5 °C. Differences between scenarios remain <1% and thawing-induced CO_2 emissions generally decrease over time comparing 2015, 2050 and 2070. With this spatial approximation at a regional scale, a first area-wide estimate of potential CO_2 emissions for 2050 and 2070 from permafrost soils of the Qinghai-Tibet Plateau is provided. This offers support of assessing potential area-specific greenhouse gas emissions and more differentiated climate change models.

Keywords

Permafrost soil, Carbon, Carbon dioxide, Soil respiration, Qinghai-Tibet Plateau, Climate change scenarios

1. Introduction[3]

Carbon dioxide (CO_2) emissions from soils to the atmosphere substantially affect the global carbon (C) cycle (Chen et al., 2010). For the global carbon budget, this soil efflux represents the main source of C, second to oceans´ releases, by approximated 98 ±12 Pg C per year (Bond-Lamberty and Thomson, 2010a; Schlesinger and Andrews, 2000; Valentini et al., 2000). Further, soils store most carbon in terrestrial ecosystems (Amundson, 2001) and their respiration amounts to ~10% of the atmospheric CO_2 cycle budget (Bond-Lamberty and Thomson, 2010b). Hence, slight increases in soil CO_2 emissions can seriously impact atmospheric CO_2 concentrations, possibly amplifying global warming (Rodeghiero and Cescatti, 2005, 2013; Davidson

[3] Abbreviations: soil respiration (SR), carbon (C), carbon dioxide (CO_2), mean annual precipitation (MAP), representative concentration pathway (RCP), belowground biomass (BGB).

and Janssens, 2006; Schlesinger and Andrews, 2000). However, climate warming itself presumably accounts for the rising global loss of soil carbon to the atmosphere in the main (Jones et al., 2003). It potentially increases belowground biomass (BGB), which in turn increases autotrophic respiration and probably also stimulates microorganisms which accordingly leads to a higher heterotrophic respiration supported by more exudates and C-input of roots (Kirschbaum, 1995; Wang et al., 2014). However, especially higher C loss through augmented autotrophic respiration as consequence of an elevated rate of photosynthesis is expected to be neutralized by a higher plant uptake of C and its sequestration (Schuur et al., 2015). Higher temperatures, extended growing seasons and a higher concentration of atmospheric CO_2 potentially intensify plant growth (Shaver et al., 2000). Uptaken C can be sequestered in larger above- and belowground biomass (Sistla et al., 2013).

Understanding the different responses of autotrophic and heterotrophic respiration to global warming in permafrost soils is particularly important (Hicks Pries et al., 2013). Higher soil CO_2 emissions resulting from thawing permafrost are, if at all, only partly offset by this negative feedback to global warming through enhanced soil respiration (Schuur et al., 2015). Permafrost is commonly defined as ground (soil or rock and included ice or organic material) at or below 0 °C for at least two consecutive years. Temperatures at or below 0 °C in permafrost soils shrink microbial activity and inhibits active microbial decomposition of the soil´s accumulated organic matter (Harden et al., 1992). Consequently, warmer temperatures and concomitant thawing of permafrost resulting from climate change will expose a large amount of soil organic C to microbial breakdown that has been frozen before (Xue et al., 2016; Schuur et al., 2009). As a result, high quantities of C may be released to the atmosphere (Dutta et al., 2006). Lately, permafrost was estimated to contain more than 1600 Pg soil organic C (Schuur et al., 2008), which is twice the atmospheric CO_2-C pool (Jia et al., 2006). Considering the remarkable C stock of permafrost and its wide-spread climate change induced degradation, its soil CO_2 emissions are of global importance in view of the greenhouse gas-driven climate change (Schaefer et al., 2011; Ding et al., 2016). Hence, the quantification of future CO_2 emissions from permafrost soil gains high relevance for more comprehensive scenarios of climate change. This importance further results from the fact that permafrost soils have functioned as C sinks so far (Hicks Pries et al., 2012).

A key region for examining such processes due to its sensitivity and comparably low human impact is seen in the ecologically fragile Qinghai-Tibet Plateau with its extensive and sensitive permafrost area (Fan et al., 2010; Yang et al., 2009; Liu and Chen, 2000). Also because of its important role in the global carbon cycle and remarkable contribution to the global carbon budget, the plateau is generally of high significance for studies on CO_2 emissions (Geng et al., 2012). As highest and spatially most extended plateau on earth, the Qinghai-Tibet Plateau influences both regional and global climates significantly (Zhong et al., 2010; Wang et al., 2006). Also its effects by means of thermal and mechanical forces (Kutzbach et al., 2008; Duan and Wu, 2005; Manabe and Terpstra, 1974) earns him the reputation of being a 'driving force' or an 'amplifier' of global warming (Kang et al., 2010). However, global climate change likewise influences the Qinghai-Tibet Plateau (Zhang et al., 2010). It is a region of high sensitiveness to global warming mainly due to its extreme elevation (Zhong et al., 2010; Zhang et al., 2007; Luo et al., 2002). The plateau´s temperature is expected to increase far above average in the future (Wang et al., 2008; Christensen et al., 2007; Liu and Chen, 2000). The cryosphere, commonly considered as the most sensitive indicator to climate change, undergoes rapid changes on the Qinghai-Tibet Plateau (Kang et al., 2010), where earth´s largest high-altitude and low-latitude permafrost zone, with more than half of its total area influenced by permafrost (Cheng, 2005), shows increasing permafrost degradation (Böhner and Lehmkuhl, 2005; Baumann et al., 2009). This process has been advancing even stronger than in other high-latitude, low-altitude permafrost regions over the last few decades (Yang et al., 2004). As expected, the further degradation of Tibetan permafrost (Böhner and Lehmkuhl, 2005; Wang et al., 2000) will highly influence soils mainly reflected by their changes in temperature and moisture (Doerfer et al., 2013; Zhang et al., 2003). Global warming so impacts permafrost stability and distribution as well as vegetation and soil characteristics that intensively interact with CO_2 emissions through complex processes (Chapin et al., 2005). The thaw of permafrost resulting from global warming will release organic C frozen till then and potentially provide a positive feedback to climate change through higher respiration rates (Koven et al., 2011). This calls attention to the need of a deep understanding of the quantity of potential CO_2 emission rates with future climate change with special regard to the heterotrophic component in thawing permafrost soils on the Qinghai-Tibet Plateau (Geng et al., 2012). This is especially difficult to quantify because of high uncertainties and only few laboratory experiments that have been

conducted so far concerning thawing-induced CO_2 emissions from permafrost. Widely varying approximations have not been overcome yet (Lawrence et al., 2015). Empirical regression models for predicting soil respiration on the Qinghai-Tibet Plateau have already been applied effectively (Bosch et al., 2016), with process-based models generally being limited in their applicability to large regions due to more difficulties when parametrizing. This approach has been successful when applied for likewise complex processes such as rainfall erosivity in other regions of China (e.g. Schönbrodt-Stitt et al., 2013). For thawing-induced CO_2 emissions, no formulated regression models exist, why results of laboratory experiments are transferred to the study area in structural analogy to regression models. Further, as to the difficulty of quantifying soil CO_2 emissions on the Qinghai-Tibet Plateau, limitations in data availability is particularly challenging. Despite its unique role in climate change studies due to its ecological sensibility, the inaccessible and complex terrain of the plateau additionally aggravates research activities and causes a general data scarcity due to enormous time and cost efforts required for data collection. Various data sets lack of a fine (about 1 km^2) resolution that captures spatial environmental variability appropriately. Others are not spatially comprehensive, existent, available or highly cost-intensive. On the other hand, several freely available global databases exist for selected environmental variables. They are have often acceptable or useful resolution to reasonably interpret empirical model results (about 1 km^2) and are developed through the harmonization of different data sets with elaborated methods. For area-explicit, efficient calculations for the Qinghai-Tibet Plateau on a regional scale, they are, therefore, advantageous.

Facing these issues, we aim at a first, efficient estimate of potential CO_2 emissions from permafrost soils on the Qinghai-Tibet Plateau in future based on freely accessible data. Against the background of different scenarios of climate change, the potential CO_2 release is approximated with special regard to the higher heterotrophic respiration induced by the increased microbial decomposition of soil organic C resulting from thawing permafrost.

2. Material and methods

2.1. Study area

Our study area, the permafrost soils on the Qinghai-Tibet Plateau, is located in southwestern China. The Qinghai-Tibet Plateau extends from 26°00′12" N to 39°46′50" N and from 73°18′52" E to 104°46′59" E with a maximum length of approx.

2945 km from east to west and approx. 1532 km from south to north. The altitude of the highest and youngest plateau amounts to 4380 m on average (Baumann et al., 2009; Zhang et al., 2002). On this plateau, earth´s largest high-altitude and low-latitude permafrost zone is located, with more than half of its total area influenced by permafrost (Cheng, 2005). Covering about 1.050×10^6 km^2, the permafrost zone is mainly part of the southwestern and central plateau (Fig. 1).

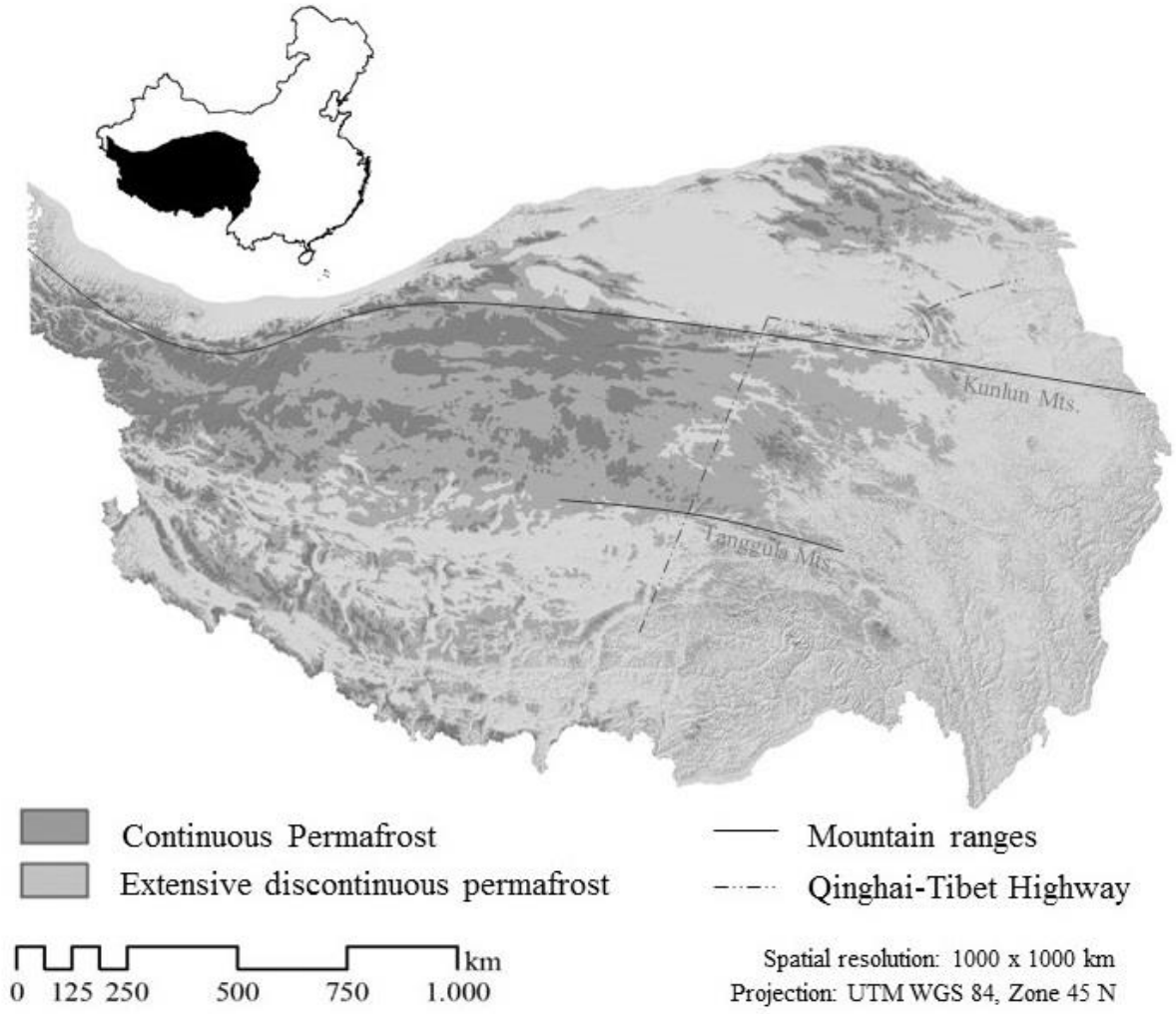

Fig. 1. Spatial extension of continuous and extensive discontinuous permafrost on the Qinghai-Tibet Plateau. The spatial resolution of the grids is 1000 x 1000 m.

Continuous permafrost mostly occurs in the interior and western Qinghai-Tibet Plateau, extending to the south of the Kunlun Mountains. Boundaries of the permafrost zone in the south are the Tanggula Mountains and the 94 ° longitude in the east. Discontinuous permafrost can be found in the northern and southern regions on the Qinghai-Tibet Plateau with more pronounced relief characterized by ground that

seasonally freezes and shows sporadic permafrost (Cheng and Jin, 2013). Along the Qinghai-Tibet highway, the permafrost zones stretches with a length of 550 km from north to south (Wang et al., 2006). The unique geographical position of the Qinghai-Tibet Plateau prevails an azonal plateau climate (Zhuang et al., 2010; Zhong et al., 2010) with strong solar radiation, low air temperature, large daily temperature variations and low differences between annual mean temperatures (Zhong et al., 2010). Generally, a decrease both in temperature and in precipitation from the south-eastern to the north-western part of the plateau is apparent (Immerzeel et al., 2005). For the plateau, the mean temperature of July, as warmest month, varies from 7 °C to 15 °C and from -1 °C to -7 °C in January, as coldest month. Average annual temperature is 1.6 °C (Yang et al., 2009). Precipitation amounts to about 413.6 mm a year (Yang et al., 2009), with more than 60-90% falling in the wet and humid summers (June-September) and 10% at maximum in the cool, arid winters (November-February) (Xu et al., 2008). The topographic setting as well as atmospheric conditions determine the sequence of alpine meadows, steppes and deserts from southeast to northwest (Pei et al., 2009; Zheng, D., 1996). Alpine steppes and meadows dominate the undisturbed vegetation, with *Stipa* species respectively *Kobresia* meadows as major vegetation types. According to the long freezing periods, relatively short growing seasons characterize the plateau`s climate (Yu et al., 2010). Its vegetation is regarded as comparatively natural (Schroeder and Winjum, 1995). Continuous, complex pedogenetic processes on the Qinghai-Tibet Plateau typically result in young and highly diverse soils with distinct degradation characteristics, exhibiting a strong influence by permafrost regimes (Baumann et al., 2014).

2.2. Geodatabase and processing

For the estimation of potential CO_2 emissions, different data sets were used in this case study. All data sets were projected into the Universal Transverse Mercator coordinate system WGS 1984, Zone 45 N. The data set for current MAP was obtained from the WorldClim data set available at http://worldclim.com (for basic statistics on current MAP see Table 1). This was compiled from a considerable number of various sources, such as the Global Historical Climate Network, World Meteorological Organization and the Food and Agricultural Organization, with a resolution of 1 x 1 km and representing the current climate conditions from circa 1950 to 2000. Data from more than 71,000 climate stations worldwide recording for precipitation, and more than

45,000 climate stations recording for temperature are integrated, with the Qinghai-Tibet Plateau as area with less densely distributed measurement points. These were, however, interpolated using a thin-plate smoothing spline algorithm. Latitude, longitude and altitude served as independent variables. Elevation data were used from the Shuttle Radar Topography Mission with a spatial resolution of 1 x 1 km (for more detailed information see Hijmans et al., 2005).

The data sets for MAP in 2050 and 2070 under different scenarios of climate change originate from the WorldClim data sets as well (for basic statistics on MAP in 2050 and 2070 under different scenarios see Table 1).

Table 1. Statistics on input data sets on MAP [mm] based on WorldClim data sets (Hijmans et al., 2005).

Year **Scenario**	**2015**	**2050 RCP2.6**	**2050 RCP4.5**	**2050 RCP6.0**	**2050 RCP8.5**	**2070 RCP2.6**	**2070 RCP4.5**	**2070 RCP6.0**	**2070 RCP8.5**
					[mm]				
Mean	222.05	232.49	235.13	233.69	241.79	231.78	234.98	235.36	243.44
Min	32.36	35.36	34.58	35.08	35.44	34.40	33.36	35.40	36.40
Max	1237.18	1291.94	1287.11	1261.01	1243.34	1295.14	1338.14	1247.18	1303.71
Range	1204.82	1256.58	1252.53	1225.93	1207.9	1260.74	234.98	1211.78	1267.31
SD	137.67	143.70	145.73	144.207	148.66	143.81	147.32	145.33	151.12

For 2050 and 2070, representing the average of modeled climate conditions from 2041 to 2060 and 2061 – 2080, respectively, there are four climate scenarios. We used the projections of the global climate model ‘Community Climate System Model Version 4’ as one of the most common and current one that is employed in the Fifth Assessment IPCC report as well and has been developed in international collaboration (Gent et al., 2011). The model is a coupled model combining four separate models that simulate the sea-ice, the atmosphere, oceans and land surface of the earth, and a fifth component that allows for an exchange of fluxes between these models. It is regarded to provide realistic simulations of the earth´s climate system at a resolution of 1 x 1 km with reasonable fidelity. WorldClim 1.4 served as reference for the downscaling and calibration of this model results (for more details see Gent et al., 2011; http://worldclim.com). The four scenarios are projected by the global climate model for four different representative concentration pathways (RCP) with a spatial resolution of 1 x 1 km (van Vuuren et al., 2011). The RCP each describe different climate scenarios that are regarded being possible depending on future amounts of greenhouse gas

emissions, land use change and air pollutants, covering a wide range of scenarios presented in the existing literature. They incorporate various different technological, political, social and economic futures influencing climate change. Each RCP has been developed under the usage of a different model. For RCP2.6, greenhouse gas emissions are assumed to be very low, for RCP4.5 medium-low, for RCP6.0 medium, and RCP8.5 is seen as high emission scenario. Air pollution is assumed to be medium-low for RCP2.6, medium for RCP4.5 and RCP6.0, and medium-high for RCP8.5. Data were harmonized, downscaled or converted using e. g. a carbon-cycle climate model or atmospheric chemistry model for emission data to be transformed into concentration data (for more details see van Vuuren et al., 2011).

The data sets for organic C content, gravel content and bulk density were obtained from the WISE30sec data set available at http://isric.org with a spatial resolution of 1 x 1 km up to a depth of 2 m (for basic statistics on the soil properties see Table 2).

Table 2. Statistics of organic carbon content [g C kg^{-1}], bulk density [kg dm^{-3}] and coarse fragments (> 2 mm) [vol. %] of the continuous and extensive discontinuous permafrost area on the Qinghai-Tibet Plateau based on WISE30sec data sets (Batjes, 2015).

Soil property	**Organic carbon content** [g C kg^{-1}]	**Bulk density** [kg dm^{-3}]	**Coarse fragments (> 2 mm)** [vol. %]
Mean	31.03	1.25	14.34
Min	2.42	0.14	1
Max	425.23	1.62	46
Range	422.81	1.48	45
SD	42.26	0.19	6.88

The WISE30sec data set was compiled from different sources, such as the Harmonized World Soil Database, version 1.21 with marginal corrections, a climate zones map (Köppen-Geiger) used as co-variate and soil property estimations based on the ISRIC-WISE soil profile database. Soil properties were estimated based on statistical analyses of about 21 000 soil profiles. This was undertaken using an elaborate system of taxonomy-based transfer rules combined with expert-rules, which assess the consistency of the predictions within the pedons. These rules implemented in the derivations were marked to support in indicating the possible confidence in the estimated data regarding their lineage. WISE30sec is generally regarded as being appropriate for exploratory assessments at a resolution of 1 x 1 km (for more detailed information see Batjes, 2015).

The data to determine the spatial extension of the permafrost zone of the Qinghai-Tibet Plateau were obtained from the Global Permafrost Zonation Index Map available at http://www.geo.uzh.ch with a spatial resolution of 1 x 1 km. The model underlying this map is based on established relationships between air temperature and occurring permafrost, which have been transformed into this model. Its parametrization has been undertaken based on published approximations. Air temperature and elevation represent the input parameters for the model. The input data to derive the modeled spatial permafrost extension are based on various climatic and physical-geographic data sets such as the CRU TS 2.0, NCEP30 and SRTM30. Permafrost extension classes used in the data are: continuous permafrost (90–100%), extensive discontinuous permafrost (50–90%), sporadic discontinuous permafrost (10–50%) and isolated patches (smaller than 10%) (for more details see Gruber et al., 2012). In our study, continuous and extensive discontinuous permafrost are considered.

2.3. Calculation of potential CO_2 emissions

The calculation of potential CO_2 emissions consists of two compartments: (i) General CO_2 emission rates for the Qinghai-Tibet Plateau as rather general soil respiration and (ii) specific CO_2 emission rates, i.e. thawing-induced CO_2 emissions, that focus on the additional source of C made available by climate change through permafrost thaw on the Qinghai-Tibet Plateau.

General CO_2 emission rates (i) as general soil respiration were calculated based on MAP for each scenario in 2050 and 2070 and the current situation using the regression model by Raich and Schlesinger (1992):

$$SR = 0.391P + 155 \quad (1)$$

where SR is the annual soil respiration rate (g C/m^2/yr) and P represents MAP (mm). This regression model performs best for estimating soil respiration on the Qinghai-Tibet Plateau according to a comparison of different regression models by Bosch et al. (2016).

As global model, however, this regression model does not consider the situation of the Qinghai-Tibet Plateau specifically concerning thawing permafrost under global warming, inhering a further source of CO_2 evolving from the soil. We therefore estimated these particular thawing-induced CO_2 emissions (ii) additionally based on estimates from a synthesis of incubation experiments with soil samples from the arctic

region by Schädel et al. (2014). On average, 23.1% of the organic C can potentially be lost within 50 incubation years through permafrost thawing (Schädel et al., 2014), which corresponds to approximately 0.012‰ per day on average. With 166 frost-free days per year on the Qinghai-Tibet Plateau as average from 1960 to 2000 and approximately additional 3 days per further decade because of global warming (Zhang et al., 2014), the potential C loss from thawing permafrost C stocks is hence 0.222% on average per year from 2015 to 2050 and from 2015 to 2070 on average 0.226% per year. Accordingly, the potential organic C loss from 2015 to 2050 amounts to 7.78% and to 12.45% until 2070 of the organic C stock in 2015. As the amount of released CO_2 in the process of permafrost thaw is rather independent from the exact temperature (Schädel et al., 2014), a further differentiation according to the RCPs used in this study would not yield deeper insights.

C stocks for *k* layers as prerequsite for a calculation of thawing-induced soil CO_2 emissions were estimated as follows:

$$T_d = \sum_{i=1}^{k} \rho_i P_i D_i (1 - S_i), \quad (2)$$

where T_d represents the total amount of organic carbon (Mg m^{-2}) over depth *d*, ρ_i is bulk density (Mg m^{-3}) of the layer *i*, P_i equals the proportion of organic carbon in layer *i* (g C g^{-1}), D_i is the thickness of this layer (m), and S_i is the volume of coarse fragments (> 2 mm) (Batjes, 1996).

With the potential C loss from current C stocks, the amount of the CO_2 equivalent as potential greenhouse gas emissions from the process of permafrost thaw for 2050 and 2070 can be calculated. This potential CO_2 emission rate is added to the CO_2 emission rates that were calculated for each scenario of 2050 and 2070 based on MAP for obtaining total CO_2 emissions. The proportion of thawing-induced CO_2 emissions to total CO_2 emissions was obtained as ratio for each year. To calculate this, means of total CO_2 emissions of all scenarios were averaged for each year.

3. Results

3.1. CO_2 emission scenarios for 2050

The four scenarios for 2050 project total CO_2 emissions ranging from lowest 1420.22 g CO_2 m^{-2} y^{-1} (RCP2.6) to highest 1433.46 g CO_2 m^{-2} y^{-1} on average (RCP8.5) (see Table 3).

Table 3. Statistics of potential CO_2 emissions: total CO_2 emissions, consisting of general soil respiration (I) and thawing-induced CO_2 emission (II) in g CO_2 m^{-2} y^{-1} [g C m^{-2} y^{-1}].

Year	Scenario	Type of CO_2 emission	Mean	Min	Max	Median	Range
2050	**RCP2.6**	Total	1420.22 [387.59]	739.02 [201.68]	4188.95 [1143.20]	1255.98 [342.77]	3449.92 [941.51]
		I	901.02 [245.90]	618.59 [168.82]	2418.89 [660.14]	855.15 [233.38]	1800.30 [491.32]
	RCP4.5	Total	1423.87 [388.58]	737.90 [201.38]	4190.54 [1143.64]	1260.37 [343.96]	3452.64 [942.26]
		I	904.80 [246.93]	617.49 [168.52]	2412.00 [658.26]	860.21 [234.76]	1794.51 [489.74]
	RCP6.0	Total	1421.76 [388.01]	738.62 [201.57]	4195.69 [1145.04]	1254.03 [342.23]	3457.06 [943.46]
		I	902.75 [246.37]	618.18 [168.71]	2374.59 [648.05]	855.26 [233.41]	1756.40 [479.34]
	RCP8.5	Total	1433.46 [391.20]	739.13 [201.71]	4224.77 [1152.98]	1267.53 [345.92]	3485.63 [951.26]
		I	914.34 [249.54]	622.36 [169.85]	2349.27 [641.14]	859.62 [236.60]	1726.91 [471.29]
2070	**RCP2.6**	Total	1409.73 [384.73]	735.46 [200.71]	4149.22 [1132.36]	1245.85 [340.00]	3413.76 [931.65]
		I	900.00 [245.62]	617.23 [168.45]	2423.50 [661.40]	755.633 [206.22]	1806.27 [492.95]
	RCP4.5	Total	1414.14 [385.93]	733.97 [200.30]	4143.43 [1130.78]	1249.51 [341.00]	3409.45 [930.47]
		I	904.62 [246.88]	615.73 [168.04]	2485.10 [678.21]	757.06 [206.61]	1869.37 [510.17]
	RCP6.0	Total	1414.88 [386.13]	736.89 [201.10]	4129.10 [1126.87]	1251.36 [341.51]	3392.20 [925.76]
		I	905.13 [247.02]	618.66 [168.84]	2354.76 [642.64]	757.06 [206.61]	1736.10 [473.8]
	RCP8.5	Total	1426.25 [389.24]	738.32 [201.49]	4158.69 [1134.95]	1263.96 [344.94]	3420.37 [933.45]
		I	916.78 [250.18]	620.09 [169.23]	2435.97 [664.75]	765.63 [208.95]	1815.68 [495.52]
2015	**Schädel et al. (2014)**	II	529.91 [144.62]	53.20 [14.52]	3134.91 [855.55]	236.19 [64.46]	3008.31 [821.03]
2050	**Schädel et al. (2014)**	II	519.75 [141.84]	52.18 [14.24]	3002.82 [819.49]	231.69 [63.23]	2950.63 [805.25]
2070	**Schädel et al. (2014)**	II	510.30 [139.26]	51.23 [13.98]	2948.25 [804.60]	227.47 [62.08]	2897.01 [790.62]
2015	**Bosch et al. (2016)**	Total	1415.59 [386.33]	737.08 [201.15]	4224.34 [1152.86]	1246.86 [340.28]	3487.25 [951.70]
		I	886.92 [242.05]	614.32 [167.73]	2340.46 [638.73]	863.83 [235.75]	1726.14 [471.08]

The difference between the lowest and highest mean CO_2 emission rate is hence 9.23‰. Differences in the minima and maxima of the different scenarios are likewise similar ranging from 737.90 g CO_2 m^{-2} y^{-1} (RCP4.5) to 739.13 g CO_2 m^{-2} y^{-1} (RCP8.5) (minima) and between 4188.95 g CO_2 m^{-2} y^{-1} (RCP2.6) and 4224.77 g CO_2 m^{-2} y^{-1} (RCP8.5) (maxima). The mean of the thawing-induced CO_2 emissions adds up to 36.47% of the averaged means of the total CO_2 emissions. In all scenarios, more values exceed the respective averages as reflected by the median values from 1254.03 g CO_2 m^{-2} y^{-1} (RCP6.0) to 1267.53 y^{-1} (RCP8.5). The frequency distribution of all thawing induced values differs strongly from those of the total CO_2 emissions, that is to say their medians amount to less than half of the mean. Highest decreases in total CO_2 emissions compared to the total CO_2 emissions in 2015 are located in the central part of the plateau (Fig. 3). With regard to the abundance of CO_2 emission values for CO_2 emission classes, most values (69.13% - 69.90%) occur in the low class (>0 – 916.05 g CO_2 m^{-2} y^{-1}) throughout all scenarios (see Table 4).

Table 4. Abundance of CO_2 emission values of per class of CO_2 emissions for the Qinghai-Tibet Plateau. CO_2 emission classes represent very low (>0 – 250 g C m^{-2} y^{-1} / >0 – 916.05 g CO_2 m^{-2} y^{-1}), low (>250 – 500 g C m^{-2} y^{-1} / >916.05 – 1832.10 g CO_2 m^{-2} y^{-1}), medium (>1832.10 g CO_2 m^{-2} y^{-1} – 3664.21 g CO_2 m^{-2} y^{-1} / >500 – 1000 g C m^{-2} y^{-1}), high (>3664.21 g CO_2 m^{-2} y^{-1} / >1000 g C m^{-2} y^{-1}) and no (≤0 g CO_2 m^{-2} y^{-1} / ≤0 g C m^{-2} y^{-1}] CO_2 emissions. Italicized values specify the area on the Qinghai-Tibet Plateau assigned to the respective CO_2 emission class.

Classes	**Scenario**	**RCP2.6**		**RCP4.5**		**RCP6.0**		**RCP8.5**	
	Year	**2050**	**2070**	**2050**	**2070**	**2050**	**2070**	**2050**	**2070**
		% [m^{-2}]							
Very low		13.27 *135,902*	13.50 *138,276*	13.29 *136,118*	13.50 *138,286*	12.72 *130,224*	13.06 *133,737*	12.21 *125,037*	12.99 *132,997*
Low		69.25 *708,955*	69.18 *708,160*	69.13 *707,685*	69.00 *709,400*	69.74 *713,895*	69.57 *712,163*	69.90 *715,538*	69.33 *709,707*
Medium		17.36 *177,789*	17.24 *176,273*	17.49 *178,843*	17.11 *175,058*	17.44 *178,528*	17.27 *176,802*	17.78 *182,068*	17.83 *182,560*
High		0.09 *976*	0.08 *912*	0.09 *976*	0.08 *878*	0.09 *977*	0.08 *920*	0.09 *979*	0.09 *969*
No		0.00 *0*	0.00 *0*	0.00 *0*	0.00 *0*	0.00 *0*	0.00 *0*	0.00 *0*	0.00 *0*

In the highest class (>3664.21 g CO_2 m^{-2} y^{-1}), only <1‰ of the values appears, which corresponds to an area of 976 – 979 m^2. Differences between the scenarios show to

be small (Fig. 2) amounting to less than <1% for all scenarios in all CO_2 emission classes.

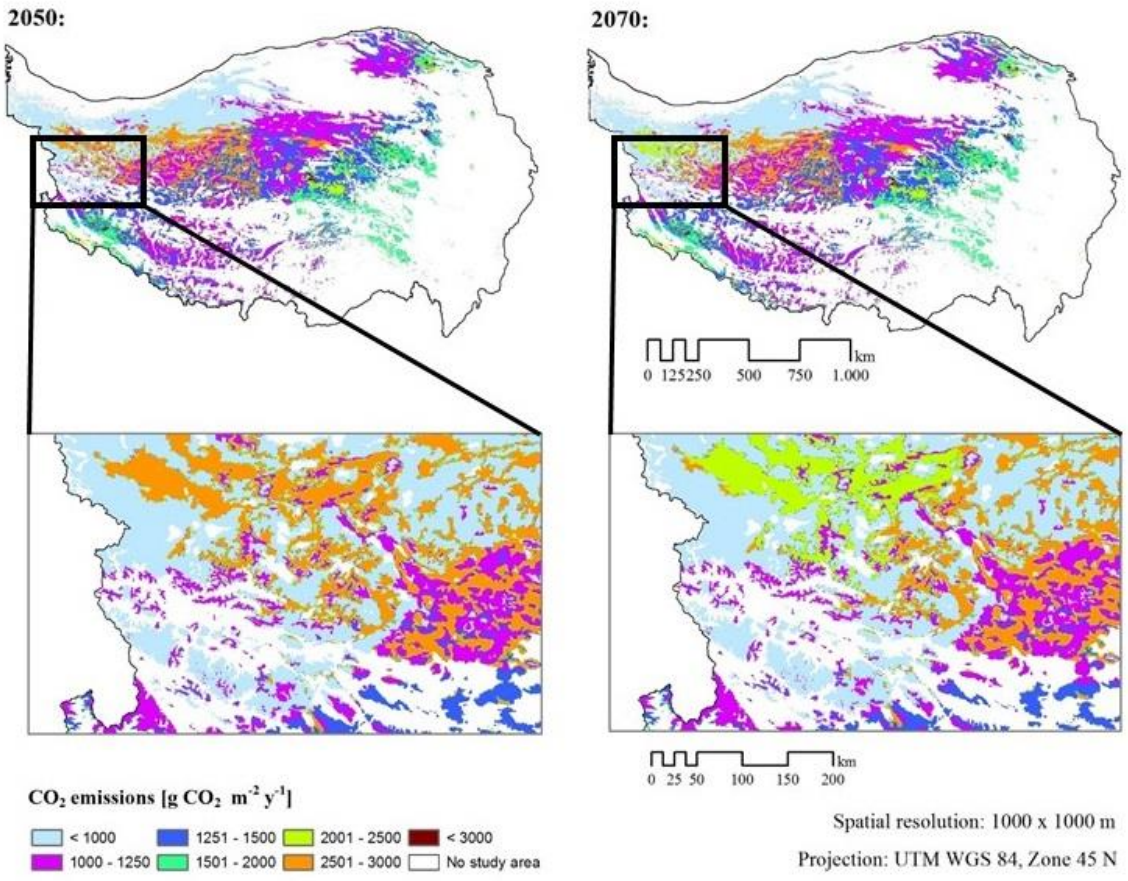

Fig. 2. Spatial distribution of total potential CO_2 emissions from permafrost-affected areas on the Qinghai-Tibet Plateau in 2050 and 2070 according to the RCP2.6 scenarios. Unit of CO_2 emissions is g CO_2 m^{-2} y^{-1}. The spatial resolution of the grids is 1000 x 1000 m.

It has to be considered, however, in terms of area, that the difference between RCP2.6 and RCP8.5 is up to 10865 m^2 in the lowest class and up to 7853 m^2 in the low class as examples. In this case, the CO_2 input to the atmosphere from more than 10 000 m^2 of the permafrost soils of the Qinghai-Tibet Plateau would be instead of 0 – 916.05 g CO_2 m^{-2} at least >916.05 – 1832.10 g CO_2 m^{-2} or even >1832.10 – 3664.21 g CO_2 m^{-2} within one year, which is two to four times more.

3.2. CO_2 emission scenarios for 2070

Mean CO_2 emissions of all scenarios for 2070 range from lowest 1409.73 g CO_2 m^{-2} y^{-1} (RCP2.6) to 1426.25 g CO_2 m^{-2} y^{-1} (RCP8.5). The strongest difference between two scenarios therefore remains 1.15%. Like for the scenarios in 2050, minima (733.97 – 738.32 g CO_2 m^{-2} y^{-1}) and maxima (4129.10 – 4158.69 g CO_2 m^{-2} y^{-1}) are also very

close. Median values lie about 150 g CO_2 m^{-2} y^{-1} below averages (1245.85 – 1263.96 g CO_2 m^{-2} y^{-1}). For all scenarios, CO_2 emissions appear to be less than the CO_2 emissions of 2050. Again, as for the projections of 2050, the statistical means of the general soil respiration follows the same patterns corresponding to the one´s of the total CO_2 emissions. The mean of the thawing-induced CO_2 emissions adds up to 36.03% of the averaged means of the total CO_2 emissions. Like for 2050, the medians of the thawing-induced values amount to less than half of the mean. For all scenarios, the range of the thawing-induced values appears to be broader than the range of the general soil respiration, which is also true for the projections of 2050. Like for 2050, strongest decreases in total CO_2 emissions compared to the total CO_2 emissions in 2015 are located in the central part of the plateau (Fig. 3).

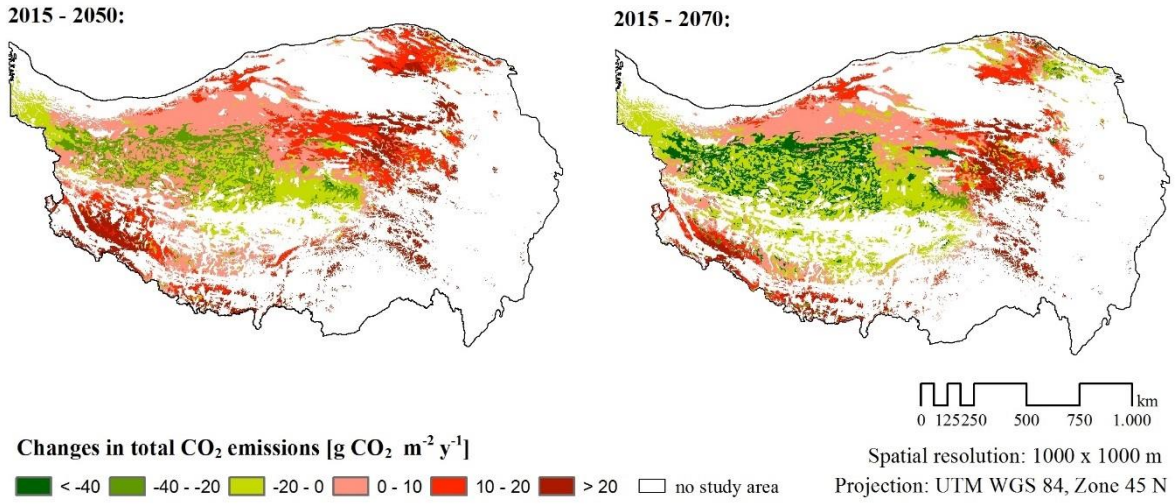

Fig. 3. Spatial distribution of absolute differences in total potential CO_2 emissions from permafrost-affected areas on the Qinghai-Tibet Plateau between 2015 and 2050 and between 2015 and 2070 according to the RCP2.6 scenarios. Unit of changes in total CO_2 emissions is g CO_2 m^{-2} y^{-1}. The spatial resolution of the grids is 1000 x 1000 m.

Basic patterns of the abundance of total CO_2 emissions of 2050 and 2070 in their respective classes resemble each other strongly. Most values occur in the low class (69.00 – 69.33%) and in the class for high CO_2 emission rates, again <1‰ is found. Differences between the scenarios follow the structures of the values´ distribution for 2050. Except for the entire lowest class and the medium class for the RCP8.5 scenario, more value of CO_2 emissions can generally be found in all scenarios of 2050. This corresponds to the result of general higher total CO_2 emissions in 2050. The highest

difference between years and scenarios within one class amounts to 1.29% at the most.

3.3. C stocks

In the permafrost soils of the Qinghai-Tibet Plateau, on average, 67.00 kg C m^{-2} for 2015, 61.79 kg C m^{-2} and 58.66 kg C m^{-2} for 2050 and 2070 are stored according to our estimations based on the WISE30sec data set (see Table 5).

Table 5. Statistics of the soil C stocks of the Qinghai-Tibet Plateau in 2015, 2050 and 2070 in kg C m^{-2} up to a depth of 2 m.

Year	Mean	Min	Max	Median	Range	Sum [Pg C]	Sum of thawing-induced C loss since 2015 [Pg C]
	kg C m^{-2}						
2015	67.00	6.72	387.13	29.87	380.40	68.59	-
2050	61.79	6.20	356.98	27.54	350.78	63.25	5.34
2070	58.66	5.88	338.92	26.15	333.03	60.05	8.54

Minima range from 5.88 kg C m^{-2} (2070) to 6.72 kg C m^{-2} (2015) and maxima from 338.92 kg C m^{-2} (2070) to 387.13 kg C m^{-2} (2015). Highest C stocks occur in the central part of the plateau (Fig. 4).

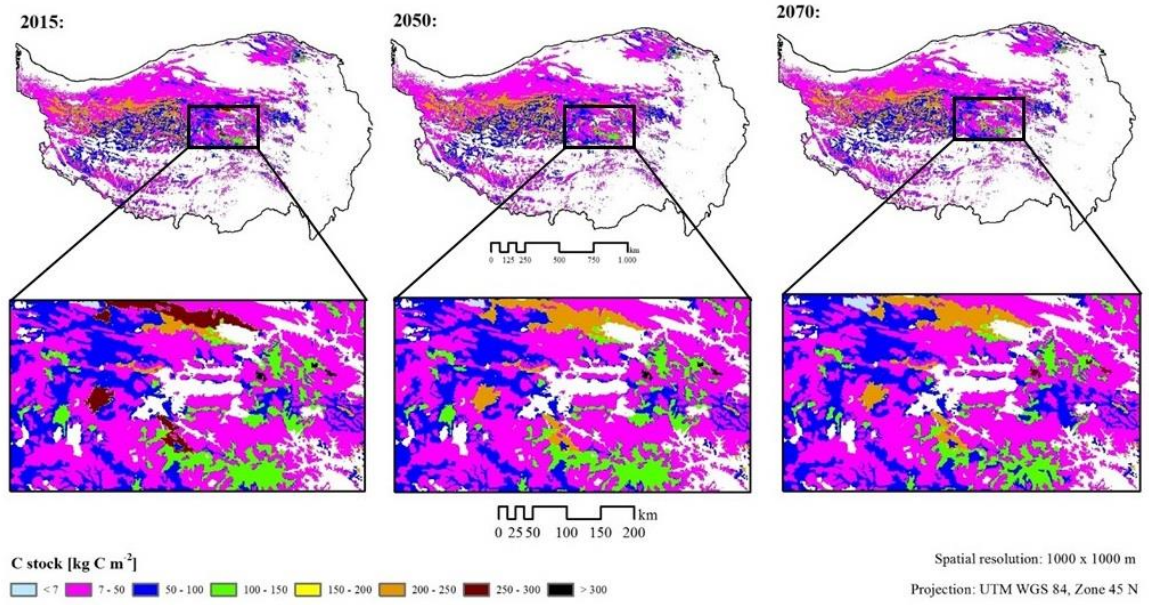

Fig. 4. Spatial distribution of C stocks of the permafrost-affected areas on the Qinghai-Tibet Plateau for 2015, 2050 and 2070. C stocks are in SI unit (kg m^{-2}). The spatial resolution of the grids is 1000 x 1000 m.

For the permafrost-affected area of the Qinghai-Tibet Plateau, C stocks in 2015 add up to 68.59 Pg and to 63.25 Pg and 60.05 Pg for 2050 and 2070 respectively. The climate change-induced increase of microbial activity releases 5.42 Pg C from these permafrost soils between 2015 and 2050 and 8.54 Pg C between 2015 and 2070. The consequent decrease of C stocks is highest on the central part of the plateau for both 2050 and 2070 (Fig. 5).

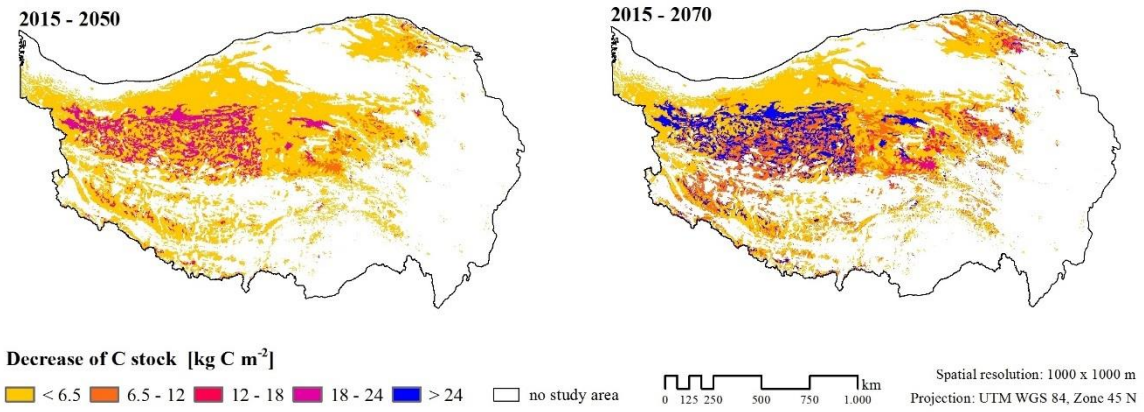

Fig. 5. Spatial distribution of absolute differences in C stocks of the permafrost-affected areas on the Qinghai-Tibet Plateau between 2015 and 2050 and between 2015 and 2070. Absolute differences in C stocks are in SI unit (kg m^{-2}). The spatial resolution of the grids is 1000 x 1000 m.

4. Discussion

Overall, total CO_2 emissions for both 2050 and 2070 remain within the same order of magnitude of soil respiration generally measured on the Qinghai-Tibetan Plateau (2550.29 g CO_2 m^{-2} y^{-1} as average of four years) (Wang et al., 2014) and further show a proportion of general soil respiration and thawing-induced CO_2 emissions comparably to the results of Peng et al. (2015) and Hicks Pries et al. (2013). The field measured results of Peng et al. (2015) with the amount of C additionally released due to warming and thawing permafrost, reach 18 to 29% in an alpine meadow on the plateau. In that study, there is no differentiation between altered soil CO_2 emissions induced by permafrost thaw and altered general soil CO_2 emissions due to a general higher plant and microbial metabolic activity as consequence of higher temperatures. However, it is to assume that most of the increase is related to the additional available permafrost C as Hicks Pries et al. (2013) obtained similar results when focusing on soil CO_2 emissions originating from permafrost C. In that study, old soil heterotrophic soil

CO_2 emissions comprised up to approximately 18% of the remaining parts of soil CO_2 emissions under thawing permafrost.

The differences between the scenarios of total soil CO_2 emissions fully result from the differences between the general soil respiration rates for each scenario as the potential thawing-induced CO_2 emissions are represented by only one value per year due to their different calculation. Accordingly, values of mean, minimum, maximum and median share proportionally the same trends for total CO_2 emissions and general soil respiration. Differences between the scenarios of general soil CO_2 emissions appear to be about 1% what reflects the small differences between the scenarios of MAP as fully accounting for this.

The variability of the general soil respiration results from the variation in MAP, naturally not following static patterns as depending on complex influencing factors as partly considered in the RCPs. As the mean CO_2 emission rate of the RCP6.0 is lower than the one of the RCP4.5 in 2050, the CO_2 emission rate reflects that there is no general linear correlation to the radiative forcing values. For all scenarios of 2070, CO_2 emissions appear to be less than the CO_2 emissions of 2050. This results mostly from the thawing-induced CO_2 loss, which is calculated as percentage of the respective C-stock, consequently decreasing with temporal progression. Differences between the years 2050 and 2070 in thawing-induced CO_2 emissions reflect their linear calculation and decreasing C-stocks. As natural process, thawing of permafrost does, however, not progress strict linearily. Nevertheless, the relative high independence of temperature (Schädel et al., 2014) does not require further differentiations of different temperature scenarios.

Regarding the abundance of values in 2050, except for the entire lowest class and the medium class for the RCP8.5 scenario, more value of CO_2 emissions can generally be found in all scenarios of 2050. This corresponds to the result of general higher total CO_2 emissions in 2050, resulting from decreasing carbon stocks in the end.

With regard to the C stored in the permafrost soils of the Qinghai-Tibet Plateau, the decrease from 2015 to 2070 (Table 5) generally reflects the steady decrease caused by the raised C decomposition. The C stocks in general appear to be reasonable in view of other studies on C stocks. They fit the order of magnitude of field measured data with about 10 kg C m^{-2} in permafrost soils of alpine grasslands of the Qinghai-Tibet Plateau to a depth of <1 m (Genxu et al., 2008; Doerfer et al., 2013) or 56.5 kg

C m^{-2} in meadows (Mu et al., 2015) as examples. The global C stock estimates by Batjes (2015) clearly show the same patterns of the spatial distribution of C stocks on the Qinghai-Tibet Plateau overall with highest C stocks on the Qinghai-Tibet Plateau reaching global maxima. Carvalhais et al. (2014) approximates the global maximum for soil C stocks to 243 kg C m^{-2}, which is comparable to the maxima in this study. Compared to 450 Pg C (Zimov et al., 2006) in the Siberian loess permafrost (1 x 10^6 km^2), the C stock estimated in this study appears to be much lower, resulting from the fact that it covers only a depth to 2 m in contrast to 25 m as reported in Zimov et al. (2006). They also include roots and partly organic matter in their less spatially differentiated approximations as not considering coarse fragments in their calculations and using only one standard value for organic C content and bulk density which accounts for much higher values. Their uncertainty is further assessed as possibly deviating by several hundred Pg (McGuire et al., 2010). Moreover, an extreme spatial variability of soil organic C stocks on the Qinghai-Tibet Plateau has been reported (Mu et al., 2015), leading generally to a wide range in area-wide estimations. C stocks for the permafrost region on the Qinghai-Tibet Plateau were calculated with about 160 Pg C up to 25 m in a similar order of magnitude by Mu et al. (2015) compared to the estimates for the Siberian loess permafrost. However, the strong methodological differences to this study are to a large extent very similar next to a broader definition of the permafrost area. Wang et al. (2002) estimate the C stock of the plateau´s grasslands to 33.5 Pg. However, they only consider the first 70 cm of the soil. The estimation of Mu et al. (2015) for the first two meters amount to about 27.9 Pg C for the permafrost soils on the Qinghai-Tibet Plateau indicating that estimates in this study are reasonable. Since the calculations by Mu et al. (2015) are based on literature data from different studies, they expect deviations of several 10% regarding the C contents as base for their calculations due to different methodological approaches.

With about 0.54 Pg CO_2 $year^{-1}$, the thawing-induced soil CO_2 emissions of the entire study area are, although in the same order of magnitude, about three times higher than what would be supposed based on the results of Schuur et al. (2009). They estimate 1 Pg C $year^{-1}$ (3.66 Pg CO_2 $year^{-1}$) as global C flux assuming an estimated area of global permafrost with about 22 * 10^6 km^2 according to Gruber (2012). Also, the estimates of Koven et al. (2011), who projected emissions from permafrost soils to a depth of 3 m to 7 - 17 Pg CO_2 until 2100, are lower than the results of this thesis (7.3.2). These and comparable estimates by Harden et al. (2012) are even considered being

overestimated (Schädel et al., 2014). However, the results of Schuur et al. (2009) are highly uncertain since they are based on measurements on only one site. A recent, model-based study by Schuur et al. (2015) approximated 37 – 174 Pg C to lose from the global permafrost zone by 2100 under the RCP8.5 scenario. This corresponds to 0.09 Pg C $year^{-1}$ from the plateau on average, which is distinctly closer to an average of 0.15 Pg C $year^{-1}$ (Section 7.3.2). Generally, global annual soil CO_2 emissions are approximated to 63 – 120 Pg C (Raich and Schlesinger, 1992; Raich and Potter, 1995; Reichstein and Beer, 2008). This gives rise to the assumption that the calculated heterotrophic soil CO_2 emissions induced by permafrost thaw are as a whole to be revised upwards after further research.

The spatial distribution of CO_2 emissions with a concentration of highest values in the central part of the plateau (Fig. 2) resembles the spatial distribution of the C:N ratio in the study area. There, the C:N ratio ranges from 0 – 25 (Batjes 2015). Highest C losses occur in this area (Fig. 5), confirming the results of Schädel et al., (2014) that present the C:N ratio as most reliable predictor of C loss compared to either C or N concentration. The permafrost conditions, conserving fragmentary decomposed organic matter, may account for this positive relationship, which reflects the stabile presence of N in the system (Schädel et al., 2014).

Uncertainties of the presented potential CO_2 emissions result from various sources. Input data limitations restrict the estimations´ reliability in all cases. The WorldClim data sets generally show lower precision for poorly sampled regions like the Qinghai-Tibet Plateau (Maussion et al., 2011; Böhner, 2006; Hijmans et al., 2005). The same holds true for areas on the plateau with complex topography where a 1 x 1 km resolution does not capture all potential variation (Hijmans et al., 2005).

The projections of the global climate model Community Climate System Model Version 4 show uncertainties for precipitation on the Qinghai-Tibetan Plateau up to 10 mm per day compared to reference models. The RCP projections generally inhere deficiencies resulting from the process of harmonizing different scenarios and models underlying the RCPs (Van Vuuren et al., 2011). As the years 2050 and 2070 represent an average from 2041 to 60 and 2061 to 80 respectively, likely variation is not represented. Assumptions are too general or static such as a general stronger and stronger regulation of air pollution (Van Vuuren et al., 2011). They also may not only occur model-specifically but are important for other RCP such as reforestation policies

included in RCP 4.5 but potentially also relevant to RCP 2.6. Further uncertainties arise from the transfer of emissions to concentrations and radiative forcing (Van Vuuren et al., 2011). The RCP do not represent those various possible translations (Van Vuuren et al., 2011). Moreover, the respective socio-economic scenario for each RCP is not representing the variety of possible developments (Van Vuuren et al., 2011).

The data input sets from the WISE30sec data inhere deficiencies that arise from processing simplifications resulting in prediction accuracies from 23 to 51% (point-based). Potential biases occur especially for soil characteristics “not observed” as the volumetric gravel content that was calculated using taxotransfer rules. The pragmatic combination of soil profile data from different sources led in the process of harmonizing and reclassification to generalizations (Batjes et al., 2015). With different soil analytical methods in nearly each country, even possibly varying between laboratories, comparability remains critical. To some extend these differences result from the fact that the analytical procedures depend on the soil type. However, no straightforward method of harmonization of the data exists (Batjes, 1999), why the synthesis of the data has proceeded pragmatically as in studies before at this scale (Batjes, 2002). Also, soil geographic as well as taxonomic gaps do exist. Generally, the soil profiles are spatially irregularly distributed. Further uncertainties originating from the spatial data and processes of aggregation, are not yet possible to be quantified at present (Batjes et al., 2015). Despite their limitations, however, the WISE30sec data sets provide the most recent, appropriate, area-explicit information on soil properties for the Qinghai-Tibet Plateau needed to calculate C stocks at a resolution of 1 x 1 km to a depth of 2 m in order to assess potential soil CO_2 emissions on the Qinghai-Tibet Plateau.

In the Global Permafrost Zonation Index Map, main uncertainties also occur for less weakly researched areas like the Qinghai-Tibet Plateau (Gruber et al., 2012). Generally, the high spatial variability of permafrost is not captured by the resolution at hand. The occurrence of permafrost is a result of the interaction of various influencing factors. The Global Permafrost Zonation Index Map, however, solely determines the existence of permafrost based on mean annual air temperature leading to deficiencies. Excluding topographic effects such as the exposition of hills to sun or temperature effects of snow warming the underground are not represented. Likewise is deep permafrost not considered with its influence on near-surface conditions. The model on

which the map is based on, further does not reproduce effects of valleys and depressions where inversions and the drainage of cold air often impact ground temperature. Vegetation effects and thermal characteristics of the ground are further not considered. Sub-grid variability may differ between grids which is also not reproduced by the map as well as transient effects (Gruber et al., 2012). Given the variety of definitions of permafrost, differences in the determination of the area covered by permafrost may occur (Gruber et al., 2012).

To sum up, using these freely accessible data inheres several limitations and uncertainties in general that have partly not even been quantified yet. Therefore, estimations based on them have to be used with caution in view of their deficiencies. In combining the different data sets with their respective limitations in data quality, the deficiencies become even more complex and less quantified. Also, the order of magnitude of potential deviations may change and results may not be as comparable e.g. absolute changes of general soil CO_2 emissions over time may range in a different order of magnitude than the changes over time of the thawing-induced soil CO_2 emissions in absolute numbers. In adding them up to total soil CO_2 emissions, this difference is less obvious and the results need to be interpreted carefully. However, on a regional scale as well as for exploratory investigations, the individual data sets are considered both appropriate and advantageous as highly efficient suppliers of area-explicit data at a high resolution. Their combination increases the inaccuracies of the results, why they as a matter of principle cannot reach the precision of using a fully consistent data set. This approach obtains its appropriateness in view of the early stage of this research area together with its relevance to the vital problem of climate change necessitating results in a timely manner, and other approaches still being highly uncertain as well.

With regard to the computation of the general soil respiration, limitations arise from the background of the regression model by Raich and Schlesinger (1992). Indicated by its coefficient of determination (r^2 = 0.34), it is not capable to fully explain the data variability reflecting highly complex interdependencies between soil respiration and all its controlling factors.

Next to this, high small-scale variability of CO_2 emission rates especially in alpine meadows is not captured by a data resolution of 1 x 1 km. The comparatively very high values in alpine meadows of especially the *Kobresia tibetica* plant communities cannot

not be predicted with this spatial resolution. This strong difference in CO_2 emission rates between this communities and other alpine meadow plant communities results in wide differences of CO_2 emissions within short distances which can only be represented by a higher spatial resolution.

Moreover, the degradation of vegetation and grazing effects comprising about 35% of the Qinghai-Tibet Plateau with decreasing influence on soil respiration (Wen et al., 2013; Cao et al., 2004) is not integrated in our estimations and constraints these predictions of CO_2 emissions. Grazing influences permafrost thawing as decreasing vegetation cover reduces the insulating effect of vegetation, resulting in quicker permafrost thaw on the Qinghai-Tibet Plateau (Hu et al., 2009) and consequently to higher CO_2 emissions induced by permafrost thaw. Although the mechanisms of the relations have in general not been sufficiently clarified yet, changes in soil CO_2 emissions by grazing are relatively high with a decrease by about 50% when doubling grazing intensity on the Qinghai-Tibet Plateau (Cao et al., 2004). Moderate grazing reduces the C uptake in *Kobresia* turfs (Babel et al., 2014) indicating decreasing CO_2 emissions. Johnson and Matchett (2001) concluded that grazing resulted in a decrease of soil CO_2 emissions compared to an ungrazed tallgrass prairie, however, grazed prairie exhibited more soil CO_2 emissions than ungrazed prairie (Frank et al., 2002). Thus, although important, grazing effects do not exceed the order of magnitude of the remaining soil CO_2 emissions (Cao et al., 2004).

Another limitation of the potential thawing-induced CO_2 emissions in the presented results arise from the transfer of the incubation experiments as base for the calculations. The soil samples of the experiments originate from the Arctic with different climatic and environmental conditions. As the soil samples are taken from different studies, their sampling methods are not fully consistent inhering a potential source of uncertainty. Further, the thawing experiments are executed under laboratory conditions that may deviate from the process in natural environment due to strong simplifications. Fresh litter additionally incorporated into the soil is not regarded as well as it is assumed that abiotic factors do not change in contrast to a natural environment (Schädel et al., 2014). Of special importance are drainage conditions altering thawing-induced C loss by 9 – 75% (Elberling et al., 2013). Uncertainty further arises from the extrapolation of the results up to 50 years, disregarding potential variation over time. It is further to expect that the linear developement of C loss over time assumed for the

calculations presented here does not correspond to the natural course as climate change is characterized by a high complexity.

Next to that limitation, we did not include areas with permafrost soils covering <50% of the area indicating that our estimates are possibly biased low. However, their inclusion would potentially have caused a stronger bias.

Moreover, the permafrost of the Qinghai-Tibet Plateau may reach a depth up to more than 130 m (Wang and French, 1995) and soil C stocks at least several 10 m (Mu et al., 2015). Consequently, the C stocks must be higher than the $WISE_{30sec}$ data set captures with a depth of 2 m. Thus, the thawing-induced CO_2 emissions in the field are higher, however, it is to assume that the permafrost thawing process does not reach this depth within the addressed years (Pang et al., 2012).

5. Conclusion

Estimates of potential CO_2 emissions from permafrost soils are crucial to understanding feedback mechanisms of global warming to project future scenarios of climate change. The magnitude of future CO_2 emissions is challenging to predict because of existing high uncertainties about quantity and velocity of the release of organic C from permafrost. Especially for the Qinghai-Tibet Plateau as key region, uncertainties in area-wide data are high as data collection requires extremely high time and cost efforts. Data at a sufficient spatial resolution for large areas, especially for the Qinghai-Tibet Plateau, are generally scarce.

Using different scenarios, a regression model that can be run with climate data, results from laboratory experiments with soil samples from the northern circumpolar permafrost zone, and C stock estimations, we provide an area-wide, highly resoluted, first estimate of potential CO_2 emissions for 2050 and 2070 from permafrost soils of the Qinghai-Tibet Plateau, thus being advantageous for an area-wide calculation of stronger differentiated climate change scenarios.

From our estimates, we conclude that thawing-induced soil CO_2 emissions from permafrost soils on the Qinghai-Tibet Plateau increase general soil respiration by at least about one third, considering that an incorporation of deep permafrost carbon would further distinctly raise CO_2 emissions. Differences between scenarios remain <1% and thawing-induced CO_2 emissions generally decrease comparing 2015, 2050 and 2070. Our approach of aiming at a first estimate of CO_2 emissions of permafrost

soils of the Qinghai-Tibet Plateau under climate change conditions is consistent to measurements of C loss from thawing permafrost soils measured within other studies. The spatially distinct CO_2 emissions calculation at a comparably high spatial resolution allows for assessing both an area-specific future permafrost carbon feedback to climate change from the highly vulnerable permafrost carbon of the Qinghai-Tibet Plateau and spatially distinct future potential greenhouse gas emissions.

6. Acknowledgements

We thank the Ev. Studienwerk Villigst e. V. that funded this study conducted within the framework of the research project PERMATRANS. The support by the German Federal Ministry for Education and Research (BMBF, grant No. 03G0810A) is highly acknowledged. We further appreciate very much the assisstance with data processing of Sarah Schönbrodt-Stitt (University of Tuebingen).

7. References

Amundson, R., 2001. The carbon budget in soils. Annu. Rev. Earth Planet. Sci. 29, 535-562.

Babel, W., Biermann, T., Coners, H., Falge, E., Seeber, E., Ingrisch, J., Schleuß, P.-M., Gerken, T., Leonbacher, J., Leipold, Willinghöfer, S., Schützenmeister, K., Shibistova, O., Becker, L., Hafner, S., Spielvogel, S., Li, X., Xu, X., Sun, Y., Zhang, L., Yang, Y., Ma, Y., Wesche, K., Graf, H.-F., Leuschner, C., Guggenberger, G., Kuzyakov, Y., Miehe, G., Foken, 2014. Pasture degradation modifies the water and carbon cycles of the Tibetan highlands. Biogeosciences 11, 6633-6656.

Batjes, N.H., 1996. Total carbon and nitrogen in the soils of the world. Eur. J. Soil Sci. 47, 151-163.

Batjes, N.H., 1999. Soil vulnerability mapping in Central and Eastern Europe: Issues of data acquisition, quality control and sharing. In: Naff, T. (Ed.), Data Sharing for International Water Resource Management: Eastern Europe, Russia and the CIS. NATO Science Series 2: Environmental Security (Vol. 61). Kluwer Academic Publishers, Dordrecht, pp 187-206.

Batjes, N.H., 2002. Soil parameter estimates for the soil types of the world for use in global and regional modelling (Version 2.1). ISRIC Report 2002/02c,

International Food Policy Research Institute (IFPRI) and International Soil Reference and Information Centre (ISRIC), Wageningen. Available at:

http://www.isric.org/isric/webdocs/Docs/ISRIC_Report_2002_02c.pdf; accessed 12/2008., 58 p.

Batjes, N.H., 2015. World soil propertiy estimates for broad-scale modelling (WISE30sec). Report 2015/01, ISRIC – World Soil Information, Wageningen.

Baumann, F., He, J.-S., Schmidt, K., Kühn, P., Scholten, T., 2009. Pedogenesis, permafrost, and soil moisture as controlling factors for soil nitrogen and carbon contents across the Tibetan Plateau. *Glob. Chang. Biol.* 15, 3001-3017.

Baumann, F., Schmidt, K., Doerfer, C., He, J.-S., Scholten, T., Kühn, P., 2014. Pedogenesis, permafrost, substrate and topography: plot and landscape scale interrelations of weathering processes on the central-eastern Tibetan Plateau. Geoderma 226-227, 300-316.

Böhner, J., 2006. General climatic controls and topoclimatic variations in Central and High Asia, Boreas 35, 279-295.

Böhner, J., Lehmkuhl, F., 2005. Environmental change modelling for Central and High Asia: Pleistocene, present and future scenarios. Boreas 34, 220-231.

Bond-Lamberty, B., Thomson, A., 2010a. Temperature-associated increases in the global soil respiration record. Nature 464, 579-582.

Bond-Lamberty, B., Thomson, A., 2010b. A global database of soil respiration data. Biogeosciences 7, 1915-1926.

Bosch, A., Doerfer, C., He, J.-S., Schmidt, K., Scholten, T., 2016. Predicting soil respiration for the Qinghai-Tibet Plateau: an empirical comparison of regression models. Pedobiologia, 59, 41-49.

Cao, G., Tang, Y., Mo, W., Wang, Y., Li, Y., Zhao, X., 2004. Grazing intensity alters soil respiration in an alpine meadow on the Tibetan plateau. Soil Biol. Biochem. 36, 237-243.

Carvalhais, N., Forkel, M., Khomik, M., Bellarby, J., Jung, M., Migliavacca, M., Mu, M., Saatchi, S., Santoro, S., Santoro, M., Thurner, M., Weber, U., Ahrens, B., Beer, C., Cescatti, A., Randerson, J.T., Reichstein, M., 2014. Global covariation of

carbon turnover times with climate in terrestrial ecosystems. Nature 514, 213-217.

Chapin III, F.S., Sturm, M., Serreze, M.C., McFadden, J.P., Key, J.R., Lloyd, A.H., McGuire, A.D., Rupp, T.S., Lynch, A.H., Schimel, J.P., Beringer, J., Chapman, W.L., Epstein, H.E., Euskirchen, E.S., Hinzman, L.D., Jia, G., Ping, C.-L., Tape, K.D., Thompson, C.D.C., Walker, D.A., Welker, J.M., 2005. Role of land-surface changes in Arctic summer warming. Science 310, 657–660.

Chen, X., Post, W., Norby, R., Classen, A., 2010. Modeling soil respiration and variations in source components using a multi-factor global climate change experiment. Clim. Chang., 1-22.

Cheng, G., 2005. Permafrost studies in the Qinghai-Tibet Plateau for road construction. J. Cold Reg. Eng. 19, 19-29.

Cheng, G., Jin, H., 2013. Permafrost and groundwater on the Qinghai-Tibet Plateau and in northeast China. Hydrogeol. J. 21, 5-23.

Christensen, J.H., Hewitson, B., Busuioc, A., Chen, A., Gao, X., Held, I., Jones, R., Kolli, R.K., Kwon, W.T., Laprise, R., Rueda, V.M., Mearns, L., Menéndez, C.G., Räisänen, J., Rinke, A., Sarr, A., Whetton, P., 2007. Regional Climate Projections. In: Solomon, S., Qin, D., Manning, M., Chen, Z., Marquis, M., Averyt, K.B., Tignor, M., Miller, H.L. (Eds.), Climate Change 2007: The Physical Science Basis. Contribution of Working Group I to the Fourth Assessment Report of the Intergovernmental Panel on Climate Change. Cambridge University Press, Cambridge, pp. 848-940.

Davidson, E.A., Janssens, I.A., 2006. Temperature sensitivity of soil carbon decomposition and feedbacks to climate change. Nature 440, 165-173.

Ding, J., Li, F., Yang, G., Chen, L., Zhang, B., Liu, L., Fang, K., Qin, S., Chen, Y., Peng, Y., Ji, C., He, H., Smith, P., Yang, Y., 2016. The permafrost carbon inventory on the Tibetan Plateau: a new evaluation using deep sediment cores. Glob. Chang. Biol., doi:10.1111/gcb.13257

Doerfer, C., Kuehn, P., Baumann, F., He, J.-S., Scholten, T., 2013. Soil organic carbon pools and stocks in permafrost-affected soils on the Tibetan Plateau. PLoS One 8(2): e57024.

Duan, A.M., Wu, G.X., 2005. Role of the Tibetan Plateau thermal forcing in the summer climate patterns over subtropical Asia. Clim. Dyn. 24, 793-807.

Dutta, K., Schurr, E.A.G., Neff, J.C., Zimov, S.A., 2006. Potential carbon release from permafrost soils of Northeastern Sibiria. Glob. Change Biol. 12, 2336-2351.

Elberling, B., Michelsen, A., Schädel, C., Schuur, E.A.G., Christiansen, H.H., Berg, L., Tamstorf, M.P., Sigsgaard, C., 2013. Long-term CO_2 production following permafrost thaw. Nat. Clim. Chang. 3, 890-894.

Fan, J.-W., Shao, Q.-Q., Liu, J.-Y., Wang, J.-B., Harris, W., Chen, Z.-Q., Zhong, H.-P., Xu, X.-L., Liu, R.-G., 2010. Assessment of effects of climate change and grazing activity on grassland yield in the Three Rivers Headwaters Region of Qinghai-Tibet Plateau, China. Environ. Monit. Assess. 170, 571–584.

Frank, A.B., Liebig, M.A., Hanson, J.D., 2002. Soil carbon dioxide fluxes in northern semiarid grasslands. Soil Biol. Biochem. 34, 1235-1241.

Geng, Y., Wang, Y., Yang, K., Wang, S., Zeng, H., Baumann, F., Kuehn, P., Scholten, T., He, J.-S., 2012. Soil respiration in Tibetan alpine grasslands: belowground biomass and soil moisture, but not soil temperature, best explain the large-scale patterns. PLoS One 7, 1-12.

Gent, P.R., Danabasoglu, G., Donner, L.J., Holland, M.M., Hunke, E.C., Jayne, S.R., Lawrence, D.M., Neale, R.B., Rasch, P.J., Vertenstein, M., Worley, P.H., Yang, Z.-L., Zhang, M., 2011. The community climate system model version 4. J. Clim. 24, 4973-4991.

Genxu, W., Yuanshou, L., Yibo, W., Qingbo, W., 2008. Effects of permafrost thawing on vegetation and soil carbon pool losses on the Qinghai.Tibet Plateau, China. Geoderma 143, 143-152.

Gruber, S., 2012. Derivation and analysis of a high-resolution estimate of global permafrost zonation. Cryosphere 6, 221-233.

Harden, J.W., Sundquist, E.T., Stallard, R.F., Mark, R.K., 1992. Dynamics of soil carbon during deglaciation of the Laurentide Ice Sheet. Sciene 258, 1921-1924.

Hicks Pries, C.E., Schuur, E.A.G., Crummer, K.G., 2012. Holocene carbon stocks and carbon accumulation rates altered in soils undergoing permafrost thaw. Ecosystems 15, 162-173.

Hicks Pries, C., Schuur, E.A.G., Crummer, K.G., 2013. Thawing permafrost increases old soil and autotrophic respiration in tundra: partitioning ecosystem respiration using $\delta^{13}C$ and $\Delta^{14}C$. Glob. Change Biol. 19, 649-661.

Hijmans, R.J., Cameron, S.E., Parra, J.L., Jones, P.G., Jarvis, A., 2005. Very high resolution interpolated climate surfaces for global land areas. Int. J. Climat. 25, 1965-1978.

Hu, H., Wang, G., Liu, G., Li, T., Ren, D., Wang, Y., Cheng, H., Wang, J., 2009. Influences of alpine ecosystem degradation on soil temperature in the freezing-thawing process on Qinghai– Tibet Plateau. Environ. Geol. 57, 1391–1397.

Immerzeel, W., Quiroz, R., Jong, S., 2005. Understanding precipitation patterns and land use interaction in Tibet using harmonic analysis of SPOT VGT-S10 NDVI time series. Int. J. Remote Sens. 26, 2281–2296.

Jia, B., Zhou, G., Wang, Y., Wang, F., Wang, X., 2006. Effects of temperature and soil water-content on soil respiration of grazed and ungrazed *Leymus chinensis* steppes, Inner Mongolia. J. Arid Environ. 67, 60-76.

Johnson, L.C., Matchett, J.R., 2001. Fire and grazing regulate belowground processes in a tallgrass prairie. Ecology 82, 3377-3389.

Jones, C.D., Cox, P.M., Essery, R.L.H., Roberts, D.L., Woodage, M.J., 2003. Strong carbon cycle feedbacks in a climate model with interactive CO_2 and sulphate aerosols. Geophys. Res. Lett. 30, 1-4.

Kang, S., Xu, Y., You, Q., Flügel, W.-A., Pepin, N., Yao, T., 2010. Review of climate and cryospheric change in the Tibetan Plateau. Environ. Res. Lett. 5, 1-8.

Kirschbaum M.U.F., 1995. The temperature dependence of soil organic matter decomposition, and the effect of global warming on soil organic storage. Soil Biol. Biochem. 27, 753-760.

Koven, C.D., Ringeval, B., Friedlingstein, P., Ciais, P., Cadule, P., Khvorostyanov, D., Krinner, G., Tarnocai, C., 2011. Permafrost carbon-climate feedbacks accelerate global warming. Proc. Natl. Acad. Sci. U.S.A. 108, 14769-14774.

Kutzbach, J.E., Liu, X., Liu, Z., Chen, G., 2008. Simulation of the evolutionary response of global summer monsoons to orbital forcing over the past 280,000 years. Clim. Dyn. 30, 567-579.

Lawrence, D.M., Koven, C.D., Swenson, S.C., Riley., W.J., Slater, A.G., 2015. Permafrost thaw and resulting soil moisture changes regulate projected high-latitude CO_2 and CH_4 emissions. Environ. Res. Lett. 10, 1-11.

Liu, X., Chen, B., 2000. Climatic warming in the Tibetan Plateau during recent decades. Int. J. Climat. 20, 1729-1742.

Luo, T., Li, W., Zhu, H., 2002. Estimated biomass and productivity of natural vegetation on the Tibetan Plateau. Ecol. Appl. 12, 980-997.

Manabe, S., Terpstra, T., 1974. The effects of mountains on the general circulation of the atmosphere as identified by numerical experiments. J. Atmos. Sci. 31, 3-42.

Maussion, F., Scherer, D., Finkelnburg, R., Richter, J., Yang, W., Yao, T., 2011. WRF simulation of a precipitation event over the Tibetan Plateau, China – an assessment using remote sensing and ground observations, Hydrol. Earth Syst. Sci. 15, 1795-1817.

McGuire, A.D., Macdonals, R.W., Schuur, E.A.G., Harden, J., Kuhry, P., Hayes, D.J., Christensen, T.R., Heimann, M., 2010. The cabon budget of the northern cryosphere region. Curr. Opin. Environ. Sustain. 2, 231-236.

Mu, C., Zhang, T., Wu, Q., Peng, X., Cao, B., Zhang, X., Cao, B., Cheng, G., 2015. Editorial: organic carbon pools in permafrost regions on the Qinghai-Xizang (Tibetan) Plateau. Cryosphere 9, 479-486.

Pang, Q., Zhao, L., Li, S., Ding, Y., 2012. Active layer thickness variations on the Qinghai-Tibet Plateau under the scenarios of climate change. Environmental Earth Sciences 66, 849-857.

Pei, Z.-Y., Ouyang, H., Zhou, C.-P., Xu, X.-L., 2009. Carbon balance in an alpine steppe in the Qinghai-Tibet Plateau. J. Integr. Plant Biol. 51, 521-526.

Raich, J.W., Potter, C.S., 1995. Global patterns of carbon dioxide emissions from soils. Glob. Biogeochem. Cycles 9, 23-36.

Raich, J.W., Schlesinger, W.H., 1992. The global carbon dioxide flux in soil respiration and its relationship to vegetation and climate. Tellus 44B, 81-99.

Reichstein, M., Beer, C., 2008. Soil respiration across scales: the importance of a model-data integration framework for data interpretation. J. Plant Nutr. Soil Sci. 171, 344-354.

Rodeghiero, M., Cescatti, A., 2005. Main determinants of forest soil respiration along an elevation/temperature gradient in the Italian Alps. Glob. Chang. Biol. 11, 1024–1041.

Rodeghiero, M., Churkina, G. Martinez, C., Scholten, T. Gianelle, D., Cescatti. A., 2013. Components of forest soil CO_2 efflux estimated from $\Delta^{14}C$ values of soil organic matter. Plant Soil 364/1, 55-68.

Schädel, C., Schuur, E.A.G., Bracho, R., Elberling, B., Knoblauch, C., Lee, H., Luo, Y., Shaver, G.R., Turetsky, M.R., 2014. Circumpolar assessment of permafrost C quality and its vulnerability over time using long-term incubation data. Glob. Change Biol. 20, 641-652.

Schaefer, K., Zhang, T., Bruhwiler, L., Barrett, A.P., 2011. Amount and timing of permafrost carbon release in response to climate warming. Tellus 63B, 165-180.

Schlesinger, W.H., Andrews, J.A., 2000. Soil respiration and the global carbon cycle. Biogeochemistry 48, 7-20.

Schoenbrodt-Stitt, S., Bosch, A., Behrens, T., Hartmann, H., Xuezheng, S., Scholten, T., 2013. Approximation and spatial regionalization of rainfall erosivity based on sparse data in a mountainous catchment of the Yangtze River in Central China. Environ. Sci. Pollut. Res. 20, 6917-6933.

Schroeder, P.E., Winjum, J.K., 1995. Assessing Brazil's carbon budget I. Biotic carbon pools. For. Ecol. Manage. 75, 77-86.

Schuur, E.A.G., Bockheim, J., Canadell, J.G., Euskirchen, E., Field, C.B., Goryachkin, S.V., Hagemann, S., Kuhry, P., Lafleur, P.M., Lee, H., Mazhitova, G., Nelson, F.E., Rinke, A., Romanovsky, V.E., Shiklomanov, N., Tarnocai, C., Venensky, S., Vogel, J., Zimov, S.A., 2008. Vulnerability of permafrost carbon to climate change: Implications for the global carbon cycle. Bioscience 58, 710-714.

Schuur, E.A.G., Vogel, J.G., Crummer, K.G., Lee, H., Sickman, J.O., Osterkamp, T.E., 2009. The effect of permafrost thaw on old carbon release and net carbon exchange from tundra. Nature 459, 556-559.

Schuur, E.A.G., McGuire, A.D., Schädel, C., Grosse, G., Harden, J.W., Hayes, D.J., Hugelius, G., Koven, C.D., Kuhry, P., Lawrence, D.M., Natalo, S.M., Olefeldt, D., Romanovsky, V.E., Schaefer, K., Turetsky, M.R., Treat, C.C., Vonk, J.E., 2015. Climate change and the permafrost carbon feedback. Nature 520, 171-179.

Shaver, G.R., Canadell, J., Chapin III, F.S., Gurevitch, J., Harte, J., Henry, J., Inseon, P., Jonasson, S., Melillo, J., Pitelka, L., Rustad, L., 2000. Global warming and terrestrial ecosystems: a conceptual framework for analysis. Bioscience 50, 871-882.

Sistla, S.A., Moore, J.C., Simpson, R.T., Gough, L., Shaver, G.R., Schimel, J.P., 2013. Long-term warming restructures Arctic tundra without changing net soil carbon storage. Nature 497, 615-618.

Valentini, R., Matteucci, G., Dolman, A.J., Schulze, E.-D., Rebmann, C., Moors, E., J., Granier, A., Gross, P., Jensen, N.O., Pilegaard, K., Lindroth, A., Grelle, A., Bernhofer, C., Grünwald, T., Aubinet, M., Ceulemans, R., Kowalski, A.S., Vesala, T., Rannik, Ü., Berbigier, P., Loustau, D., Guðmundsson, J., Thorgeirsson, H., Ibrom, A., Morgenstern., Clement, R., Moncrieff, J., Montagnani, L., Minerbi, S., Jarvis, P.G. 2000. Respiration as the main determinant of carbon balance in European forests. Nature 404, 861-865.

van Vuuren, D.P., Edmonds, J., Kainuma, M., Riahi, K., Thomson, A., Hibbard, K., Hurtt, G.C., Kram, T., Krey, V., Nakicenovic, N., Smith, S.J., Rose, S.K., 2011. The representative concentration pathways: an overview. Clim. Chang. 109, 5-31.

Wang, B., French, H., 1995. Permafrost on the Tibet Plateau, China. Quat. Sci. Rev. 14, 225-274.

Wang, B., Bao, Q., Hoskins, B., Wu, G., Liu, Y., 2008. Tibetan Plateau warming and precipitation change in East Asia. Geophys. Res. Lett. 35.

Wang, S., Jin, H., Li, S., Zhao, L., 2000. Permafrost degradation on the Qinghai-Tibet Plateau and its environmental impacts. Permafrost Periglacial Process. 11, 43-53.

Wang, W.Y., Wang, Q.J., Li, S.X., Wang, G., 2006. Distribution and species diversity of plant communities along transect on the Northeastern Tibetan plateau. Biodivers. Conserv. 15, 1811–1828.

Wang, X., Liu, L., Piao, S., Janssens, I.A., Tang, J., Liu, W., Chi, Y., Wang, J., Xu, S., 2014a. Soil respiration under climate warming: differential response of heterotrophic and autotrophic respiration, Glob. Chang. Biol. 20, 3229-3237.

Wang, Y., Liu, H., Chung, H., Yu, L., Mi, Z., Geng, Y., Jing, X., Wang, S., Zeng, H., Cao, G., Zhao, X., He, J.-S., 2014b. Non-growing-season soil respiration is controlled by freezing and thawing processes in the summer monsoon-dominated Tibetan alpine grassland. Global Biochem. Cy. 28, 1081-1095.

Wen, L., Dong, S., Li, Y., Wang, X., Li, X., Shi, J., Dong, Q., 2013. The impact of land degradation on the C pools in alpine grasslands of the Qinghai- Tibet Plateau, Plant Soil 368, 329-340.

Xu, Z.X., Gong, T., L., Li, J.Y., 2008. Decadal trend of climate in the Tibetan Plateau - regional temperature and precipitation. Hydrol. Process. 22, 3056-3065.

Xue, K.M., Yuan, M.J., Shi, Z., Qin, Y., Deng, Y., Cheng, L., Wu, L., He, Z., Van Nostrand, J.D., Bracho, R., Natali, S., Schuur, E.A.G., Luo, C., Konstantinidis, K.T., Wang, Q., Cole, J.R., Tiedje, J.M., Luo, Y., Zhou, J., 2016. Tundra soil carbon is vulnerable to rapid microbial decomposition under climate warming. Nature Clim. Change, advance online publication.

Yang, M., Wang, S., Yao, T., Gou, X., Lu, A., Guo, X., 2004. Desertification and its relationship with permafrost degradation in Qinghai-Xizang (Tibet) plateau. Cold Reg. Sci. Technol. 39, 47-53.

Yang, Y., Fang J., Smith, P.,Tang, Y., Chen, A., Ji, C., Hu, H., Rao, S., Tan K.U.N., He, J.-S., 2009. Changes in topsoil carbon stock in the Tibetan grasslands between the 1980s and 2004. Glob. Chang. Biol. 15, 2723-2729.

Yu, H.Y., Luedeling, E., Xu, J.C., 2010. Winter and spring warming result in delayed spring phenology on the Tibetan Plateau. Proc. Natl. Acad. Sci. U. S. A. 107, 22151–22156.

Zhang Y., Bingyuan, L., Du, Z., 2002. The area and boundary of Qinghai-Tibet Plateau. Geogr. Res., 21, 1–8. (in Chinese)

Zhang, D., Xu, W., Li, J., Cai, Z., An, D., 2014. Frost-free season lenghtening and ist potential cause in the Tibetan Plateau from 1960 to 2010. Theor. Appl. Climatol. 115, 441-450.

Zhang, Y., Ohata, T., Kodata, T., 2003. Land-surface hydrological processes in the permafrost region of the eastern Tibetan Plateau. J. Hydrol. 283, 41-56.

Zhang, Y., Tang, Y., Jiang, J., Yang, Y., 2007. Characterizing the dynamics of soil organic carbon in grasslands on the Qinghai-Tibetan Plateau. Sci. China Ser. D 50, 113-120.

Zhang, Y., Wang, G., Wang, Y., 2010. Response of biomass spatial pattern of alpine vegetation to climate change in permafrost region of the Qinghai-Tibet Plateau, China. J. Mt. Sci. 7, 301-314.

Zheng, D., 1996. The system of physico-geographical regions of the Qinghai-Xizang (Tibet) Plateau. Sci. China Ser. D 39, 410-417.

Zhong, L., Ma, Y., Salama M.S., Su, Z., 2010. Assessment of vegetation dynamics and their response to variations in precipitation and temperature in the Tibetan Plateau. Clim. Chang. 103, 519-535.

Zhuang, Q., He, J., Lu, Y., Ji, L., Xiao, J., Luo, T., 2010. Carbon dynamics of terrestrial ecosystems on the Tibetan Plateau during the 20th century: an analysis with a process-based biogeochemical model. Glob. Ecol. Biogeogr. 19, 649-662.

Zimov, S.A., Davydov, S.P., Zimova, G.M., Davydova, A.I., Schuur, E.A.G., Dutta, K., Chapin III, F.S., 2006. Permafrost carbon: stock and decomposability of a globally significant carbon pool. Geophys. Res. Lett. 33, L20502.

Table 1

Table 1. Regression models to approximate soil respiration.

Type of regression	Region, vegetation type	Equation	Parameters	Author(s)
Regression based on temperature		$R_s = a * e^{bT}$	*Rs* = soil respiration (n/a), *T* = temperature (n/a), *a*, *b* = empirical regression coefficient	Luo and Zhou (2006) from van´t Hoff (1894)
	Inner Mongolia, *Leymus chinensis* steppe	$F = a + bT$ with: a = -76.91; -56.34 b = 16.59; 9.52 (ungrazed; grazed)	*F* = soil respiration rate (mg m^{-2} h^{-1}), *T* = temperature (°C), *a, b* = parameters	Jia et al. (2006)
	Inner Mongolia, *Leymus chinensis* steppe	$F = a + bT + cT^2$ with: a = -47.51; -66.98 b = 12.79; -7.18 c = 0.11; 0.50 (ungrazed; grazed)	*F* = soil respiration rate (mg m^{-2} h^{-1}), *T* = temperature (°C), *a, b, c* = parameters	Jia et al. (2006)
	Inner Mongolia, *Leymus chinensis* steppe	$F = aT^b$ with: a = 22.70; 1.43 b = 0.71; 1.46 (ungrazed; grazed)	*F* = soil respiration rate (mg m^{-2} h^{-1}), *T* = temperature (°C), *a, b* = parameters	Jia et al. (2006)
	Inner Mongolia, *Leymus chinensis* steppe	$F = a(T + 10)^b$ with: a = 0.07; 0.02 b = 2.31; 2.56 (ungrazed; grazed)	*F* = soil respiration rate (mg m^{-2} h^{-1}), *T* = temperature (°C), *a, b* = parameters	Jia et al. (2006)
	Inner Mongolia, *Leymus chinensis* steppe	$F = a(T - T_{min})^b$ with: a = 4.22 * 10-4; 3.21 * 10-26 b = 3.48; 12.98 Tmin = -22.02; -112.61 (ungrazed; grazed)	*F* = soil respiration rate (mg m^{-2} h^{-1}), *T* = temperature (°C), *a, b* = parameters	Jia et al. (2006)
	Inner Mongolia, *Leymus chinensis* steppe	$F = ae^{bT}$ with: a = 29.94; 14.75 b = 0.09; 0.10 (ungrazed; grazed)	*F* = soil respiration rate (mg m^{-2} h^{-1}), *T* = temperature (°C), *a, b* = parameters	Jia et al. (2006)

Inner Mongolia, *Leymus chinensis* steppe	$F = a * \exp(bT + cT^2)$ with: a = 18.17; 14.01 b = 0.16; 0.11 c = -0.002; -0.0002 (ungrazed; grazed)	*F* = soil respiration rate (mg m^{-2} h^{-1}), *T* = temperature (°C), *a, b, c* = parameters	Jia et al. (2006)
Inner Mongolia, *Leymus chinensis* steppe	$F = a * \exp(-E/R(T + 273.2))$ with: a = 2.91*1013; E = 6.31*104; R = 8.31 J mol^{-1} K^{-1}	*F* = soil respiration rate (m^{-2} h^{-1}), *T* = temperature (°C), *E* = gas constant (J mol^{-1} K^{-1}), *a, R* = parameters	Jia et al. (2006)
Inner Mongolia, *Leymus chinensis* steppe	$F = a * \exp(-E_0/(T + 273.2 - T_0))$ with: a = 5.99*104; 1.96*1011 E0 = 444.02; 4610.03 T0= 219.78; 75.50 (ungrazed; grazed)	*F* = soil respiration rate (mg m^{-2} h^{-1}), *T* = temperature (°C), *a, E_0, T_0* = parameters	Jia et al. (2006)
	$R = R_c e^{\frac{E}{T - T_c}}$	*R* = respiration rate, *T* = absolute temperature (K), R_c= fitted parameter, *E* = fitted parameter, T_c = fitted parameter	Lloyd and Taylor (1994) ("Lloyd and Taylor equation")
Lab in-cubations	$Y = aexp(\frac{E}{R(T + 273.2)} \frac{T - 10}{283.2}$ with: a = 0.06648; 0.02992 E = 6.141*104; 8.361 * 104 (farmland soil; forest soil)	*Y* = soil respiration (mg CO_2 m^{-2} s^{-1}), *T* = temperature (°C), *a, E* = parameters, *R* = (n/a)	Fang and Moncrieff (2001) ("Arrhenius type equation")
Inner Mongolia, *Leymus chinensis* steppe	$F = ae^{(-\frac{E}{R(T+273.2)})}$ with: a = 6.14 * 10-6; 3.06 * 10-7 b = 0.15; 0.14 E = 3.34 *104; 3.87 *104 R = 8.31 J mol-1 K-1; 8.31 J mol-1K-1 (ungrazed; grazed)	*F* = soil respiration rate (mg m^{-2} h^{-1}), *T* = temperature, *E* = gas constant (J mol^{-1} K^{-1}), *a, b, R* = parameters	Jia et al. (2006)
Bacteria	$\sqrt{r} = b\ (T - T_0)$	*r* = growth rate constant, *b* = regression coefficient, *T* = temperature (K), T_0 = conceptual temperature of no metabolic significance	Ratkowsky et al. (1982)
Utah, *Atriplex-confertifolia*	$R_T = R_{10} + 6.187 * 10^{-3}(T - 10)^2$	R_T = respiration (μmolkg^{-1} s^{-1}), *T* = temperature (°C), R_{10} = seasonally adjusted respiration rate at 10 °C	Holthausen and Caldwell (1980)
Ten-nessee	$R_s = f * T$	R_s = soil respiration (μmol m^{-2} s^{-1}),	Chen et al. (2010)

		T = temperature (°C), *f* = coefficient	
Qinghai-Tibet Plateau, *Kobresia* meadow	$F = R_0 \exp(kT)$ with: $R_0 = 0.273$	*F* = CO_2 emission rate (µmol CO_2 m^{-2} s^{-1}), R_0 = CO_2 emission rate at 0 °C (µmol CO_2 m^{-2} s^{-1}), *k* = activation energy ($°C^{-1}$), *T* = temperature (°C)	Kato et al. (2005)
Japan, agri-cultural field	$SR = aexp(bx)$	*SR* = soil respiration rate (mg CO_2 m^{-2} s^{-1}), *x* = temperature at different heights (°C), *a*, *b* = coefficient	Nakadai et al. (2002)
China, desert	$R_s = ae^{bTa}$ with: a = 0.322; 0.21; 0.142; 0.222 b = 0.03; 0.034; 0.042; 0.034 (*Haloxylonammodendron; Anabasis aphylla; Halostachyscaspica, all*)	R_s= soil respiration (µmol CO_2 m^{-2} s^{-1}), *Ta* = air temperature (°C), *a, b* = fitted parameter	Zhang et al. (2010)
China, desert	$R_s = ae^{(-E/R(Ta+273.2))}$ with: a = 3796.515; 2248.805; 74042.548; 6416.267 E = 21200.55; 20817.8; 29932.56; 23193.9 (*Haloxylonammodendron; Anabasis aphylla; Halostachyscaspica, all*)	R_s= soil respiration (µmol CO_2 m^{-2} s^{-1}), Ta = air temperature (°C), *a*, *E* = fitted parameter, *R* = universal gas constant (kJ mol^{-1} k^{-1})	Zhang et al. (2010)
China, desert	$y = 0.322e^{0.0305x}$	*y* = soil respiration at *Haloxylonammodendron*site (µmol CO_2 m^{-2} s^{-1}), *x* = air temperature (°C)	Zhang et al. (2010)
China, desert	$y = 0.2103e^{0.0366x}$	*y* = soil respiration at *Anabasis aphylla* site (µmol CO_2 m^{-2} s^{-1}), y = air temperature (°C)	Zhang et al. (2010)
China, desert	$y = 0.1424e^{0.0422x}$	*y* = soil respiration at *Halostachyscaspica* site (µmol CO_2 m^{-2} s^{-1}), *x* = air temperature (°C)	Zhang et al. (2010)
China, desert	$y = 0.222e^{0.0339x}$	*y* = soil respiration at *Haloxylonammodendron, Anabasis aphylla and Halostachyscaspica* site (µmol CO_2 m^{-2} s^{-1}), *x* = air temperature (°C)	Zhang et al. (2010)
	$R_s = R_0 Q_{10}^{\frac{T-T_0}{10}}$	R_s =soil respiration (n/a), R_0 = respiration at temperature T_0, Q_{10} = representing the relative increase R/R_0 as temperature increases by 10°C	Luo and Zhou (2006) from van´t Hoff (1894) ("Q_{10}mo-del")
	$R = A\, e^{-\frac{E_0}{R_0 T}}$ with: R_0 = 8.314	*R* = respiration rate, *T* = absolute temperature (K), *A* = Arrhenius coefficient, E_0 = activation energy for the chemical reaction, R_0 = gas constant ($JK^{-1}mol^{-1}$)	Qi et al. (2002) ("Arrhenius equation")

	Oregon, citrus seedlings	$r = 1.11^{(0.0739T)}$	*r* = root respiration rate (nmol CO_2 (g DW)$^{-1}$ s^{-1}), *T* = temperature (°C)	Bouma et al. (1997)
	Massa-chusetts, forest	$R_{mass} = -0.0227T + 0.748$ (organic soils) $R_{mass} = -0.0179T + 0.491$ (mineral soils)	R_{mass}= rates of microbial respiration at 15 °C (µg C g microbial biomass^{-1} day^{-1}), *T* = temperature (°C)	Bradford et al. (2008)
Regression based on mean annual tempera-ture *T*		$SR = 25.6T + 300$	*SR* = annual soil respiration rate (g C/m^2/yr), *T* = mean annual temperature (°C),	Raich and Schlesinger (1992)
	Micro-nesia and Hawaii, peatlands	$Y = 265.9 + (27.7 * MAT)$	*Y* = annual soil respiration rate (g C m^{-2} yr^{-1}), *MAT* = mean annual temperature (°C)	Chimner (2004)
		$R_S = 36.2 + 3.32 * T$	R_S = annual global soil respiration (g C y^{-1}), *T* = mean annual air temperature over land (°C)	Raich et al. (2002)
Regression based on mean monthly air tempera-ture *T*	Analysis of published field fluxes of CO_2	$\log SR = 0.282 + (0.0271 * T)$ with: $SR = e^{logSR} - 1.0$	*SR* = soil CO_2 efflux (g C m^{-2} d^{-1}), *T* = mean monthly air temperature (°C)	Raich and Potter (1995)
	Analysis of published field fluxes of CO_2	$SR = 0.286 + (0.0568 * T)$	*SR* = soil CO_2 efflux (g C m^{-2} d^{-1}), *T* = mean monthly air temperature (°C)	Raich and Potter (1995)
	Qinghai-Tibet Plateau	$G_1(t;T) = 0.16$T(t)+2.24	G_1 *(t;T)* = mean monthly soil release of carbon for temperate/boreal needle-leaved vegetation (g C m^{-2} d^{-1}), *T(t)* = monthly surface air temperature (°C)	Fung et al. (1987)
	Qinghai-Tibet Plateau	$G_2(t;T) = 0.44$ T(t)+2.76	G_2 *(t;T)* = mean monthly soil release of for temperate/boreal broad-leaved vegetation (g C m^{-2} d^{-1}), *T(t)* = monthly surface air temperature (°C)	Fung et al. (1987)
	Qinghai-Tibet Plateau	$G_3(t;T)/G_{max} = 0.78$ T(t)/T_{max}+2.76	G_3 *(t;T)* = mean monthly soil release of carbon for tropical/subtropical woody vegetation (g C m^{-2} d^{-1}), *T(t)* = monthly surface air temperature (°C), G_{max} = maximum monthly soil respiration rate, T_{max} = local maximum monthly air temperature	Fung et al. (1987)
	Qinghai-Tibet Plateau	$G_4(t;T)/G_{max} = 0.77$ T(t)/T_{max}+0.03	G_4 *(t;T)* = mean monthly soil release of carbon for grasslands (g C m^{-2} d^{-1}), *T(t)* = monthly surface air temperature (°C), G_{max} = maximum monthly soil respiration rate,	Fung et al. (1987)

			T_{max} = local maximum monthly air temperature	
Regression based on mean weekly air temperature *wTa*	Colorado, crop field	$lnCO_2 = 7.8156 + 0.05995wTa$	CO_2 = amount of CO_2 evolved from the soil (g m^{-2} d^{-1}), *wTa* = mean weekly air temperature (°C)	Buyanovsky et al. (1986)
Regression based on soil temperature	Great Plains of USA, tall grass prairie	$R_s = ae^{bT}$ with: a = 0.267; 0.332; 0.333; 0.430 b = 0.104; 0.085; 0.086; 0.070 (unclipped/unwarmed; unclipped/warmed; clipped/unwarmed; clipped/warmed)	R_s = soil respiration (µmol m^{-2} s^{-1}), *T* = soil temperature (°C), *a* = intercept of soil respiration when temperature is zero, *b* = temperature sensitivity coefficients	Luo (2001)
		$R = R_0 e^{\beta T}$ with: $e^{10\beta} = Q_{10} = \frac{R_{T+10}}{R}$	*R* = soil respiration (µmol $m^{-2}s^{-1}$), R_0 = basal respiration at temperature of 0°C, *T* = soil temperature over 0-10cm (°C), *β* = temperature coefficient	Rey et al. (2002)
	Northeast China, grass-lands with *L. chinensis*	$Y = 1.282e^{0.077x}$	*Y* = soil respiration (g CO_2 $m^{-2}d^{-1}$), *x* = soil temperature at 10 cm soil depth (°C)	Wang et al. (2007)
	Northeast China, grass-lands with *P. tenuiflora*	$Y = 0.741e^{0.086x}$	*Y* = soil respiration (g CO_2 $m^{-2}d^{-1}$), *x* = soil temperature at 10 cm soil depth (°C)	Wang et al. (2007)
	Colorado Plateau, cold desert	$y = -0.65 + 0.15\ (X)$	*y* = soil respiration (µmoles CO_2 m^{-2} s^{-1}), *x* = soil temperature ≤ 15.7 (°C)	Fernandez et al. (2006)
	Colorado Plateau, cold desert	$y = -3.24 + 51.14\ (X)$	*y* = soil respiration (µmoles CO_2 m^{-2} s^{-1}), *x* = soil temperature > 15.7 (°C)	Fernandez et al. (2006)
	Tibetan Plateau, low grazed alpine meadow	$y = 115.7exp^{0.117x}$	*y* = soil respiration rate (mg CO_2 m^{-2} h^{-1}), *x* = soil temperature at 5 cm depth (°C)	Cao et al. (2004)
	Tibetan Plateau, high grazed alpine meadow	$y = 90.21exp^{0.1016x}$	*y* = soil respiration rate (mg CO_2 m^{-2} h^{-1}), *x* = soil temperature at 5 cm depth (°C)	Cao et al. (2004)
	Central Massa-chusetts, forest	$Flux = 21.13 * e^{(0.1371*temp)}$	*Flux* = soil respiration (mg $C/m^2/hr$), *temp* = soil temperature at 10 cm (°C)	Davidson et al. (1998)
	Alaska, tundra	$Y = 89.78 + 1.54X + 5X^2$	*Y* = daily mean dark CO_2 flux (mg CO_2 m^{-2} hr^{-1}, *X* = daily mean soil temperature (°C)	Peterson and Billings (1975)

Korea, forest	$y = 0.14e^{0.113x}$	y = soil respiration (g CO_2 m^{-2} h^{-1}), x = soil temperature (°C)	Kang et al. (2003)
Min-nesota, forest	$CO_2 = e^{C+B_1T+B_2MI}$ with: C = -2.63; -2.07; -2.06 B1 = 0.11; 0.07; 0.08 B2 = 0.04; 0.03; 0.04 (oak forest; marginal fen; cedar swamp)	CO_2 = CO_2 evolution rate (gm CO_2/m^2/hr), C = constant, B_1 = coefficient for soil temperature, B_2 = coefficient for moisture index, T = soil temperature (°C), MI = moisture index	Reiners (1968)
Great Plains	$Soil\ flux = ((A_1, A_2, A_3)^z) * maximum\ flux$ with: A1 = (Tmax-T)/(Tmax-Topt), A2 = (T-Tmin)/(Topt-Tmin), A3 = (Topt-Tmin)/(Tmax – Topt), z = 1.5, maximum flux rate = 8.4 g CO_2-C m^{-2} d^{-1}	*Soil flux* = soil CO_2 flux (g CO_2-C m^{-2} d^{-1}), T = measured soil temperature (°C), T_{max} = maximum soil temperature, T_{min}= minimum soil temperature, T_{opt} = optimum soil temperature for soil CO_2 flux	Frank et al. (2002)
Finland, agri-cultural eco-system with peat soil	$SR = 122.65 \exp(0.0718ST)$	SR = soil respiration (mg CO_2 m^{-2} h^{-1}), ST = soil temperature at 2.0 cm depth (°C)	Koizumi et al. (1999)
Finland, agri-cultural eco-system with clay soil	$SR = 16.07ST + 91.95)$	SR = soil respiration (mg CO_2 m^{-2} h^{-1}), ST = soil temperature at 2.0 cm depth (°C)	Koizumi et al. (1999)
Australia, *Eu-calyptus pauciflora* forest	$\ln(resp) = 4.83 + 0.092 * (stemp)$ for: < 10 °C $\ln(resp) = 5.45 + 0.041 * (stemp)$ for: >10 °C	*resp* = soil CO_2 efflux (mg CO_2 m^{-2} hr^{-1}), *temp* = soil temperature at 10 cm (°C)	Keith et al. (1997)
Arctic	$R_s = R_{10}e^{308.56(\frac{1}{36.02} - \frac{1}{T_s - 227.13})}$	R_s = soil respiration (µmol m^{-2} s^{-1}), R_{10} = soil respiration rate at 10°C (µmol m^{-2} s^{-1}), T_s = soil temperature (°C)	Lloyd (2001)
Canada, agri-cultural fields	$Rsoil = -0.74 + 0.2\ Tsoil$ (volumetric soil moisture content 10 – 35%)	*Rsoil* = soil respiration (µmol$CO_2$$m^{-2}$ s^{-1}), *Tsoil* = soil temperature (°C)	Rochette et al. (1991)
Missouri, tallgrass prairie	$\ln Y = a + b \ln(X + 10)$	Y = CO_2 evolution rate (mg CO_2 m^{-2} hr^{-1}), a = constant, b = temperature coefficient, X = soil temperature (°C)	Kucera and Kirkham (1971)

Sweden, forest	$R = 0.041 \exp(0.1559 T_s)$	R = soil respiration (mg $m^{-2} s^{-1}$), T_s = soil temperature at 5 cm (°C)	Morén and Lindroth (2000)
California, grass savanna	$R_s = -0.12 + 0.029 T_s$	T_s = soil respiration of an open area in June (μmol $m^{-2} s^{-1}$), T_s = soil temperature at 8 cm depth (°C)	Tang et al. (2005)
California, grass savanna	$R_s = -0.37 + 0.024 T_s$	T_s = soil respiration of an open area in July (μmol $m^{-2} s^{-1}$), T_s = soil temperature at 8 cm depth (°C)	Tang et al. (2005)
California, grass savanna	$R_s = -0.26 + 0.017 T_s$	T_s = soil respiration of an open area in September (μmol $m^{-2} s^{-1}$), T_s = soil temperature at 8 cm depth (°C)	Tang et al. (2005)
California, grass savanna	$R_s = 5.33 + 0.040 T_s$	T_s = soil respiration under a tree in June (μmol $m^{-2} s^{-1}$), T_s = soil temperature at 8 cm depth (°C)	Tang et al. (2005)
California, grass savanna	$R_s = 5.15 - 0.028 T_s$	T_s = soil respiration under a tree in July (μmol $m^{-2} s^{-1}$), T_s = soil temperature at 8 cm depth (°C)	Tang et al. (2005)
California, grass savanna	$R_s = 1.59 - 0.015 T_s$	T_s = soil respiration under a tree in September (μmol $m^{-2} s^{-1}$), T_s = soil temperature at 8 cm depth (°C)	Tang et al. (2005)
California, forest	$F = \beta_0 e^{\beta, T}$	F = soil efflux rate (μmol $m^{-2} s^{-1}$), T = soil temperature at a certain depth (°C), β_0 = constant fitted with the least squares techniques, β_1 = constant fitted with the least squares techniques	Xu and Qi (2001)
China, forest	$y = \frac{b_1}{1 + \exp(b_2(b_3 - x))}$	y = soil respiration (μmol $m^{-2} s^{-1}$), x = soil temperature at 10 cm depth, b_1, b_2, b_3 = regression parameter	Yu et al. (2011)
Brazil, forest	$R_s = 0.29 * \exp(0.14 * T)$	Rs = mean monthly soil respiration (μmol $m^{-2} s^{-1}$), T = soil temperature (°C)	Zanchi et al. (2009)
Brazil, forest	$R_s = R_0 * e^{(\beta_0 * T_{soil})}$ $Q_{10} = e^{10 * \beta_0}$ with: $R_0 = 0.02; 0.04; 0.18; 0.28$ $b_0 = 0.25; 0.22; 0.15; 0.14$ $Q_{10} = 12.00; 8.80; 4.30; 3.90$ (dry class; intermediate; wet class; whole period)	R_s = soil respiration (μmol CO_2 $m^{-2} s^{-1}$), T_{soil} = soil temperature at 15 cm depth (°C), R_0, β_0 = fitted parameter, Q_{10} = sensitivity parameter of the respiration variation with a variation in temperature of 10 °C	Zanchi et al. (2009)
Wyoming, mature forest	$Y = 1.406 * e^{(0.038 * X)}$	Y = soil-surface CO_2 efflux in August (μmol CO_2 $m^{-2} s^{-1}$), X = soil temperature (°C)	Litton et al. (2003)
Wyoming, mature forest	$Y = 1.782 * e^{(0.035 * X)}$	Y = soil-surface CO_2 efflux in June (μmol CO_2 $m^{-2} s^{-1}$), X = soil temperature (°C)	Litton et al. (2003)

	Wyoming, young forest	$Y = 0.299 * e^{(0.064*X)}$	Y = soil-surface CO_2 efflux in August (µmol CO_2 m^{-2} s^{-1}), X = soil temperature (°C)	Litton et al. (2003)
	Wyoming, young forest	$Y = 0.827 * e^{(0.061*X)}$	Y = soil-surface CO_2 efflux in June (µmol CO_2 m^{-2} s^{-1}), X = soil temperature (°C)	Litton et al. (2003)
	Brazil, forest	$R = R_0 e^{kT}$	R = CO_2 efflux(µmol m^{-2} s^{-1}), R_0= CO_2 efflux at average soil temperature (µmol m^{-2} s^{-1}), k = CO_2 efflux exponential response coefficient for temperature, T = soil temperature at 5 cm depth (°C)	Sotta et al. (2004)
	China, moso bamboo forest	$y = 0.990e^{0.078x}$	y = soil CO_2 efflux (µmol m^{-2} s^{-1}), x = soil temperature at 0.05 m depth (°C)	Song et al. (2013)
	China, Chinese fir forest	$y = 0.302e^{0.114x}$	y = soil CO_2 efflux (µmol m^{-2} s^{-1}), x = soil temperature at 0.05 m depth (°C)	Song et al. (2013)
		$SR = a/(1 + b\ exp(-kT))$	SR = soil respiration rate (µmol CO_2 $m^{-2}s^{-1}$), T = soil temperature (°C), a = maximum soil respiration rate, b = elongation along x axis, k = steepness of curve at inflection point	Richards (1959)
	Tibetan Plateau, alpine grassland	$y = 17.759e^{0.0475x}$	y = soil respiration (mg m^{-2} h^{-1}), x = soil temperature at 0 cm depth (°C)	Zhang et al. (2005)
	Tibetan Plateau, alpine grassland	$y = 15.132e^{0.0819x}$	y = soil respiration (mg m^{-2} h^{-1}), x = soil temperature at 5 cm depth (°C)	Zhang et al. (2005)
	Tibet, alpine meadow	$R_s = 0.808e^{0.123T}$ (growing season) $R_s = 0.254e^{0.256T}$ (non-growing season)	R_s = soil respiration rate (µmol m^{-2} s^{-1}), T = soil temperature at 5 cm depth (°C)	Li and Sun (2011)
	Colorado, crop field	$lnCO_2 = 7.0687 + 0.1329Ts_{10} - 0.00197{Ts_{10}}^2$	CO_2 = amount of CO_2 evolved from the soil (g m^{-2} d^{-1}), Ts_{10} = soil temperature at 10 cm depth (°C)	Buyanovsky et al. (1986)
	Colorado, crop field	$lnCO_2 = 7.579 + 0.061Ts_{10}$	CO_2 = amount of CO_2 evolved from the soil (g m^{-2} d^{-1}), Ts_{10} = soil temperature at 10 cm depth (°C)	Buyanovsky et al. (1986)
Regression based on litter temperature T	South-western Australia, litter of Eucalypt forest	$A(T) = \exp(\alpha + \beta T + \gamma T^2)$	A = maximum substrate-limited respiration rate (mg CO_2 g^{-1} litter day^{-1}), T = litter temperature (°C), α, β, γ = constants	O´Connell (1990)
Regression based on moss temperature T_m	Sweden, forest	$R = 0.0599 \exp(0.1067T_m)$	R = soil respiration (mg $m^{-2}s^{-1}$), T_m = moss temperature (°C)	Morén and Lindroth (2000)

Regression based on chamber temperature T_{ch}	Sweden, forest	$R = 0.1092 \exp(0.0638 T_{ch})$	R = soil respiration (mg $m^{-2}s^{-1}$), T_{ch} = chamber temperature (°C)	Morén and Lindroth (2000)
Regression based on temperature T, root biomass B	China, spring maize ecosystem	$SR = ae^{bT}B + cT + d$ with: a = 0.1022; 0.0341; 0.0422; 0.0214; 0.0389 b = 0.0381; 0.0540; 0.0401; 0.038; 0.0069 c = 0.0807; - 0.0379; - 0.0563; - 0.0170; 0.0165 d = - 0.3459; 1.8813; 0.829; 1.0225; 0.4292 (June 5; June 28; July 28; August 28; September 22)	SR = soil respiration rate (µmol m^{-2} s^{-1}), B = root biomass in the soil collars (gm^{-2}), T = temperature (°C), a, b, c, d = parameters	Han et al. (2007)
Regression based on temperature T, soil organic matter SOM	Various ecosystems	$RCR(t) = RCR_0[1 + \alpha(T)\Delta T(t)]\frac{SOM}{SOM_0}$	RCR = evolution of CO_2 from soil (mg $m^{-2}h^{-1}$), T = temperature (°C), $\alpha(T)$ = CO_2 response to temperature T (°C), SOM = soil organic matter (n/a)	Schleser (1982)
Regression based on soil temperature T_{soil}, NDVI I_{NDVI}	Spain, barley	$F_{soil} = 0.052(2.684T_{soil} - 0.092T_{soil}^2 * \exp(2.79I_{NDVI})$	F_{soil} = soil CO_2 efflux (µmol m^{-2} s^{-1}), T_{soil}= soil temperature at 10 cm depth (°C), I_{NDVI} = normalized difference vegetation index	Sánchez et al. (2003)
Regression based on temperature T, depth z, max. depth of respiration L		$q(z) = Qg_Tg_\Theta(1 - \frac{z}{L})^n$ with: n = 1 (soil gas transport) n = 0.25 (CO2 transport) $g_T = \exp\frac{-E_0}{T - T_o}$	$q(z)$= soil respiration rate (kg m^{-3} s^{-1}), Q = surface soil respiration rate (kg m^{-3} s^{-1}), z = depth (m), L = depth to which respiration occurs (m), n = dimensionless attenuation coefficient, g_T = relationship between soil respiration and temperature, g_Θ = relationship between soil respiration and water content (Θ, m^3 m^{-3}), E_0 =308.6 K, T = temperature (K), T_0= 227.1 K	Cook et al. (1998), Lloyd and Taylor (1994), Glinski and Stepniewski (1985)
Regression based on mean annual precipitation P		$SR = 0.391P + 155$	SR = annual soil respiration rate (gC/m^2/yr), P = mean annual precipitation (mm)	Raich and Schlesinger (1992)
Regression based on soil moisture	Colorado Plateau, cold desert	$y = -1.00 + 32.56\ (X)$	y = soil respiration (µmoles$CO_2m^{-2}s^{-1}$), x = soil moisture ≤ 9.5 (%)	Fernandez et al. (2006)
	Colorado Plateau, cold desert	$y = 0.20 + 0.01\ (X)$	y = soil respiration (µmoles CO_2 m^{-2} s^{-1}), x = soil moisture > 9.5 (%)	Fernandez et al. (2006)
	Inner Mongolia, *Stipa*	$y = 3.469log10x - 2.053$	y = CO_2-release rate (g C m^{-2} d^{-1}), x = soil moisture (%)	Chen et al. (1999)

grandis steppe			
Inner Mongolia, *Leymus chinensis* steppe	$F = a + bW$ with: a = -250.64; -71.54 b = 47.91, 18.93 (ungrazed; grazed)	*F* = soil respiration rate (mg m^{-2} h^{-1}), *W* = soil moisture (%), *a, b* = parameters	Jia et al. (2006)
Inner Mongolia, *Leymus chinensis* steppe	$F = a + bW$+cW^2 with: a = -102.85; -371.08 b = 20.00; 79.64 c = 1.17; -2.80 (ungrazed; grazed)	*F* = soil respiration rate (mg m^{-2} h^{-1}), *W* = soil water content (%), *a, b, c* = parameters	Jia et al. (2006)
Inner Mongolia, *Leymus chinensis* steppe	$F = a + bW^3$ with: a = 87.19; 61.06 b = 0.10, 0.04 (ungrazed; grazed)	*F* = soil respiration rate (mg m^{-2} h^{-1}),*W* = soil water content (%), *a, b* = parameters	Jia et al. (2006)
Inner Mongolia, *Leymus chinensis* steppe	$F = ae^{bW}$ with: a = 25.67; 14.34 b = 0.18; 0.19 (ungrazed; grazed)	*F* = soil respiration rate (mg m^{-2} h^{-1}), *W* = soil water content (%), *a, b* = parameters	Jia et al. (2006)
Inner Mongolia, *Leymus chinensis* steppe	$F = a + b\mathrm{Log}\,W$ with: a = -933.41; -331.64 b = 1191.04; 458.92 (ungrazed; grazed)	*F* = soil respiration rate (mg m^{-2} h^{-1}), *W* = soil water content (%), *a, b* = parameters	Jia et al. (2006)
Australia, *Eucalyptus pauciflora* forest	$\ln(resp) = 5.37 - 0.0011 * (soilm)$ for: < 10 °C $\ln(resp) = 5.31 + 0.0193 * (soilm)$ for: >10 °C	*resp* = soil CO_2 efflux (mg CO_2 m^{-2} hr^{-1}), *soilm* = soil moisture content (%)	Keith et al. (1997)
Australia, *Eucalyptus pauciflora* forest	$\ln(resp) = 5.27 - 0.0005 * (litterm)$ for: < 10 °C $\ln(resp) = 5.76 + 0.0052 * (litterm)$ for: >10 °C	*resp* = soil CO_2 efflux (mg CO_2 m^{-2} hr^{-1}), *litterm* = soil moisture content (%)	Keith et al. (1997)

	Sweden, forest	$R = -0.9024\Theta + 0.3341$	*R* = soil respiration (mg $m^{-2}s^{-1}$), *Θ* = soil water content at 10 cm (%)	Morén and Lindroth (2000)
	Okla-homa, field	$R = 0.664 * \frac{(W-25)}{7.88 + (W-25)}$	*R* = soil CO_2 efflux (µmol m^{-2} s^{-1}), *W* = soil moisture (g kg^{-1})	Liu et al. (2002)
	Ten-nessee	$R_s = g * RSW$	R_s = soil respiration (µmol m^{-2} s^{-1}), *RSW* = relative soil water content (%), *g* = coefficient	Chen et al. (2010)
	Brazil, forest	$R_s = -1.0753 + 17.58 * \ln(0) - 6.299 * ln^2(0)$	*Rs* = mean monthly soil respiration (µmol m^{-2} s^{-1}), *T* = soil moisture (m^3 m^{-3})	Zanchi et al. (2009)
	Brazil, forest	$R_s = a + b * \ln(\theta) + c * ln^2(\theta)$ with: $a_0 = 2213;\ -44.70;\ 18.00;\ -12.50$ $b_0 = 1934;\ -65.30;\ 19.80;\ -30.30$ $c_0 = 423.80;\ -19.00;\ 12.00;\ -9.60$ (dry class; intermediate; wet class; whole period)	*Rs* = soil respiration (µmol CO_2 m^{-2} s^{-1}), *Θ* = volumetric soil moisture content (m^3 m^{-3}), *a* = soil activation energy (n/a), *b* = parameter for the soil respiration close to the water field capacity, *c* = soil respiration decrease when Θ>0.25m^3 m^{-3} or Θ<0.15 m^3 m^{-3}	Zanchi et al. (2009)
	Brazil, forest	$CO_2 = 1.902(\Theta^3) + 0.14$	CO_2 = CO_2 flux (g C m^{-2} hr^{-1}), *Θ* = volumetric water content *(cm^3 H_2O cm^{-3})*	Davidson et al. (2000)
	Brazil, cattle pasture	$CO_2 = 3.461(\Theta^3) + 0.09$	CO_2 = CO_2 flux (g C m^{-2} hr^{-1}), *Θ* = volumetric water content *(cm^3 H_2O cm^{-3})*	Davidson et al. (2000)
		$P = \begin{cases} \alpha\theta_v^f \\ \beta(\varepsilon - \theta_v)^g \end{cases}$	*P* = evolved CO_2 (mg CO_2/g soil), θ_v = relative water content (n/a), α, β, ε, f, g = parameter	Skopp et al. (1990)
	China, grassland *Lymus chinesis*	$y = 126.51x - 6.5121$	*y* = CO_2 release rate of soil respiration (g m^{-2} d^{-1}), *x* = soil water content at 0-10 cm depth (%)	Wang et al. (2002)
	China, grassland *Pucci-nellia tenuiflora*	$y = 60.425x - 1.7024$	*y* = CO_2 release rate of soil respiration (g m^{-2} d^{-1}), *x* = soil water content at 0-10 cm depth (%)	Wang et al. (2002)
Regression based on water potential	Lab in-cubations	$A = -0.167\ln(-\psi) + 0.95$	*A* = microbial activity indexing CO_2 evolution (µl CO_2 g^{-1} h^{-1}), *ψ* = water potential (MPa)	Orchard and Cook (1983)
	Brazil, forest	$CO_2 = -0.0431Log(-\psi) + 0.16$	CO_2 = CO_2 flux (g C m^{-2} hr^{-1}), *ψ* = matric potential *(MPa)*	Davidson et al. (2000)
	Brazil, cattle pasture	$CO_2 = -0.0472Log(-\psi) + 0.19$	CO_2 = CO_2 flux (g C m^{-2} hr^{-1}), *ψ* = matric potential *(MPa)*	Davidson et al. (2000)
Regression based on mean annual tempera-ture *T*, mean annual pre-cipitation *P*		$SR = 0.0178TP + 311$	*SR* = annual soil respiration rate (gC/m^2/yr), *T* = mean annual temperature (°C), *P* = mean annual precipitation (mm)	Raich and Schlesinger (1992)
		$SR = (18.6T) + (0.192P) + 175$	*SR* = annual soil respiration rate (gC/m^2/yr), *T* = mean annual temperature (°C), *P* = mean annual precipitation (mm)	Raich and Schlesinger (1992)

		$SR = (9.26T) + (0.0127TP) + 289$	*SR* = annual soil respiration rate (gC/m^2/yr), *T* = mean annual temperature (°C), *P* = mean annual precipitation (mm)	Raich and Schlesinger (1992)
		$SR = (9.88T) + (0.0344P) + (0.0112TP) + 268$	*SR* = annual soil respiration rate (gC/m^2/yr), *T* = mean annual temperature (°C), *P* = mean annual precipitation (mm)	Raich and Schlesinger (1992)
Regression based on mean monthly air temperature, mean monthly precipitation		$R_S = 1.250 * e^{(0.05452*T_a)} * [P/(4.259 + P)]$	R_s = mean monthly soil-CO_2 efflux (gCm^{-2}d^{-1}), T_a = mean monthly air temperature (°C), *P* = mean monthly precipitation (cm)	Raich et al. (2002)
	China	$R'_s = f * e^{b_x*T_a)} * [\frac{P}{k+P}]$ with: $b_x = LnQ_{10}(x)/10$ $f = 1.250$ $k = 4.259$	*R's* = mean monthly soil respiration (g C/m^2*d), b_x = estimated temperature sensitivity at spatial grid x, T_a = mean monthly air temperature (°C), *P* = monthly precipitation (cm), *f*, *k* = constant	Zhou et al. (2009)
	Analysis of published field fluxes of CO_2	$R_S = F * e^{(Q*T_a)} * [P/(K+P)]$	R_S = mean monthly soil-CO_2 efflux (g C m^{-2} d^{-1}), T_a = mean monthly air temperature (°C), *P* = mean monthly precipitation (cm), *F* = soil respiration rate when mean monthly air temperature = 0°C, *Q* = rate of change of soil respiration rate with respect to temperature (°C^{-1}), *K* = half-saturation constant of the hyperbolic relationship between soil respiration with monthly precipitation (mm mo^{-1})	Raich and Potter (1995)
	Global	$moRs = F * e^{(aT-bT^2)} * \frac{\alpha P + (1-\alpha)P_{m-1}}{K + \alpha P + (1-\alpha)P_{m-1}}$	*moRs* = mean monthly soil respiration (g C m^{-2} d^{-1}), F = parameter (g C m^{-2} d^{-1}), K = parameter (cm mol^{-1}), a = parameter for the temperature function (°C^{-1}), b = parameter for the temperature function (°C^{-2}), *α* = parameter for the precipitation function, P_{m-1} = precipitation of the previous month (cm)	Hashimoto et al. (2015)
Regression based on temperature, precipitation	n.a., forest	$\widehat{CO}_2 = 0.715 + 0.210T_a + 0.285P_{3-1} + 0.083P_{7-4}$	*C^O$_2$* = evolution of CO_2 (g CO_2 m^{-2} d^{-1}), T_a = ambient air temperature (°C), P_{3-1}= rainfall within the 3 days preceding sampling (cm), P_{7-4} = rainfall from day 7 to day 4 preceding sampling (cm)	Reinke et al. (1981)
Regression based on temperature,	northern Great	$Daily\ flux = -4.20 + (0.33Ts) + (8.47SWC)$	*Daily flux* = daily soil flux (g CO_2-C m^{-2}d^{-1}), *Ts* = soil	Frank et al. (2002)

soil water content	Plains, prairie		temperature, *SWC* = soil water content	
	North-eastern France, young beech forest	$y = A\theta_v e^{BT}$ with: A = 1.13 B = 0.136	Θ_v = soil volumetric water content at -10 cm, *T* = soil temperature at -10 cm, *A, B* = fitting parameter	Epron et al. (1999)
	Japan, forest	$Fx = 0.000197e^{0.045t} * (\theta v - 21.42) * (58.54 - \theta v)^{4.46}$	*Fx* = soil CO_2 flux (mg CO_2 m^{-2} h^{-1}), *t* = soil temperature (°C), *θv* = soil water content (%)	Lee et al. (2002)
	Inner Mongolia, *Leymus chinensis* steppe	$F = a + bTW$ with: a = -109.17, -31.84 b = 1.68; 0.80 (ungrazed; grazed)	*F* = soil respiration rate (mg m^{-2} h^{-1}), *T* = temperature (°C), *W* = soil water content (%), *a, b* = parameters	Jia et al. (2006)
	Inner Mongolia, *Leymus chinensis*s teppe	$F = a + bT + cW$ with: a = -381.83; -148.50 b = 8.85; 6.40 c = 43.63; 15.01 (ungrazed; grazed)	*F* = soil respiration rate (mg m^{-2} h^{-1}), *T* = temperature (°C), *W* = soil water content (%), *a, b, c* = parameters	Jia et al. (2006)
	Inner Mongolia, *Leymus chinensis* steppe	$F = a + bT + cW + dTW$ with: a = 75.80; 100.11 b = -13.40; -8.27 c = -7.54; -13.20 d = 2.42; 1.60 (ungrazed; grazed)	*F* = soil respiration rate (mg m^{-2} h^{-1}), *T* = temperature (°C), *W* = soil water content (%), *a, b, c, d* = parameters	Jia et al. (2006)
	Inner Mongolia, *Leymus chinensis* steppe	$\mathrm{Ln}F = a + bT + cW$ with: a = 2.33; 1.81 b = 0.06; 0.07 c = 0.15; 0.14 (ungrazed; grazed)	*F* = soil respiration rate (mg m^{-2} h^{-1}), *T* = temperature (°C), *W* = soil water content (%), *a, b, c* = parameters	Jia et al. (2006)
	Inner Mongolia, *Leymus chinensis* steppe	$\mathrm{Ln}F = a + bT + cW + dTW$ with: a = 2.79; 1.96 b = 0.04; 0.06 c = 0.10; 0.13 d = 0.002; 0.001 (ungrazed; grazed)	*F* = soil respiration rate (mg m^{-2} h^{-1}), *T* = temperature (°C), *W* = soil water content (%), *a, b, c, d* = parameters	Jia et al. (2006)
	Inner Mongolia, *Leymus*	$F = ae^{bT}W^c$ with:	*F* = soil respiration rate (mg m^{-2} h^{-1}), *T* = temperature, *W* = soil	Jia et al. (2006)

chinensis steppe	a = 1.19; 0.94 b = 0.06; 0.07 c = 1.65; 1.52 (ungrazed; grazed)	water content (%), *a, b, c* = parameters	
Inner Mongolia, *Leymus chinensis* steppe	$F = ae^{bT}(W - c)(d - W)^f$ with: a = 1.63 * 105; 2.39 * 1039 b = 0.06; 0.07 c = -1.89* 104; 1.99 d = 45.16; 603.18 f = -5.06; -13.99 (ungrazed; grazed)	*F* = soil respiration rate (mg m^{-2} h^{-1}), *T* = temperature, *W* = soil water content (%), *a, b, c, d, f* = parameters	Jia et al. (2006)
Korea Seoul, oak forest	$R_{soil} = 124.3\exp(0.097T_s) - 55.3(M_s)^2 + 2931.9(M_s) - 38516$ for: $R_{soil(T)} > 0$ °C, Ts ≥ 0 °C	R_{soil} = total soil CO_2 efflux (mg CO_2 $m^{-2}h^{-1}$), T_s = soil temperature at 5 cm depth (°C), M_s = soil moisture content (%)	Joo et al. (2012)
Texas	$flux = (6.42 * e^{0.087*temp}) * (2.12 * ((\theta_v - 0.10) * (0.7 - \theta_v)^{1.46})$	*flux* = CO_2-C flux (g CO_2-C $m^{-2}d^{-1}$), *temp* = soil temperature (°C), θ_v = volumetric water content (m^3 m^{-3})	Mielnick and Dugas (2000)
Alaska, forest	$flux = \alpha e^{(\beta T)} * \chi M$	*flux* = CO_2 flux (g CO_2-C $m^{-2}d^{-1}$), α = flux rate at 0 °C (g CO_2-C $m^{-2}d^{-1}$), β = temperature response coefficient, *T* = soil temperature (°C), *M* = soil moisture (g H_2O/g dry soil), χ = moisture response constant	Gulledge and Schimel (2000)
Alaska, forest	$flux = \alpha e^{(\beta T)} - (M - \delta)^2$	*flux* = CO_2 flux (g CO_2-C $m^{-2}d^{-1}$), α = flux rate at 0 °C (g CO_2-C $m^{-2}d^{-1}$), β = temperature response coefficient, *T* = soil temperature (°C), *M* = soil moisture (g H_2O/g dry soil), δ = moisture response constant	Gulledge and Schimel (2000)
Alaska, forest	$flux = \alpha e^{(\beta T)} * (M/(M + \varepsilon))$	*flux* = CO_2 flux (g CO_2-C $m^{-2}d^{-1}$), α = flux rate at 0 °C (g CO_2-C $m^{-2}d^{-1}$), β = temperature response coefficient, *T* = soil temperature (°C), *M* = soil moisture (g H_2O/g dry soil), ε = moisture response constant	Gulledge and Schimel (2000)
Washing-ton, arid grassland	$y = (0.88 \pm 0.15) + (0.013 \pm 0.002)(w) * (t)$	*y* = rate of carbon dioxide evolution (g C $(m^2)^{-1}$ d^{-1}), *w* = soil water (%), *t* = soil temperature (°C)	Wildung et al. (1975)
California, forest	$F = 0.33W^{0.69}e^{0.042T}$ (W < 19%)	*F* = soil CO_2 efflux (µmol m^{-2} s^{-1}), *T* = soil temperature at 10 cm depth	Xu and Qi (2001)

	$F = 26.17W^{-0.82}e^{0.047T}$ (W > 19%)	(°C), *W* = soil water content (%)	
Alaska, tundra	$R_s = C * e^{(-\frac{E}{R*T_k})} * e^{(S_{wt})}$ with: $S_{wt} = A * W_t/(W_t + B)$	*Rs* = rate of CO_2 efflux (µmol m^{-2} s^{-1}), *C* = constant (m^{-2} s^{-1}), *R* = gas constant (8.31 J $mol^{-1}°K^{-1}$), T_k = soil temperature at 1 cm depth (°K), *E* = apparent activation energy (J mol^{-1}), S_{wt} = function of soil water table, W_t = depth to water table below soil surface (cm), *A*, *B* = regression coefficient	Oberbauer et al. (1992)
California, forest	$R = 0.2439M^{0.4199}T^{0.5581}$	*R* = soil CO_2 efflux (µmol m^{-2} s^{-1}), *T* = soil temperature (°C), *M* = soil moisture (m^3/m^3 %)	Qi et al. (2002)
Lab	$\rho(T,M) = \frac{M}{116+M} * \frac{2.820}{2.820+M} * 232 * 3.74^{(\frac{T-10}{T})}$	$\rho(T,M)$ = rate of microbial respiration (µl CO_2 g^{-1} h^{-1}), *M* = moisture content (% dry weight), *T* = temperature (°C)	Bunnell et al. (1977)
Australia, forest	$FRESP = \frac{M}{a_1+M}\frac{M}{a_2+M}a_3A_4^{\frac{T-10}{10}}$ with: $A_4 = \frac{1}{a_6 + a_4^{M-10}} + a_5$ $a_6 = \frac{1}{upper\ limit\ for\ Q_{10}} - a_5$ $a_1 = 17.8$ $a_2 = 17.8$ $a_3 = 29.3$ $a_4 = 1.55$ $a_5 = 0.54$ $a_6 = 0.75$	*FRESP* = respiration rate (g CO_2 m^{-2} h^{-1}), *T* = temperature (°C), *M* = moisture (% dry weight), a_1 = moisture content at half field capacity (%), a_2 = moisture content at half saturation (%), a_3 = theoretically maximum respiration rate at 10 °C when moisture is non-limiting, a_4 = parameter linking Q_{10} to substrate moisture content, a_5 = lower limit for the Q_{10} quotient, a_6 = coefficient, A_4 = Q_{10} quotient depending on soil moisture content	Carlyle and Than (1988)
Colorado, wheat/ fallow field and Wyoming, sub-alpine meadow	$R_H = F(T_{soil}) * F(RWC)$ $F(T_{soil}) = 0.56 + (1.46 * \frac{\arctan(\pi * 0.0309) * (T_{soil} - 15.7)}{\pi})$ $F(RSW) = 5 * (0.287 + \frac{\arctan(\pi * 0.009 * (RWC - 17.47))}{\pi})$	R_H = heterotrophic respiration (kg CO_2C ha^{-1} d^{-1}), *RWC* = measured relative soil water content (%), T_{soil}= soil temperature (°C)	del Grosso et al. (2005)
Wis-consin, forest	$\ln(R_s) = b_0 + b_1(soilT) + b_2(soilT^2) + b_3(SWC) + b_4(SWC^2) + b_5(soilT * SWC) + b_6(site\ code\ or\ site/soil\ characteristics)$	R_S = soil respiration (µmol CO_2 m^{-2} sec^{-1}), *soilT* = soil temperature (°C, at 10 cm), *SWC* = soil moisture (volumetric soil water content, g water 100 $soil^{-1}$, at 15 cm), *b* = coefficient, *site code* = nominal term to designate site	Martin and Bolstad (2005)

East Coast of USA, forest	$R = \left\{Aexp\left[\frac{-338.2°K}{T-329.2°K}\right]\right\} + [40.7 - 58.9(soil\ moisture)]$	*R* = soil respiration (mg C m^{-2} hr^{-1}), *T* = soil temperature at 10 cm soil depth (°K), *A* = site-specific factor, *soil moisture* = soil moisture (cm^3 H_2O cm^{-3} soil)	Savage and Davidson (2001)
China, desert	$Rs = -2.180 + 0.261Ws - 0.006Ws$	*y* = soil respiration at *Halostachyscaspica* site (µmol CO_2 m^{-2} s^{-1}), *y* = air temperature (°C), *Ws* = soil water content (%)	Zhang et al. (2010)
China, desert	$Rs = a + b(TW)$ with: a = 0.061; 0.207; 0.109; 0.576 b = 0.004; 0.001; 0.002; 1.112* 10-6 (*Haloxylonammodendron; Anabasis aphylla; Halostachyscaspica, all*)	*Rs* = soil respiration (µmol CO_2 m^{-2} s^{-1}), *T* = air temperature (°C), *W* = soil water content (%), *a*, *b* = regression parameter	Zhang et al. (2010)
China, desert	$Rs = a + bT + cW$ with: a = -0.362; -0.077; -0.257; 0.241 b = 0.026; 0.014; 0.018; 0.017 c = 0.061; 0.014; 0.012; -0.008 (*Haloxylonammodendron; Anabasis aphylla; Halostachyscaspica, all*)	*Rs* = soil respiration (µmol CO_2 m^{-2} s^{-1}), *T* = air temperature (°C), *W* = soil water content (%), *a*, *b*, *c* = regression parameter	Zhang et al. (2010)
China, desert	$Rs = aT^bW^c$ with: a = 0.005; 0.019; 0.002; 0.082 b = 1.036; 0.644; 1.078; 0.714 c = 0.819; 0.448; 0.640; -0.156 (*Haloxylonammodendron; Anabasis aphylla; Halostachyscaspica, all*)	*Rs* = soil respiration (µmol CO_2 m^{-2} s^{-1}), *T* = air temperature (°C), *W* = soil water content (%), *a*, *b, c* = regression parameter	Zhang et al. (2010)
China, desert	$Rs = ae^{bT}W^c$ with: a = 0.037; 0.064; 0.021; 0.361 b = 0.045; 0.029; 0.045; 0.030 c = 0.919; 0.475; 0.633; -0.146 (*Haloxylonammodendron; Anabasis aphylla; Halostachyscaspica, all*)	*Rs* = soil respiration (µmol CO_2 m^{-2} s^{-1}), *T* = air temperature (°C), *W* = soil water content (%), *a*, *b*, *c* = regression parameter	Zhang et al. (2010)
China, desert	$Rs = a + bT + cW + dTW$ with: a = 0.408; 0.011; -0.141; 0.156 b = -0.011; 0.011; 0.012; 0.020 c = -0.054; 0.008; 0.004; 0.0005 d = 0.006; 0.0002; 0.001; 0.0003 (*Haloxylonammodendron; Anabasis aphylla; Halostachyscaspica, all*)	*Rs* = soil respiration (µmol CO_2 m^{-2} s^{-1}), *T* = air temperature (°C), *W* = soil water content (%), *a*, *b*, *c*, *d* = regression parameter	Zhang et al. (2010)

Brazil, forest	$R_s = R_0 * e^{(\beta_0 * T_{soil})}$ $Q_{10} = e^{10*\beta_0}$ with: $R_0 = 0.02; 0.04; 0.18; 0.28$ $b_0 = 0.25; 0.22; 0.15; 0.14$ $Q_{10} = 12.00; 8.80; 4.30; 3.90$ (dry class; intermediate; wet class; whole period)	R_s = soil respiration (μmol CO_2 m^{-2} s^{-1}), T_{soil} = soil temperature at 15 cm depth (°C), R_0, β_0 = fitted parameter, Q_{10} = sensitivity parameter of the respiration variation with a variation in temperature of 10 °C	Zanchi et al. (2009)
Brazil, forest	$R_s = R_{Ref} * f(T_{soil,RSWC}) * g(RSWC)$ with: $f\ (T_{soil}, RSWC) = e^{E_0(RSWC)}(\frac{1}{T_{ref} - T_0}\frac{1}{T_{soil} - T_0})$ $g(RSWC) = \frac{RSWC}{RSWC_{1/2}} + RSWC$ $E_0(RSWC) = aREW + bREW * RSWC$ $RSWC = \frac{SWC}{SWC_{1/2}}$ with: $R_{ref} = 10.50; 12.08; 8.15; 10.84$ $RSWC = 0.41; 0.52; 1.24; 0.63$ $E_0 = 1045.80; 851.30; 598.80; 316.80$ (dry class; intermediate; wet class; whole period)	R_s = soil respiration (μmol CO_2 m^{-2} s^{-1}), R_{ref} = soil respiration at the reference temperature T_{ref} = 25 °C, E_0 = activation energy (K^{-1}), T_0 = lower temperature limit for the soil respiration (-46 °C), T_{soil} = soil temperature at 15 cm depth (°C), *RSWC* = water content relative to the soil water content at field capacity (n/a), $RSWC_{1/2}$ = soil water content with half-maximal respiration at a given temperature, *a* = n/a, *b* = n/a, *REW* = n/a	Zanchi et al. (2009)
Ten-nessee	$R_s = i * T + j * RSW$	R_s = soil respiration (μmol m^{-2} s^{-1}), *T* = temperature (°C), *RSW* = relative soil water content (%), *I, j* = coefficients	Chen et al. (2010)
Ten-nessee	$R_s = \lambda e^{k*t+l*w}$	R_s = soil respiration (μmol m^{-2} s^{-1}), λ = soil respiration at temperature of 0 °C (μmol CO_2 $m^{-2}s^{-1}$), *t* = temperature (°C), *RSW* = relative soil water content (%), *k*, *l* = coefficients	Chen et al. (2010)
France, forest	$y = 1.13\theta_v e^{0.136T}$	*y* = soil CO_2 efflux (μmol m^{-2} s^{-1}), Θ_v = volumetric water content (n/a), *T* = temperature (°C)	Epron et al. (1999)
Iowa, crop fields, riperian grass buffers	$\ln(SR) = 0.0865T + 0.0246M - 0.264$	*SR* = soil respiration rate (g C m^{-2} d^{-1}), *T* = morning surface-soil (0-5 cm depth) temperature (°C), *M* = surface-soil (0-5 cm depth) gravimetric moisture content (% H_2O)	Tufekcioglu et al. (2001)
Belgium, forest	$SR = SR_{10}Q_{10}^{(T-10)/10}$ with:	*SR* = predicted soil respiration (μmol m^{-2} s^{-1}), SR_{10} = simulated SR at	Curiel Yuste et al. (2003)

	$Q_{10} = 1.93$, $SR_{10} = 1.06$ (whole year), $Q_{10} = 2.74$, $SR_{10} = 1.02$ (winter), $Q_{10} = 1.24$, $SR_{10} = 1.38$ (growing season), $Q_{10} = 3.21$, $SR_{10} = 1.15$ (fall), $SR = f(T) * f(SWC)$ (SWC below WHC) with: $f(SWC) = 5.2SWC - 0.05$	10 °C (µmol m^{-2} s^{-1}), Q_{10} = respiratory flux at one temperature over the flux at a temperature 10 °C lower (µmol m^{-2} s^{-1}), *T* = soil temperature at 2 cm depth (°C), *f (T)* = Q_{10} function, *SWC* = soil water content (m^3 m^{-3}), *WHC* = water holding capacity (m^3 m^{-3})	
Alaska, forest	$BRESP = \frac{M}{a_1 + M} * \frac{a_2}{a_2 + M} * a_3 * \left(\frac{1}{a_6 + a_4^{\left(\frac{T-10}{10}\right)}} + a_5\right)$ with: a_1 = 76.5; 158.0; 135.0 a_2 = 355.9; 167.6; 109.9 a_3 = 1.60; 3.56; 3.63 a_4 = 11.07; 14.12; 9.24 a_5 = 0.25; 0.25; 0.25 a_6 = 2.0; 2.0; 2.0 (aspen; birch; white spruce)	*BRESP* = soil respiration (g CO_2 m^{-2} h^{-1}), *T* = soil temperature at 15 cm depth (°C), *M* = percent soil moisture dry weight basis (%), a_1, a_2 = coefficient, a_3 = scaling factor, a_4 = Q_{10} related parameter, a_5 = lower limit of CO_2 evolution, $a_6 = a_5 + 1/a_6$	Schlentner and van Cleve (1984)
Germany, agroeco-systems	$A = A_R + A_F + A_S$ with: $A_R = A_R^0 \eta f(T)$, $A_F = k_F C_F f(\Theta) f(T)$, $A_S = k_S C_S f(\Theta) f(T)$, $f(\Theta) = \frac{\exp[(\frac{\Theta}{\Theta_c} - 1)]^\alpha}{[\frac{\Theta - \Theta_c}{\beta} + 1]^\alpha}$, $f(T) = [\exp(aT - b)]^c$, c = cT+cDR, $c_T = \frac{m - \sum_{t-30}^{t-1}(T)}{n}$, $c_{DR}^t = c_{DR}^{t-1} + \omega - r c_{DR}^{t-1}$, ω = 0 if Θt-1< Θcand Θt - Θt-1 ≥0.25* Θc, Θc= 60% of FC, a = 6.10; 5.13 b = 0.85; 0.96 m = 1479; 1180 n = 1248; 1210	*A*= daily mean soil respiration (mg CO_2 m^{-2} h^{-1}), A_R = root and rhizosphere respiration (mg CO_2 m^{-2} h^{-1}), A_F = respiration of fast organic matter fraction (mg CO_2 m^{-2} h^{-1}), A_S = respiration of slow organic matter fraction (mg CO_2 m^{-2} h^{-1}), A_R^0= maximum root and rhizosphere respiration (mg CO_2 m^{-2} h^{-1}), η = representing root growth *(>0, <1), T* = temperature (°C), Θ = actual soil water content at 10 cm depth (%), C_F = concentration (kg C ha^{-1}), C_S = concentration (kg C ha^{-1}), k_F = rate constant (d^{-1}), k_S= rate constant (d^{-1}), Θ_c = maximum water content at 10 cm depth = *1,* α, β = empirical fitting parameter (% field capacity FC^{-2}), *a, n* = fitted parameter ($°C^{-1}$), *b* = fitted parameter,	Kutsch and Kappen (1997)

		ω = 0.3; 0.25 r = 12; 34 k_F^{-1}= 965; 576 k_S^{-1}= 24950; 21533 k_{FS}^{-1}=510; 319 α = 0.25; 0.36 β = 1000, 1000 (maize monoculture; crop rotation)	*m*= fitted parameter (°C), *r* = empirically determined recovery coefficient, *c* = parameter for sensitivity of the system to short-term temperature variations, c_T = running 30-day T-sum, c_{DR} = drying and rewetting	
Regression based on mean weekly air temperature *wTa,* soil moisture M_{20}	Colorado, crop field	$CO_2 = -3193 + 392wTa + 175M_{20}$	CO_2 = amount of CO_2 evolved from the soil (g m^{-2} d^{-1}), *wTa* = mean weekly air temperature (°C), M_{20} = soil moisture at 20-30 cm (n/a)	Buyanovsky et al. (1986)
	Colorado, crop field	$CO_2 = -10860 + 509wTa + 419M_{20}$	CO_2 = amount of CO_2 evolved from the soil (g m^{-2} d^{-1}), *wTa* = mean weekly air temperature (°C), M_{20} = soil moisture at 20-30 cm (n/a)	Buyanovsky et al. (1986)
Regression based on air temperature *Ta*, soil temperature *Ts*, soil water content *SWC*	Northern Great Plains of USA, grazed prairie	$Daily\ flux = -0.57 - (0.12\,Ta) + (0.36\,Ts) + (4.70SWC)$	*Daily flux* = daily soil flux (g CO_2-C m^{-2} d^{-1}), *Ts* = soil temperature, *Ta* = air temperature, *SWC* = soil water content	Frank et al. (2002)
	North-eastern Great Plains of USA, western wheat-grass	$Daily\ flux = -2.45 + (0.26\,Ts) + (7.06SWC)$	*Daily flux* = daily soil flux (g CO_2-C m^{-2} d^{-1}), *Ts* = soil temperature, *SWC* = soil water content	Frank et al. (2002)
Regression based on temperature *T*, soil water content *W*, precipitation *R*	India, tropical grassland	$Y\hat{} = 61.17+7.78T+7.17W-0.54R$	*Y^* = CO_2 output (mg CO_2 m^{-2} h^{-1}), *T* = temperature (°C), *W* = soil water (%), *R* = rainfall (mm)	Gupta and Singh (1981)
Regression based on soil temperature, soil moisture	Colorado, crop field	$lnCO_2 = 5.025 + 0.7312Ts_{10} + 0.7308lnM_{20}$	CO_2 = amount of CO_2 evolved from the soil (g m^{-2} d^{-1}), Ts_{10} = soil temperature at 10-20 cm depth, M_{20} = soil moisture at 20-30 cm (n/a)	Buyanovsky et al. (1986)
	Colorado, crop field	$CO_2 = 17190 - 801Ts_{10} + 35.8\,Ts_{10}{}^2 - 354M_{10}$	CO_2 = amount of CO_2 evolved from the soil (g m^{-2} d^{-1}), Ts_{10} = soil temperature at 10-20 cm depth, M_{10} = soil moisture at 20-30 cm (n/a)	Buyanovsky et al. (1986)
	Colorado, crop field	$lnCO_2 = 2.306 + 0.087Ts_{10} + 1.51lnM_{20}$	CO_2 = amount of CO_2 evolved from the soil (g m^{-2} d^{-1}), Ts_{10} = soil temperature at 10-20 cm depth, M_{20} = soil moisture at 20-30 cm (n/a)	Buyanovsky et al. (1986)

Regression based on daily mean temperature *T*, daily precipitation *P*	Qinghai-Tibet Plateau, alpine Steppe	$E_{carbon} = 0.22(\exp(0.09T) + \ln(0.31P + 1))$	E_{carbon} = soil respiration (g/m^2 per day), *T* = daily mean temperature (°C), *P* = total daily precipitation (mm),	Pei et al. (2009)
Regression based on soil temperature *T*, water matrix potential ψ	East Cost, forest	$R = \left\{Aexp\left[\frac{-350.6°K}{T - 231.2°K}\right]\right\} - [7.044 + 0.103(\psi)]$ (ψ ≤ - 150kPa) $R = \left\{Aexp\left[\frac{-350.6°K}{T - 231.2°K}\right]\right\}$ (ψ > - 150kPa)	*R* = soil respiration (mg C m^{-2} hr^{-1}), *T* = soil temperature at 10 cm soil depth (°K), *A* = site-specific factor, *ψ* = water matrix potential (kPa)	Savage and Davidson (2001)
Regression based on soil temperature T_s, soil water potential *ψ*	Canada, forest	$\hat{r}_s = (ce^{d\psi_s})e^{b(T_s - 10)}$	$\hat{r}_s$ = soil respiration (µmol m^{-2} s^{-1}), T_s = soil temperature at 5 cm depth (°C), *a*, *b*, *c*, *d* = regression coefficient, ψ_s = soil water potential (MPa)	Lavigne et al. (2004)
Regression based on soil temperature T_s, soil water content W_s, coarse fraction in the soil C_f	Tennessee, forest	$FF_{cer} = \left(R_b Q^{\left(\frac{T_s}{10}\right)}\right)\left(1 - \frac{Cf}{100}\right)$ with: $R_b = (kW_s R_{\max})/((kW_s) + R_{max})$	*FFcer* = efflux of CO_2 from forest floor (µmol m^{-2} s^{-1}), R_b= effect of soil water content on FF_{cer},, *Q* = rate of change in FF_{cer} for a 10 °C increase in soil temperature, T_s = soil temperature (°C), *Cf*= coarse fraction in the soil (%), W_s= soil water content (vol%), *k* = constant determining rate of change of R_b with respect to W_s, R_{max} = maximum value of R_b when W_s= 100%	Hanson et al. (1993)
Regression based on soil temperature, soil water content, leaf area index	Europe and North America, forest and shrubland	$R = R_{ref}(LAI_{max}) * f(T_{soil}, RSWC) * g(RSWC)$ with: $R_{ref}(LAI_{max}) = a_{LAI} + b_{LAI} * LAI_{max}$ $f(T_{soil}, RSWC) = e^{E_0(RSWC)*\left(\frac{1}{T_{ref} - T_0} - \frac{1}{T_{soil} - T_0}\right)}$ $g(RSWC) = \frac{RSWC}{RSWC_{1/2} + RSWC}$ $E_0(RSWC) = a_{E0} + b_{E0} * RSWC$ $RSWC = \frac{SWC}{SWC_{FC}}$	*R* = soil respiration (µmol m^{-2} s^{-1}), T_{soil} = soil temperature (°C), *RSWC* = relative soil water content (n/a), *SWC* = actual soil water content (m^3 m^{-3}), SWC_{FC} = soil water content at field capacity (n/a), R_{ref} = soil respiration rate under standard conditions (T_{ref} = 18 °C, non-limiting water) (µmol m^{-2} s^{-1}), R_{ref} *(*LAI_{max}*)* = site-specific soil respiration rates corrected for soil moisture and soil temperature depending on maximum site leaf area index (µmol m^{-2} s^{-1}), LAI_{max}= maximum site leaf area index (m^2 m^{-2}), T_{ref} = reference temperature (°C), T_0 = lower temperature limit for the soil respiration R, $RSWC_{1/2}$= soil water content at half-maximal respiration at a given temperature (fraction), E_0 = activation-	Reichstein et al. (2003)

			energy-type parameter of Lloyd and Taylor (1994) (K^{-1}), a_{LAI} , b_{LAI} = regression parameter (µmol m^{-2} s^{-1}), a_{E0}, b_{E0} = regression parameter (K^{-1})	
Regression based on soil temperature, soil water content, soil carbon	Italian Alps, forest	$SR = (c + dS_C + wS_{RW})/(1 + bT_M \exp(-(m + nT_{IQR})T_i))$	*SR* = mean soil CO_2 efflux (µmol CO_2 m^{-2} s^{-1}), T_M = soil mean annual temperature at soil depth of 10 cm (°C), S_C = average site soil carbon (kg m^{-2}), S_{RW} = relative soil water content at depth of 6 cm (n/a), *c, d, m, n* *w* = fitting parameter , T_{IQR} = soil temperature interquartile range (°C), T_i = (n/a)	Rodeghiero and Cescatti (2005)
Regression based on soil temperature, soil water content, litter	Belgium, forest	$Rs = Rs_{10} Q_{10}^{(T-10)/10}$ with: $Q_{10} = 5.65$, $Rs_{10} = 1.67$ (2001), $Q_{10} = 5.9$, $Rs_{10} = 1.66$ (2003), $Rs(non-stressed) = f(T) * f(I_s)$ (SWC below WHC) $Rs(drought) = f(T) * f(SWC) * f(I_s)$ (SWC below WHC) $Rs(rewetting) = 1.1 * (f(T) * f(I_s))$ (SWC below WHC) with: $I_s = d * \ln(L + e)$ with: $f(SWC) = a * SWC + b$ with: a = 6.9701; 6.3533 b = -0.2423; -0.1922 (2001; 2003) d = 0.60071 e = 3.789	*Rs* = predicted soil respiration (µmol m^{-2} s^{-1}), Rs_{10} = simulated Rs at 10 °C (µmol m^{-2} s^{-1}), Q_{10} = respiratory flux at one temperature over the flux at a temperature 10 °C lower (µmol m^{-2} s^{-1}), *T* = soil temperature at 2 cm depth (°C), *f (T)* = Q_{10} function, *SWC* = soil water content (m^3 m^{-3}), *WHC* = water holding capacity (m^3 m^{-3}), I_s = index of seasonality, *Rs(non-stressed)* = soil CO_2 efflux with SWC > 0.16 m^3 m^{-3} (µmol m^{-2} s^{-1}), *Rs(drought)* = soil CO_2 efflux with SWC < 0.16 m^3 m^{-3} and Iw< -0.7(µmol m^{-2} s^{-1}), *Rs(rewetting)* = soil CO_2 efflux with SWC below 0.16 m^3 m^{-3} and Iw> -0.7 (µmol m^{-2} s^{-1}), *L* = cumulative aboveground fine litter during the year (ton C ha^{-1})	Curiel Yuste et al. (2005)
Regression based on temperature, soil moisture, root biomass, net primary production	China, spring maize eco-system	$SR = (aW + b)e^{cT}B + (dNPP + e)T + f$ with: a = 0.1022; 0.0341; 0.0422; 0.0214; 0.0389 b = 0.0381; 0.0540; 0.0401; 0.038; 0.0069 c = 0.0807; - 0.0379; - 0.0563; - 0.0170; 0.0165	*SR* = soil respiration rate (µmol m^{-2} s^{-1}), *B* = root biomass in the soil collars (gm^{-2}), *T* = temperature (°C), *W* = soil moisture (%), *NPP* = net primary production (n/a.), *a, b, c, d, e, f* = parameters to be determined	Han et al. (2007)

		d = - 0.3459; 1.8813; 0.829; 1.0225; 0.4292 (June 5; June 28; July 28; August 28; September 22)		
Regression based on soil temperature, monthly mean soil water content, monthly precipitation, leaf area index		$R_{month} = (R_{LAI=0} + S_{LAI} * LAI)e^{QT_a}\frac{P+P_0}{K+P+P_0}$	R_{month} = monthly mean soil respiration (g C m^{-2} mo^{-1}), $R_{LAI=0}$ = soil respiration at LAI = 0 and at 0 °C without moisture limitation (g C m^{-2} mo^{-1}), Q = temperature sensitivity parameter to determine the exponential relationship between soil respiration and temperature ($°C^{-1}$), T_a = monthly average soil temperature (°C), K = half-saturation constant of the hyperbolic relationship of soil respiration with monthly precipitation, P = monthly precipitation sum (cm), S_{LAI} = basal rates of soil respiration (n/a), LAI = site peak leaf area index, P_0 = related to soil respiration in months without rains (n/a)	Luo and Zhou (2006) (in-corporating LAI in equation of Raich and Potter (1995)
Regression based on soil temperature, soil water content, monthly precipitation, soil matric water potential, leaf area index	Ten-nessee	$R_s = a * R_h + R_a$ with: $R_a = b * r_m + c * r_g$ $r_m = (0.058N + 0.622M)e^{0.098T}$ $R_h = d * M * F(t) * F(w)$ $F(t) = 0.56 + (1.46 * \frac{\arctan(\pi * 0.0309) * (t - 15.7)}{\pi})$ $F(w) = 5 * (0.287 + \frac{\arctan(\pi * 0.009 * (w - 17.47))}{\pi})$	R_s = soil respiration (µmol m^{-2} s^{-1}), R_h = heterotrophic respiration (µmol m^{-2} s^{-1}), R_a = autotrophic respiration (µmol m^{-2} s^{-1}), a = coefficient, r_m = root maintenance respiration(µmol m^{-2} s^{-1}), r_g = root growth respiration (µmol m^{-2} s^{-1}), b, c, d = coefficient, N = root nitrogen concentration (g kg^{-1}), M = soil matric water potential (MPa), T = soil temperature at 15 cm depth (°C), M = maximal soil respiration for different biomes according to Del Grosso et al. (2005) (µmol m^{-2} s^{-1}), $F(t)$ = temperature limitation function, $f(w)$ = water limitation function, t = temperature (°C), w = relative soil water content (%),	Chen et al. (2010)
Regression based on root mass, soil temperature, soil water content, pH value	Germany	$R_{soil} = R_{ref} * F(T_{soil}) * g(RSWC) * h(pH)$ $R_{ref} = h_{resp} + a_{resp}$ $a_{resp} = RRM * rf$ $f(T_{soil}) = \exp(E_0 * (\frac{1}{T_{ref} - T_0} - \frac{1}{T_{soil} - T_0}))$	R_{soil} = soil CO_2 efflux (µmol CO_2 m^{-2} s^{-1}), R_{ref} = emission under standard conditions (µmol CO_2 m^{-2} s^{-1}), h_{resp} = heterotrophic respiration (µmol CO_2 m^{-2} s^{-1}), a_{resp} = autotrophic respiration (µmol CO_2 m^{-2} s^{-1}), RRM = root mass per dry soil	Reth et al. (2005)

		$g(RSWC) = \frac{RSWC - RSWC_0}{(RSWC_{1/2} - RSWC_0) + (RSWC - RS}$ $h(pH) = \exp(-\left(\frac{pH - phOpt}{pHSens}\right)^2)$ with: $h_{resp} = 9.11$ $E_0 = 247.78$ $RWSC_0 = 9$ $RWSC_{1/2} = 1$ $phOpt = 9.35$ $phSens = -4.87$ $rf = 19.91$	mass (%), *rf* = parameter, E_0 = free parameter analogue to the activation energy in the standard Arrhenius model (K), T_{ref} = reference soil temperature (°C), T_0 = lower temperature limit for R_{soil} (°C), *RSWC* = relative soil water content, $RSWC_{1/2}$ = RSWC at half-maximum soil CO_2 efflux (%), $RSWC_0$ = residual soil water content, below which efflux ceases (%), *pH* = pH value, *pHOpt* = parameter for optimal pH value, *pHSens* = parameter for sensivity of soil CO_2 efflux to deviation from the optimal value	
Regression based on temperature, moisture, time, organic carbon	Lab, heavy clay soil	$C_{flux} = \sum C_{tot}\alpha_i k_i f(T,w)\exp(-k_i f\ (T,w)t$ with: $\sum \alpha_i = 1$	C_{flux} = measured CO_2 evolution rate (mg kg^{-1} $soil^{-1}$), *t* = time (days), C_{tot} = total initial amount of carbon (mg g $soil^{-1}$), α_i = fraction of each of the assumed organic carbon pools (% of initial amount), *i* = indices referring labile (*l*) and refractory (*r*) organic C pools, added straw (*TS*) or roots (*TR*), k_i = corresponding decomposition rate constant (% day^{-1}), *f (T, w)* = response function representing the modification of the rate constants for the effects of temperature (T) (°C) and moisture (w) (% H_2O)	Lomander et al. (1998)
Regression based on temperature, moisture, age, geo-graphical position, mineral coarse fragment mass	Virginia, forest	$Efflux = -0.05195 + 0.44652(temp) - 0.73176(lntemp) - 0.00625(temp^2) - 0.01739(temp * pos) + 0.00037936(temp * moist * age) - 0.00133(moist * age * pos) - 0.0000077(temp * moist * cfrags)$ with: temp = 0.446520 lntemp = -0.731760 (temp)2 = -0.006250 temp*pos = -0.017390 temp*moist*age = 0.000379 moist*age*pos = -0.001330 temp*moist*cfrags = -0.000008	*Efflux* = mean annual soil CO_2 efflux (µmol m^{-2} s^{-1}), *temp* = parameter, *lntemp* = parameter, *temp2* = parameter, *temp*pos* = parameter, *temp*moist*age* = parameter, *moist*age*pos* = parameter, *temp*moist*cfrags* = parameter,	Wiseman and Seiler (2004)
Regression based on	India, tropical forest soil	$y = 0.37x + 178.03$	*y* = soil respiration (mg CO_2 m^{-2} h^{-1}), *x* = large root biomass (g m^{-2})	Behera et al. (1990)

root biomass	India, tropical forest soil	$y = 2.40x + 163.6$	*y* = soil respiration (mg CO_2 m^{-2} h^{-1}), *x* = fine root biomass (g m^{-2})	Behera et al. (1990)
	India, tropical forest soil	$y = 0.32x + 176.6$	*y* = soil respiration (mg CO_2 m^{-2} h^{-1}), *x* = total root biomass (g m^{-2})	Behera et al. (1990)
	Japan, mixed grassland	$Y = 4.19x + 3.3$ (6 am)	*Y* = soil respiration (µmol m^{-2} s^{-1}), *x* = root biomass (kg m^{-2})	Wang et al. (2005)
	Japan, mixed grassland	$Y = 3.69x + 4.5$ (8 am)	*Y* = soil respiration (µmol m^{-2} s^{-1}), *x* = root biomass (kg m^{-2})	Wang et al. (2005)
	Japan, mixed grassland	$Y = 4.42x + 5.16$ (10 am)	*Y* = soil respiration (µmol m^{-2} s^{-1}), *x* = root biomass (kg m^{-2})	Wang et al. (2005)
	Japan, mixed grassland	$Y = 5.12x + 5.34$ (12 am)	*Y* = soil respiration (µmol m^{-2} s^{-1}), *x* = root biomass (kg m^{-2})	Wang et al. (2005)
	Japan, mixed grassland	$Y = 4.19x + 5.84$ (2 pm)	*Y* = soil respiration (µmol m^{-2} s^{-1}), *x* = root biomass (kg m^{-2})	Wang et al. (2005)
	Japan, mixed grassland	$Y = 4.41x + 4.08$ (4 pm)	*Y* = soil respiration (µmol m^{-2} s^{-1}), *x* = root biomass (kg m^{-2})	Wang et al. (2005)
	Japan, mixed grassland	$Y = 3.66x + 3.2$ (6 pm)	*Y* = soil respiration (µmol m^{-2} s^{-1}), *x* = root biomass (kg m^{-2})	Wang et al. (2005)
	Japan, mixed grassland	$Y = 5.14x + 3.79$ (May 26)	*Y* = soil respiration (µmol m^{-2} s^{-1}), *x* = root biomass (kg m^{-2})	Wang et al. (2005)
	Japan, mixed grassland	$Y = 8.03x + 5.71$ (Aug. 8)	*Y* = soil respiration (µmol m^{-2} s^{-1}), *x* = root biomass (kg m^{-2})	Wang et al. (2005)
	Japan, mixed grassland	$Y = 2.05x + 3.7$ (Oct. 29)	*Y* = soil respiration (µmol m^{-2} s^{-1}), *x* = root biomass (kg m^{-2})	Wang et al. (2005)
	Japan, mixed grassland	$Y = 2.95x + 2.59$ (Apr. 15)	*Y* = soil respiration (µmol m^{-2} s^{-1}), *x* = root biomass (kg m^{-2})	Wang et al. (2005)
	Japan, mixed grassland	$Y = 2.83x + 3.37$ (May 10)	*Y* = soil respiration (µmol m^{-2} s^{-1}), *x* = root biomass (kg m^{-2})	Wang et al. (2005)
	Japan, mixed grassland	$Y = 5.12x + 5.33$ (Jun. 5)	*Y* = soil respiration (µmol m^{-2} s^{-1}), *x* = root biomass (kg m^{-2})	Wang et al. (2005)
	Northern hemi-sphere, temperate eco-systems	$y = 382 + 1.13x$	*y* = soil respiration (g C $m^{-2}y^{-1}$), *x* = fine roots (g C m^{-2})	Hibbard et al. (2005)
	China, spring maize eco-system	$SR = \alpha B + \beta$ with: α = 0.0885; 0.0866; 0.0909; 0.1000; 0.1025; 0.0983; 0.1160; 0.1195; 0.1268; 0.1282; 0.1281; 0.1322; 0.1294 β = -0.4839; - 0.3298; - 0.2549; - 0.2324; - 0.3072; - 0.0728; -	*SR* = soil respiration rate (µmol m^{-2} s^{-1}), *B* = root biomass in the soil collars (gm^{-2}), *α*, *β* = parameters	Han et al. (2007)

		0.4122; - 0.3742; - 0.7169; - 0.8339; - 0.8156; - 1.0059; - 0.8742 (6 am; 7 am; 8 am; 9 am; 10 am; 11 am; 12 am; 1 pm; 2 pm; 3 pm; 4 pm; 5 pm; 6 pm)		
	Qinghai-Tibet Plateau, *Kobresia* meadow	$y = 0.00\ x + 2.78$	*y* = soil respiration (µmol CO_2 m^{-2} s^{-1}), *x* = belowground biomass of *Kobresia pygmaea* (g D. W. m^{-2})	Zhang et al. (2009)
	Qinghai-Tibet Plateau, *Kobresia* meadow	$y = 0.00\ x + 6.00$	*y* = soil respiration (µmol CO_2 m^{-2} s^{-1}), *x* = belowground biomass of *Kobresia humilis* (g D. W. m^{-2})	Zhang et al. (2009)
	Qinghai-Tibet Plateau, *Kobresia* meadow	$y = 0.00\ x + 7.56$	*y* = soil respiration (µmol CO_2 m^{-2} s^{-1}), *x* = belowground biomass of *Kobresia tibetica* (g D. W. m^{-2})	Zhang et al. (2009)
	China, rape field	$Rs = aB + b$ with: a =1.29; 0.75; 0.33; 0.35; 0.41; 0.43 b = 129.90; 70.67; 99.28; 103.14; 183.77; 176.20 (Nov.; Dec.; Jan., Feb., Mar.; Apr.)	*Rs* = soil respiration rate (mg CO_2/m^2/h), *B* = root biomass in the soil collars (g/m^2), *a, b* = parameter	Hao and Jiang (2014)
Regression based on carbon *x*	Colorado Plateau, cold desert	$y = 0.21 + 0.30\ (X)$	*y* = soil respiration (µmoles CO_2 m^{-2} s^{-1}), *x* = carbon ≤ 0.196 (%)	Fernandez et al. (2006)
	Colorado Plateau, cold desert	$y = 0.35 + 0.29\ (X)$	*y* = soil respiration (µmoles CO_2 m^{-2} s^{-1}), *x* = carbon > 0.196 (%)	Fernandez et al. (2006)
Regression based on nitrogen *x*	Colorado Plateau, cold desert	$y = 0.25 - 18.77\ (X)$	*y* = soil respiration (µmoles CO_2 m^{-2} s^{-1}), *x* = nitrogen ≤ 0.005 (%)	Fernandez et al. (2006)
	Colorado Plateau, cold desert	$y = 0.24 - 1.61\ (X)$	*y* = soil respiration (µmoles CO_2 m^{-2} s^{-1}), *x* = nitrogen > 0.005 (%)	Fernandez et al. (2006)
Regression based on organic layer thick-ness *OL*	Central Ireland, Sitka Spruce	$SR = 24.46 + 47.33\ OL$ (10 years old)	*SR* = soil respiration (mg C m^{-2} h^{-1}), *OL* = organic layer thickness	Saiz et al. (2006)
	Central Ireland, Sitka Spruce	$SR = 40.60 + 15.47\ OL$ (15 years old)	*SR* = soil respiration (mg C m^{-2} h^{-1}), *OL* = organic layer thickness	Saiz et al. (2006)
	Central Ireland, Sitka Spruce	$SR = 19.44 + 23.85\ OL$ (31 years old)	*SR* = soil respiration (mg C m^{-2} h^{-1}), *OL* = organic layer thickness	Saiz et al. (2006)
	Central Ireland, Sitka Spruce	$SR = -9.89 + 38.97\ OL$ (47 years old)	*SR* = soil respiration (mg C m^{-2} h^{-1}), *OL* = organic layer thickness	Saiz et al. (2006)

	Central Ireland, Sitka Spruce (all stand ages)	$SR = 21.85 + 25.59\ OL$	*SR* = soil respiration (mg C m^{-2} h^{-1}), *OL* = organic layer thickness	Saiz et al. (2006)
Regression based on Leaf Area Index *x*	Northern hemi-sphere, temperate eco-systems	$y = 419 + 77x$	*y* = soil respiration (g C $m^{-2}y^{-1}$), *x* = Leaf Area Index (m^2 m^{-2})	Hibbard et al. (2005)
Regression based on NDVI	Tibet, alpine grass-lands	$R_s = 0.9805 * e^{2.5763*(0.9655*NDVI\_MODIS+0.0166)}$	R_s = diurnal soil respiration (g C m^{-2} d^{-1}), *NDVI_MODIS* = normalized difference vegetation index calculated from Moderate-resolution Imaging Spectroradiometer	Huang and Zheng (2013)
Regression based on mean annual gross primary pro-ductivity P_g	Europe, forests	$R_s = -552 + 0.913P_g$	R_s = mean annual soil respiration (g C m^{-2} s^{-1}), P_g = mean annual gross primary productivity (g C m^{-2} s^{-1})	Janssens et al. (2001)
Regression based on ambient CO_2 con-centration *x*	Japan, agri-cultural field	$SR = a + bx$	*SR* = soil respiration rate (mg CO_2 m^{-2} s^{-1}), *x* = ambient CO_2 concentration (µl l^{-1}), *a*, *b* = coefficient	Nakadai et al. (2002)
	Belgium, forest	$Fc = Fs = \frac{v_z * C - D * \frac{\delta C}{\delta z}}{V_{mol}}$	*Fc* = *Fs* = soil CO_2 efflux (µmol m^{-2} s^{-1}), *vz* = air vertical velocity (m s^{-1}), *C* = air CO_2 concentration (µmol mol^{-1}), *D* = molecular diffusion coefficient of CO_2 in the air (m^2 s^{-1}), *δC/δz* = vertical gradient of the air CO_2 concentration (µmol mol^{-1} m^{-1}), V_{mol} = molecular volume (m^3 mol^{-1})	Longdoz et al. (2000)
Regression based on photo-synthesis P_s	California, grass savanna	$R_s = 6.19 - 0.031P_s$	T_s = soil respiration under a tree in June (µmol m^{-2} s^{-1}), P_s= photosynthesis (µmol m^{-2} s^{-1})	Tang et al. (2005)
	California, grass savanna	$R_s = 4.30 - 0.062P_s$	T_s = soil respiration under a tree in July (µmol m^{-2} s^{-1}), P_s = photosynthesis (µmol m^{-2} s^{-1})	Tang et al. (2005)
	California, grass savanna	$R_s = 1.22 - 0.044T_s$	T_s = soil respiration under a tree in September (µmol m^{-2} s^{-1}), P_s = photosynthesis (µmol m^{-2} s^{-1})	Tang et al. (2005)
Regression based on thawed soil thickness *H*	Qinghai-Tibet Plateau	$F = 1.84e^{0.023H} + 5.06$	*F* = soil CO_2 efflux (mgm^{-2} d^{-1}), *H* = thawed soil thickness (cm)	Wang and Wu. (2013)
Regression based on time *t*	Belgium, forest	$Q_{CO_2} = at + B(1 - e^{kt})$	Q_{CO2} = amount of CO_2 evolved at time t (g m^{-2} h^{-1}), *t* = time, *a* = constant representing the zero order rate, *B* = constant representing the flash of mineralization resulting from disturbance of the soil sample, *k* = time	Thierron and Laudelout (1996)

			constant of the transient phase before zero-order kinetics begin	
	Okla-homa, field	$Y = Y_0 + ate^{-bt}$	Y = soil CO_2 efflux (µmol m^{-2} s^{-1}), Y_0 =soil CO_2 efflux before water treatment, t = time (h), a, b = coefficient	Liu et al. (2002)
	Ten-nessee	$R_s = \lambda e^{\beta t}$ λ = 0.9506 *µmol CO_2 $m^{-2}s^{-1}$*	R_s= soil respiration (µmol m^{-2} s^{-1}), λ = soil respiration at temperature of 0 °C (µmol CO_2 $m^{-2}s^{-1}$), β = coefficient, t = temperature (°C)	Chen et al. (2010)
Regression based on gas con-centration, depth, max. depth of respiration		$\frac{d(\frac{DdC}{dz})}{dz}$ = -q $q(z) = Q[1 - (\frac{Z}{L})^k]$ with: k = 1 (soil gas transport) k = 0.25 (CO_2 transport)	D = diffusion coefficient of CO_2 in the gas-filled pore space (m^2 s^{-1}), z = depth (m), C = concentration of the gas in the gas-filled pore space (kg m^{-3}), $q(z)$= soil respiration rate (kg m^{-3} s^{-1}), Q = surface soil respiration rate (kg m^{-3} s^{-1}), L = depth to which respiration occurs (m), k = dimensionless attenuation coefficient	Cook et al. (1998), Glinski and Stepniewski (1985)
Regression based on CO_2 con-centration, weight of root sample	Oregon, forest	$k = \frac{\Delta CO_2}{100}\frac{1}{ODW}\frac{1}{IP} * V * 41.0339 * 12$	k = respiration rate of decomposing root (µg C per gram dry-root per hour), ΔCO_2 = net percentage increase of CO_2 concentration during incubation (%), ODW = oven-dry weight of root sample (g), IP = incubation period (h), V = net volume of headspace	Chen et al. (2000)
Regression based on total area of vegetation, number of vegetation types	Qinghai-Tibet Plateau, grassland	$Ec_1 = \sum_{j=1}^{m} \beta_j F_j (1 - \lambda_j)$	Ec_1 = carbon emission from soil-associated respiration (Mg C $year^{-1}$), β_j = total respiration rate measured below ground (Mg C $year^{-1}$), F_j = total area of vegetation (ha), m = number of vegetation types, λ_j = percentage of plant root respiration to total below-ground respiration (%), j = 1, 2, …, m	Genxu et al. (2002)

Table 2

Table 2. Regression functions to approximate belowground biomass

Type of regression	Region, vegetation type	Equation	Parameters	Author(s)
Regression based on above-ground biomass	World-wide, different grassland sites	$BNPP = BGB\frac{\text{Live}BGB}{BGB}turnover$ with: $BGB = 0.79\ (AGBIO) - 33.3\ (MAT + 10) + 1289;$ $LiveBGB = 0.6\ BGB;$ $turnover = 0.2884e^{0.046\ MAT}$	*BNPP* = belowground netto primary production, *BGB* = belowground biomass (g m^{-2}), *AGBIO* = peak aboveground live biomass (g m^{-2}), *MAT* = mean annual temperature (°C)	Gill et al. (2002)
	USA	$BGBD = \exp[-1.085 + 0.9256 * \ln(AGBD)]$	*BGBG* = belowground biomass density (Mg/ha), *AGBD* = aboveground biomass density (Mg/ha)	Jenkins et al. (2001)
	USA, smooth cordgrass	$\ln(LiveBelow) = 0.713\ln(TotalAbove) + 2.235$	*Live Below* = live belowground biomass (g), *Total Above* = live and dead aboveground biomasse (g)	Gross et al. (1991)
	World-wide, forest and woodland	$y = 0.489x^{0.890}$	*y* = root biomass, *x* = shoot biomass	Mokany et al. (2006)
	World´s upland forests	$Y = exp[-1.0850 + 0.9256(lnA)]$	*Y* = root biomass density (Mg/ha), *A* = aboveground biomass density (Mg/ha)	Cairns et al. (1997)
	World´s upland forests	$Y = \exp[-1.3267 + 0.8877(lnA) + 0.1045\ (lnB)$	*Y* = root biomass density (Mg/ha), *A* = aboveground biomass density (Mg/ha), *B* = age (year)	Cairns et al. (1997)
	World´s tropical forests	$Y = \exp[-1.0587 + 0.8836(lnA) + 0.2840\ (lnC) + 0.1874\ (lnD)$ with: $C = 0;$ $D = 0$	*Y* = root biomass density (Mg/ha), *A* = aboveground biomass density (Mg/ha), *B* = age (year), *c* and *d* = parameters for the latitudinal zone	Cairns et al. (1997)
	World´s temperate forests	$Y = \exp[-1.0587 + 0.8836(lnA) + 0.2840\ (lnC) + 0.1874\ (lnD)$	*Y* = root biomass density (Mg/ha), *A* = aboveground biomass density (Mg/ha), *B* = age (year),	Cairns et al. (1997)

		with: $C = 1$; $D = 0$	*c* and *d* = parameters for the latitudinal zone	
	World´s boreal forests	$Y = \exp[-1.0587 + 0.8836(lnA) + 0.2840\,(lnC) + 0.1874\,(lnD)$ with: $C = 0$; $D = 1$	*Y* = root biomass density (Mg/ha), *A* = aboveground biomass density (Mg/ha), *B* = age (year), *c* and *d* = parameters for the latitudinal zone	Cairns et al. (1997)
	Non-woody plants	$M_B = \frac{\beta_2}{(\beta_2 + 1)\beta_3} M_A = \beta_4 M_A$	M_B = belowground biomass, M_A =aboveground biomass, β_2 = allometric constant = annual leaf growth rate, β_3 = allometric constant = annual stem growth rate, β_4 = allometric constant = annual root growth rate	Niklas (2005)
Regression based on softwood root biomass RB_s and hardwood root biomass RB_h	Canada, forest	$RB = RB_s + RB_h$ with: $RB_s = 0.222 AB_s$; $RB_h = 1.576 AB_s^{0.615}$	*RB* = total root biomass (Mg ha^{-1}), RB_s = softwood root biomass (Mg ha^{-1}), RB_h = hardwood root biomass (Mg ha^{-1}), AB_s = softwood aboveground biomass (Mg ha^{-1}), AB_h = hardwood aboveground biomass (Mg ha^{-1})	Li et al. (2003)
	Canada, forest	$RB = RB_s + RB_h$ with: $RB_s = 0.2317 AB_s$; $RB_h = e^{0.359} AB_h^{0.639}$	*RB* = total root biomass (Mg ha^{-1}), RB_s = softwood root biomass (Mg ha^{-1}), RB_h = hardwood root biomass (Mg ha^{-1}), AB_s = softwood aboveground biomass (Mg ha^{-1}), AB_h= hardwood aboveground biomass (Mg ha^{-1})	Kurz et al. (1996)
Regression based on diameter at breast height	Central Highlands of Vietnam, evergreen broad leaved forest	$BGB = exp^{(-4.91842 + 2.41957 \ln(DBH))}$	*BGB* = belowground biomass (kg), *DBH* = diameter at breast height (cm)	Huy et al. (2012)
	Taiwan, Mahogany	$W_{below} = 61.65\, DBH^{2.19}$	W_{below} = Belowground biomass (g), *DBH* = diameter at breast height (cm)	Tsai et al. (2012)

	Western Kenya, trees in agricultural land-scapes	$BGB = 0.048\ dbh^{2.303}$	*BGB* = below-ground biomass (Mg tree $^{-1}$), *dbh* = diameter at breast height (cm)	Kuyah et al. (2012)
	Australia, open woodland	$totalmeasuredrootbiomass = 0.62\ DBH - 19.72$	*Total measured root biomass* = total belowground biomass (kg m^{-2} ground area), *DBH* = diameter at breast height (cm)	Macinnis-Ng et al. (2010)
	Finland, birch	$\ln(y_{ki}) = b_0 + b_1 \frac{d_{Ski}}{(d_{Ski} + 26)} + b_2 \ln(h_{ki}) + u_{9k} + e_{9ki}$	y_{ki}= biomass component or total biomass of tree *i* in stand *k* (kg), d_{ki} = tree diameter at breast height of tree *i* in stand *k* (cm), d_{Ski} = 2 + 1.25 *d* (cm), h_{ki} = tree height of tree *i* in stand *k* (m), *u* = vector of random effects, *e* = vector of random errors	Repola (2008)
Regression based on inside/ outside bark basal diameter *X*	Wyoming, 13-year-old *Pinus contorta* var. *latifolia*	$Y = aX^b$ with: $a = 6.563$; $b = 2.205$ (outside bark basal diameter) and with: $a = 7.691$; $b = 2.289$ (inside bark basal diameter)	*Y* = total coarse root biomass (g d.m.), *X* = inside/outside bark basal diameter (cm), *a, b* = constants	Litton et al. (2003)
Regression based on basal diameter *D*	Chile, *notho-fagus pumilio*	$Y = 0.001185459\ D^{1.762} H^{0.588}$	*Y* = belowground biomass (kg), *D* = basal diameter (cm), *H* = total height (cm)	Schmidt et al. (2009)
Regression based on January mean tempera-ture *x*	Tibet	$y = 200/(1 + \exp(-0.1434x + 1.0789))$	*y* = root biomass density (Mg/ha), *x* = january mean temperature (°C)	Luo et al. (2005)
Regression based on July mean tempera-ture *x*	Tibet	$y = 200/(1 + \exp(-0.2245x + 4.6125))$	*y* = root biomass density (Mg/ha), *x* = july mean temperature (°C)	Luo et al. (2005)

Regression based on annual mean tempera-ture *x*	Tibet	$y = 200/(1 + \exp(-0.1750x + 2.5543))$	*y* = root biomass density (Mg/ha), *x* = annual mean temperature (°C)	Luo et al. (2005)
Regression based on annual precipitation *x*	Tibet	$y = 200/(1 + \exp(-2.14E-06x^2 - 0.00575x + 4.78))$	*y* = root biomass density (Mg/ha), *x* = annual precipitation (mm)	Luo et al. (2005)
Regression based on annual mean temperature and annual precipitation *x*	Tibet	$y = 200/(1 + \exp(-0.0001594x + 2.5869))$	*y* = root biomass density (Mg/ha), *x* = annual mean temperature x annual precipitation (°C x mm)	Luo et al. (2005)
Regression based on altitude *x*	Tibet	$y = -0.0209x + 104.89$	*y* = root biomass density (Mg/ha), *x* = altitude (m)	Luo et al. (2005)

Acknowledgements

First of all, I would like to thank Prof. Dr. Thomas Scholten for supervising this thesis and providing the necessary framework for it. I am further grateful for his support, advice and various helpful impulses while working on this thesis.

Further, I would like to thank my co-supervisor Prof. Dr. Volker Hochschild for supervising, supporting as well as refereeing this thesis.

I am also very grateful to my third supervisor, Dr. Karsten Schmidt especially for valuable discussions, ideas, advice, GIS- and general support, and providing a critical and constructive perspective.

I further thank Corina Dörfer very much for several supportive discussions, productive ideas and suggestions, highly acknowledging her various helpful support.

Very special words of thanks go to Dr. Sarah Schönbrodt-Stitt who has taught me much of scientific working before. Next to this, I especially and highly acknowledge her extraordinary, helpful and manifold support and advice. Besides this, I am grateful for her proofreading - and last, but not least for all her instructions and help with GIS.

I would also like to express my gratitude to Philipp Gries very much, as I thankfully and highly appreciate his GIS help and proofreading.

Next to the Evangelische Studienwerk e.V. Villigst in general, I especially would like to thank Prof. Dr. Eberhard Müller and Dr. Almuth Hattenbach for mentoring this project and providing support and advice.

Further thanks go to several PhD students of the Ev. Studienwerk e.V. Villigst for support in literature procurement, manifold discussions, and interdisciplinary exchange on different occasions.

Moreover, I would like to thank Katie Tay overseas for her proofreading.

Finally, I would like to thank explicitly *each and everyone* in my family for his or her support in many ways very much. In particular, however, I would like to thank my parents for their support.